



# CHALMERS

## Thorium Fuels for Light Water Reactors

Steps towards commercialization

KLARA INSULANDER BJÖRK

---

Department of Applied Physics  
CHALMERS UNIVERSITY OF TECHNOLOGY  
Göteborg, Sweden 2015



THESIS FOR THE DEGREE OF DOCTOR OF PHILOSOPHY IN APPLIED  
PHYSICS

# Thorium Fuels for Light Water Reactors

Steps towards commercialization

KLARA INSULANDER BJÖRK

Department of Applied Physics

Division of Nuclear Engineering

CHALMERS UNIVERSITY OF TECHNOLOGY

Göteborg, Sweden 2015

Thorium Fuels for Light Water Reactors  
Steps towards commercialization  
KLARA INSULANDER BJÖRK  
ISBN 978-91-7597-191-9

© KLARA INSULANDER BJÖRK, 2015

Doktorsavhandlingar vid Chalmers tekniska högskola  
Ny serie nr. 3872  
ISSN 0346-718X  
Department of Applied Physics  
Division of Nuclear Engineering  
Chalmers University of Technology  
SE-412 96 Göteborg  
Sweden  
Telephone: +46 (0)31-772 1000

Chalmers Reproservice  
Göteborg, Sweden 2015

Thorium Fuels for Light Water Reactors  
Steps towards commercialization  
Thesis for the degree of Doctor of Philosophy in Applied Physics  
KLARA INSULANDER BJÖRK  
Department of Applied Physics  
Division of Nuclear Engineering  
Chalmers University of Technology

## ABSTRACT

Thorium-containing nuclear fuel is proposed as a means of gaining a number of benefits in the operation of light water reactors, some related to the nuclear properties of thorium and some related to the material properties of thorium dioxide. This thesis aims to investigate some of these benefits and to widen the knowledge base on thorium fuel behaviour, in order to pave the way for its commercial use.

Part of the work is dedicated to finding ways of utilizing thorium in currently operating light water reactors which are beneficial to the reactor operator from a neutronic point of view. The effects of adding different fissile components to the fertile thorium matrix are compared, and the neutronic properties of the preferred alternative (plutonium) are more closely investigated. The possibility to use thorium as a minor component in conventional uranium dioxide fuel is also subject to study.

Another part of the work is related to the thermal-mechanical behaviour of thorium-containing nuclear fuel under irradiation. To assess this behaviour, an irradiation experiment has been designed and is ongoing in the Halden research reactor. Existing software for prediction of thermal-mechanical fuel behaviour has been modified for application to mixed thorium and plutonium oxide fuel, and the preliminary simulation output is compared with irradiation data.

The conclusion of the research conducted for this thesis is that the adoption of thorium-containing fuel in light water reactors is indeed technically feasible and could also be attractive to reactor operators in a number of different aspects. Some steps have been taken towards a more complete knowledge of the behaviour of such fuel and therewith towards its commercial use.

Keywords: Thorium, plutonium, light water reactors, neutronic simulations, Halden research reactor, fuel performance



*To my father, a firm believer in the saving of humankind through technical development.*



## PREFACE

This thesis is the result of work performed within the framework of an industrial PhD program. I am employed by the company Thor Energy, based in Oslo, Norway, and the research subjects have been chosen to fit the research needs of Thor Energy. For this reason, a commercial focus has been held throughout the work, meaning that primarily aspects of interest to commercial actors in the nuclear field have been studied. The industrial context has also had the consequence that some of the work performed has been documented in the form of patent applications instead of academic journal articles. The groundwork forming the basis for one of the two patent applications is presented herein.

As a part of the research and development strategy of a commercial company, the work presented herein does not have the character of a single well-defined project, but rather a part, limited in time and scope, of a large and long-term research undertaking. For example, the irradiation experiment which has formed a large part of the work performed during the PhD project is at the time of writing still ongoing, and work to expand its scope is in progress. The results presented herein are thus only the first parts of the more comprehensive data set that will ultimately be generated.

There is currently considerable interest for thorium as a nuclear fuel also from parties not directly involved in the field of nuclear technology, and misperceptions are common. For this reason, the thesis begins with an introduction to thorium as a nuclear fuel, aimed towards explaining the basics of the thorium fuel cycle and relating it to comparable uranium utilization schemes.

It is my hope as the author of this thesis that it will be readable and interesting not only within academia but also to readers within the energy industry.

*Klara Insulander Björk,  
Göteborg 2015.04.07*



## LIST OF PUBLICATIONS

- Paper I** K. Insulander Björk, V. Fhager, and C. Demazière (2011). Comparison of thorium-based fuels with different fissile components in existing boiling water reactors. *Progress in Nuclear Energy* **53**, 618–625  
*The present author performed all simulations and the main part of the analysis and wrote the manuscript.*
- Paper II** K. Insulander Björk, S. Mittag, R. Nabbi, A. Rineiski, O. Schitthelm, and B. Vezzoni (2013a). Irradiation of a Thorium-Plutonium rodlet: Experiment and benchmark calculations. *Progress in Nuclear Energy* **66**, 73–79  
*The present author performed one out of four reported benchmark simulations, participated in the analysis of the results and wrote the manuscript.*
- Paper III** K. Insulander Björk and V. Fhager (2009). “Comparison of Thorium-Plutonium fuel and MOX fuel for PWRs”. *Proceedings of Global 2009*. September 6-11. Paris, France  
*The present author performed all simulations and the main part of the analysis and wrote the manuscript.*
- Paper IV** K. Insulander Björk, C. W. Lau, H. Nylén, and U. Sandberg (2013b). Study of Thorium-Plutonium Fuel for Possible Operating Cycle Extension in PWRs. *Science and Technology of Nuclear Installations* **2013**. Paper 867561  
*The present author performed the lattice simulations, participated in the data analysis and wrote the manuscript.*
- Paper V** K. Insulander Björk (2013). A BWR fuel assembly design for efficient use of plutonium in thorium-plutonium fuel. *Progress in Nuclear Energy* **65**, 56–63  
*The present author performed all simulations and analysis and wrote the manuscript.*

K. Insulander Björk, S. S. Drera, J. F. Kelly, C. Vitanza, C. Helsengreen, T. Tverberg, M. Sobieska, B. C. Oberländer, H. Tuomisto, L. Kekkonen, J. Wright, U. Bergmann, and D. P. Mathers (2015). Commercial thorium fuel manufacture and irradiation: Testing (Th,Pu)O<sub>2</sub> and (Th,U)O<sub>2</sub> in the “Seven-Thirty” program. *Annals of Nuclear Energy* **75**, 79–86

**Paper VI**

*The present author wrote the manuscript and is the manager of the described research program, a task which has comprised choosing and procuring materials for irradiation and deciding on instrumentation and irradiation conditions together with the co-authors associated with IFE. The author has also organized meetings collecting advice on the conduction of the research program from the co-authors associated with the collaboration partners Fortum, Westinghouse and NNL, and participated in the analysis of the irradiation data.*

K. Insulander Björk and P. Fredriksson (2014). “Development of a fuel performance code for thorium-plutonium fuel”. *Proceedings of PHYSOR 2014*. September 28 - October 3. Kyoto, Japan

**Paper VII**

*The present author performed all thermal-mechanical modeling and programming, supervised the student performing the neutronic modeling and programming and wrote the manuscript.*

K. Insulander Björk and L. Kekkonen (2015). Thermal-mechanical performance modelling of thorium-plutonium oxide fuel and comparison with experimental data. Submitted to *Journal of Nuclear Materials*

**Paper VIII**

*The present author performed all simulations and programming, participated in the experiment data analysis and wrote the manuscript.*

### Other publications related to this thesis:

K. Insulander Björk, V. Fhager, and C. Demazière (2009a). “Method for investigating the applicability of thorium-based fuels in existing BWRs”. *Proceedings of ICAPP '09*. May 10-14. Tokyo, Japan

K. Insulander Björk, V. Fhager, and C. Demazière (2009b). “Comparison of thorium-based fuels with different fissile components in existing BWRs”. *Proceedings of ICAPP '09*. May 10-14. Tokyo, Japan

K. Insulander Björk, V. Fhager, and C. Demazière (2009c). “Comparison of thorium-based fuels with different fissile components in existing boiling water reactors”. *Proceedings of Advances in Nuclear Fuel Management (ANFM) IV*. April 12-15. Hilton Head Island, South Carolina, USA

O. Schitthelm, R. Nabbi, B. Vezzoni, A. Rineiski, S. Mittag, and K. Insulander Björk (2011). *A thorium-plutonium pin benchmark based on the experimental results from the KWO irradiation*. Tech. rep. LWR-DEPUTY D11. Forschungszentrum Jülich

K. Insulander Björk (2012). “Thorium-plutonium fuel for long operating cycles in PWRs - preliminary calculations”. *Proceedings of the SAIMM conference on Thorium and Rare Earths*. February 21-22. Cape Town, South Africa

K. Insulander Björk and S. Helmersson (Oct. 30, 2013). “A fuel assembly for a nuclear reactor”. Patent application filed by the European Patent Organization.

C. W. Lau, H. Nylén, K. Insulander Björk, and U. Sandberg (2014a). Feasibility Study of 1/3 Thorium-Plutonium Mixed Oxide Core. *Science and Technology of Nuclear Installations* **2014**. Paper 709415

C. W. Lau, V. Dykin, H. Nylén, K. Insulander Björk, and U. Sandberg (2014b). Conceptual study on Axial Offset Fluctuations by Stepwise Power Changes in a Thorium-Plutonium Core to Improve Load-Following Conditions. *Annals of Nuclear Energy* **72**, 84–89

K. Insulander Björk and Ø. Asphjell (Oct. 17, 2014). “Fuel assembly for a nuclear power boiling water reactor”. Patent application filed by the European Patent Organization.

S. S. Drera, J. F. Kelly, Ø. Asphjell, and K. Insulander Björk (2014a). “Overview of the Thor Energy thorium fuel development program”. *ANS Winter Meeting and Nuclear Technology Expo 2014*. November 9-13. Anaheim, California, USA

S. S. Drera, H. Feinroth, J. F. Kelly, and K. Insulander Björk (2014b). “Development of LWR fuels utilizing thorium dioxide in conjunction with both zirconium-based and SiC cladding”. *ANS Winter Meeting and Nuclear Technology Expo 2014*. November 9-13. Anaheim, California, USA

S. S. Drera, J. F. Kelly, Ø. Asphjell, K. Insulander Björk, M. Sobieska, and B. C. Oberländer (2014c). “Ceria-thoria materials testing and pellet manufacturing in preparation for thoria-plutonia Th-MOX LWR fuel production”. *2014 Water Reactor Fuel Performance Meeting / Top Fuel / LWR fuel performance meeting*. September 14-17. Sendai, Japan

S. S. Drera, J. F. Kelly, Ø. Asphjell, K. Insulander Björk, M. Sobieska, and B. C. Oberländer (2015). Ceria-thoria pellet manufacturing in preparation for plutonia-thoria LWR fuel production. Submitted to Nuclear Technology

# CONTENTS

<b>Abstract</b>	<b>v</b>
<b>Preface</b>	<b>ix</b>
<b>List of Publications</b>	<b>xi</b>
<b>Contents</b>	<b>xv</b>
<b>Nomenclature</b>	<b>xviii</b>
<b>I EXTENDED SUMMARY</b>	<b>1</b>
<b>1 Introduction</b>	<b>2</b>
1.1 Objective and limitations . . . . .	2
1.2 Outline of this thesis . . . . .	3
<b>2 Thorium as a Nuclear Fuel - Background</b>	<b>4</b>
2.1 History of thorium fuels . . . . .	4
2.2 Basic nuclear reactions . . . . .	5
2.2.1 Fissile components . . . . .	6
2.2.2 Reaction products . . . . .	7
2.3 Fuel cycles and reactor types . . . . .	7
2.3.1 Reactor types . . . . .	8
2.3.2 Spent nuclear fuel handling . . . . .	9
2.4 Safety and security aspects . . . . .	10
2.4.1 Safe reactor operation . . . . .	11
2.4.2 Radiotoxicity issues . . . . .	11

2.4.3	Proliferation concerns . . . . .	12
2.5	Material properties . . . . .	12
2.6	Commercial viability of thorium fuel . . . . .	13
2.7	Research needs . . . . .	14
<b>3</b>	<b>Choice of Fuel Types</b>	<b>16</b>
3.1	Comparison of fissile components - Paper I . . . . .	16
3.1.1	Results . . . . .	17
3.1.2	Conclusions . . . . .	19
3.2	Thorium as an additive to uranium fuel . . . . .	21
3.2.1	Assembly design with thorium additive . . . . .	22
3.2.2	Neutronic properties of the Th-Add BWR fuel . . . . .	23
<b>4</b>	<b>Neutronic Properties of Thorium-Plutonium Fuel</b>	<b>26</b>
4.1	Th-MOX modelling with CASMO-5 . . . . .	26
4.1.1	CASMO-5 . . . . .	27
4.1.2	Cross section libraries . . . . .	29
4.1.3	Benchmark based on irradiated Th-MOX rodlet - Paper II . . . . .	29
4.2	Th-MOX fuel in PWRs . . . . .	32
4.2.1	Lattice simulations - Paper III . . . . .	32
4.2.2	Full core simulations - Paper IV . . . . .	35
4.3	BWR fuel assembly design for efficient use of plutonium - Paper V . . . . .	37
<b>5</b>	<b>Thermal-Mechanical Properties of Thorium Fuel Materials</b>	<b>41</b>
5.1	Instrumented irradiation experiment . . . . .	41
5.1.1	Rig IFA-730 in the Halden research reactor - Paper VI . . . . .	42
5.1.2	Results of the irradiation . . . . .	45
5.2	Fuel performance modelling and benchmarking . . . . .	48

5.2.1	FRAPCON 3.4 . . . . .	49
5.2.2	Material properties . . . . .	50
5.2.3	Fission gas release . . . . .	51
5.2.4	Radial power profiles - Paper VII . . . . .	52
5.2.5	Comparison with irradiation data - Paper VIII . . . . .	54
<b>6</b>	<b>Summary and Future Work</b>	<b>57</b>
6.1	Summary . . . . .	57
6.1.1	Choice of fuel types . . . . .	57
6.1.2	Neutronic properties of Th-MOX fuel . . . . .	58
6.1.3	Thermal-mechanical properties of thorium fuel materials . . . . .	59
6.1.4	Conclusion . . . . .	59
6.2	Future work . . . . .	60
	<b>Acknowledgements</b>	<b>61</b>
	<b>References</b>	<b>61</b>
<b>II</b>	<b>APPENDED PAPERS I–VIII</b>	<b>69</b>

# NOMENCLATURE

## ABBREVIATIONS

2RPu	Twice recycled plutonium
ABWR	Advanced boiling water reactor
AmPu	RGPu with an ingrowth of americium
BOL	Beginning of life
BWR	Boiling water reactor
CERN	European Center for Nuclear Research
DPC	Doppler power coefficient
EOL	End of life
FGR	Fission gas release
FTC	Fuel temperature (Doppler) coefficient
H/HM ratio	Hydrogen-to-heavy metal ratio
HCS	Hot-to-cold reactivity swing
HEU	High enriched uranium
IFBA	Integral fuel burnable absorber
IFE	The Norwegian Institute for Energy Technology
ITC	Isothermal temperature coefficient
JRC-ITU	Joint Research Center - Institute for Transuranium Elements
LEU	Low enriched uranium
LHGR	Linear heat generation rate
LWR	Light water reactor
MA	Minor actinides
MTC	Moderator temperature coefficient
MWd/kgHM	Mega-Watt days per kilogram of heavy metal (unit of burnup)
NatU	Natural uranium
PIE	Post-irradiation examination
PWR	Pressurised water reactor
RGPu	Reactor grade plutonium
TD	Theoretical density
Th-MOX	Mixed thorium and plutonium oxides
TMOL	Thermal-mechanical operating limit
U-MOX	Mixed uranium and plutonium oxides
UOX	Uranium oxide
USNRC	United States Nuclear Regulatory Commission
VC	Void coefficient
WGPu	Weapon's grade plutonium

## OTHER NOTATION

$\beta_{\text{eff}}$	Effective delayed neutron fraction
$\eta$	Average number of neutrons released per neutron absorbed in the isotope
$T_C$	Fuel centerline temperature
$k_\infty$	Infinite multiplication factor

## GLOSSARY

<i>actinide</i>	Element with atomic number 89–103, e.g. thorium, uranium and plutonium
<i>closed fuel cycle</i>	Fuel cycle in which a major part of the spent fuel is recycled
<i>cross section</i>	Measure of the probability of interaction
<i>epithermal neutron</i>	Neutron with an energy intermediate between <i>fast</i> and <i>thermal</i>
<i>fast neutron</i>	Neutron with an energy in the order of MeV
<i>fertile</i>	Can be converted to a fissile isotope upon absorption of a neutron
<i>fissile</i>	Can undergo fission upon absorption of a thermal neutron
<i>moderator</i>	Medium that slows down neutrons from fast to thermal energies
<i>neutronic</i>	Related to neutron-induced nuclear reactions
<i>open fuel cycle</i>	Fuel cycle where a minor or no part of the fuel is recycled
<i>thermal neutron</i>	Neutron with an energy of about 0.025 eV



# Part I

## EXTENDED SUMMARY

---

---

# CHAPTER 1

---

## INTRODUCTION

*This chapter describes the objectives and limitations of the work described in this thesis and outlines the contents of the following chapters.*

### 1.1 Objective and limitations

Thorium based nuclear fuel has been subject to much research and a wide range of applications have been proposed. This thesis focuses on thorium based fuel for Light Water Reactors (LWRs), and in particular on two specific thorium oxide containing fuel types. In this context, Boiling Water Reactors (BWRs) and Pressurised Water Reactors (PWRs) are included in the notion of LWRs. The objective of this work is to identify and investigate some of the most important areas where more research is needed for thorium fuel to be considered as an attractive alternative for LWR operators and for the fuel to be licensable for use within the current nuclear regulatory framework. The goal of these investigations is to take some of the steps remaining before thorium based nuclear fuels can be commercially used in LWRs.

Even though the scope has been narrowed down to two fuel types in two closely related reactor types, several aspects will have to be left out of the current work. This thesis focuses on the area of most direct relevance to a reactor operator - the behaviour of the fuel during reactor operation. The first step in the value chain, i.e. thorium mining and thorium oxide powder production, is not investigated here. The subject of

fuel manufacture is very briefly touched upon, since it is a necessary part of realising an experiment where the thermal-mechanical behaviour is assessed. The properties of spent thorium based fuel, in terms of its isotopic content, are also touched upon, but the direct consequences for preliminary storage in spent fuel pools are not evaluated and final storage of all or parts of the spent fuel is only synoptically discussed. Chemical properties and possible reprocessing methods for thorium based fuel are not part of this work.

## 1.2 Outline of this thesis

The thesis commences with an introduction to thorium as a nuclear fuel, putting it into the context of nuclear fuel cycles. This chapter is written for a reader not familiar with nuclear technology, although some basic knowledge of physical concepts is required. The purpose is to motivate the choice of subject for this work, i.e. to explain why thorium fuel is relevant, and why it is worthwhile to investigate its behaviour in LWRs.

The remaining chapters will demand a certain level of familiarity with nuclear technology from the reader. Chapter 3 describes how the research area was narrowed down to two specific fuel types by scoping studies of the neutronic properties of a number of alternatives. The detailed investigation of the operational behaviour of the chosen fuel types is then presented in the following chapters. The operational behaviour of the fuel can be subdivided into two closely interrelated categories – The *neutronic* behaviour, related to the neutron-induced nuclear reactions taking place inside the reactor and the *thermal-mechanical* performance, i.e. how material properties like thermal expansion and conductivity interact to determine parameters such as the temperature and dimensional changes of the fuel.

Chapter 4 focuses on the neutronic behaviour. One particular area which is pointed out as important for licensing of any fuel type is that its neutronic behaviour can be accurately modeled by dedicated software. An attempt at validation of a particular computer code for neutronic modelling of thorium fuel is described, and the detailed properties of the fuel are then investigated using this software. The thermal-mechanical performance is discussed in Chapter 5. This behaviour has to be assessed experimentally and an experiment designed for this purpose is described. Also some results of this experiment are presented, including a comparison with theoretical predictions. Finally, the work is summarised in Chapter 6 and some future work, both ongoing and proposed, is outlined.

---

---

# CHAPTER 2

---

## THORIUM AS A NUCLEAR FUEL - BACKGROUND

*This chapter gives an introduction to the nuclear fuel cycle, and in particular to thorium as a nuclear fuel, based on open literature. The intention is to provide a background for a reader not familiar with nuclear technology.*

### 2.1 History of thorium fuels

The history of thorium use for nuclear applications is almost as old as that of uranium. The possibility to convert thorium into fissile material, from which energy can be extracted, was discovered in 1941, and it was proposed that this should be utilized in the development of nuclear weapons. The relative simplicity and maturity of uranium-based technologies however made thorium a less attractive alternative (Seaborg 1976, 1977, 1978, 1979, 1980). When nuclear development later turned towards more peaceful purposes, research on the use of thorium based nuclear fuels was carried out in parallel with that on uranium, although with less intensity. The main reason for favouring the uranium based alternatives was, at that time, the fact that the still not fully developed breeder reactor concept<sup>1</sup> seemed to favour the use of a uranium based nuclear fuel cycle (Moir and Teller 2005),

---

<sup>1</sup>Breeder reactors can be described as reactors which produce their own fuel, enabling a closed fuel cycle where spent fuel is reprocessed and the main part of it is re-inserted into the reactor.

see also Section 2.3.1. The use of non-breeding reactors was at that time regarded as a transition phase towards the more sustainable era of breeder reactors. Nevertheless, the feasibility of using thorium based fuel was demonstrated in several research programs (Baumer and Kalinowski 1991; Gottaut and Krüger 1990; Haubenreich and Engel 1970; Price 2012; Walker 1978), most notably in the Shippingport reactor in the USA, where breeding was demonstrated in an LWR under very specifically tailored conditions (Clayton 1993).

Since the seventies, the main rationale for research into thorium based fuel has been to provide an alternative to uranium based fuel, would the uranium resources ever become depleted (Onufriev 1987). Consequently, the intensity of the related research has to some extent followed the uranium price. India has been an exception to this trend because the country has large thorium reserves and limited access to imported uranium<sup>2</sup>. For this reason, thorium has formed an important part of India's nuclear program since 1958 (Bucher 2009). The latest surge in thorium fuel research occurred in connection with the rapid increase in the uranium price in 2007.

At this time, several decades have gone by without the projected transition to large scale deployment of breeder reactors. The primary reasons for this delay have been that new uranium findings have reduced anxiety that these resources would become depleted in the near future, and that breeder reactors are not economical to operate at their current state of development and today's relatively low uranium prices. Meanwhile, non-breeding LWRs have become the dominating reactor type, providing almost 90% of the world's nuclear electricity generating capacity (World Nuclear Association 2015a). In this context, thorium fuel research is increasingly becoming directed towards LWR applications, and to some extent towards heavy water reactor applications in countries where this reactor type is more common (Dekoussar et al. 2005).

Although the uranium resources may be very large, it is recognized that the thorium content of the earth's crust is about three times larger, reflecting its longer half-life. In the long term, this means that the thorium resources can expand the nuclear fuel resource base significantly. Due to the low demand for thorium, no mining activities are being directed towards retrieval of thorium today, but it often occurs as a by-product of rare earth element mining. As a result, large thorium stockpiles are available over ground today. Only the US thorium stockpile of about 1500 metric tonnes (Hedrick 2004) would suffice for roughly 60 years of reactor operation using thorium based fuel.

## 2.2 Basic nuclear reactions

Naturally occurring thorium has only one isotope, Th-232. This isotope is not *fissile*, meaning that a thermal neutron can not induce fission of a Th-232 nucleus. The probability of different nuclear reactions are quantified in terms of their *cross section*, which depends

---

<sup>2</sup>India has not signed the nuclear Non-Proliferation Treaty, for which reason uranium trading with India has been restricted. An agreement was however reached in 2008, loosening the restrictions.

on which reaction is considered, which nucleus is involved and on the energy of the incoming neutrons<sup>3</sup>. Thus, the fission cross section of Th-232 is very low in thermal reactors such as LWRs, where the neutrons are predominantly thermal.

The nuclear fission is the primary reaction by which energy is released in a nuclear reactor. It is thus not possible to generate energy directly from thorium in a thermal reactor, but it has first to be converted to a fissile isotope. Such conversion takes place when a thorium nucleus captures a neutron, a reaction which has a comparatively high cross section in a thermal reactor. Nuclei, such as Th-232, which are convertible into fissile nuclei are called *fertile*. The fissile isotope formed from Th-232 is U-233<sup>4</sup>. This isotope is not only fissile, but has also a high neutron yield per neutron absorbed (a parameter commonly denoted  $\eta$ ) compared with other fissile isotopes.

### 2.2.1 Fissile components

The neutrons required for conversion to take place must be made available, and the most practical way to do this is to place the thorium in a nuclear reactor where neutrons are produced by fission reactions. This, of course, demands that not only thorium but also some fissile isotopes are present in the reactor. In the context of LWRs, the practical way to introduce these fissile isotopes is to include them in the fuel by mixing them with the thorium itself or by concentrating them in so-called seed zones, whereas the zones where the thorium resides are referred to as blanket zones. The number of fissile nuclei relative to the fertile nuclei must be high enough to sustain a fission chain reaction, i.e. that the number of neutrons generated by fission is equal to the number of neutrons being consumed, primarily by inducing fission in fissile nuclei or being captured by fertile nuclei.

In practice, there are only a few alternatives available for these fissile nuclei.

One alternative is U-235. Since natural uranium only contains 0.71% of the fissile isotope U-235 (the rest being fertile U-238), natural uranium has to be enriched in U-235 in order to provide sufficient fissile material for both maintaining a fission chain reaction and providing extra neutrons for the conversion of Th-232 into U-233.

Another alternative is to use plutonium. Plutonium does not occur naturally, but can be recovered from spent uranium-based nuclear fuel, where various plutonium isotopes are formed as a result of neutron captures in U-238. One neutron capture in U-238 leads to the formation of Pu-239<sup>5</sup>, and consecutive neutron captures lead to formation of the higher plutonium isotopes Pu-240, Pu-241 and Pu-242. Also some Pu-238 is formed from a chain of neutron captures in U-235. Of these isotopes only Pu-239 and Pu-241 are fissile. However, isotopic separation of plutonium is not practiced, so these isotopes always occur together, although in different proportions, depending on the origin of the plutonium.

---

<sup>3</sup>The term is also used for other reactions than those induced by neutrons.

<sup>4</sup>This reaction goes via the intermediate isotopes Th-233 and Pa-233.

<sup>5</sup>This reaction goes via the intermediate isotopes U-239 and Np-239.

The third alternative is to use U-233, which may be obtained from reprocessing of spent thorium fuel. Since there is no use and reprocessing of thorium on an industrial scale, this option is currently not available except for laboratory or pilot scale operations.

Thorium, uranium and plutonium, together with a number of other heavy elements, are collectively called *actinides*, referring to their placement in the periodic table.

## 2.2.2 Reaction products

An often mentioned advantage of thorium fuels is the low amounts of long-lived nuclear waste formed during its irradiation. The reason for this is that the most long-lived and strongly radiotoxic isotopes, mainly plutonium, americium and curium, are formed in very low quantities, due to the long series of low cross section neutron captures required to form these heavy actinides from Th-232. This can be compared with the relatively few steps required to form these elements when the mother isotope is U-238. However, some other undesirable isotopes are formed, most importantly U-232, which will be further discussed in Section 2.4.

For a fuel cycle based exclusively on thorium and its fissile daughter product U-233, the radiotoxic inventory of the actinide waste to be disposed of is about a tenth of that pertaining to the closed uranium-plutonium fuel cycle, for the first 10 000 years after disposal (Gruppelaar and Schapira 2000). However, when a fissile component such as plutonium or enriched uranium is needed the matter is much more complicated, since neutron captures in these materials produce the aforementioned heavy actinides.

In addition to the actinides, the spent nuclear fuel also contains the fission products, i.e. the nuclei resulting from fission reactions. The fissioning nucleus generally splits in two fragments, each with an atomic weight approximately half that of the original nucleus<sup>6</sup>. The set of fission products is similar but not identical for different fissile nuclei. The fission products are often highly radioactive and are responsible for the main part of the waste radiotoxicity for the first few hundred years.

## 2.3 Fuel cycles and reactor types

The practical relevance of the above described nuclear reactions does not become apparent until it is put into a context - a nuclear fuel cycle. The description of a nuclear fuel cycle involves, of course, the nuclear fuel itself, the reactor in which it is used and also the scheme deployed to handle the spent nuclear fuel.

---

<sup>6</sup>In fact, the fission products very rarely have a mass exactly half that of the fissioning nucleus, but rather slightly above or below, i.e. about 100 or 140 u.

### 2.3.1 Reactor types

The most basic classification of nuclear reactors refers to the typical energy of the neutrons causing the fission reactions, which broadly divides reactor types into two classes: *Thermal* reactors, in which the neutrons inducing fission typically have relatively low energies (around 0.025 eV) and *fast* reactors, in which the neutrons have high energies (around 1 MeV). These classifications of neutron energies are somewhat arbitrary, but the numbers give an impression of the orders of magnitude. As noted above, the cross section of a nuclear reaction, such as fission or capture, depends on the energy of the neutron inducing it, which makes these two reactor types fundamentally different. However, there is of course a continuum of neutron energy spectra between the two extremes and reactors can also operate with intermediate neutron energy spectra, often referred to as *epithermal*. The energy dependence of the cross sections is different for different nuclei, which is the most fundamental reason for thorium based fuel being different to uranium based fuel.

There are several ways of constructing a thermal reactor but the thermal LWR fuelled with enriched uranium dominates the world of nuclear power production, accounting for 88% of the total capacity. The perhaps most important reason for this dominance is that ordinary water serves excellently both as a coolant, transporting the generated energy from the fuel to ordinary steam turbines, and a neutron *moderator*, slowing down the fast neutrons produced by a fission reaction to thermal energies<sup>7</sup>. This reactor type has the advantage of being comparatively cheap, well proven and relatively easy to operate, and, with the prevailing operation schemes, the disadvantage of using less than one percent of the energy stored in the fuel, leaving large volumes of radioactive waste to be handled.

By allowing the water to boil intensively, its density and thereby its neutron moderating effect can be reduced so that an epithermal spectrum is achieved, which opens a possibility for more efficient fuel usage, especially with thorium fuel. This can not be directly implemented in currently operating LWRs, but given the similarities, a reduced moderation core may be retrofitted into a sufficiently modern LWR such as the Advanced Boiling Water Reactor (ABWR) (Uchikawa et al. 2007).

Fast reactors are devised to make significantly better use of their fuel than thermal reactors do, an improvement mostly attributed to the fact that  $\eta$  is higher for fissions induced by fast neutrons, rendering an excess number of neutrons for conversion of fertile isotopes to fissile. Fast reactors can generally be designed to be breeder reactors creating more fissile material than they consume, i.e. the production of fissile material from fertile is high enough to compensate for the loss of fissile material through fission. An additional feature of fast neutrons is that they can induce fission not only in thermally fissile nuclei, but also in the heavier actinides, reducing the radiological problem that the production of these isotopes constitutes.

In principle, all reactor types may be fuelled with thorium, but some are more suited to thorium fuel than others. A “thorium reactor”, as is sometimes discussed, is thus

---

<sup>7</sup>Heavy water serves the same purpose in heavy water reactors, which stand for another 6.5% of the world’s nuclear power production.

not a well-defined concept. It should however be pointed out that U-233 has a high  $\eta$  value in the epithermal spectrum, compared with U-235 and Pu-239, making thorium an advantageous fuel for the reduced moderation epithermal LWRs. This option has been investigated by several researchers (Kim and Downar 2002; Lindley et al. 2014; Shaposhnik et al. 2013), concluding that breeding can indeed be achieved.

The reactor types most commonly referred to as “thorium reactors” are molten salt reactors and accelerator driven systems. Thorium fuelled molten salt reactors have been investigated both in theory (e.g. (Heuer et al. 2014)) and practice (Haubenreich and Engel 1970) and have received much recent attention in China where in 2011 a very large research program was launched, aiming to develop a thorium fuelled molten salt reactor for commercial power production starting in 2032 (World Nuclear Association 2015b). Thorium fuelled accelerator driven systems gained much attention in the 1990’s due to Nobel laureate Carlo Rubbia’s embracement of the concept and development of the so-called “Energy Amplifier” (Rubbia et al. 1995). Both concepts are promising in that they may provide a means of generating energy from the abundant thorium resources while simultaneously incinerating the long-lived radiotoxic waste generated by today’s nuclear reactors. The two concepts can even be combined into an economical and safe system for nuclear waste reduction (Salvatores et al. 2001). The drawback of these technologies is that they are still comparatively immature and much research and development work remains until they are ready for deployment, as indicated by e.g. the projected (and probably quite optimistically so) commercialization time for the Chinese project.

### 2.3.2 Spent nuclear fuel handling

There are two major strategies for the handling of spent nuclear fuel and different strategies are adopted by different countries. The one adopted in Sweden and some other countries is direct disposal, i.e. the spent nuclear fuel (with over 99% of its potentially recoverable energy remaining) is disposed of, preferably in deep geological repositories, where it must remain separated from the biosphere for several hundreds of thousands of years. The other approach is reprocessing, which involves separating the constituents of the spent fuel, making use of some of them.

Despite the obvious drawbacks of the direct disposal option, reprocessing is not very widely practiced. This is partly due to the high costs connected with reprocessing activities and the manufacture of new fuel from their products, and partly to the perception that separation of material which is to some extent fissile (such as plutonium with its main fissile isotope Pu-239) constitutes a nuclear weapon proliferation risk. However, reprocessing is a necessary tool for improving fuel utilization. Irrespective of which reactor type is used, the fuel will degrade with burnup and will need to be reprocessed if the majority of the fissile isotopes produced are to come to use.

About 3% of the spent LWR fuel consists of fission products. These are often

radioactive, with mostly relatively short half-lives compared with the actinides<sup>8</sup>, and need to be disposed of. The rest of the spent fuel is made up of actinides, which may be re-used in nuclear fuel. Most of the actinide content is just the original fertile isotopes (U-238 or Th-232), which have not undergone any nuclear reaction. In addition, there are the new isotopes generated by neutron captures. These are e.g. U-233 or Pu-239 which may readily be re-used for nuclear fuel manufacture, but especially in the case of uranium based fuel, there are also small quantities of heavier actinides.

Reprocessing of uranium fuel is an established process which is being widely practiced in e.g. France, where the separated plutonium is mixed with natural uranium and re-used in so-called mixed oxide fuel<sup>9</sup>, enabling uranium savings of up to 30%. Reprocessing of thorium based fuel has never been practiced on an industrial scale. A process for thorium based fuel recycling, THOREX, was devised already in the 1960's, and continued development is ongoing in India (Das and Bharadwaj 2013). The reprocessing of thorium based oxide fuel (which is the most commonly used chemical form of fuel material) is more difficult than that of uranium fuel, due to the fact that thorium dioxide is relatively chemically inert and hence difficult to dissolve.

Whereas reprocessing is optional in the current fuel management scheme, it is crucial for a breeding cycle to make sense, since it is required in order to make use of the produced fissile isotopes. A fuel cycle including reactors which produce enough fissile material to be self-sustaining and reprocessing of the spent fuel with recycling of the major part of the spent fuel is referred to as a *closed fuel cycle*. For the case of the uranium based fuel cycle, despite many decades of research, there are some unresolved technical issues with manufacturing and using fuel containing the complete set of actinides produced in this cycle. There are conceptual designs of closed fuel cycle systems in which all actinides are recycled, but they are still under development, see e.g. Somers (2011); Ikeda et al. (2014).

It is thus clear that a breeding reactor combined with reprocessing is required in order to achieve the closed, self-sustaining, low-waste producing thorium fuel cycle which is often referred to by thorium proponents. Although the technology to reprocess thorium based fuel is still immature, it is ultimately possible to establish.

## 2.4 Safety and security aspects

In addition to the central aspects of the nuclear fuel cycle - reactors and reprocessing - there are additional aspects that need to be discussed, related to safety and security concerns connected with nuclear activities.

---

<sup>8</sup>There are some long-lived exceptions to this, with the consequence that the radioactivity of the fission products as a collective decreases very rapidly for the first few hundred years and then settles at a low level, remaining there for a few million years.

<sup>9</sup>The term U-MOX will be used in this work to distinguish mixed uranium and plutonium oxides from mixed thorium and plutonium oxides (Th-MOX)

### 2.4.1 Safe reactor operation

The specific nuclear properties of the isotopes central to the thorium cycle, U-233 and Th-232, makes the fuel different from uranium based fuel in terms of reactor operation. Most importantly, the differences affect how the reactor responds to changes in operation conditions, i.e. the dynamic characteristics of the reactor. This directly affects the possibilities to safely operate a thorium fuelled reactor.

The dynamic characteristics are often described in terms of reactivity coefficients, i.e. how the reactivity changes when a certain parameter such as the fuel temperatures changes. The efficiency of the different mechanisms used to control the reactor, such as control rods, are also affected by the nuclear properties of the fuel. How the reactivity coefficients and the control mechanism efficiency change when thorium fuel is introduced depends strongly on which fissile component is used.

Another important aspect for reactor safety is the delayed neutron fraction, i.e. the fraction of the total number of neutrons emitted with some delay after the fission event. This parameter determines how rapidly the reactor responds to changes in operational conditions. It depends on which isotope is fissioning, and is lower for U-233 than for U-235 and Pu-239, meaning that a reactor in which U-233 is the predominant isotope responds more rapidly and is hence more difficult to control. The importance of this of course depends on how much U-233 is actually present in the core.

All of these aspects are much more thoroughly discussed in Chapters 3 and 4.

### 2.4.2 Radiotoxicity issues

One safety related topic has already been touched upon: The radiotoxicity of the materials to be handled. One part of this problem is the final waste to be disposed of. In the case of a closed fuel cycle, this waste consists of fission products and some actinides which inevitably are lost to the waste stream during reprocessing. The losses are usually of the order of 0.1 - 1%. The fission products dominate the waste radiotoxicity for the first few hundred years, after which the actinides take over as the major component. As stated earlier, thorium has an advantage of an order of magnitude lower radiotoxicity of the actinide waste up to about 10 000 years (Gruppelaar and Schapira 2000). However, it is important to note that thorium based fuel adds a complication to reprocessing and manufacture of fuel from reprocessed material. The reason is that a small quantity of radioactive U-232 is produced during irradiation, whose decay chain results in emission of high-energetic  $\gamma$ -rays (in particular from Tl-208). This makes it necessary to deploy remote-controlled manufacture of recycled fuel, whereas glove-box handling is sufficient in the uranium case. This makes recycled thorium fuel manufacture more expensive.

For fuel cycles with no reprocessing, the radiotoxicity of (and heat production in) spent thorium fuel depends heavily on the fissile component. The addition of a fissile

component inevitably brings U-238 or heavier actinides into the fuel cycle<sup>10</sup>, meaning that long-lived radiotoxic isotopes are nevertheless produced in the fuel, although not primarily from the thorium itself.

In case of direct disposal of spent fuel, thorium oxide fuel also has an advantage due to its chemical inertness. This means that the thorium fuel matrix, which effectively encapsulates most of the fission products and heavy actinides, will remain intact for a longer time than a uranium matrix, even if groundwater would permeate to the fuel in the deep geological repository (Greeneche and Chhor 2012; Gruppelaar and Schapira 2000).

Irrespective of whether the fuel is reprocessed or taken to final disposal, the emission of high energy  $\gamma$ -radiation adds a complication to the handling of spent fuel already at the reactor site. Additional shielding will be needed already at fuel discharge and intermediate storage (Ade et al. 2014).

### 2.4.3 Proliferation concerns

Resistance to nuclear proliferation, i.e. the proliferation of nuclear weapon related materials and technology, is often mentioned as a possible advantage of the thorium fuel cycle. This perception comes mostly from the fact that no plutonium is produced. In fact, if plutonium is used as the fissile component of thorium fuel, the plutonium is efficiently destroyed, which will also be discussed further in Chapter 4. This method of plutonium incineration has been judged to offer non-proliferation benefits (Gruppelaar and Schapira 2000; Trellue et al. 2011).

Although no plutonium is produced from thorium, so is U-233, from which nuclear weapons can also be manufactured if the fuel is reprocessed. It can however be argued that this uranium is extremely difficult to use for bomb making due to its contamination with  $\gamma$ -ray producing U-232, and it has also been suggested to “denature” the U-233 by adding some U-238 to the thorium fuel. It would in principle be possible to obtain pure U-233 by separation of its precursor Pa-233. This is not practical for spent solid fuel, but in principle possible for molten salt reactors in which the liquid fuel is continuously reprocessed during reactor operation. Considering all these aspects, it can nevertheless be concluded that the thorium cycle causes slightly less proliferation concerns than the uranium cycle (Dekoussar et al. 2005; Pellaud 2013).

## 2.5 Material properties

Also the material properties of thorium distinguishes it from uranium. The chemical form of uranium predominantly used in nuclear fuels is uranium dioxide,  $\text{UO}_2$ , and it

---

<sup>10</sup>This can almost completely be avoided by using high-enriched uranium (Rose et al. 2011), which however adds significant concerns related to nuclear weapon proliferation and enrichment costs.

is assumed that thorium will be used in the same way, i.e. as thorium dioxide,  $\text{ThO}_2$ .  $\text{ThO}_2$  has some features which are beneficial for its use as a nuclear fuel. It has a much higher melting point compared with that of  $\text{UO}_2$ , a lower thermal expansion and a higher thermal conductivity. In particular the thermal conductivity is important, since it leads to a lower inner fuel temperature. The fuel temperature in turn drives many processes deteriorating the performance of the fuel. These properties are of course affected by the addition of the necessary fissile component (also assumed to be in oxide form) and will be more thoroughly discussed in Chapter 5. To a first approximation, though, these beneficial properties makes it reasonable to assume that  $\text{ThO}_2$ -based fuel should be able to operate at higher power levels and/or to a higher *burnup*, i.e. to a higher amount of energy released per unit mass of the fuel material.

## 2.6 Commercial viability of thorium fuel

With this background information on the historical, physical, technical, safety and security related aspects of thorium as a nuclear fuel, the utility of using it commercially can now be discussed.

It is clear that a long-term sustainable nuclear fuel cycle must involve breeding reactors and reprocessing of spent fuel. It seems plausible that a transition to such a cycle must eventually occur, although several decades of research on closed uranium based fuel cycles have not yet resulted in an economically competitive alternative. It can however be stated, based on the above, that thorium could potentially provide a faster and cheaper way to such a cycle, through deployment of the mentioned thorium fuelled reduced moderation LWRs. Due to the similarity to existing LWR technology, the transition to such systems would be evolutionary rather than revolutionary, moving gradually to higher conversion systems. In addition, such a fuel cycle would lead to lower production of radiotoxic waste compared with its uranium counterpart, provide some non-proliferation benefits and make use of an abundant resource.

From the economical perspective, it is clear that the establishment of a closed fuel cycle based on either thorium or uranium requires very large investment in both research and fuel cycle infrastructure. The question then becomes how to realise the first step in this evolutionary development, i.e. how thorium can offer economical advantages in the current reality of the nuclear industry, while simultaneously working towards the goal of a self sustaining thorium fuel cycle by gaining operational experience and also by generating U-233 for the next generations of thorium fuelled reactors.

As mentioned, thorium can be used in almost any reactor type, including existing LWRs. Given the dominance of LWRs in current nuclear power production and the potential for a transition to a breeding cycle using closely related technology, the development of thorium based fuel for LWRs makes sense both from the perspective of near-term commercial viability and eventual sustainability. Thus, the objective of the following chapters is to investigate the potential advantages of thorium fuel usage in currently operating LWRs.

## 2.7 Research needs

The United States Nuclear Regulatory Commission (USNRC) released a report in 2014 titled “Safety and Regulatory Issues of the Thorium Fuel Cycle” (Ade et al. 2014). The regulatory framework formulated and enforced by the USNRC is the reference framework in many countries, at least in the western world, and the regulatory framework in many countries is similar to that in the US. This report is thus a useful starting point for outlining the research needs.

The report states that the most likely near-term application of thorium in the US is in currently operating light water reactors. The report then outlines the research needs that are most important from a regulatory point of view. The related issues have been divided into six categories: Physical properties, nuclear data, fuel performance, reactor safety, front-end issues and back-end issues. The physical properties (thermal conductivity, melting point etc.) of thorium oxide and mixtures with uranium or plutonium oxides are partially known and research is ongoing, in particular at the Institute for Transuranium elements (ITU), see e.g. Cozzo et al. (2011), Vălu et al. (2014) and Böhler et al. (2015). The nuclear data relevant for thorium fuel cycles are generally known, although not with the same high level of confidence as the corresponding data related to the uranium fuel cycle. Measurement of nuclear data is a discipline of basic research generally undertaken by universities and research institutes with access to large and expensive machinery, and research is being carried out at e.g. CERN (Belloni et al. 2012). As previously noted, front- and back-end issues are not considered in this work.

In the field of fuel performance, the USNRC report states that “it is likely that fuel irradiation experiments would be needed to generate and validate fuel performance data and codes”. Such an irradiation experiment forms a major part of the current work. With respect to reactor safety, the report comprises a computational assessment of neutronic safety parameters, and concludes that “Further study should be initiated when realistic fuel design information becomes available” and that “Whole core analyses are required”. This work aims to find such realistic fuel design information, with the interpretation that a realistic fuel design is a design which is acceptable both from economic and safety perspectives. A whole core analysis is also performed. In addition, it is noted that these analyses must be carried out with validated software, an issue which is also addressed in this work.

Neutronic analysis of thorium based nuclear fuels in existing LWRs has indeed been carried out in several contexts. Most of these propose unconventional features, such as heterogeneous fuel assemblies with partly metallic fuel (Galperin et al. 2000), micro-heterogeneous fuel (Shwageraus et al. 2004a) or annular fuel (Caner and Dugan 2000). Many of these features are primarily intended to improve conversion of Th-232 to U-233, which is beneficial for the fuel economy but adds an aspect that could be considered challenging by both reactor operators and regulatory bodies. With the view to make the initial step of thorium fuel adoption as small as possible, the proposed solution should only entail replacement of uranium with thorium while not altering any other parameters.

Other proposed concepts are based completely or partly on U-233 as the fissile component (Baldova et al. 2014a,b; Rose et al. 2011), an alternative which is currently not available.

Quite a few researchers have simulated PWRs with homogeneous thorium oxide fuel with U-235 or Pu-239 as the fissile isotope (Ade et al. 2014; Arkhipov 2000; Gruppelaar and Schapira 2000; Herring et al. 2001; Puill 2002). The reports are basically similar in that they conclude that the introduction of thorium in current PWRs is indeed feasible, that thorium-plutonium mixed oxide fuel (Th-MOX) is similar to uranium-plutonium mixed oxide fuel (U-MOX) and that for unaltered reactor operation conditions, replacing some of the uranium with thorium does not lead to U-235 savings.

Only few studies have been made of thorium fuelled BWRs: Núñez-Carrera et al. (2008) studied thorium fuelled BWRs with a heterogeneous fuel assembly concept involving metallic fuel, and some similar studies have been published after the publication of the papers included in this thesis by Galahom et al. (2015). This imbalance is probably due to the relative dominance of PWRs over BWRs (273 PWRs and 81 BWRs were in operation in 2015 (World Nuclear Association 2015a)). However, BWRs could potentially offer an advantage due to their slightly faster spectrum, which emphasizes the good breeding properties of thorium fuels.

---

---

# CHAPTER 3

---

## CHOICE OF FUEL TYPES

*This chapter describes scoping studies providing a basis for the continued work, by investigating the basic properties of a range of thorium-containing fuel types. The aim is to determine which fuel types are particularly promising and which have inherent properties making them ineligible for further study. This chapter is based on the content of Paper I and calculations made in preparation for a patent application (Insulander Björk and Asphjell 2014).*

### 3.1 Comparison of fissile components - Paper I

The basic properties of four different thorium based fuel types were investigated using CASMO-5 (J. Rhodes et al. 2007), a multi-group transport theory code for depletion simulations of nuclear fuel assemblies in a two-dimensional geometry. The suitability of this code for the purpose will be further discussed in Section 4.1. The infinite multiplication factor  $k_{\infty}$  of the fuel assembly can be calculated for different burnup and operational conditions, so information on the fuel behaviour can be deduced from these simulations, which can be used for comparing the basic properties of different fuel types. The operational parameters were modeled on the Swedish BWR Forsmark 3 and the fuel assembly design chosen for this study was GE14-N, a modern design used in Forsmark 3 as well as in many other BWRs worldwide. The operational parameters can be found in Paper I.

As explained in Section 2.2.1, a fissile component must be added to the thorium in order to make a fuel capable of sustaining a fission chain reaction. The four thorium-containing fuel types investigated in this study all consist mainly of thorium and are distinguished by the respective fissile component used, namely:

- *Reactor grade plutonium (RGPu)* - plutonium with an isotope vector typical for reprocessed LWR fuel with a burnup of 40-50 MWd/kgHM. The one used in this study is 2.5% Pu-238, 54.2% Pu-239, 23.8% Pu-248, 12.6% Pu-241 and 6.9% Pu-242. The feature distinguishing RGPu from weapons' grade plutonium (WGPu) is that it has a much lower content of the fissile isotope Pu-239, which makes it unsuitable for nuclear weapon production.
- *Low Enriched Uranium (LEU)* - uranium enriched to 20% in U-235. Enrichments up to 20% count as low, whereas uranium with higher enrichments (High Enriched Uranium, HEU) is subject to much harder restrictions due to proliferation concerns.
- *U-233* - Isotopically pure U-233 is not available in practice, but this alternative is included to understand the basic characteristics of this fissile isotope and the consequences of its introduction in the fuel in relation to the alternatives.
- *Recovered uranium and RGPu (UPu)* - The uranium recovered from one spent Th+RGPu-assembly (containing 89% U-233 and 11% U-234) is used for one assembly of this type and combined with RGPu to provide sufficient reactivity.

In addition to the four thorium based fuel types, two reference cases were also included in the study - one uranium oxide (UOX) fuel assembly and one assembly with mixed uranium and plutonium oxides (U-MOX). In order to compare equivalent fuel assemblies, the amount of the fissile component in each assembly was adjusted to yield equal amounts of energy, determined by the linear reactivity model as explained in Paper I. Reactivity coefficients were estimated by perturbation calculations and the control rod worth by comparing  $k_{\infty}$  with or without control rods inserted in the simulated infinite lattice. Pin power distributions, delayed neutron fractions and decay heat are routinely calculated by CASMO-5.

### 3.1.1 Results

The composition of each fuel type at the beginning of life (BOL), as determined by the condition of equal energy yield, is given in Table 3.1, in terms of kg per fuel assembly. The plutonium and U-233 content of each fuel type is also given at the end of life (EOL). Already this table offers some information relevant for the choice of fuel type. It is seen that the total U-235 mass needed, and therewith the natural uranium requirements, is higher for Th+LEU than for the UOX reference. The U-MOX and Th+RGPu cases can be compared from the point of view of plutonium destruction. It is then clear that Th-RGPu offers an advantage both in terms of total plutonium mass reduction (8.3 kg for

Th+RGPu versus 4.6 kg for U-MOX) and in terms of the fissile fraction of the discharged plutonium (39% for Th+RGPu versus 48% for U-MOX). The Th+UPu case also offers a small advantage in terms of plutonium destruction compared with U-MOX. It is also clear that the system is far from breeding, given the large reduction of the U-233 mass for the Th+U-233 case. The Th+UPu case is close to self-sustaining in terms of U-233, but requires the addition of RGPu.

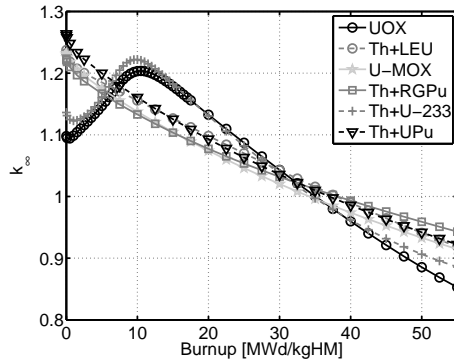


**Figure 3.1:** The infinite multiplication factor for the investigated fuel types.

The multiplication factor, plotted in Figure 3.1 in itself is not directly relevant to reactor operation, but offers some insight into the fundamental processes leading to the differences between the fuel types. Firstly, it is clear that the slope of the  $k_\infty$  curve is steeper for the UOX and Th+U-233 cases, compared with the other cases. For this reason, the burnable absorber gadolinium is routinely used in UOX fuel, and it was chosen to use this also for the Th+U-233 case. The use of gadolinium causes a gradually decreasing suppression of  $k_\infty$  at the beginning of life in these two cases, so that  $k_\infty$  is actually increasing while the gadolinium is burnt out.

The differences in the rates of decrease of  $k_\infty$  depends on the balance between consumption of fissile material through fission and production of fissile material through the neutron captures in the fertile material. Efficient conversion gives a continuous buildup of new fissile isotopes, sustaining  $k_\infty$  at a higher level. Conversion is improved in the Th+RGPu and U-MOX cases by the presence of Pu-240, having a capture cross section two orders of magnitude larger than U-238. Also in the Th+LEU case, conversion is improved by the simultaneous presence of Th-232 and U-238, providing a double set of absorption resonances and in addition the high thermal absorption in Th-232.

Reactivity coefficients, control rod worth, delayed neutron fractions and short term decay heat are central to the safe operation of a reactor. The most important reactivity coefficients for a BWR is the fuel temperature coefficient (FTC), the moderator temperature coefficient (MTC), the void coefficient (VC) and the isothermal temperature coefficient (ITC). All these need to be negative in order to avoid positive feedback loops

leading to uncontrollable reactivity increase. They may however not be too negative, i.e. negative and too large in amplitude, since this may have an adverse impact in some transient scenarios. The estimates based on lattice simulations are only indicative for the fuel behaviour, and are in this context only used for comparison of the different cases. Full core simulations of cases similar to the Th+U-233, Th+LEU and Th+RGPu cases have been carried out in a previous study (Insulander Björk 2008), providing a useful reference. The safety parameters, also listed in Table 3.1, were similar for all cases, and acceptable as far as can be judged based on the present simulations, with some important exceptions:

- The MTC and VC are positive for the Th+U-233 case. The reason for this is further discussed in Section 4.3. Full core simulations, taking e.g. the presence of control rods and leakage effects into account, show a negative VC for Th+U-233 under normal operational conditions, but significantly closer to zero than the reference, yielding unacceptably low margins.
- The FTC is negative and very large in amplitude in the Th+LEU case, because the Doppler effect, i.e. the broadening of the capture resonances with increased temperature, is amplified by the simultaneous presence of Th-232 and U-238.
- The control rod worth (CRW) is strongly reduced for the plutonium containing fuel types U-MOX and Th+RGPu and somewhat reduced also for Th+UPu. This is a known phenomenon from U-MOX usage and is attributed to the hardening of the neutron spectrum caused by the presence of the large thermal absorption resonances in several of the plutonium isotopes.
- The effective delayed neutron fraction  $\beta_{\text{eff}}$  for the U-MOX, Th+RGPu, Th+U-233 and Th+UPu cases is significantly lower than for the UOX reference. This mirrors directly the lower delayed neutron yields for fission of U-233 and Pu-239 compared with U-235. U-MOX fuel is routinely used in LWRs and full U-MOX core loadings are considered for most Generation III+ LWRs, so this is not expected to be an insurmountable problem since the delayed neutron fractions calculated for the thorium fuel types are not significantly lower than that for U-MOX fuel.

### 3.1.2 Conclusions

Based on these results and the background information provided in the previous chapter, an informed choice can be made about which fuel type should be subject to continued research.

The Th+LEU option adds many complications compared with standard UOX fuel. More enrichment work is needed to enrich uranium up to 20%, and in addition, commercial fuel factories are in general not licensed to handle uranium with an enrichment above 5%. The manufacture of a two-component fuel can also be expected to be more expensive

**Table 3.1:** Key safety parameters and balance of the most relevant elements.

Fuel type	UOX	Th+LEU	U-MOX	Th+RGPu	Th+U-233	Th+UPu
Fuel composition data, in terms of kg per fuel assembly						
Initial U-235	7.2	8.0	0.5	-	-	-
Initial RGPu	-	-	13.2	15.6	-	8.3
Initial U-233	-	-	-	-	5.8	2.9
Final total Pu	1.8	0.56	8.6	7.3	$\approx 0$	2.7
Final fissile Pu	1.0	0.34	4.1	2.8	-	0.76
Final U-233	-	1.8	-	2.1	2.5	2.8
Burnup averaged safety parameters						
MTC [pcm/K]	-10.2	-7.5	-17.3	-7.1	14.3	-2.6
VC [pcm/%void]	-56	-50	-52	-38	6	-34
FTC [pcm/K]	-2.4	-3.6	-2.5	-2.9	-2.7	-3.0
CRW [arbitrary]	20.0	20.1	17.2	17.2	21.5	18.2
$\beta_{\text{eff}}$ [pcm]	555	547	395	357	333	360

than standard UOX fabrication. This alternative is in practice only justifiable if it can offer natural uranium savings, which it according to this study does not.

The alternatives involving U-233, i.e. Th+U-233 and Th+UPu, are, as stated earlier, not practically available at present. There are however two conclusions to be drawn from this study. The fact that the VC and MTC of the Th+U-233 fuel is positive means that it has a higher reactivity at lower moderation. This indicates that the fuel is over-moderated also in a BWR and would perform better at lower moderation, which is in line with previous studies e.g. by Kim and Downar (2002). For the normal BWR operational conditions simulated, it is clearly far from being self-sustaining, given that the U-233 content decreases during life even with the initial addition of RGPu.

This leaves us with the option of RGPu as the fissile component. The present study does indeed not indicate any showstoppers, but rather a big similarity with U-MOX. Although RGPu was the plutonium type investigated in this work, other plutonium vectors may also be considered, such as for example WGPu, which is becoming available when nuclear weapons are decommissioned. Having excluded the other alternatives involving mixtures of thorium oxide with uranium oxide, the mixture of thorium oxide with plutonium oxide will in the following be referred to as Th-MOX, to underline its analogy with U-MOX.

Th-MOX as an option for management of plutonium (and other transuranic elements) has been considered many times before as a means to reduce the large and growing stockpiles of these elements resulting from the operation of the current generation of uranium fuelled LWRs. A comprehensive report on the potential of this concept in PWRs was compiled by Gruppelaar and Schapira (2000), and it has also been investigated by other researchers (Dziadosz et al. 2004; Shwageraus et al. 2004b). These studies show,

just like the BWR-calculations presented here, that Th-MOX offers clear benefits over U-MOX in terms of plutonium destruction. The reason for this is that new plutonium is generated from the U-238 mixed with the plutonium in U-MOX fuel, whereas no new plutonium is produced when Th-232 is the fertile component. As mentioned, the fissile isotope U-233 is produced instead, but the Th-MOX concept nevertheless has some merits over U-MOX from a non-proliferation point of view (Trellue et al. 2011).

Seen from another viewpoint: if the long term goal of thorium fuel usage is deployment of breeding, thorium-fuelled reduced-moderation LWRs, U-233 should be viewed as an asset rather than a proliferation concern. With this perspective, plutonium as the fissile component offers another advantage over LEU in that no U-238 is present in the fuel that would make the uranium isotope vector unsuitable for further use as a fissile component in this context.

However, both the perspectives of proliferation safety and long-term nuclear strategy are relevant rather on national or global level, but not so much for nuclear reactor operators. There is of course a possibility that a national-level decision will be made in some country to deploy thorium based fuels for reasons of e.g sustainability, proliferation, waste management or resource self-sufficiency (as has been done in India), but a shorter way to adoption of thorium based fuel may be to appeal directly to the reactor operators. In order to do so, it must first of course be demonstrated that Th-MOX indeed provides an advantage, and an advantage than can be converted into an economic benefit for the operator, while in no way compromising the safe operation of the reactor. The advantage must also, in most situations, be not only over U-MOX but also over UOX fuel.

Showing an advantage is however not sufficient. It must also be possible to provide a very high degree of confidence in any predictions made regarding the fuel behaviour. This is a big challenge. The very small experience base regarding thorium fuel operation is probably one of its largest drawbacks, which has followed it since the uranium cycle got a headstart of a few years in the 1950's. The following chapters will deal with both potential advantages of Th-MOX, and with a few steps taken towards providing the required level of confidence.

## 3.2 Thorium as an additive to uranium fuel

Although the simulations described above seemed to disfavour the combination of thorium with LEU, another promising option for thorium usage together with uranium in PWRs was proposed by Lau et al. (2012). This option involves only a minor fraction of thorium, so low that the uranium enrichment does not need to exceed the 5%-limit held by commercial fuel manufacture plants. It was found that in a fuel assembly operated under typical operational conditions in the Swedish reactor Ringhals 3, a thorium fraction of 7% would allow for similar discharge burnup as the currently used UOX assemblies in that reactor. Full core simulations (Lau et al. 2013; Lau et al. 2014c) indicated some promising features, such as improved core stability and favourable power distributions. The original intention

was to utilize thorium's absorbing properties to reduce the need for burnable absorbers, a goal which was indeed reached. However, it was also found that the natural uranium requirements were higher than for the pure UOX alternative, and also the enrichment costs would increase due to the higher enrichment level required.

In spite of the results with respect to the economic prospects of this concept being discouraging, it was clear that the margins to becoming economically feasible were much smaller than for the obviously un-economical Th-LEU case described in the previous section. It was also recognized that this concept would constitute an even smaller first step in the evolutionary approach to thorium fuel adoption. For these reasons, simulations were performed for a similar concept for usage in BWRs. Due to the status of thorium as an additive in this concept, it is hereafter referred to as thorium-additive fuel or Th-Add for short. The initial investigations by Lau et al. (2012) also aroused enough interest in the concept so that it was decided to include two rods of a representative material, i.e. UO<sub>2</sub> with with 7% ThO<sub>2</sub>, in the irradiation experiment described in Chapter 5.

The neutronic calculations performed have not been reported in an academic publication. Instead, a patent application was filed with the European Patent Organization. Being written for a legal rather than an academic context, the patent application is not suitable for inclusion in this thesis.

### 3.2.1 Assembly design with thorium additive

Nuclear fuel design in a BWR is a complicated matter, as compared with the PWR case. Since cruciform control rods are inserted between the fuel assemblies, there are large water gaps to accommodate for these, giving an uneven moderation in the assembly. Due to this fact, the enrichment must be low in the well-moderated rods closest to the water gaps to prevent high power peaks there, whereas the less moderated rods must have a higher enrichment to be able to sustain their power share. In the PWR assembly proposed by Lau et al., all rods had the same enrichment and the same thorium fraction (7%), a design which cannot be used in a BWR assembly. Instead, the design strategy was to start from a reference BWR fuel assembly design with only UOX fuel with varying enrichments, let the U-235 fraction remain unchanged and thorium only introduced to replace some of the U-238. In practice, this could be done by enriching all uranium up to e.g. 4.95%<sup>1</sup> and mixing it with thorium in different fractions. In a BWR assembly, the enrichment typically varies from about 1% in the most well-moderated areas of the fuel assembly to 4.95% in the least well-moderated areas. In the rods which have a 4.95% enrichment in the reference UOX assembly, no thorium can be introduced without lowering the U-235 fraction and hence the reactivity. In the rods with a lower enrichment in the reference UOX assembly, however, the corresponding rods in a Th-Add assembly may contain some thorium while maintaining the same U-235 fraction and still using uranium with an enrichment below the maximum allowed 4.95%. The maximum allowable thorium fraction

---

<sup>1</sup>Commercial fuel factories are designed and licensed for handling uranium with a maximum enrichment of 5%, and a margin of 0.05 percentage points to the maximum is usually held.

$f_{\text{Th}}$  for a rod with the desired U-235 fraction  $x\%$  can be calculated as  $f_{\text{Th}} = 1 - \frac{x}{4.95}$ .

There are some exceptions to be made to this simple recipe. Firstly, there exists no experience at all with mixtures of thorium, uranium and gadolinium oxides, and their properties would be difficult to predict even theoretically. In order to avoid the introduction of such an exotic mixture, it was chosen to let the burnable absorber rods consist of only gadolinium and uranium oxides. Secondly, preliminary simulations showed that high thorium fractions (over 40%) in the well-moderated corner rods resulted in too efficient breeding of U-233, resulting in very high peaking factors towards the end of life. A lower thorium content was therefore used in these rods, and the uranium enrichment consequently reduced.

Just as for the PWR concept investigated by Lau et al., the need for burnable absorbers is quite significantly reduced by the introduction of thorium (a reduction of 20 - 30% seems possible, depending on the application). The most important effect of this is that the number of burnable absorber rods can be reduced. This makes it easier to achieve low power peaking factors early in the life of the fuel assembly, since the number of rods running at a low power level due to their burnable absorber content is reduced, so that more rods can share the power load. Also the fraction of gadolinium in the remaining burnable absorber rods could be reduced. Finally, the power peaking factor could be further reduced by altering the thorium content in some of the rods slightly, optimising the design. All these considerations resulted in a fuel assembly design for which a number of preliminary studies have been carried out, comparing it with a reference assembly with an equal content of U-235. Preliminary full core simulations have also been carried out.

### 3.2.2 Neutronic properties of the Th-Add BWR fuel

The  $k_{\infty}$  curve plotted in Figure 3.2 already gives the key to the benefits of the Th-Add concept. Most importantly, it is noted that the lifetime energy yield of this assembly, as calculated by the methodology outlined in Paper I, is equal to that of the UOX reference. This means that the addition of thorium in this case does not increase the U-235 requirements.

The presence of thorium in the fuel makes the  $k_{\infty}$  curve slightly more level, which enables gadolinium savings. As can be seen, the initial period of suppressed reactivity is shorter for the Th-Add fuel than for the reference, and the peak  $k_{\infty}$  is still lower. The reactivity cost of the thorium at the beginning of life is paid back towards the end of life, where the reactivity remains at a higher level. This feature gives a smaller reactivity difference between the most and least reactive fuel assemblies, which is beneficial for the power balance in the core. This will reduce power peaking in the core as a whole, and also improve the shutdown margin (SDM), since clusters of highly reactive fuel can be avoided.

The effect of the reduced gadolinium requirements is also seen in the assembly power peaking factors, plotted in Figure 3.3. The power peaking is significantly reduced

throughout the lifetime of the fuel, except for the very last period when it increases because of one of the well-moderated corner pins gaining in power due to U-233 breeding, despite having a reduced initial Th-232 content.

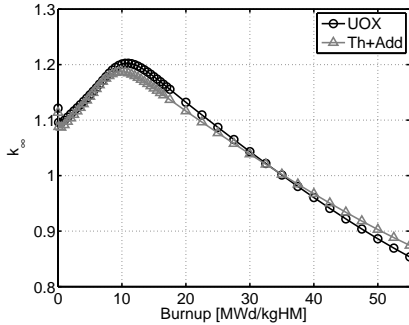


**Figure 3.2:**  $k_{\infty}$  development with burnup for Th-Add and a reference UOX fuel assembly.

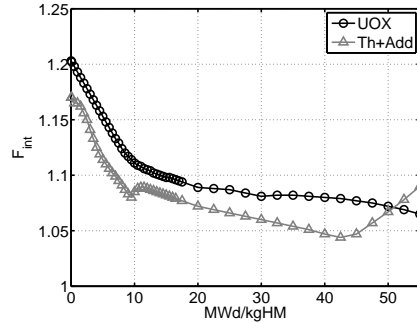
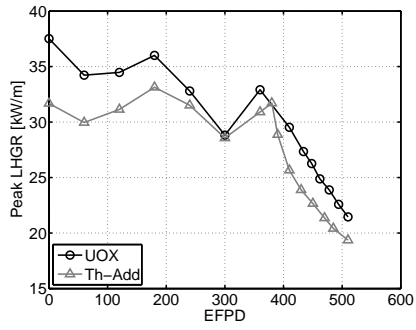


**Figure 3.3:** The assembly internal power peaking factor.

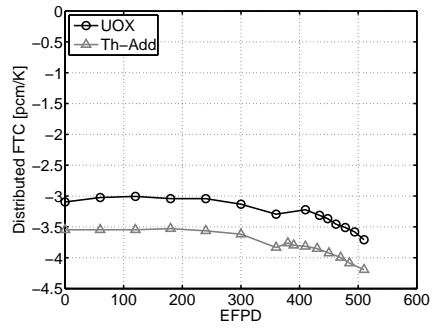
The core loading patterns and control rod sequences used in the full core simulations have not been optimised, for which reason the absolute values of shutdown margins and power peaking factors are not within acceptable ranges. Also, an unrepresentatively long coast-down period had to be modeled at the end of the cycle for the fuel to reach the target discharge burnup, also due to the loading scheme not being optimised. However, since identical core loading patterns have been used for both fuel types, relevant comparisons can nevertheless be made. The achievable cycle length was slightly shorter for the Th-Add core. However, the difference (5 days) is small enough to be rectifiable with only slight changes of the loading pattern. It can be expected that the larger thermal margins provided by the Th-Add fuel can allow for more “aggressive” loading patterns, i.e. where more fresh fuel is loaded centrally in the core, reducing neutron leakage.<sup>2</sup>

Figure 3.4 shows the peak linear heat generation rate for the two cores, which is lower for the Th-Add case throughout the cycle. The shutdown margin is negative for both cores due to the non-optimised loading pattern, but significantly better for the Th-Add case. The delayed neutron fraction is very slightly reduced by the addition of thorium, which was expected since the in-bred U-233 only stands for about 7% of the fissions in the Th-Add core and has only a slightly lower delayed neutron yield than Pu-239. The control rod worth, as estimated from the lattice simulations, is also insignificantly affected. The VC and MTC are virtually unaffected, whereas the amplitude of the (negative) FTC, shown in Figure 3.5, is increased by about 17% by the thorium additive.

<sup>2</sup>Preliminary studies for a currently operating BWR show that this is indeed the case, and that the total costs of uranium and enrichment can indeed be slightly reduced by use of Th-Add fuel.



**Figure 3.4:** The peak LHGR in the Th-Add and reference UOX cores.



**Figure 3.5:** The FTC in the Th-Add and reference UOX cores.

---

---

# CHAPTER 4

---

## NEUTRONIC PROPERTIES OF THORIUM-PLUTONIUM FUEL

*This chapter describes the aspects of the neutronic code CASMO-5 related to simulation of Th-MOX fuel and a benchmark study for Th-MOX modelling. Thereafter, studies performed with CASMO-5 and the closely related code CASMO-4 are described. The first two studies address the possible advantages of Th-MOX usage in PWRs, and the objective of the third study is to investigate possible improvements in performance of Th-MOX fuel for BWRs. This chapter is based mainly on the content of Papers II - V.*

### 4.1 Th-MOX modelling with CASMO-5

For detailed studies of the neutronic behaviour of Th-MOX fuel, it is important to investigate the applicability of the software used for this purpose. Due to its widespread use in the nuclear industry, the neutronic simulation code CASMO has been used. Most simulations have been carried out using CASMO-5 whereas the older version CASMO-4E was used for the simulations performed for Paper IV, since this is the code used in normal operation of the simulated reactor. The specificities of CASMO-5 are outlined below whereas the differences to CASMO-4E are briefly discussed in Section 4.2.

Validation is not only necessary in order to make sure that the calculations carried out in this work are relevant. It is also a prerequisite for loading of this fuel in a commercial

reactor. A regulatory body will generally demand that the in-core neutronic behaviour of a fuel can be predicted with “sufficient” accuracy. What is regarded as sufficient is generally different between different countries, having different regulatory systems, and also depends on how much fuel will be loaded, i.e. whether only a few rods, a small number of assemblies or partial or full core loadings are being considered. Whereas the benchmarking carried out within this work is certainly not sufficient for full core loadings, it may be sufficient for loading of lead test rods.

In general, Th-MOX and U-MOX fuels behave similarly, compared with UOX fuel, as concluded by several studies performed with different neutronic software (e.g. Ade et al. 2014; Gruppelaar and Schapira 2000), and also indicated by the study presented in Section 3.1. The reason for this is that the main fissile isotopes are the same. It is thus relevant to know that CASMO-5 has been benchmarked against some U-MOX experiments (Lee et al. 2008; J. Rhodes et al. 2010; Xu et al. 2010) with good results. This provides confidence that plutonium-containing fuels are generally well modelled by CASMO-5. It then remains to assess how well thorium and related isotopes are modelled.

#### 4.1.1 CASMO-5

CASMO-5 is a deterministic neutronic simulation code, based on a numerical method known as the method of characteristics. Also the method of collision probabilities is used in the pin cell calculations. The computational methodology in itself is not specific to the type of fuel being simulated. However, a number of decisions has been made in the implementation of the method, and also in the preparation of the cross section library, which are based on the assumption that the fuel may be either UOX or U-MOX, i.e. that the fuel mainly consists of U-238.

The energy group divisions in the 586-group cross section library are chosen to give the best possible results for simulation of UOX or MOX-fuelled LWRs. Due to the dominance of thermal neutrons in such reactors, the library is very fine-meshed in the thermal region, i.e. 0 – 10 eV, a feature which is equally adequate for thorium and uranium based fuels. In the resonance region, the group boundaries are chosen so that as far as possible, the U-238 absorption resonances are uniformly distributed within each group, in order to improve the accuracy in the calculation of group average cross sections. This choice is of course then not as adequate for Th-232. Since the U-238 and Th-232 resonances are randomly distributed with respect to one another, it is not obvious whether this will lead to an under- or overprediction of the resonance absorption, or in general what effect this will have on the calculated results. Comparison with experiments is thus necessary, and adaptations of the code for thorium modelling in this respect would be beneficial to provide confidence in the accuracy of the results.

A second choice of group boundaries is made for the two-dimensional transport calculation. The 586 micro-group cross sections are then condensed to 35 larger energy groups. In particular in the thermal spectrum, these boundaries are specifically chosen to

resolve some resonances typical for U-MOX fuel<sup>1</sup>, i.e. the large absorption resonances of Pu-240 (1 eV), Pu-242 (2.7 eV) and U-238 (6.6 eV). Some finer group boundary spacing is also present close to the broad resonance of Pu-239 at 0.3 eV. This choice of group boundaries is of course equally good for Th-MOX and U-MOX with respect to the plutonium isotopes and the coverage of the U-238 resonance is merely unimportant for the Th-MOX case. Th-232 does not have any low-energy resonances, so its cross section is adequately modeled with the present thermal group structure. To the small extent that U-233 is produced in the fuel, its comparatively broad and small cross section resonances are not very well covered. However, given that the U-233 number density generally remains below that of any of the Pu isotopes in Th-MOX fuel and that its resonance peaks are more than an order of magnitude below those of the plutonium isotopes, this is not expected to have any large consequences for the modeling accuracy. It could be noted that the distribution of energy groups does not take into account any features of the U-235 cross section either.

Finally, the cross section library has a slightly lower degree of precision with respect to thorium related isotopes in that cross sections for these isotopes are only evaluated at four temperatures whereas the cross sections for U-235, U-238 and the major plutonium isotopes are evaluated at ten temperatures. Larger interpolation errors can thus be expected.

With regards to the methodology, some special adaptations are being made to U-238 as the normally dominant isotope. An important one is that a resonance scatter model has been applied to correct for large scattering resonances in U-238, which gives an improvement of the modeling if the scattering cross section is large compared with the absorption cross section. This enables the modelling of upscattering in the resonance region, and is estimated to give a 10% more negative Doppler coefficient compared with codes which do not have this model (J. Rhodes et al. 2008). This model is however not applied to Th-232, the consequences of which are unknown. Trellue et al. (2011) made a comparison of reactivity coefficients and boron efficiency of Th-MOX with different plutonium vectors, calculated by CASMO-5 and the Monte Carlo-based code MonteBurns. The conclusion is that there were indeed differences in the predictions on the order of 25% but there was no clear tendency towards under- or overprediction compared with MonteBurns, so other modelling differences with respect to e.g. data libraries or pin cell/lattice/full core calculations can be assumed to play a larger role.

In addition to these considerations, it is noted that U-233 and Th-232 are treated as resonance absorbers by default, adding to the confidence in the calculated results. A correction is routinely applied for the presence of multiple resonance absorbers. Another beneficial feature of CASMO-5 for the modeling of thorium-based fuels is that the effective energy release per fission,  $Q_{\text{eff}}$  (and also the fission neutron spectra) are calculated for all fissioning isotopes, meaning that the smaller  $Q_{\text{eff}}$  of U-233 compared with e.g. U-235 and Pu-239 is taken into account.

---

<sup>1</sup>A less fine 18-group division is made for UOX cases, however the 35 group division is automatically activated by the presence of Pu isotopes, so also for Th-MOX simulations.

The general conclusion that can be drawn from the above outlined considerations is that none of the underlying assumptions in CASMO-5 are in direct conflict with the modelling of Th-MOX fuel, but since it is optimized for U-238-dominated fuel, the confidence in the results for Th-MOX is somewhat lower. Benchmark calculations are ultimately the only way to assess the fidelity of calculated results. Such a benchmark calculation has been undertaken and is addressed in the Section 4.1.3.

### 4.1.2 Cross section libraries

Although the calculation methodology can be more or less adapted to modelling of a certain isotope, as outlined above, it is ultimately the cross section data used by the code that are of most importance to the accuracy of the predictions. The cross section library integrated in CASMO-5 and used in this work builds on the Evaluated Nuclear Data File ENDF/B-VII, release 0 (Chadwick et al. 2006). It should be noted that some changes were made to the Th-232 and U-233 cross sections in ENDF/B-VII.0 short before its release (Mosteller 2008). These data sets have not been subject to the same level of testing as the other data sets in the library. Benchmarks for U-233 cross sections in the thermal spectrum show some improvement over the last ENDF/B-VI version. For Th-232 cross sections, there are not many well-vetted benchmarks. The cross section library in CASMO-5 has been subject to some change since the studies presented here were made e.g. in connection with the release of ENDF/B-VII.1. New simulations will be carried out to assess the impact of these changes on thorium fuel modeling.

### 4.1.3 Benchmark based on irradiated Th-MOX rodlet - Paper II

With the aim to create an experimental benchmark for Th-MOX fuel, a Th-MOX rodlet was irradiated in a commercially operating reactor in Obrigheim, Germany, during its last four operating cycles, 2001-2005. This activity was part of the Thorium Cycle Project (Klaassen et al. 2008). The rodlet was of 14.4 cm length and was mounted in one of the inner guide tubes of a U-MOX assembly located at the core center. After the four cycles, the rod was discharged and subjected to post-irradiation examination (PIE), as a part of the LWR-DEPUTY project (Verwerft et al. 2011). One of the analyses performed was a radiochemical analysis, determining the concentration of 28 isotopes in the pin. It should also be mentioned that the general conclusion of the PIE, including profilometry, fission gas analysis and gamma scanning, was that the Th-MOX fuel had withstood the irradiation very well.

A benchmark was formulated such that the irradiation history of the rodlet and its carrier assemblies was simulated. Four different codes or code systems participated in the study; CASMO-5, HELIOS (Villarino et al. 1992), MCBurn (Schitthelm et al. 2010) and a combination of the codes Ecco/Eranos (Rimpault 2002) and Train (Rineiski 2008) (EET). At first, the power history was simulated as measured by an aeroball system located in a next-to-neighbouring fuel assembly, although the uncertainties in the extrapolation of

these measurements to the power at the carrier assembly were known to be large. In addition, the plutonium composition in the carrier U-MOX assemblies was unknown, adding to the uncertainty in the neutronic surroundings of the Th-MOX rodlet. As a test, all participants calculated the content of the burnup indicator Cs-137 present in the fuel, resulting in large overpredictions by all codes. As a result, it was decided that all participants should recalibrate the power history with an individual factor resulting in the correct Cs-137 content being calculated by each code. Thus, the calculated results with respect to the isotopic content of the fuel rod are merely relative to the Cs-137 content.

Whereas this individual recalibration made calculated values of  $k_\infty$  and pin power distributions within the assembly difficult to compare, the calibration factors used by the respective benchmark participants gives an indication of how the power of the Th-MOX pin relative to the surrounding U-MOX pins was predicted by the respective codes. For three of the participating codes, the calibration factor was very similar; 0.778 (HELIOS), 0.759 (CASMO-5) and 0.791 (EET), whereas for MCBurn, the calibration factor was 0.663, deviating significantly from the others. This indicates that the three former codes agree reasonably (within 2%) on the relative power of Th-MOX and U-MOX fuel, which is useful for comparative studies. <sup>2</sup>

For the eight elements thorium, protactinium, uranium, plutonium, americium, curium, neodymium and europium, radial distributions were calculated by each code. The profiles for plutonium and uranium are shown in Figures 4.1 and 4.2 as examples. The CASMO-5 prediction of the shape of the radial distribution of plutonium, americium and curium agreed well with the other codes, whereas for thorium, protactinium and uranium, the profile as predicted by CASMO-5 was almost level, disagreeing strongly with the results calculated by the other codes. It is noted that the latter isotopes are the ones most strongly related to the thorium cycle. The present protactinium and uranium isotopes are in this case direct or indirect products of neutron reactions with Th-232. For the fission products europium and neodymium, the profiles predicted by CASMO-5 are slightly more level compared with the other predictions. This is explained by the fact that they stem from fissions of both Pu-239, the distribution of which is strongly periphery-peaked, and U-233, for which the profile, as modelled by CASMO-5, is almost level.

---

<sup>2</sup>A possible explanation for the deviating result of the MCBurn calculations could be that a reduction of the moderator boron fraction that took place during the last of the four irradiation cycles was not taken into account in the MCBurn simulations. The  $k_\infty$ -curve shown in Paper II indicates that this could be the case. A higher boron content gives a harder spectrum which in turn gives a higher reactivity of the Th-MOX rod compared with the U-MOX rods, since the Th-MOX rod at this late stage of the irradiation contains significant amounts of U-233 which is favoured by a harder spectrum as shown in Paper V. A higher relative power of the Th-MOX rod would explain why the Th-MOX reaches the same burnup in all simulations, despite the lower assembly power level in the MCBurn calculations. This theory is strengthened by the fact that the production of U-233 is overestimated by MCBurn and the consumption of Pu-239 is underestimated, since a harder spectrum tends to favour captures (producing U-233) over fissions (consuming Pu-239).

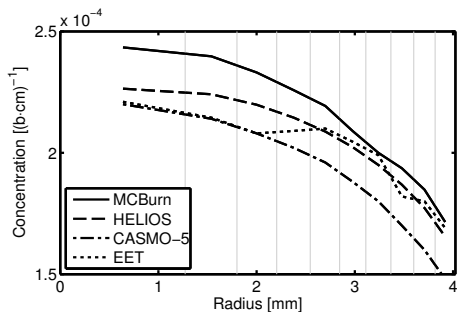


**Figure 4.1:** Modelled radial plutonium distribution in the Th-MOX rod.

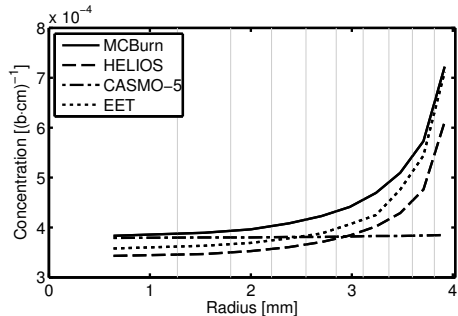


**Figure 4.2:** Modelled radial uranium distribution in the Th-MOX rod.

Unfortunately, technical problems with the electron-probe micro-analysis instrument at the JRC-ITU (Joint Research Center - Institute for Transuranium Elements) have delayed the experimental assessment of these profiles, so there is no experimental data to support any of the predictions. However, the architects of CASMO-5, Studsvik Scandpower, have confirmed that the shielding effects of Th-232 (which are more thoroughly discussed in Paper VIII) are not accounted for in the used CASMO-5 release. CASMO-5 relies on an empirical radial distribution function for the U-238 resonance integral for generating appropriate power profiles in UOX pellets, when requested by user input (Xu et al. 2009). No such function is implemented for Th-232, which can explain the present results. Xu et al. (2009) state that the radial distribution function applied to the U-238 resonance integral only affects the power profile within the fuel pellet, and not the global results with respect to  $k_{\infty}$  or generation of Pu-239. While this is not necessarily true for the Th-232 case, it at least lends some confidence in the global results calculated by CASMO-5, despite the inadequate representation of the rod internal radial distribution of the reaction rates. It is noted that a similar radial distribution function was implemented for Th-232 in a later release of CASMO-5 (J. D. Rhodes 2014).

The calculated average contents of the investigated isotopes are generally in line with the experimental results, also for CASMO-5. Most deviations could be explained by uncertainties in the cross section libraries or experimental uncertainties. The most important deviation in the CASMO-5 results is that the production of U-234 and U-235 are underestimated, and to some extent also that of U-233. This would indicate that the capture rates in Th-232 are underestimated, which could be related to the discussed issue with the radial distribution of the reaction rates.

Based on the above, it can be concluded that CASMO-5 can be used for theoretical studies of Th-MOX fuel behaviour with some confidence, since the used methodology is generally applicable to thorium. Further validation is of course required before CASMO-5 can be used for safety evaluations of actual core loadings in commercially operating reactors.

## 4.2 Th-MOX fuel in PWRs

A study was made of Th-MOX in PWRs. In a first phase, lattice simulations were made of Th-MOX with several different plutonium isotope vectors, whereafter full core simulations were performed, based on the experience gained.

### 4.2.1 Lattice simulations - Paper III

Lattice simulations were performed with CASMO-5 for PWR conditions, comparing Th-MOX and U-MOX fuels with a range of different plutonium types constituting the fissile component. The plutonium types were RGPu, WGPu, plutonium recovered from spent U-MOX fuel (2RPu) and RGPu with an in-growth of americium (AmPu). All Pu vectors represent specific plutonium management scenarios, and the purpose of the study was to investigate whether Th-MOX could offer particular benefits in some specific scenario. The two plutonium types AmPu and 2RPu can be referred to as “low quality”, and higher plutonium fractions are necessary to yield the same amount of energy compared with RGPu. A UOX case was also simulated for reference. The operating conditions and the used methodology are described in Paper III. Equivalent fuel compositions were determined and  $k_{\infty}$ , safety parameters and mass balances for plutonium, U-233 and minor actinides (MA) were calculated. Burnup averaged safety parameters and mass balance data are listed in Table 4.1, whereas plots showing the burnup dependence of the safety parameters are provided in Paper III. The results for one of the cases - where RGPu was the fissile component - could be compared with similar cases reported by Gruppelaar and Schapira (2000). The conclusions with respect to the reactivity coefficients and plutonium mass balances were in good agreement whereas no reference was provided for the delayed neutron fraction or the short term decay heat. The comparison between the Th+WGPu case and the UOX case could also be referenced against an earlier study by Dziadosz et al. (2004), and the conclusions were also in this case in agreement.

The following conclusions could be drawn from the study:

- The most notable differences between the UOX reference and the Th-MOX and U-MOX fuel types were decreased efficiency of reactivity control systems (soluble boron and control rods), a decreased delayed neutron fraction and a larger (less negative) ITC. It has been found (Shwageraus et al. 2004b) that the decreased efficiency of the reactivity control, which is due to strong thermal absorption in some plutonium isotopes, can be mitigated by increasing the moderation.
- In all cases, more plutonium was required for generating an equal amount of energy using Th-MOX fuel compared with U-MOX fuel, under current burnup constraints. The initial reactivity is reduced by the higher thermal capture cross section of Th-233, and the payback in form of more fissions in U-233 does not compensate for that in the modelled burnup period. It was estimated that one would have

to go to significantly higher burnup (almost 100 MWd/kgHM in the Th+RGPu case) to achieve plutonium savings. This way of using thorium is thus not a way to maximise the energy value of the plutonium stockpile. Also in this context, increased moderation can improve the plutonium utilization (Shwageraus et al. 2004b).

- Most of the safety parameters depend more strongly on which plutonium vector is used, or rather on the fraction of plutonium in the fuel, than on whether the fertile component is Th-232 or U-238. Differences between the different U-MOX and Th-MOX fuel types were in most cases small compared with the difference between the UOX reference and the MOX fuel types as a collective.
- An important exception to this rule was the coolant void reactivity (CVR), estimated as the  $k_\infty$  difference between normal operational conditions and a fully voided core. For the low-quality plutonium vectors AmPu and 2RPu, the coolant void reactivity was significantly closer to zero than it was for the UOX reference, but also significantly lower for Th-MOX fuel than for U-MOX fuel, representing a larger margin to a positive CVR. Th-MOX could thus be used to incinerate low-quality plutonium with larger safety margins than U-MOX.
- The slope of the  $k_\infty$  curve shown in Figure 4.3 was smaller than the reference for all plutonium types except for WGPu, in which case it was similar. This indicates that some improvement with respect to the power distribution between fuel assemblies in a core can be expected by introduction of Th-MOX or U-MOX fuel with any of the plutonium types RGPu, AmPu or 2RPu. This feature, however, is not improved by an increased moderation ratio, which generally increases fission rates at the cost of capture rates, thus making the slope of the  $k_\infty$ -curve steeper.

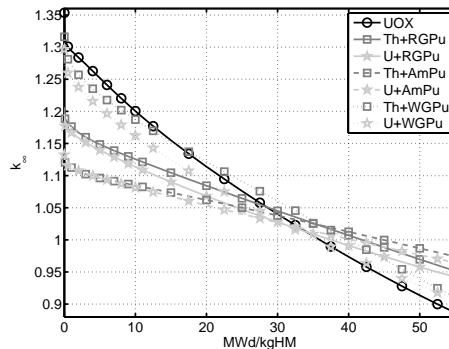


**Figure 4.3:**  $k_\infty$  development with burnup for the UOX reference and six of the investigated Th-MOX and U-MOX fuel types. The  $k_\infty$  curves for the 2RPu cases are omitted for clarity. They are very similar to those of the RGPu cases.

**Table 4.1:** Key parameters for safety and fuel design, and balance of the most relevant elements in terms of kg per fuel assembly. The units of the CRW and the CVR are arbitrary but comparable for the different cases.

Fuel type	UOX	U-RGPu	Th-RGPu	U-AmPu	Th-AmPu	U-WGPu	Th-WGPu	U-2RPU	Th-2RPU
Burnup averaged safety parameters									
CRW [arbitrary]	30	21	22	19	20	25	25	19	20
CVR [arbitrary]	26	15	16	8	12	24	24	8	11
BW [pcm/ppm]	-7.1	-3.0	-3.2	-2.4	-2.6	-4.2	-4.3	-2.5	-2.6
FTC [pcm/K]	-2.9	-3.2	-3.4	-3.0	-3.2	-3.1	-3.3	-3.3	-3.4
MTC [pcm/K]	-45	-58	-48	-50	-46	-62	-46	-48	-42
ITC [pcm/K]	-10.6	-6.4	-6.1	-6.2	-6.2	-6.9	-6.3	-6.0	-5.9
$\beta_{\text{eff}}$ [pcm]	565	399	367	378	343	360	316	417	389
Fuel composition data									
Initial Pu mass [kg]	-	38.2	41.0	49.0	49.6	22.6	26.7	54.2	55.2
Final Pu mass [kg]	5.8	27.5	18.9	37.8	26.7	14.8	7.4	41.3	31.3
Pu consumption [%]	-	28	54	23	46	35	72	24	43
Final Pu quality [%]	68	57	43	56	44	64	47	50	38
Final MA mass [kg]	0.57	1.90	1.97	3.12	3.05	0.494	0.499	3.10	3.12

With these conclusions in mind, new reflections can be made on how to use Th-MOX fuel in a sensible way. There appear to be two paths to follow: One is to leave the moderation ratio and the assembly design unaltered, and try to draw benefits from the flatter  $k_\infty$ -curve for other plutonium compositions than WGPu. This approach is held in the work presented in Section 4.2.2. The other path would be to increase the moderation ratio in order to improve plutonium utilization and possibly also safety parameters. This path is investigated in Section 4.3.

## 4.2.2 Full core simulations - Paper IV

An even power distribution in a core is not a goal in itself, but is rather necessary for maintaining a high average power without exceeding thermal limits in any assembly. Introducing Th-MOX to improve the power distribution compared with the current UOX fuel could thus give a possibility to increase the average power, i.e. a power uprate. A major power uprate would however also necessitate a number of large and expensive modifications to the whole reactor system. Another implication of the flatter  $k_\infty$  curve is that the fuel can be designed to reach a higher discharge burnup without having to bear with an excessively high initial  $k_\infty$ . This is an interesting option, since the aforementioned good material properties of thorium oxide makes it plausible that Th-MOX could sustain higher burnups than U-MOX.

A higher burnup capacity can be utilized either by decreasing the number of fuel assemblies replaced in each reload, or by extending the operating cycles. Of these two, the option of operating cycle extension was chosen. Full core simulations were performed for the Swedish PWR Ringhals 3, using CASMO-4E (J. Rhodes et al. 2009) and SIMULATE-3 (Dean 2007) since these are the codes normally used for core management in this reactor. CASMO-4E operates essentially in the same way as CASMO-5, but with fewer energy groups in the pin cell calculations and a different cross section library. In addition, the mentioned correction for multiple resonance absorbers is not implemented in CASMO-4E. The differences between CASMO-5 and CASMO-4E can be expected to affect the modeling of thorium based fuel to some extent, but CASMO-4E has previously been benchmarked for simulation of Th-MOX fuel with good results (Shwageraus et al. 2004b), so it is expected that the modeling is reasonable. The results should be regarded as indicative. SIMULATE-3 uses the homogenized macroscopic cross sections provided by CASMO-4E for two-group full core diffusion simulations, and is thus less dependent on the specific isotopes present in the fuel.

A normal UOX reload, designed for a one-year operating cycle, was used as a reference case and compared with a Th-MOX core which was designed for an 18-month operating cycle, i.e. a 50% cycle extension. As previously noted, the reactivity worth of soluble boron and control rods is reduced by the presence of plutonium, and for this reason, the Th-MOX core was modelled assuming the soluble boron to be enriched in B-10, and stronger control rods were also modelled. Another difference to the reference case was that  $Gd_2O_3$  mixed with the fuel matrix was not used, since ternary mixtures of  $ThO_2$ ,

$\text{PuO}_2$  and  $\text{Gd}_2\text{O}_3$  are difficult both to manufacture and to model. Instead, a thin layer of zirconium boride applied to the outer surface of the fuel pellet was modelled, a concept referred to as Integral Fuel Burnable Absorber (IFBA).

The conclusion of the study is that operating cycle extension using Th-MOX fuel is indeed possible, provided the above mentioned reinforcements of the reactivity control systems and that the fuel material can sustain high burnups. Despite the fuel assemblies being designed for higher burnup, the initial  $k_\infty$  is lower than that of Th-MOX as seen in Figure 4.4, partially due to the use of IFBA. The different indicators of the power distribution are in general well within the safety margins and the margin to departure from nucleate boiling is even improved as shown in Figure 4.5.

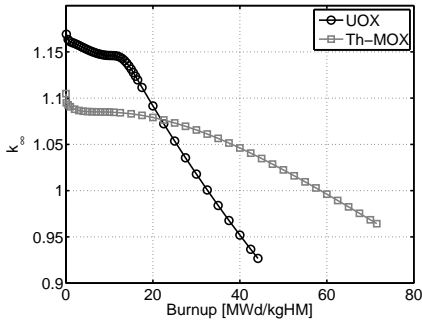


**Figure 4.4:**  $k_\infty$  development with burnup for the Th-MOX and the reference UOX fuel assembly.

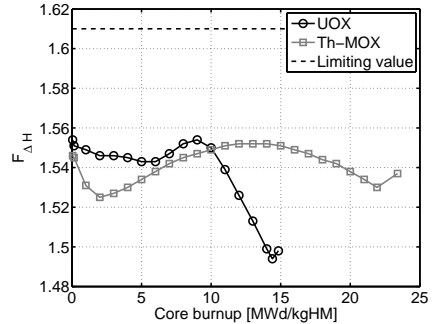


**Figure 4.5:**  $F_{\Delta H}$ , i.e. maximum rod power relative to core average rod power as a function of burnup, for the Th-MOX and the reference UOX core.

The calculated safety parameters are listed in Table 4.2 along with the limits for these applied at Ringhals 3. As can be seen, three of the safety parameters were outside the pre-defined limits:  $\beta_{\text{eff}}$ , the Doppler power coefficient (DPC) and the FTC. Transients involving these three safety parameters were qualitatively assessed, indicating that these transients would have an acceptable course with Th-MOX fuel. Details are given in Paper IV. Since Ringhals 3 is a typical PWR with no features making it especially suitable for MOX fuel, it seems that operating cycle extension using Th-MOX fuel should be possible in PWRs in general.

Later studies by Lau et al. (2014b) also found that the axial offset, i.e. the power imbalance between the upper and lower halves of the core, was reduced for the Th-MOX core. Moreover, the fluctuations in axial offset induced by rapid power changes were almost eliminated, greatly improving the core stability.

As a final remark, it is interesting to note that some but not all of the predictions made by the lattice calculations proved to be in agreement with the full core situation. The decreased delayed neutron fraction and boron and control rod worths were similarly

important. The ITC was predicted by the lattice simulations to be higher for Th-MOX, but was found to be lower in the full core simulations. Given that the full core simulations take several effects into account which are not present in the lattice simulations, most importantly presence of control rods, the full core results are likely to be more representative in this remark. The Doppler power coefficient was not calculated in the lattice simulations, but the closely related FTC was, showing no big deviation from that of UOX fuel. In the full core simulations however, these coefficients were outside of the specified limits. Referencing the results to those of Shwageraus et al. (2004b), we see that results from the full core simulations are confirmed rather than those of the lattice simulations.

**Table 4.2:** Key safety parameters for the Th-MOX core and the UOX reference.

	Limit	UOX reference	Th-MOX
Min boron worth [pcm/ppm]	-15	-8.3	-8.7
Max boron worth [pcm/ppm]	-5	-6.2	-5.2
Min SDM [pcm]	2000	2559	3895
Max rod worth [pcm]	-	6505	7808
Max MDC $[(\Delta k/k)/(g/cm^3)]$	0.50	0.41	0.34
Max MTC [pcm/K]	-	-1.3	-4.0
Max ITC [pcm/K]	0.0	-4.4	-7.9
Min DTC [pcm/K]	-4.00	-3.72	-4.53
Max DTC [pcm/K]	-1.70	-2.10	-2.36
Min DPC [pcm/%power]	-21.0	-15.5	-21.5
Max DPC [pcm/%power]	-6.5	-9.8	-14.6
Min $\beta_{\text{eff}}$ EOC [pcm]	430	502	350
Max $\beta_{\text{eff}}$ BOC [pcm]	720	647	370

### 4.3 BWR fuel assembly design for efficient use of plutonium - Paper V

Since thorium based fuel is suggested as an efficient means to manage stockpiles of plutonium and MA, it is relevant to investigate how this can be done in the most efficient way, while staying within the limits drawn by the condition of safe reactor operation. It is widely recognized (Puill 2002; Shwageraus et al. 2004b) that conventionally designed fuel assemblies loaded with plutonium-containing fuels are strongly undermoderated. A higher H/HM ratio increases the initial reactivity of the fuel by favouring fission over neutron capture, which has the additional consequence in Th-MOX fuel that the initially added plutonium is more thoroughly consumed, since less U-233 is generated to compete for the thermal neutrons.

The moderation ratio can be increased by several means. The most straightforward is

perhaps to increase the moderator density, which can be done by decreasing its temperature or by increasing the reactor pressure. Both these operations demand a change in how the reactor is operated, and quite possibly to the thermohydraulic system of the reactor. Another method which limits the change to the reactor core is to decrease the fuel volume and, consequently, increase the moderator volume. The BWR context was chosen for trying this, since there is a high degree of design flexibility within the box surrounding the BWR assembly. The consequences for different fuel types of varying the H/HM ratio are illustrated in Figure 4.6. The normalized curves represent the beginning of life  $k_{\infty}$  at different H/HM ratios, showing that the maxima occur at very different H/HM ratios. Also shown are the void coefficients at different H/HM ratios for each case, which are in effect the derivatives of the respective  $k_{\infty}$ -curves. Since a negative void coefficient is a prerequisite for safe reactor operation, the H/HM ratio must be slightly below the optimum. As shown in Table 4.3, the H/HM ratio in a standard BWR assembly is just below 5 (assuming 40% void in the coolant), varying slightly depending on the density of the fuel material. The optimum H/HM ratio for Th+U-233 fuel is below that, which explains the positive void coefficient encountered for this fuel type in Paper I. It also indicates that the H/HM ratio for Th-MOX fuel must have a reasonable margin to the optimum seen in Figure 4.6, since the increasing U-233 content of this fuel will shift the optimum towards lower values during burnup.

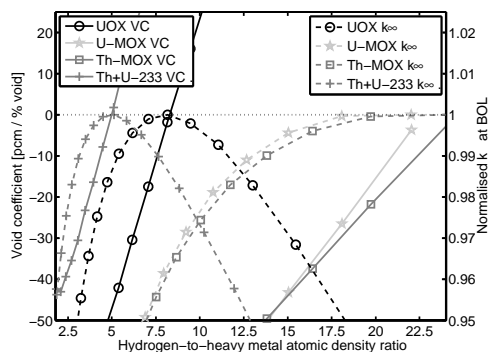


**Figure 4.6:** Normalized  $k_{\infty}$  and void coefficients for four different fuel types.

The goal of the exercise is once again to introduce as little change as possible for the reactor operator. Therefore, the new fuel assembly is designed to yield an equal amount of energy throughout its lifetime as a normal UOX BWR fuel assembly. Decreasing the fuel volume then means that the burnup must be increased, i.e. more energy must be generated per unit fuel mass. Once again, it has to be assumed that Th-MOX fuel can sustain high burnups.

A fuel assembly design was created with an almost doubled H/HM ratio compared with the reference BWR assembly, GE14-N. This increase in the H/HM ratio was realised both by removing some rods from the lattice and by decreasing the diameter of those remaining.

The results were compared with a UOX and a U-MOX reference of normal (GE14-N) design, and also with a Th-MOX assembly with unaltered design. Key parameters for all references and the modified assembly are listed in Table 4.3 and the general conclusions were the following:

- The energy generated per loaded kilogram of plutonium was increased by 19% compared with an unmodified Th-MOX assembly. The achieved value is similar to that of an unmodified U-MOX assembly.
- The fissile fraction of the discharged plutonium was only 24%, to be compared with the 49% for discharged U-MOX fuel.
- The discharged masses of U-233 and of MA were lowered.
- The reactivity coefficients were higher (less negative) but not widely different from those of the reference.
- The control rod worth was not improved relative to the unmodified Th-MOX assembly, despite the increased moderation.
- The hot-to-cold reactivity swing (HCS), i.e. the  $k_{\infty}$  difference between hot full power conditions with all rods out and cold zero power conditions with all rods in, was nevertheless improved. This is an indicator of the shutdown margin that can be expected.

It can be concluded that plutonium incineration by Th-MOX fuel in BWRs can be made even more efficient by modification of the fuel assembly design. This strategy is most suitable where there is a stockpile of plutonium to be disposed of and there is no intention to reprocess the fuel, since the amounts of fissile material in the spent fuel is minimised. In this case, the chemical inertness of the ThO<sub>2</sub> matrix is beneficial, improving the fuel's suitability for final storage.

**Table 4.3:** Key parameters for safety and fuel design, and balance of the most relevant elements.

Fuel type	UOX ref.	U-MOX ref.	Th-MOX ref.	New Th-MOX
Burnup averaged safety parameters				
CRW [arbitrary]	16	14	14	13
HCS [arbitrary]	-14	-12	-13	-14
VC [pcm/% void]	-55	-52	-37	-41
FTC [pcm/K]	-2.4	-2.5	-2.9	-2.1
ITC [pcm/K]	-28	-26	-21	-12
$\beta_{\text{eff}}$ [pcm]	551	399	365	369
Design parameters				
H/HM ratio	4.6	4.4	4.8	9.0
Fuel mass [kg]	186	192	172	108
$B_D$ [MWd/kgHM]	53	52	58	91
Fuel composition data				
Initial Pu mass [kg]	-	13.4	15.8	13.4
Pu consumption [%]	-	34	54	67
Final Pu quality [%]	59	49	40	24
Final $^{233}\text{U}$ mass [kg]	-	-	2.3	1.4
Final MA mass [kg]	0.20	0.74	0.75	0.62

---

---

# CHAPTER 5

---

## THERMAL-MECHANICAL PROPERTIES OF THORIUM FUEL MATERIALS

*This chapter describes an irradiation experiment designed to provide data on how Th-MOX and Th-Add fuel performs under irradiation with respect to its thermal-mechanical properties. Theoretical simulations of the thermal-mechanical performance of Th-MOX fuel are also described and comparisons made between the experimental results and the theoretical predictions. This chapter is based mainly on the content of Papers VI - VIII.*

### 5.1 Instrumented irradiation experiment

In the preceding chapters, it has been necessary to make some assumptions for the thermal-mechanical operating limits. In general, it has been assumed that Th-MOX fuel can withstand the same linear heat generation rates (LHGR) as uranium fuel, but that thorium fuel can operate to higher burnup. These assumptions rest upon the fact that thorium oxide has a number of beneficial material properties. However, exactly how these properties interact is difficult to foresee, especially in the presence of another component in the fuel; plutonium oxide. Furthermore, the properties change as the fuel is irradiated, making the predictions even more difficult. Experimental assessment is thus crucial to

build the necessary degree of confidence in the predictions.

### 5.1.1 Rig IFA-730 in the Halden research reactor - Paper VI

The research reactor located in Halden offers the possibility to measure the properties of nuclear fuel under irradiation. Information on fuel centerline temperature ( $T_C$ ), dimensional changes of fuel and cladding, the internal pressure in the fuel rod and a number of other parameters is conveyed on-line, during operation, from dedicated instruments located inside the core. Experimental irradiation rigs comprising up to about twelve nuclear fuel rodlets can be loaded in up to 30 locations in the reactor core and be irradiated for approximately six months per year. The reactor is the world's only boiling heavy water reactor, operating at a pressure of 33.6 bar and a coolant temperature of 240 °C. It is operated by the Norwegian Institute for Energy Technology, IFE, which also runs nuclear material laboratories at Kjeller in Norway, where all the driver fuel and some of the test fuel for the reactor is manufactured.

The experimental rig IFA-730 comprises six rods and is depicted in Figure 5.1. The rods consist of the pellet types listed in Table 5.1. All materials except for the Th-MOX material were manufactured at IFE Kjeller. As seen in Figure 5.1, there are only two short segments of Th-MOX pellets in two rods (rods one and three – *ThMOX-1* and *ThMOX-3*). These segments comprise four pellets each of the eight Th-MOX fuel pellets which were available at the start of the experiment. These were manufactured by JRC-ITU, and being originally designed for a previous experiment (Verwerft et al. 2007), they have a small diameter, not representative for LWR fuel. The remaining pellets in rods *ThMOX-1* and *ThMOX-3* are composed of the material referred to as “ThUOX” in Table 5.1. This material was designed to provide a neutronic environment for these pellets that would minimise the effects of discontinuities in the macroscopic cross sections at the ends of these short segments. Since the IFE Kjeller labs routinely handle 20% enriched uranium, this was chosen as the fissile component and was mixed with thorium in proportions chosen to give the two materials approximately equal power throughout the irradiation. One rod (rod five – *ThUOX-5*), made of only ThUOX material, was also inserted to provide a reference to rods *ThMOX-1* and *ThMOX-3*. The density of these pellets was initially measured to 94% of the theoretical density (TD), however it underwent very high densification during the early phases of the irradiation and so the density was re-measured on remaining un-irradiated pellets, and found to be about 80% of TD. A possible explanation is the low pressing force used for these pellets.

The remaining two materials are the UOX reference material (rod six - *UOX-6*) and a material representative for the Th-Add concept as modelled by Lau et al. for use in PWRs (rods two and four – *ThAdd-2* and *ThAdd-4*). The diameter of these pellets was chosen as typical for BWR fuel, i.e. significantly larger than that of the Th-MOX pellets. The uranium enrichment in these pellets was chosen so that their power would not be too high compared with that of the Th-MOX, but at the same time high enough to allow for reasonable burnup accumulation rates.

**Table 5.1:** Basic characteristics of the fuel pellets being irradiated in rig IFA-730. Compositions are given as oxide weight percentages.

Fuel type	Th-MOX	ThUOX	Th-Add	UOX
Compositions				
Th content [%]	92.1	42	7	-
Pu content [%]	7.9	-	-	-
U content [%]	-	58	93	100
U enrichment [% U-235]	-	19.8	9.0	8.4
Manufacture parameters				
Pressing force [t/cm <sup>2</sup> ]	4.1	2.5	4.0	4.0
Sintering temperature [°C]	1650	1680	1680	1680
Sintering time [ht]	6	4	4	4
Sintering atmosphere	Wet Ar/H <sub>2</sub>	Dry H <sub>2</sub>	Dry H <sub>2</sub>	Dry H <sub>2</sub>
Diameter [mm]	5.9	5.9	8.48	8.48
Density [% of TD]	97	80	95	97

As shown in Figure 5.1, all rods are instrumented with thermocouples, measuring the  $T_C$  of the pellet stacks. For the rods containing the Th-MOX pellets, these are located so that the thermocouple tip extends to the center of the Th-MOX segment. Pressure bellows with direct communication with the rod interior are mounted on rods *ThAdd-2*, *ThMOX-3*, *ThUOX-5* and *UOX-6*. Changes in pressure cause lateral movement of the bellows, which is converted to an electric signal by transducers mounted in the rig. Similarly, rods *ThMOX-1* and *ThAdd-4* are instrumented with transducers converting the lateral movement of the cladding, caused by its extension and contraction, to electric signals.

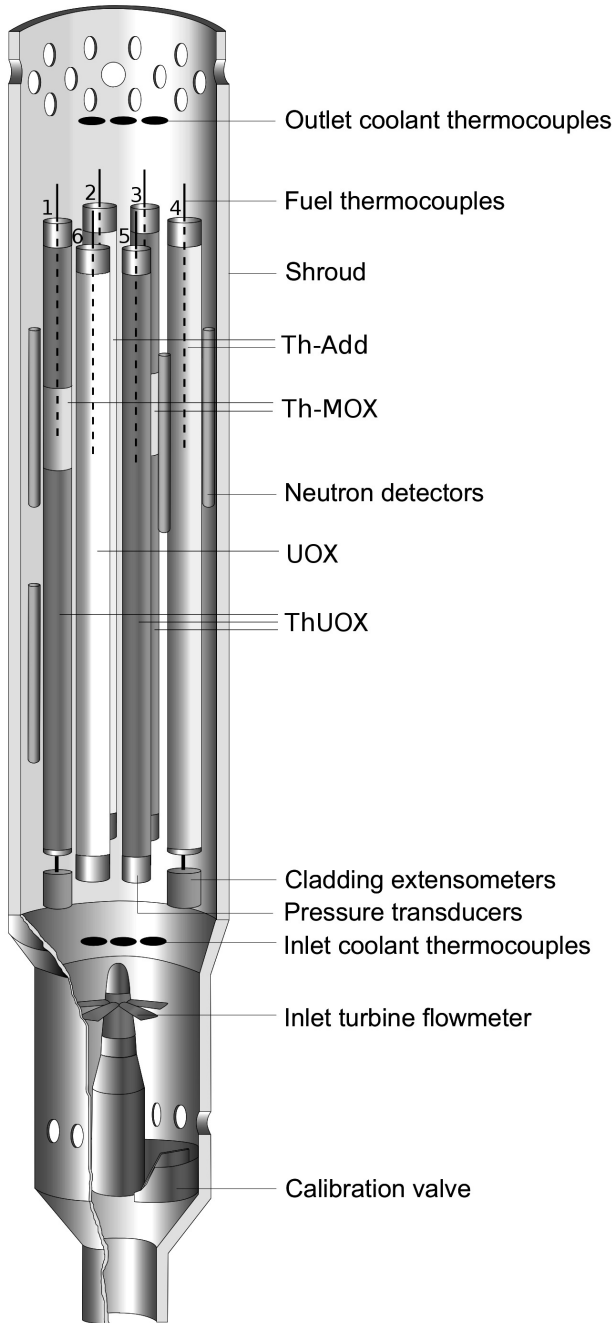


**Figure 5.1:** Schematic image of the testrig IFA-730.

## 5.1.2 Results of the irradiation

At the time of this writing (March 2015), IFA-730 has been under irradiation for 350 days. The rods with BWR dimensions, *ThAdd-2*, *ThAdd-4* and *UOX-6*, have accumulated a burnup of about 17 MWd/kgHM and the small-diameter rods *ThMOX-1*, *ThMOX-3* and *ThUOX-5*, have accumulated about 25 MWd/kgHM. Most of the instrumentation has been working well, with three exceptions. The pressure signal from rod *ThUOX-5* was lost early in the irradiation due to water penetration into the cable. The pressure bellows on rod *UOX-6* initially gave spurious signals, followed by a sudden drop, after which the instrument responded as expected to power changes but showed high absolute values of the rod internal pressure. It can however be expected that the instrument will show when fission gas release (FGR) occurs. Finally, the signal from the thermocouple on rod *ThAdd-2* made an unexpected jump during an early episode when it operated close to its operating limit of 1300°C and has since then given signals difficult to interpret.

The pin powers used for normalization of the measured data are calculated using a rig-internal pin power distribution obtained from simulations with HELIOS (Casal et al. 1991). The input power level of the rig is calibrated using measured values of the coolant flow and temperature at the rig inlet and outlet during the first startup. The calculated radial power distribution between the pins is corrected for a possible flux tilt over the rig quantified by four neutron detectors located in the same horizontal plane as the thermocouples. Finally, the axial power distribution can be calculated using a signal from a fourth neutron detector located at a different axial level. The location of the neutron detectors is shown in Figure 5.1.

The  $T_C$  for the rods with BWR dimensions are plotted in Figure 5.2, normalized to 30 kW/m, which is close to their actual operating LHGR. During the first power ramp, the two Th-Add rods had a lower normalized  $T_C$  than their UOX reference by 20 K and 35 K respectively. After this, cracking, relocation and possibly some damage to the *ThAdd-2* thermocouple caused the normalized temperatures to drift relative to each other. After a shutdown at about 90 days, during which the rig was moved and pellet fragments maybe relocated, the original relation with the Th-Add rods below the UOX reference was re-established, although the very low temperature indicated by the possibly faulty *ThAdd-2* thermocouple may be questioned. Since this result was highly unexpected it was suspected that the power predictions were not accurate enough to resolve such small differences as the ones observed. To assess this, the rig was rotated 180° after 290 days of irradiation. After this, the relation between the normalized temperatures of *ThAdd-4* and *UOX-6* was reversed. The rapid drop of the normalized temperatures of rods *ThAdd-2* and *UOX-6* is unexpected and suggests that the power levels may not be correctly calculated. This implies that the measured normalized temperature difference lies within the experimental error, if the probably erratic *ThAdd-2* signal is disregarded.

However, there is a second way to assess the thermal conductivity of the irradiated materials. When the reactor is scrammed,  $T_C$  exponentially approaches that of the coolant and the time constant for this process gives an independent indication of the conductivity. A high time constant corresponds to a low conductivity and a high  $T_C$ . As

can be seen in Figure 5.3, the time constants for rods *ThAdd-4* and *UOX-6* have the same relation as indicated by the normalized temperatures whereas the comparatively high time constants for rod *ThAdd-2* contradict the very low  $T_C$  measured for this rod, underlining that this thermocouple may indeed be unreliable. These measurements thus reconfirm the previous indication that the Th-Add material initially has a higher conductivity than the UOX rod, whereas the relation is later reversed.

Whereas the matter must of course be further investigated, it should be noted that a higher thermal conductivity for the Th-Add material would be an interesting phenomenon. Assuming a homogeneous mixture of  $\text{ThO}_2$  and  $\text{UO}_2$ , the thermal conductivity should be lower than for pure  $\text{UO}_2$ , since the  $\text{ThO}_2$  acts as a phonon-scattering impurity in the lattice, just like  $\text{PuO}_2$  in a  $\text{ThO}_2$  matrix, as discussed in Section 5.2.2. Unfortunately, no direct measurement of the thermal conductivity of  $(\text{Th,U})\text{O}_2$  with such low  $\text{ThO}_2$  fraction could be found in the literature. A hypothesis that may explain the observed behaviour is that the mixture of  $\text{ThO}_2$  and  $\text{UO}_2$  in this fuel is very inhomogeneous, possibly leading to a “network” of more well-conducting  $\text{ThO}_2$ -rich regions between less well-conducting  $\text{UO}_2$ -rich regions.

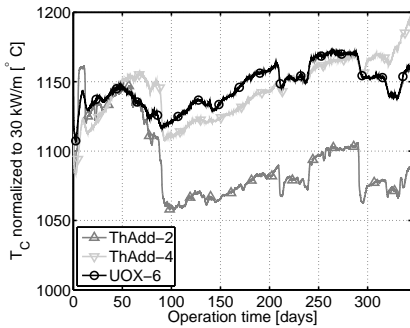


**Figure 5.2:** Measured  $T_C$  for rods *ThAdd-2*, *ThAdd-4* and *UOX-6*.

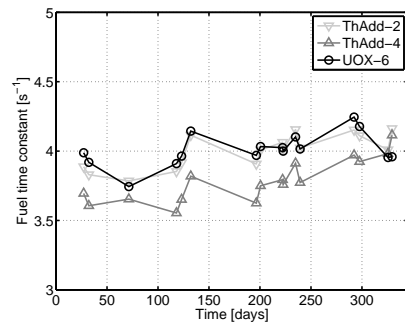


**Figure 5.3:** Scram time constants for rods *ThAdd-2*, *ThAdd-4* and *UOX-6*.

The Th-MOX rods and their reference operate at a lower LHGR than the Th-Add and UOX pins, about 20 kW/m, due to their smaller diameter. Their respective  $T_C$ , normalized to this power level, are plotted in Figure 5.4. This figure shows a simpler burnup dependence of  $T_C$  compared with Figure 5.2, possibly indicating less cracking and relocation. For the Th-MOX rods,  $T_C$  increases almost linearly, an effect of the slow decrease of the thermal conductivity caused by irradiation damage to the fuel matrix. For rod *ThUOX-5*, the normalized  $T_C$  starts at a much higher temperature due to the low conductivity of this material caused by its low density.  $T_C$  then increases rapidly as the low density material resinters during the first months of operation, increasing the pellet-cladding gap size. After this, it increases linearly at approximately the same rate as the Th-MOX rods. The scram time constants shown in Figure 5.5 confirm the recorded behaviour.

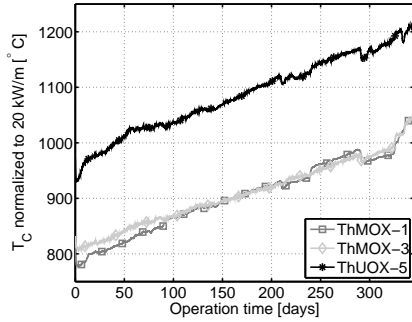


**Figure 5.4:** Measured  $T_C$  for rods *ThMOX-1*, *ThMOX-3* and *ThUOX-5*.

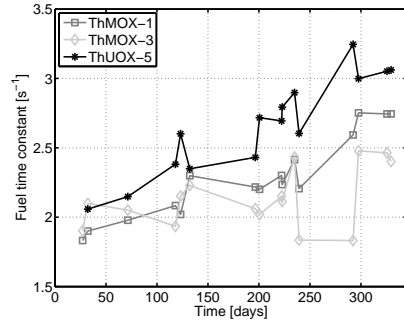


**Figure 5.5:** Scram time constants for rods *ThMOX-1*, *ThMOX-3* and *ThUOX-5*.

The cladding elongation registered for rods *ThMOX-1* and *ThAdd-4* is plotted in Figure 5.6. The slow and approximately linear elongation is due to normal irradiation swelling of the cladding material. The discontinuity at about 90 days coincides with the shutdown period during which the rig was moved, and is probably a consequence of the forces acting on the rig in connection with this. The rapid increase seen for rod *ThAdd-4* at about 300 operation days indicates that there is some contact between the pellet and the cladding, causing the cladding to expand at the same rate as the fuel during the power ramps that took place at this point in the irradiation. The rapid elongation was partly reversed by relaxation of the cladding material in connection with a shutdown at 340 days, indicating that the pellet-cladding gap is not firmly closed yet. The low pressure at which the Halden reactor operates does not cause the cladding to creep inwards towards the fuel to the same extent as it does in most commercial reactors. The current burnup is quite typical for detecting the first signs of impending gap closure for UOX fuel irradiated in the Halden reactor.

The fact that the first indications of gap closure for rod *ThAdd-4* almost coincide with the rig rotation at 290 days further complicates the interpretation of the temperature readings. Given the similarity between rods *ThAdd-4* and *UOX-6*, it is reasonable to assume that gap closure would occur at approximately the same time. Gap closure generally gives a drop in the normalized  $T_C$ , similar to what was recorded in connection with the rig rotation.

Finally, the pressure recorded for rods *ThAdd-2*, *ThMOX-3* and *UOX-6* is plotted in Figure 5.7, normalized to zero power and room temperature. The pressure for rod *ThMOX-3* behaves as expected, increasing slowly as the fuel material swells with increasing irradiation exposure. Similarly to the temperature recordings for rods *ThAdd-2* and *UOX-6*, the pressure signals from these rods drift relative to each other in an unexpected manner, but settles for a more predictive behaviour after the shutdown at 90 days. As mentioned, the pressure bellows on rod *UOX-6* showed erratic behaviour at the beginning of the irradiation, so the absolute value of the recorded pressure is likely not accurate.

However, all three rods almost simultaneously show indications of FGR at about 320 days. This coincides with a power ramp, a situation which is known to trigger FGR. It also occurs at a burnup and temperature typical for FGR, so once again, normal behaviour is confirmed. It should be recalled that the FGR in rod *ThMOX-3* is dominated by the low-density ThUOX material, and is thus not representative of Th-MOX behaviour.

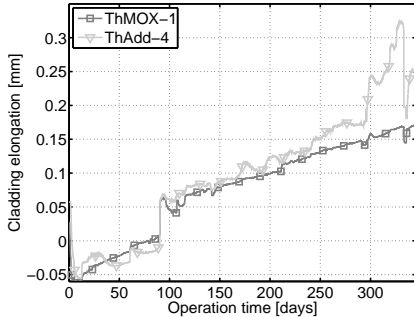


**Figure 5.6:** Cladding elongation measured for rods *ThMOX-1* and *ThAdd-4*.

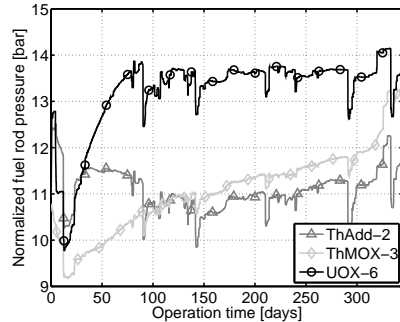


**Figure 5.7:** Fuel rod pressures measured for rods *ThAdd-2*, *ThMOX-3* and *UOX-6*.

The most interesting indication so far from this irradiation is that the temperature of the Th-Add rods may be lower than that of the UOX rod. It also seems, from the pressure readings, that the Th-Add behaviour with regards to FGR is similar to that of UOX fuel. The first indications of gap closure at rod *ThAdd-4* also occurs at a typical burnup. For the Th-MOX rods, the most useful result is the recorded  $T_C$ . This can be compared with theoretical prediction, which is the subject of the following section. The fact that the Th-MOX material only constitutes a minor part of the rods in which it is irradiated makes it impossible to draw any conclusions from the pressure and cladding elongation data, since these signals are dominated by the filler material.

## 5.2 Fuel performance modelling and benchmarking

A crucial aspect in the licensing of a nuclear fuel for use in a commercial reactor is that its thermal-mechanical behaviour can be accurately predicted for all operation conditions and at any burnup up to the projected discharged burnup. Such predictions are routinely made by fuel performance codes, making use of established correlations for the fuel material properties and their dependence on most importantly temperature, but also on burnup and the composition of the fuel. The material behaviour is also closely related to the neutronic behaviour of the fuel through the spatial distribution of the power generation within the fuel. Several well established codes exist for the prediction of UOX fuel behaviour, and most of them can also be used for U-MOX fuel. A version of the well-established code FRAPCON has also been written for prediction of (Th,U)O<sub>2</sub> fuel performance (Long et al.

2004) and recently several efforts have been directed towards the modelling of Th-MOX, e.g. by Mieloszyk et al. (2014). An earlier effort to model Th-MOX was also made within the OMICO project (Verwerft et al. 2007).

Given the uncertainties in many of the material property correlations, in particular regarding their burnup dependence, and the simplifications that are necessarily made in the codes, thorough validation through comparison with experimental data is necessary. The described irradiation experiment is intended to form part of the basis for such a validation. The efforts made to write and validate a fuel performance code for modeling of Th-MOX fuel are described in this section.

### 5.2.1 FRAPCON 3.4

The fuel performance code FRAPCON 3.4 (Geelhood et al. 2011a) has been developed for the USNRC and is used for fuel performance simulations for regulatory control. This code was used as a basis for the development of a fuel performance code for Th-MOX. FRAPCON 3.4 calculates temperature, pressure and deformation of an LWR fuel rod for steady-state operation, up to the highest burnups typical for LWR fuel. The state of the fuel rod is determined for each time step by iterative calculations until the fuel-cladding gap temperature difference and the rod internal gas pressure converge (Geelhood et al. 2011a).

FRAPCON 3.4 has a modular structure with a specific subroutine for calculation of each material property. The subroutines related to the fuel material properties have been modified as described in Paper VIII. Dependence of the material properties on density, stoichiometry and burnup has been included to the largest possible extent. Where data are lacking for Th-MOX, a best estimate has been made based on the available literature and corresponding correlations for U-MOX. The subroutine related to FGR has been left unmodified due to the lack of relevant experimental data to support a new model, but its importance is recognized and briefly discussed in Section 5.2.3. The subroutine for prediction of the radial distribution of the power generation within the fuel pin has been updated as discussed in Paper VII and outlined in Section 5.2.4. Other subroutines, related to the properties of water, the gas mixture in the fuel-cladding gap and the cladding material are left unmodified.

FRAPCON 3.5 was released during the course of the development work. The differences between the results as calculated by FRAPCON 3.5 and FRAPCON 3.4 were negligible after the same material property subroutines were modified for both codes. Since the modified subroutine for radial power profile prediction could not be directly implemented in FRAPCON 3.5, it was decided that FRAPCON 3.4 would be kept as the base for the development work, for the time being.

## 5.2.2 Material properties

The good material properties of thorium oxide have formed the basis for the assumption that thorium based fuel should be able to operate to higher discharge burnup. Whereas many investigations on the material properties of UOX and to some extent also U-MOX fuel have been carried out, much less information is available about thorium based fuel. There is some information available on the properties of  $(\text{Th,U})\text{O}_2$ , although not for mixtures with  $\text{ThO}_2$  fractions below 50%, which is unfortunate given the compositions typical for the proposed Th-Add concept. The knowledge base of Th-MOX fuel was until recently very small (Bakker et al. 1997), but has been significantly expanded by measurements performed at the JRC-ITU in the last years (Böhler et al. 2015; Cozzo et al. 2011; Vălu et al. 2014). The details of the material property correlations can be found in Paper VIII, and the most important features, related to those of  $\text{UO}_2$  are:

- Lower thermal expansion, putting less strain on the cladding during temperature increases when the pellet-cladding gap is closed, but also leaving a larger pellet-cladding gap early in life. The used correlation is plotted in Figure 5.8.
- A higher melting point; approximately 700 K higher for a composition with 8% plutonium, see Figure 5.9.
- Lower heat capacity, giving a smaller stored heat to be cooled off in transient scenarios, but also a faster fuel temperature increase in a reactivity insertion accident, see Figure 5.10.
- Higher thermal conductivity for compositions up to about 8% plutonium, see Figure 5.11.

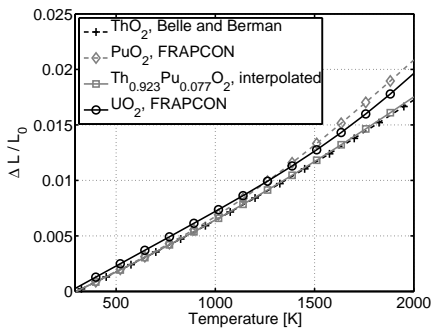


**Figure 5.8:** Thermal expansion of  $\text{ThO}_2$ ,  $\text{PuO}_2$ ,  $\text{UO}_2$  and the present Th-MOX material.

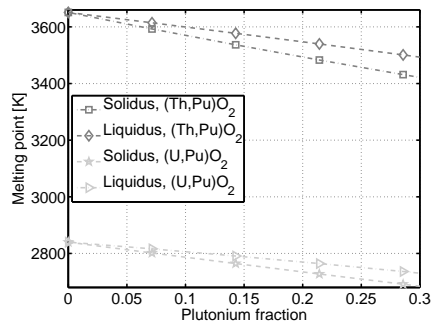


**Figure 5.9:** Solidus and liquidus temperatures for  $\text{Th}_{1-y}\text{Pu}_y\text{O}_2$  and  $\text{U}_{1-y}\text{Pu}_y\text{O}_2$  for  $\text{PuO}_2$  fractions lower than 30%.

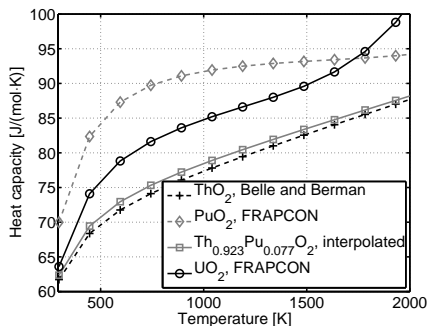


**Figure 5.10:** Heat capacity for  $\text{ThO}_2$ ,  $\text{PuO}_2$ ,  $\text{UO}_2$  and the present Th-MOX material.

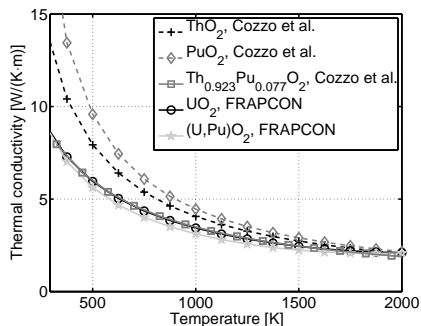


**Figure 5.11:** Thermal conductivity for  $\text{ThO}_2$ ,  $\text{PuO}_2$ ,  $\text{UO}_2$ , U-MOX fuel and the present Th-MOX material.

Equations for these curves are given in Paper VIII, further discussed in Section 5.2.5.

The thermal conductivity deserves a more thorough discussion since it is the most important material property, having a strong influence on the fuel temperature. It is noted that the correlation used in FRAPCON for the thermal conductivity of U-MOX fuel includes no dependence on the  $\text{PuO}_2$  fraction, whereas it can be seen that already a small addition of  $\text{PuO}_2$  to the  $\text{ThO}_2$  matrix causes a strong reduction of the thermal conductivity. This is primarily due to the fact that the reduction of the thermal conductivity depends on the relative mass difference and the relative lattice parameter difference between the two components (Cozzo et al. 2011). These differences are larger for the (Th,Pu) $\text{O}_2$  case than for the (U,Pu) $\text{O}_2$  case. The general conclusion is that the thermal conductivity of thorium based fuels is higher than that of uranium based fuels only under certain conditions.

### 5.2.3 Fission gas release

The fuel temperature is the driving force behind the processes, most importantly FGR, that limit the lifetime of the fuel. The onset of FGR depends largely on the diffusion rate of fission gases in the fuel matrix. The diffusion rates depend on the fuel material and are inherently lower for  $\text{ThO}_2$  than for  $\text{UO}_2$ . There is also a strong dependence on the fuel temperature, and the lower FGR seen in Th-MOX fuels (Karam et al. 2008) is mostly attributed to the lower temperature caused by the higher thermal conductivity.

Fission gases are generally modeled as being released in a stepwise process. First, the fission gas atoms are formed by fission reactions after which they migrate through the fuel matrix, ultimately being trapped at grain boundaries. There, fission gas bubbles are formed, which eventually interconnect. When a direct connection is formed with the pellet surface, the fission gases are released. This often happens in connection with power ramps,

during which the heated gases expand, putting additional strain on the fuel material. The many processes involved depend not only on the diffusion rates and fuel temperature, but also on the fission gas generation rates, the fuel microstructure and other factors. The complexity of the process makes it necessary to benchmark against experimental data. Given the very scarce data available, and in particular since no Th-MOX FGR data can be obtained from IFA-730, the development of a FGR model for Th-MOX fuel has been left for later. A new FGR model has been developed for (Th,U)O<sub>2</sub> fuel and benchmarked against existing irradiation data for this fuel type by (Long et al. 2002). The model employed for Th-MOX fuel will most likely be similar.

## 5.2.4 Radial power profiles - Paper VII

The neutronic differences between Th-MOX and UOX fuels have a direct impact on the fuel performance simulations through the radial variations of the power production within the fuel pin. This necessitates an adaptation of the subroutine determining the radial power profile in FRAPCON 3.4.

The original model for radial power profile prediction in FRAPCON 3.4, called TUBRNP (TransUranus BuRnuP equations, adopted from the fuel performance code TRANSURANUS), uses a one-group diffusion approximation for the neutron flux, solving the equation analytically assuming a homogeneous distribution of all isotopes within the fuel. This approximation is judged to hold sufficiently well for UOX fuel, and is also used for U-MOX fuel. Isotopic concentrations are determined for each radial node and local power generation is calculated from the flux and the macroscopic fission cross sections. The radial distribution of the Pu-239 production is described by an empirically derived shape function which is multiplied with the average U-238 concentration when calculating local concentrations of U-238 and Pu-239 for the power profile determination.

The first step in the adaptation to Th-MOX fuel was to extend the list of isotopes being accounted for in the evaluation with the isotopes relevant for Th-MOX fuel i.e. Th-232, U-233, U-234, U-236 and Pu-238. The Monte Carlo-based neutronic code *Serpent* (Leppänen 2012) was used to calculate power profiles for Th-MOX fuel, and it was found that these were not well reproduced by the current solution model. The radial power profiles in Th-MOX pins differ significantly from those of UOX fuel in two respects:

- The high absorption cross section for thermal neutrons in Th-232 gives a strong shielding effect for thermal neutrons, resulting in a power profile early during irradiation which is more strongly peaked towards the pellet periphery, compared with that of UOX fuel. Also the plutonium isotopes, most notably Pu-240, have large resonances around 1 eV, enhancing this effect.
- The smaller resonance capture in Th-232 gives a weaker shielding effect for epithermal neutrons, compared with UOX fuel. This gives a more homogeneous buildup of new fissile material (U-233) in the fuel pin, giving a less periphery-peaked power profile at higher burnup.

The differences between the power profiles of the respective fuel types are illustrated in Figure 5.12.

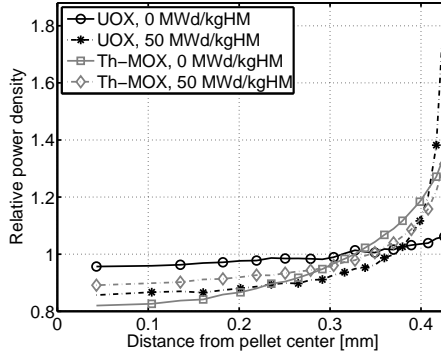


**Figure 5.12:** Radial pellet power profiles for UOX and Th-MOX fuel at 0 and 50 MWd/kgHM. The UOX fuel is enriched to 5% and the Pu concentration in the Th-MOX fuel is 8% with 80% Pu-239.

In order to calculate more representative power profiles while maintaining the simplicity of the TUBRNP subroutine, it was decided to stay with the one-group diffusion approximation, but to solve it numerically, accounting for the radial variation of the concentration of each isotope. The adopted solution scheme was the finite difference method with the boundary conditions of zero neutron current at the pellet center and the scalar flux at the pellet periphery equal to a normalization constant.

The one-group approximation cannot account for the fact that the presence of one isotope affects the flux which in turn affects the reaction rates for other isotopes. For example, the presence of Pu-239 hardens the spectrum since many thermal neutrons are absorbed by Pu-239, and the harder spectrum makes the one-group capture cross section of Th-232 lower than it would have been with no Pu-239 present. Neither can the approximation account for the radial variation in the neutron spectrum which is the direct consequence of the thermal shielding effect of Th-232, absorbing thermal neutrons already at the periphery of the pin and leaving less thermal neutrons to cause fissions at the center of the pin. The shielding effect thus cannot be directly modelled by the one-group diffusion approximation.

However, the application of TUBRNP for Th-MOX is fairly narrow. Only a small range of pin radii, a relatively small set of fuel compositions and neutron spectra typical for either LWRs or heavy water reactors need to be considered<sup>1</sup>. A sensitivity study was made, concluding that the pellet radius and composition and the neutron spectrum were the only parameters significantly affecting the power profile (Fredriksson 2014). This

<sup>1</sup>The type of reactor, LWR or HBWR (The Halden research reactor) is specified by a switch in the FRAPCON input.

means that the solution can be fine-tuned to fit the specific application, which was done by two means. Firstly, the numerical values of the one-group cross sections were adapted to give the best possible results. Furthermore, new shape functions were derived for the most significant isotopes, Pu-239 and Th-232. Since the diffusion equation was solved numerically, allowing for different cross sections in different nodes, the shape functions were multiplied directly with the macroscopic cross sections. This differs from the original scheme in FRAPCON 3.4, where the shape functions were only used in the step where the isotopic concentrations were updated.

The adaptation of the numerical values of the one-group cross sections was made by means of a genetic algorithm, as described in Paper VII. The process is described in more detail by Fredriksson (2014). Reference power profiles at burnups up to 70 MWd/kgHM were calculated with *Serpent*, for a set of 61 different pin configurations representing a realistic range of plutonium isotope vectors, plutonium fractions and pin radii, in LWR conditions. A second reference set was generated for the conditions in the Halden research reactor, given that test irradiation data from this reactor will be used for benchmarking. The genetic algorithm was then used for adjusting the one-group cross sections and the shape function parameters used in TUBRNP, so that the reference data were reproduced as closely as possible.

The initial guess for the one-group cross sections was based on the corresponding values used by Long (2002) in the THUPS subroutine, which is a version of TUBRNP adapted for (Th,U)O<sub>2</sub> fuel performance simulations. It has to be noted that the differences between the adjusted set of cross sections and this initial guess were expected to be small, but this was not the case. Whereas some of the cross sections remained similar, others, such as the capture cross section of Pu-240, were widely different from their original values, indicating that these simplified neutronic calculations did not correctly model isotopic concentrations or reaction rates. Nevertheless, the reference power profiles generated by *Serpent* were well reproduced, so the new model and modified cross sections were adopted. However, the new TUBRNP version is to be regarded as empirical, so only the calculated power profiles and not the isotopic concentrations are to be used.

### 5.2.5 Comparison with irradiation data - Paper VIII

The modified FRAPCON 3.4 version was used in its current state of development to calculate the fuel centerline temperatures of the Th-MOX rods currently being irradiated in IFA-730. Input files were generated using all the data available for the irradiated pellets and their cladding. As a reference, also the *UOX-6* pin was modelled, using the original FRAPCON 3.4. The power histories were taken from the corrected and calibrated HELIOS calculations made by IFE, but increased by 12%, in order for the calculated power of the *UOX-6* pin to agree with the measured data. There are two justifications for this adjustment:

Firstly, there is an uncertainty of about 5% in the calibration of the total rig power (not affecting the power distribution between the individual pins in the rig). The systematic

underprediction of the temperatures for all fuel rods when using the power levels given by IFEs calculations indicated that the total rig power is indeed higher than assumed, which motivates the use of a higher power for the temperature calculations.

Secondly, FRAPCON 3.4 is known to underpredict fuel temperatures for Halden research reactor conditions by up to about 7% (Geelhood et al. 2011b). The exact reason for this is unknown, but it is likely that a systematic underprediction at Halden irradiation conditions would affect UOX rods and Th-MOX rods similarly, which is why the input power is adjusted in order to eliminate this factor.

The fuel temperatures calculated with the adjusted power history are plotted in Figure 5.13 together with the measured data. It can be seen that the calculated temperatures for the Th-MOX rods are underpredicted by about 30 K, which could be explained by the fact that the ThUOX filler material located above and below the Th-MOX pellets has a considerably higher temperature, heating also the Th-MOX pellets through heat conduction in the axial direction. It can also be noted that the temperature predicted by FRAPCON 3.4 for the UOX fuel remains good until about 300 irradiation days, after which the temperature is clearly overpredicted. A possible explanation is that the pellet-cladding gap has closed, greatly improving heat conductance from the pellet to the coolant. FRAPCON 3.4 does not predict gap closure yet for this fuel pin, but the indications that the gap is nearly closed for rod *ThAdd-4* strengthen this hypothesis.

Initially, a trend of increasing underprediction of the Th-MOX rods was clearly seen, growing to almost 100 K within the current irradiation period, that is to a burnup of 25 MWd/kgHM. Since the agreement between the calculated and measured temperatures was good at the beginning of life, causes were sought among the burnup dependent factors affecting the fuel centerline temperature. A sensitivity analysis was performed, including the effects of swelling, relocation, power profile prediction and the burnup dependent term in the expression for the thermal conductivity. Causes were also sought in the neutronic modelling used for the power predictions, since an error in the predicted power of the Th-MOX segments relative to the other materials would give an error in the calculated temperature which is based on the predicted power history. It was concluded that none of the three former factors could account for the observed underprediction, whereas an increase of the burnup dependent factor of the thermal conductivity resulted in the fair agreement shown in Figure 5.13. No error could be found in the neutronic simulations, and the scram time constants plotted in Figure 5.5 strengthen the hypothesis that the increasing temperature is a real phenomenon, since these are independent of the power levels. As can be seen, the time constants for the Th-MOX rods are increasing with burnup, indicating a decreasing thermal conductivity (the two unexpectedly low time constants for rod *ThMOX-3* at 240 and 292 days have very large uncertainties). However, it cannot be excluded that a gradual increase in the temperature contribution from the axial heat conduction from the ThUOX material causes part of the observed increase of the underprediction, so a good estimate of the burnup dependent term in the expression for the thermal conductivity cannot be made based on only this set of experimental data.

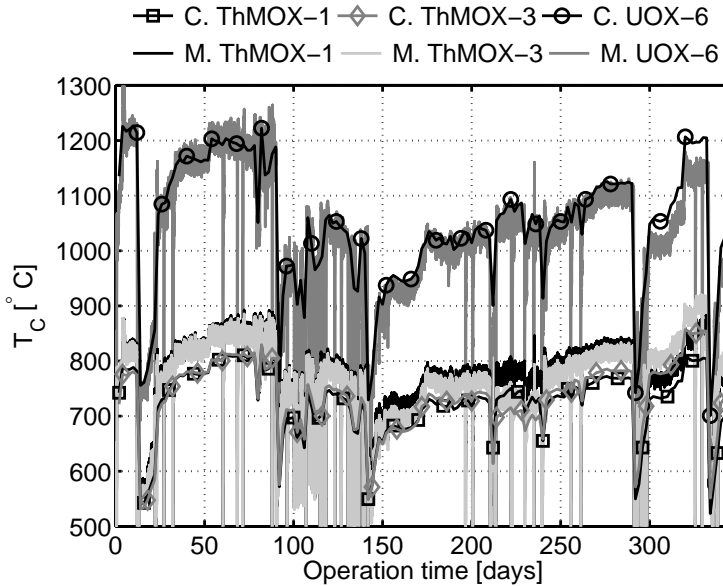


**Figure 5.13:** Calculated (C) and measured (M) fuel centerline temperatures for rods *ThMOX-1*, *ThMOX-3* and *UOX-6*.

The conclusion of the work so far is that existing data for fresh Th-MOX material<sup>2</sup>, combined with the new model for radial power profile predictions and the simulation methodology of FRAPCON 3.4 as a whole, are adequate for predicting the temperature of fresh Th-MOX material. The current results indicate that an increase of the burnup dependence of the thermal conductivity of Th-MOX gives adequate predictions also at higher burnups. The implication that the thermal conductivity of the Th-MOX material decreases more rapidly with burnup than that of UOX material is reinforced by the time constant measurements. This would cast some doubt on the previously held assumption that Th-MOX fuel can indeed sustain higher burnups than UOX and U-MOX fuel. However, this is only one data set and, as noted, the experimental uncertainties are large. Additional test irradiation data sets, preferably on full Th-MOX rods, are required in order to disentangle the many different factors affecting the fuel temperature. As previously noted, several other types of behaviour such as FGR and dimensional changes also remain unaddressed. Hence, much more validation work is needed before the code can be used for fuel performance predictions in a commercial context.

<sup>2</sup>It should be noted that the irradiated pellets are from the same batch that was used for the determination of the implemented thermal conductivity correlation, i.e. in the work by Cozzo et al. (2011). The calculated thermal conductivity can thus be expected to correspond very well to the conductivity of the irradiated pellets, but possibly worse for other pellets.

---

---

# CHAPTER 6

---

## SUMMARY AND FUTURE WORK

*In this final chapter, the previous chapters are summarised and the results are discussed from the perspective of how well the goal stated in Chapter 1 is fulfilled. Finally, some relevant research activities are outlined which would be suitable for complementing and extending the work presented.*

### 6.1 Summary

The initially stated goal of the work reported in this thesis was to take some of the steps remaining before thorium based nuclear fuels can be commercially used in LWRs. Two research areas were identified as most relevant in order to both provide motivation for using thorium based fuel and to expand the knowledge base for thorium fuel where needed to provide a basis for nuclear fuel licensing. These were the neutronic behaviour and the thermal-mechanical behaviour of thorium-containing fuels. The whole process and the conclusions are summarised below.

#### 6.1.1 Choice of fuel types

At the outset, several different thorium containing fuel types were considered. An initial scoping study singled out thorium-plutonium fuel (Th-MOX) as the most interesting alternative (Paper I). One reason for making this decision was that the fuel seemed to

have neutronic properties similar to those of commonly used U-MOX fuel, i.e. using it in LWRs seemed feasible. The other reasons were rather related to considerations of nuclear waste management and possible transitions to purely thorium based breeding fuel cycles in LWRs.

Another approach, to use thorium as an additive in BWR UOX fuel (Th-Add), was also investigated, inspired by corresponding calculations carried out for PWRs. This alternative has to date been investigated to a much lesser extent, but preliminary indications are that the requirements for burnable absorbers can be significantly reduced, improving bundle-internal power peaking factors. The high conversion in Th-232 leads to smaller reactivity differences between fresh and irradiated fuel and consequently smaller core power peaking factors and larger shutdown margin.

### 6.1.2 Neutronic properties of Th-MOX fuel

A necessary prerequisite for the licensing of thorium based fuels is to provide confidence that the neutronic behaviour of the fuel can be adequately modeled (Paper II). A step in this direction was taken through the participation in a benchmarking activity, where predictions of four different codes were compared with experimental data. Due to experimental uncertainties, the benchmark exercise could not fully satisfy its goal to provide confidence in the modelled results through experimental confirmation. Nevertheless, two conclusions could be made regarding the performance of CASMO-5. One is that the power of Th-MOX fuel relative to that of U-MOX fuel was predicted similarly by three of the codes, including CASMO-5, which provides some confidence in this respect. Furthermore it was concluded that the radial distribution of the reaction rates characteristic to the thorium chain were not well modeled, an issue which has been attended to in later releases of CASMO-5.

The neutronic properties of Th-MOX fuel were further investigated using CASMO-5. PWR lattice simulations confirmed its similarity with U-MOX, with the exception of the coolant void reactivity, which was significantly more negative for Th-MOX than for U-MOX at high plutonium contents (Paper III). It was also noted, for both MOX fuel types, that the high conversion could give rise to advantages in the context of operating cycle extensions. Thus, full-core simulations were performed investigating this possibility, and the conclusions were that this application of Th-MOX fuel seems indeed to be feasible (Paper IV).

It is generally known that plutonium containing fuel benefits from a higher moderation ratio than UOX fuel, and the possibility to increase the moderation in a BWR fuel assembly has been investigated. It was concluded that both the energy generated from a fixed amount of plutonium and the incinerated fraction of the loaded plutonium could be increased in this way. Acceptable safety parameters, as evaluated by neutronic lattice simulations, were obtained, but the discharge burnup of the fuel assembly had to be significantly increased to reach this result (Paper V).

### 6.1.3 Thermal-mechanical properties of thorium fuel materials

Th MOX pellets and material representative of the Th-Add application have been irradiated in the Halden research reactor (Paper VI). The conclusions for the Th-Add material is that it behaves similarly to UOX fuel and may, surprisingly, exhibit lower fuel temperatures. The recorded centerline temperatures of the Th-MOX pellets have been used for initial validation of a thermal-mechanical fuel performance code for Th-MOX fuel.

The fuel performance code FRAPCON 3.4 has been modified, introducing new algorithms for calculations of pellet power profiles (Paper VII) and Th-MOX material properties. The initial validation shows good reproduction of fresh fuel temperatures, and assuming a faster decrease of the thermal conductivity of the Th-MOX material the predictions are also good for higher burnups (Paper VIII).

### 6.1.4 Conclusion

It can be concluded that the stated goal has been fulfilled since some steps have indeed been taken towards the commercial use of thorium fuels in LWRs:

- The experience base for neutronic modelling of thorium based fuel has been extended and some conclusions could be drawn which have lead to improved modeling of thorium based fuel in CASMO-5.
- Detailed full-core simulations of Th-MOX fuel have been performed, indicating the feasibility of Th-MOX fuel use for operating cycle extension, providing a motivation for reactor owners to consider this alternative.
- A novel concept for thorium use as an additive to UOX fuel for BWRs has been developed, providing another potentially attractive option for thorium fuel usage.
- The scarce irradiation experience of thorium based fuel has been extended through an instrumented irradiation experiment performed in the Halden research reactor.
- The work towards establishing a fuel performance code for prediction of thermal-mechanical performance of thorium based fuel has been initiated.

## 6.2 Future work

Some of the work described herein is currently being extended with continued research. These projects include:

- The irradiation of IFA-730 is ongoing, accumulating more data and higher burnup information. The project is scheduled to continue at least until 2017.
- Th-MOX fuel manufacture is being prepared at the IFE Kjeller, with the first Th-MOX trial run scheduled for March 2015.
- A second phase of the irradiation program is being planned, including Th-MOX pellets manufactured at IFE Kjeller and two more (Th,U)O<sub>2</sub> compositions representative of the BWR application.
- The reasons for the unexpected signals from the irradiated Th-Add rods in IFA-730 are being sought by more detailed modelling.
- The detailed properties of Th-Add fuel is being evaluated by full-core simulations, using a model of a currently operating BWR.

In addition to these ongoing projects, the following research activities would be highly relevant for taking the next steps towards thorium fuel adoption:

- The thermal conductivity of (Th,U)O<sub>2</sub> with low ThO<sub>2</sub> fractions should be measured directly, since there is a paucity of data for these compositions.
- The development of a fuel performance code for Th-MOX must be finished, and complemented with a code for transient fuel performance simulations.
- The detailed properties of spent thorium fuels must be evaluated from the viewpoint of intermediate and possibly also final storage.
- The argument that thorium fuel usage in today's LWRs is a step towards later adoption of advanced breeding LWRs is of course only valid if reprocessing technology for thorium based fuel is being developed. Research on the THOREX process is being done in India, but parallel efforts may be relevant.

## ACKNOWLEDGEMENTS

I would like to thank the people that have been directly involved in the process of, ultimately, making this PhD thesis a reality. Imre Pázsit for warmly welcoming me back to academia after my brief visit to the outside world, Valentin Fhager for initially defining the project (although it has been redefined multiple times after that) and guiding me through its early phases, and Christophe Demazière for being a helpful supervisor and patiently improving my understanding of neutronics.

I would also like to thank the many people who have in different ways been involved in the research projects I have had the pleasure to participate in. Many of you appear as co-authors of the appended papers - thank you, all of you. I would like to specially mention Cheuk Wah Lau for spawning the first Th-Add idea, Sture Helmersson for sharing his immense knowledge of BWR fuel design, Joe Somers for his wise thoughts on fuel materials and Laura Kekkonen for promptly, accurately and friendly answering every thinkable question regarding fuel performance modelling and irradiation. If I start naming all friends and colleagues at IFE who have been crucial in making the IFA-730 experiment come true, I will not know where to stop. Please accept my gratitude as a collective.

None of this research whatsoever would have been conducted if it had not been for my dear colleagues at Thor Energy and their tireless hunt for sponsors and partners for realizing the research program of which this thesis forms a part. Thank you, Lise Chatwin Olsen, Julian Kelly, Saleem Drera and last but definitely not least Øystein Asphjell for supporting me all the way through this, trusting me with great responsibilities and always encouraging me.

The Norwegian Research Council also deserves thanks for supporting me economically through the industrial PhD Program, and the “Kungliga och Hvitfeldtska stiftelsen” for supporting my stay at Villa Martinson, without which this thesis would have remained half-written.

I want to thank both former and present colleagues and co-students at Chalmers for all the nice moments of coffee, collaboration, cakes, help, parties and just plain silent working side by side. I want to thank my parents for a lot of things, but right now, most importantly, for imprinting in me that everything is doable with a little (or a lot of) effort. I want to thank all of my family for helping me and bearing with me when I have been absorbed by this work, and I want to direct my most sincere thanks to my beloved husband Martin for supporting me, no, carrying me, all the way... Thank you so much.

---

# REFERENCES

- Ade, B., A. Worrall, J. Powers, S. Bowman, G. Flanagan, and J. Gehin (2014). *Safety and regulatory issues of the thorium fuel cycle*. Tech. rep. NUREG/CR-7176, ORNL/TM/2013/543. United States Nuclear Regulatory Commission.
- Arkhipov, V. (2000). *Thorium based fuel options for the generation of electricity: Development in the 1990s*. Tech. rep. IAEA-TECDOC-1155. International Atomic Energy Agency.
- Bakker, K., E. H. P. Cordfunke, R. J. M. Konings, and R. P. C. Schram (Nov. 1997). Critical evaluation of the thermal properties of  $\text{ThO}_2$  and  $\text{Th}_{1-y}\text{U}_y\text{O}_2$  and a survey of the literature data on  $\text{Th}_{1-y}\text{Pu}_y\text{O}_2$ . *Journal of Nuclear Materials* **250**.1, 1–12.
- Baldova, D., E. Fridman, and E. Shwageraus (2014a). High conversion Th-U233 fuel for current generation of PWRs: Part I – Assembly level analysis. *Annals of Nuclear Energy* **73**, 552–559.
- Baldova, D., E. Fridman, and E. Shwageraus (2014b). High conversion Th-U233 fuel for current generation of PWRs: Part II – 3D full core analysis. *Annals of Nuclear Energy* **73**, 560–566.
- Baumer, R. and I. Kalinowski (1991). THTR commissioning and operating experience. *Energy* **16**.1–2, 59–70.
- Belloni, F. et al. (2012). Neutron-induced fission cross section measurement of  $^{233}\text{U}$ ,  $^{241}\text{Am}$  and  $^{243}\text{Am}$  in the energy range  $0.5 \text{ MeV} \leq E_n \leq 20 \text{ MeV}$  at n\_TOF at CERN. *Physica Scripta* **2012**.T150, 014005.
- Böhler, R., P. Çakır, O. Beneš, H. Hein, R. Konings, and D. Manara (2015). High temperature phase transition of mixed ( $\text{PuO}_2+\text{ThO}_2$ ) investigated by laser melting. *The Journal of Chemical Thermodynamics* **81**, 245–252.
- Bucher, R. (2009). *India's Baseline Plan for Nuclear Energy Self-sufficiency*. Tech. rep. ANL/NE-09/03. Argonne National Laboratory.
- Caner, M. and E. T. Dugan (2000). ThO<sub>2</sub>-UO<sub>2</sub> annular pins for high burnup fuels. *Annals of Nuclear Energy* **27**.9, 759–770.

- Casal, J., R. Stammler, E. Villarino, and A. Ferri (1991). “HELIOS: Geometric Capabilities of a New Fuel Assembly Program”. *Intl. Topical Meeting on Advances in Mathematics, Computations and Reactor Physics*. Pittsburgh, Pennsylvania, USA.
- Chadwick, M. et al. (2006). ENDF/B-VII.0: Next Generation Evaluated Nuclear Data Library for Nuclear Science and Technology. English. *Nuclear Data Sheets* **107**.12, 2931–3060.
- Clayton, J. (Oct. 1993). *The Shippingport Pressurized Water Reactor and Light Water Breeder Reactor*. Tech. rep. WAPD-T-3007. Westinghouse Bettis Atomic Power Laboratory.
- Cozzo, C., D. Staicu, J. Somers, A. Fernandez, and R. Konings (Sept. 2011). Thermal diffusivity and conductivity of thorium-plutonium mixed oxides. *Journal of Nuclear Materials* **416**.1-2, 135–141.
- Das, D. and S. R. Bharadwaj, eds. (2013). *Thoria based Nuclear Fuels*. London, UK: Springer.
- Dean, D. W. (2007). *SIMULATE-3 Advanced Three-Dimensional Two-Group Reactor Analysis Code*. Studsvik Scandpower, Inc.
- Dekoussar, V., G. Dyck, A. Galperin, C. Ganguly, M. Todosow, and M. Yamawaki (2005). *Thorium fuel cycle - Potential benefits and challenges*. Tech. rep. IAEA-TECDOC-1450. Vienna: International Atomic Energy Agency.
- Drera, S. S., J. F. Kelly, Ø. Asphjell, and K. Insulander Björk (2014a). “Overview of the Thor Energy thorium fuel development program”. *ANS Winter Meeting and Nuclear Technology Expo 2014*. November 9-13. Anaheim, California, USA.
- Drera, S. S., H. Feinroth, J. F. Kelly, and K. Insulander Björk (2014b). “Development of LWR fuels utilizing thorium dioxide in conjunction with both zirconium-based and SiC cladding”. *ANS Winter Meeting and Nuclear Technology Expo 2014*. November 9-13. Anaheim, California, USA.
- Drera, S. S., J. F. Kelly, Ø. Asphjell, K. Insulander Björk, M. Sobieska, and B. C. Oberländer (2014c). “Ceria-thoria materials testing and pellet manufacturing in preparation for thorium-plutonia Th-MOX LWR fuel production”. *2014 Water Reactor Fuel Performance Meeting / Top Fuel / LWR fuel performance meeting*. September 14-17. Sendai, Japan.
- Drera, S. S., J. F. Kelly, Ø. Asphjell, K. Insulander Björk, M. Sobieska, and B. C. Oberländer (2015). Ceria-thoria pellet manufacturing in preparation for plutonia-thoria LWR fuel production. Submitted to Nuclear Technology.
- Dziadosz, D., T. N. Ake, M. Saglam, and J. J. Sapyta (2004). Weapons-grade plutonium-thorium PWR assembly design and core safety analysis. *Nuclear Technology* **147**.1, 69–83.
- Fredriksson, P. (2014). “Determination of radial power profiles in thorium-plutonium mixed oxide fuel pellets”. MSc thesis. Göteborg, Sweden: Chalmers University of Technology.
- Galperin, A., M. Segev, and M. Todosow (2000). Pressurized water reactor plutonium incinerator based on thorium fuel and seed-blanket assembly geometry. English. *Nuclear Technology* **132**.2, 214–226. ISSN: 00295450.
- Galahom, A. A., I. Bashter, and M. Aziz (2015). Design of an MCNPX model to simulate the performance of BWRs using thorium as fuel and its validation with HELIOS code. *Annals of Nuclear Energy* **77**, 393–401.

- Geelhood, K., W. Luscher, and C. Beyer (Mar. 2011a). *FRAPCON-3.4: A Computer Code for the Calculation of Steady-State Thermal-Mechanical Behavior of Oxide Fuel Rods for High Burnup*. NUREG/CR-7022. Pacific Northwest National Laboratory. P.O. Box 999, Richland, WA 99352.
- Geelhood, K., W. Luscher, and C. Beyer (Mar. 2011b). *FRAPCON-3.4: Integral Assessment*. NUREG/CR-7022. Pacific Northwest National Laboratory. P.O. Box 999, Richland, WA 99352.
- Gottaut, H. and K. Krüger (1990). Results of experiments at the AVR reactor. *Nuclear Engineering and Design* **121.2**, 143–153.
- Greneche, D. and M. Chhor (2012). *Nuclear Fuel Cycle Science and Engineering*. Ed. by I. Crossland. Woodhead Publishing Limited. Chap. 8.
- Gruppelaar, H. and J. P. Schapira (2000). *Thorium as a waste management option, final report*. Tech. rep. EUR 19142 EN. European Commission.
- Haubenreich, P. and J. Engel (1970). Experience with the Molten-Salt Reactor Experiment. *Nuclear Applications and Technology* **8**, 118–136.
- Hedrick, J. B. (2004). *Thorium*. Tech. rep. U.S. Geological Survey.
- Herring, J. S., P. E. MacDonald, K. D. Weaver, and C. Kullberg (2001). Low cost, proliferation resistant, uranium-thorium dioxide fuels for light water reactors. *Nuclear Engineering and Design* **203**, 65–85.
- Heuer, D., E. Merle-Lucotte, M. Allibert, M. Brovchenko, V. Ghetta, and P. Rubiolo (2014). Towards the thorium fuel cycle with molten salt fast reactors. *Annals of Nuclear Energy* **64**, 421–429.
- Ikeda, K., S.-i. Koyama, M. Kurata, Y. Morita, K. Tsujimoto, and K. Minato (2014). Technology readiness assessment of partitioning and transmutation in Japan and issues toward closed fuel cycle. *Progress in Nuclear Energy* **74**, 242–263.
- Insulander Björk, K. (2008). “Nuclear design of a thorium fuelled boiling water reactor”. MSc thesis. Göteborg, Sweden: Chalmers University of Technology.
- Insulander Björk, K. and V. Fhager (2009). “Comparison of Thorium-Plutonium fuel and MOX fuel for PWRs”. *Proceedings of Global 2009*. September 6-11. Paris, France.
- Insulander Björk, K., V. Fhager, and C. Demazière (2009a). “Method for investigating the applicability of thorium-based fuels in existing BWRs”. *Proceedings of ICAPP '09*. May 10-14. Tokyo, Japan.
- Insulander Björk, K., V. Fhager, and C. Demazière (2009b). “Comparison of thorium-based fuels with different fissile components in existing BWRs”. *Proceedings of ICAPP '09*. May 10-14. Tokyo, Japan.
- Insulander Björk, K., V. Fhager, and C. Demazière (2009c). “Comparison of thorium-based fuels with different fissile components in existing boiling water reactors”. *Proceedings of Advances in Nuclear Fuel Management (ANFM) IV*. April 12-15. Hilton Head Island, South Carolina, USA.
- Insulander Björk, K., V. Fhager, and C. Demazière (2011). Comparison of thorium-based fuels with different fissile components in existing boiling water reactors. *Progress in Nuclear Energy* **53**, 618–625.
- Insulander Björk, K. (2012). “Thorium-plutonium fuel for long operating cycles in PWRs - preliminary calculations”. *Proceedings of the SAIMM conference on Thorium and Rare Earths*. February 21-22. Cape Town, South Africa.

- Insulander Björk, K., S. Mittag, R. Nabbi, A. Rineiski, O. Schitthelm, and B. Vezzoni (2013a). Irradiation of a Thorium-Plutonium rodlet: Experiment and benchmark calculations. *Progress in Nuclear Energy* **66**, 73–79.
- Insulander Björk, K., C. W. Lau, H. Nylén, and U. Sandberg (2013b). Study of Thorium-Plutonium Fuel for Possible Operating Cycle Extension in PWRs. *Science and Technology of Nuclear Installations* **2013**. Paper 867561.
- Insulander Björk, K. and S. Helmersson (Oct. 30, 2013). “A fuel assembly for a nuclear reactor”. Patent application filed by the European Patent Organization.
- Insulander Björk, K. (2013). A BWR fuel assembly design for efficient use of plutonium in thorium-plutonium fuel. *Progress in Nuclear Energy* **65**, 56–63.
- Insulander Björk, K. and P. Fredriksson (2014). “Development of a fuel performance code for thorium-plutonium fuel”. *Proceedings of PHYSOR 2014*. September 28 - October 3. Kyoto, Japan.
- Insulander Björk, K. and Ø. Asphjell (Oct. 17, 2014). “Fuel assembly for a nuclear power boiling water reactor”. Patent application filed by the European Patent Organization.
- Insulander Björk, K., S. S. Drera, J. F. Kelly, C. Vitanza, C. Helsingreen, T. Tverberg, M. Sobieska, B. C. Oberländer, H. Tuomisto, L. Kekkonen, J. Wright, U. Bergmann, and D. P. Mathers (2015). Commercial thorium fuel manufacture and irradiation: Testing (Th,Pu)O<sub>2</sub> and (Th,U)O<sub>2</sub> in the “Seven-Thirty” program. *Annals of Nuclear Energy* **75**, 79–86.
- Insulander Björk, K. and L. Kekkonen (2015). Thermal-mechanical performance modelling of thorium-plutonium oxide fuel and comparison with experimental data. Submitted to Journal of Nuclear Materials.
- Karam, M., F. Dimayuga, and J. Montin (2008). *Fission Gas Release of (Th,Pu)O<sub>2</sub> CANDU Fuel*. Tech. rep. CW-124950-CONF-002. Atomic Energy of Canada Limited.
- Kim, S. K. and T. J. Downar (2002). Thorium fuel performance in a tight-pitch light water reactor lattice. *Nuclear Technology* **138**, 17–29.
- Klaassen, F. C., J. C. Kuijper, K. Bakker, and R. P. C. Schram (Oct. 2008). *THORIUM CYCLE: Development Steps for PWR and ADS Applications*. Tech. rep. Th5-DOC-041. NRG.
- Lau, C. W., C. Demazière, H. Nylén, and U. Sandberg (2012). Improvement of LWR thermal margins by introducing thorium. *Progress in Nuclear Energy* **61**, 48–56.
- Lau, C. W., H. Nylén, C. Demazière, and U. Sandberg (2013). “Investigation of the equilibrium core characteristics for the Ringhals 3 PWR with improved thermal margins using uranium-thorium fuel”. *International Congress on Advances in Nuclear Power Plants*. Jeju Island, South Korea.
- Lau, C. W., H. Nylén, K. Insulander Björk, and U. Sandberg (2014a). Feasibility Study of 1/3 Thorium-Plutonium Mixed Oxide Core. *Science and Technology of Nuclear Installations* **2014**. Paper 709415.
- Lau, C. W., V. Dykin, H. Nylén, K. Insulander Björk, and U. Sandberg (2014b). Conceptual study on Axial Offset Fluctuations by Stepwise Power Changes in a Thorium-Plutonium Core to Improve Load-Following Conditions. *Annals of Nuclear Energy* **72**, 84–89.
- Lau, C. W., H. Nylén, C. Demazière, and U. Sandberg (2014c). Reducing axial offset and improving stability in PWRs by using uranium–thorium fuel. *Progress in Nuclear Energy* **76**, 137–147.

- Lee, D., J. Rhodes, and K. Smith (2008). CASMO-5 Solutions for the Two-Dimensional C5G7 MOX Benchmark Problem. *Transactions of the American Nuclear Society* **99**, 680–682.
- Leppänen, J. (2012). *Serpent - a Continuous-energy Monte Carlo Reactor Physics Burnup Calculation Code*. VTT Technical Research Centre of Finland.
- Lindley, B. A., C. Fiorina, F. Franceschini, E. J. Lahoda, and G. T. Parks (2014). Thorium breeder and burner fuel cycles in reduced-moderation LWRs compared to fast reactors. *Progress in Nuclear Energy* **77**, 107–123.
- Long, Y., Y. Yuan, M. S. Kazimi, R. G. Ballinger, and E. E. Pilat (2002). A fission gas release model for high-burnup LWR ThO<sub>2</sub>-UO<sub>2</sub> fuel. *Nuclear Technology* **138**, 260–272.
- Long, Y. (2002). “Modeling the performance of high burnup thoria and urania fuel”. PhD thesis. Massachusetts Institute of Technology.
- Long, Y., L. J. Siefken, P. Hejzlar, E. P. Loewen, J. K. Hohorst, P. E. MacDonald, and M. S. Kazimi (July 2004). The behavior of ThO<sub>2</sub>-based fuel rods during normal operation and transient events in LWRs. *Nuclear Technology* **147**, 120–139.
- Mieloszyk, A., Y. Sukjai, S. Xu, and M. S. Kazimi (2014). “FRAPCON-MIT: A fuel performance tool for innovative fuel designs”. *Proceedings of TopFuel*.
- Moir, R. W. and E. Teller (2005). Thorium fuelled underground power plant based on molten salt technology. *Nuclear Technology* **151**.
- Mosteller, R. (2008). “ENDF/B-VII.0, ENDF/B-VI, JEFF-3.1, and JENDL-3.3 results for the MCNP criticality validation suite and other criticality benchmarks”. *International Conference on the Physics of Reactors 2008, PHYSOR 08*. Vol. 1, pp. 376–383.
- Núñez-Carrera, A., J. L. F. Lacouture, C. M. del Campo, and G. Espinosa-Paredes (2008). Feasibility study of boiling water reactor core based on thorium–uranium fuel concept. *Energy Conversion and Management* **49**.1, 47–53.
- Onufriev, V. (1987). *Thorium Based Nuclear Fuel: Current Status and Perspectives*. Tech. rep. IAEA-TECDOC-412. International Atomic Energy Agency.
- Pellaud, B. (2013). *Kernenergie Schweiz*. Zürich, Switzerland: Orell Füssli Verlag AG.
- Price, M. (2012). The Dragon Project origins, achievements and legacies. *Nuclear Engineering and Design* **251**, 60–68.
- Puill, A. (2002). “Thorium utilization in PWRs. Neutronics studies.” *Thorium fuel utilization: Options and trends*. IAEA-TECDOC-1319. Vienna: International Atomic Energy Agency, pp. 185–197.
- Rhodes, J., L. Deokjung, and K. Smith (2007). *CASMO-5/CASMO-5M, A Fuel Assembly Burnup Program, User’s Manual*. Studsvik Scandpower, Inc.
- Rhodes, J., D. Lee, and K. Smith (2008). *CASMO-5/CASMO-5M, A Fuel Assembly Burnup Program, Methodology Manual*. Studsvik Scandpower, Inc.
- Rhodes, J., D. Lee, and K. Smith (2009). *CASMO-4E: Extended Capability CASMO-4 - User’s Manual*. Studsvik Scandpower, Inc.
- Rhodes, J., N. Gheorghiu, Z. Xu, and K. Smith (2010). “CASMO5 status and validation”. *Studsvik Light Water Reactor Seminar*. Fukuoka, Japan.
- Rhodes, J. D. (2014). *Summary of CASMO-5 changes*. Tech. rep. SSP-11/406 Rev 6. Studsvik.

- Rimpault, G. (2002). “The ERANOS code and Data System for Fast Reactor Neutronic Analyses”. *International Conference on the Physics of Reactors*. Seoul, Korea.
- Rineiski, A. (2008). Decay heat production in a TRU burner. *Progress in Nuclear Energy* **50**, 377–381.
- Rose, S., J. Wilson, N. Capellan, S. David, P. Guillemain, E. Ivanov, O. Méplan, A. Nuttin, and S. Siem (2011). Minimization of actinide waste by multi-recycling of thoriated fuels in the EPR reactor. *Annals of Nuclear Energy* **38**.11, 2619–2624.
- Rubbia, C., J. Rubio, S. Buono, N. F. F. Carminati, J. Galvez, C. Gelès, Y. Kadi, R. Klapisch, P. Mandrillon, J. Revol, and C. Roche (1995). *Conceptual design of a fast neutron operated high power energy amplifier*. Tech. rep. CERN/AT/95-44 (ET). European Organization for Nuclear Research (CERN).
- Salvatores, M., I. Slessarev, and V. Berthou (2001). Review and proposals about the role of accelerator driven systems nuclear power. *Progress in Nuclear Energy* **38**.1–2, 167–178.
- Schitthelm, O., R. Nabbi, and F. Simons (2010). “A MCNP high resolution approach for the simulation of the LWR fuel element configurations”. *Jahrestagung Kerntechnik*. Berlin, Germany.
- Schitthelm, O., R. Nabbi, B. Vezzoni, A. Rineiski, S. Mittag, and K. Insulander Björk (2011). *A thorium-plutonium pin benchmark based on the experimental results from the KWO irradiation*. Tech. rep. LWR-DEPUTY D11. Forschungszentrum Jülich.
- Seaborg, G. T. (1976). *Early History of Heavy Isotope Research at Berkeley*. Lawrence Berkeley Laboratory, University of California, Berkeley, United States.
- Seaborg, G. T. (1977). *History of Met Lab Section C-I*. Vol. 1. Lawrence Berkeley Laboratory, University of California, Berkeley, United States.
- Seaborg, G. T. (1978). *History of Met Lab Section C-I*. Vol. 2. Lawrence Berkeley Laboratory, University of California, Berkeley, United States.
- Seaborg, G. T. (1979). *History of Met Lab Section C-I*. Vol. 3. Lawrence Berkeley Laboratory, University of California, Berkeley, United States.
- Seaborg, G. T. (1980). *History of Met Lab Section C-I*. Vol. 4. Lawrence Berkeley Laboratory, University of California, Berkeley, United States.
- Shaposhnik, Y., E. Shwageraus, and E. Elias (2013). Core design options for high conversion BWRs operating in Th-233U fuel cycle. *Nuclear Engineering and Design* **263**, 193–205.
- Shwageraus, E., X. Zhao, M. Driscoll, P. Hejzlar, M. Kazimi, and J. Herring (2004a). Microheterogeneous thorium-urania fuels for pressurized water reactors. *Nuclear Technology* **147**.1, 20–36.
- Shwageraus, E., P. Hejzlar, and M. S. Kazimi (2004b). Use of Thorium for Transmutation of Plutonium and Minor Actinides in PWRs. *Nuclear Technology* **147**.1, 53–68.
- Somers, J. (2011). Minor Actinide Bearing Fuels: Fabrication and Irradiation Experience in Europe. *Energy Procedia* **7**, 169–176.
- Trellue, H. R., C. G. Bathke, and P. Sadasivan (2011). Neutronics and material attractiveness for PWR thorium systems using monte carlo techniques. *Progress in Nuclear Energy* **53**.6, 698–707.
- Uchikawa, S., T. Okubo, T. Kugo, H. Akie, R. Takeda, Y. Nakano, A. Ohunki, and T. Iwamura (2007). Conceptual design of innovative water reactor for flexible fuel cycle

- (FLWR) and its recycle characteristics. *Journal of nuclear science and technology* **44.3**, 277–284.
- Válu, O., O. Benes, R. Konings, and H. Hein (2014). The high temperature heat capacity of the (Th,Pu)O<sub>2</sub> system. *The Journal of Chemical Thermodynamics* **68**, 122–127.
- Verwerft, M. et al. (2007). *OMICCO Final Report*. Tech. rep. EUR 23104. FIKS-CT-2001-00141. European Commission.
- Verwerft, M. et al. (Dec. 2011). *LWR-DEPUTY Final Report*. External Report SCK-CEN-ER-200. FI6W-036421. Boeretang 200, BE-2400 Mol, Belgium: SCK-CEN.
- Villarino, E., R. Stamm'ler, A. Ferri, and J. Casal (1992). HELIOS: Angularly dependent collision probabilities. *Nuclear Science and Engineering* **112**, 16–31.
- Walker, R. (1978). Experience with the Fort St. Vrain reactor. *Annals of Nuclear Energy* **5.8–10**, 337–356.
- World Nuclear Association (2015a). *Nuclear Power Reactors*. URL: <http://www.world-nuclear.org/info/Nuclear-Fuel-Cycle/Power-Reactors/Nuclear-Power-Reactors/> (visited on 02/05/2015).
- World Nuclear Association (2015b). *Molten Salt Reactors*. URL: <http://www.world-nuclear.org/info/Current-and-Future-Generation/Molten-Salt-Reactors/> (visited on 02/05/2015).
- Xu, Z., J. Rhodes, and K. Smith (2009). “CASMO-5 versus MCNP-5 benchmark of radial power profile in a fuel pin”. *International conference on mathematics, computational methods & reactor physics (M&C)*. Saratoga Springs, New York.
- Xu, Z., K. Smith, and J. Rhodes (2010). “Benchmarking CASMO5 Against PNL Mixed Oxide Criticals”. *ICAPP '10*. Paper 10216. San Diego, CA, UCA.

Part II

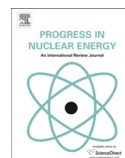
APPENDED PAPERS I–VIII



# Paper I

**Comparison of thorium-based fuels with different fissile components in existing boiling water reactors**





## Comparison of thorium-based fuels with different fissile components in existing boiling water reactors

Klara Insulander Björk<sup>a,b,\*</sup>, Valentin Fhager<sup>a</sup>, Christophe Demazière<sup>b</sup>

<sup>a</sup>Thor Energy, Sommersrogaten 13–15, NO-0255 Oslo, Norway

<sup>b</sup>Chalmers University of Technology, Department of Nuclear Engineering, SE-412 96 Göteborg, Sweden

### A B S T R A C T

#### Keywords:

Thorium  
BWR  
Neutronics

With the aim of investigating the technical feasibility of fuelling a conventional BWR (Boiling Water Reactor) with thorium-based fuel, computer simulations were carried out in a 2D infinite lattice model using CASMO-5. Four different fissile components were each homogeneously combined with thorium to form mixed oxide pellets: Uranium enriched to 20% U-235 (LEU), plutonium recovered from spent LWR fuel (RGPu), pure U-233 and a mixture of RGPu and uranium recovered from spent thorium-based fuel. Based on these fuel types, four BWR nuclear fuel assembly designs were formed, using a conventional assembly geometry (GE14-N). The fissile content was chosen to give a total energy release equivalent to that of a UOX fuel bundle reaching a discharge burnup of about 55 MWd/kgHM. The radial distribution of fissile material was optimized to achieve low bundle internal radial power peaking. Reactor physical parameters were computed, and the results were compared to those of reference LEU and MOX bundle designs. It was concluded that a viable thorium-based BWR nuclear fuel assembly design, based on any of the fissile components, can be achieved. Neutronic parameters that are essential for reactor safety, like reactivity coefficients and control rod worths, are in most cases similar to those of LEU and MOX fuel. This is also true for the decay heat produced in irradiated fuel. However when Th is mixed with U-233, the void coefficient (calculated in 2D) can be positive under some conditions. It was concluded that it is very difficult to make savings of natural uranium by mixing LEU (20% U-235) homogeneously with thorium and that mixing RGPu with thorium leads to more efficient consumption of Pu compared to MOX fuel.

© 2010 Elsevier Ltd. All rights reserved.

### 1. Introduction

Thorium-based fuel is steadily gaining interest in the nuclear industry due to advantageous thermal and chemical properties and low actinide production. Furthermore, the retrievable thorium resources of the world are expected to be several times larger than the known uranium resources, so the use of thorium-based nuclear fuel has the possibility of significantly extending the long-term horizon of nuclear power.

The majority of options for utilizing thorium previously proposed have relied on highly innovative fuel or reactor concepts, such as accelerator driven systems (Salvatores et al., 1997), molten salt reactors (Merle-Lucotte et al., 2008) and advanced seed-and-blanket designs in LWRs utilizing new fuel materials (Galperin and Radkowsky, 1999; Núñez-Carrera et al., 2005). The development efforts, including licensing processes for such concepts are, and justifiably so, often thought to be extensive. Studies of the use of

thorium with existing reactor and fuel technology have also been published (Puill, 1999), in most cases PWR specific.

In this paper, we investigate the properties of thorium-based oxide fuel designed for use in existing BWRs. Lacking a naturally occurring fissile isotope, thorium must be combined with some fissile material, and three different alternatives for driver materials, containing a fissile component, have been investigated: reactor-grade plutonium, uranium enriched to 20% in U-235 and U-233. We seek to demonstrate that the use of all these different fuel types is basically feasible in present day BWRs, and to find potential issues that need further attention. Since the use of MOX fuel is standard practice in many countries today, we pay special attention to the reactor physical consequences of mixing the recovered Pu from spent uranium fuel with thorium instead of depleted uranium (DU), i.e. using Th + RGPu fuel instead of MOX.

The study presented in this paper partly builds on an M.Sc. thesis work carried out at Chalmers University of Technology in 2007–2008, in cooperation with Vattenfall Nuclear Fuel (Insulander Björk, 2008). More calculation cases have been added, upgraded software has been used, including a different nuclear data library, and the methodology has been refined.

\* Corresponding author.

E-mail address: [klara.insulander@scatec.no](mailto:klara.insulander@scatec.no) (K. Insulander Björk).

The premises and assumptions made for this study are presented in Section 2. In Section 3, the methodology for design optimization and neutronic analysis is described. The results of the study, in terms of reactivity coefficients, delayed neutron fractions, control rod worths and decay heat for the different fuel designs, are presented in Section 4, and the conclusions drawn from these results are summarized in Section 5.

## 2. Premises

### 2.1. Reactor specifications

The Swedish BWR Forsmark-3 was chosen to model the reactor geometry in which the thorium-based fuels were studied. Some of the operating parameters, which are used in this study, are shown in Table 1.

It was assumed that the total neutron leakage from the Forsmark-3 reactor represents a lowering of the effective neutron multiplication factor,  $k_{\text{eff}}$ , that amounts to 2000 pcm, which was used to adjust the target infinite neutron multiplication factor,  $k_{\infty}$ , in the 2D infinite lattice model.

### 2.2. Fuel assembly geometry

The fuel assembly model chosen was GE14-N, designed by Global Nuclear Fuel, as fabricated for the Swedish Forsmark-3 BWR. This is a modern and commercially available fuel assembly design. The assembly has an active fuel length of 368 cm. Fuel pins are arranged in a 10-by-10 lattice, in which eight pins are replaced by two centrally placed water channels and 14 are part length and vanish in the upper third of the fuel assembly. When using normal uranium fuel, mainly consisting of uranium dioxide, the heavy metal weight in a GE14-N fuel assembly is approximately 176 kg.

### 2.3. Fissile components

Uranium with an enrichment of less than 20% in U-235 is denoted *Low-Enriched Uranium* (LEU). This material is not subject to the same hard safeguard restrictions as uranium of higher enrichment (high-enriched uranium, HEU). For this reason, 20% enriched U is considered a feasible driver material in a thorium-fuelled reactor. It is noted that most large-scale enrichment plants of today operate with a license for up to 5 weight % U-235, and that obtaining large amounts of uranium with an enrichment of 20% in U-235 may not be straightforward.

*Reactor-Grade Plutonium* (RGPu) is obtained from reprocessing of spent uranium-based fuel. It is composed by a mix of plutonium isotopes. In this study we have used an isotope vector which is

typical for pressurized water reactor fuel discharged at about 41 MWd/kgU<sup>1</sup>. The presence of Am-241 in the Pu vector was neglected in this work, but previous work (Insulander Björk and Fhager, 2009) suggests that the main consequence of taking the presence of Am-241 into account is that the amount of Pu needs to be increased to compensate for the additional neutron captures in this isotope. RGPu is the principal fissile material in MOX fuel, which is used in over 30 reactors worldwide.

U-233 does not occur naturally and is only produced in very small amounts in uranium-fuelled reactors. However, it is produced by neutron irradiation of Th-232, for example in a nuclear reactor, and subsequent spent fuel separation. It can be argued that the use of pure U-233 in this study is somewhat unrealistic, since U-233 is not the only uranium isotope which is produced when thorium is irradiated. Furthermore, a BWR will under almost all circumstances produce less U-233 than it consumes, so a closed self-sustained BWR fuel cycle based entirely on U-233 and thorium is not possible. However, U-233 will play a major role in any application of a closed thorium cycle and it is of high interest to investigate the neutronic properties of this fissile component.

*Recovered Uranium* (RU) denotes, in this paper, a composition of uranium roughly corresponding to the uranium vector in Th + RGPu fuel burnt to 55 MWd/kgHM. The uranium vector used in this case consists of 89 weight % U-233 and 11 weight % U-234, and the smaller amounts of other uranium isotopes (mainly U-235) were neglected.

### 2.4. Fuel cycle scenarios

Six different fuel types have been studied, each representing a fuel cycle scenario:

<b>Once through:</b> LEU (reference)	The standard fuel cycle used in most LWRs today.
Th + LEU	This effectively corresponds to replacing most of the fertile matrix of U-238 in LEU fuel with Th-232. The main reason for doing so would be to reduce the natural uranium consumption by efficient conversion of Th-232.
MOX (reference)	The way MOX is applied today is a once-through usage of recovered Pu.
Th + RGPu	This translates into replacing the DU matrix in ordinary MOX. The reason to do this could be to improve Pu utilization or to more efficiently burn stockpile Pu while capturing its energy content.
<b>(Semi)-closed:</b> Th+U-233	In this case, it is assumed that a stockpile of pure U-233 is available, e.g. from preceding irradiation of Th-232. This is then mixed with Th.
Th + RU + RGPu	Here, the uranium recovered from one spent Th + RGPu fuel bundle is re-inserted into a fresh fuel bundle, mixed with Th. Supplementary RGPu is added to provide sufficient reactivity.

In all cases, a homogenous mix of the components into mixed oxide pellets was modelled.

**Table 1**  
Reactor operating parameters.

Parameter	Notation	Value
Number of fuel assemblies	$N$	700
Number of fuel batches	$n$	6
Cycle length [days]	$t_c$	350
Reactor thermal power [MW]	$P_{\text{th}}$	3300
Neutron leakage [pcm]	$\Delta k$	2000
<b>At hot full power (HFP):</b>		
Power density [kW/dm <sup>3</sup> ]		53.5
Coolant/moderator temp. [K]		559
Fuel temperature [K]		800
Void fraction [%]		40
<b>At cold zero power (CZP):</b>		
Power density [kW/dm <sup>3</sup> ]		0
Coolant/moderator temp. [K]		293
Fuel temperature [K]		293
Void fraction [%]		0

<sup>1</sup> The exact isotope vector is: 2.5% Pu-238, 54.2% Pu-239, 23.8% Pu-240, 12.6% Pu-241 and 6.9% Pu-242.

### 3. Methodology

#### 3.1. Determining the initial average fissile content

The total energy release demanded from each fuel assembly during its lifetime can be calculated according to Equation (1), inserting the operation parameters given in Table 1.

$$E_{\text{tot}} = \frac{P_{\text{th}} \cdot T_C \cdot n}{N} \quad (1)$$

The total energy released from a fuel assembly during its lifetime can also be calculated as the product of its mass  $M$  and its discharge burnup  $B_D$ , according to Equation (2).

$$E_{\text{tot}} = M \cdot B_D \quad (2)$$

The different fuel types all have different densities, and as the same different assembly geometry is used in each case, this implies that they also have different total fuel mass per assembly. Thus, the lighter fuel types must be designed to reach a slightly higher discharge burnup, in order for the total energy release to satisfy Equation (1). The total fuel mass per assembly is given in Table 2.

The discharge burnup for a certain fuel composition is calculated from  $k_{\infty}$ , which is given in the CASMO-5 output data, by means of the linear reactivity model as described in (Graves, 1979). In a core composed of fuel from  $n$  batches and with no control rods inserted, the effective multiplication factor,  $k_{\text{eff}}$ , equals the average infinite multiplication factor of the different fuel batches, minus the assumed lowering of the  $k_{\text{eff}}$  due to neutron leakage,  $\Delta k$ , see Table 1.  $k_{\text{eff}}$  can thus be calculated from Equation (3), where the infinite multiplication factor of fuel batch  $m$  is denoted  $k_m$ , which is a function of the burnup  $B$ .

$$k_{\text{eff}} = \frac{1}{n} \sum_{m=1}^n k_m(B) - \Delta k \quad (3)$$

If it is assumed that a fuel assembly accumulates the same burnup  $B_C$  in each operating cycle,  $B_C$  must equal  $B_D/n$ . The effective multiplication factor at the end of each cycle can, under this assumption, be calculated by Equation (4), where  $k_{\infty}$  of batch  $m$  at EOC has been taken as the value of  $k_{\infty}$  at a burnup of  $m$  times  $B_C$ .

$$k_{\text{eff,EOC}} = \frac{1}{n} \sum_{m=1}^n k_{\infty}(B_C \cdot m) - \Delta k \quad (4)$$

The basic criticality condition for the core is that  $k_{\text{eff}}$  should be unity at EOC with all control rods withdrawn. A suitable initial fissile content can thus be found iteratively by calculating  $k_{\infty}$  in the burnup range of interest, calculating  $k_{\text{eff,EOC}}$  and adjusting the fissile content for achieving an increased or decreased  $k_{\infty}$  as demanded for fulfilling the criticality condition. This procedure was gone through for all the different fuel types.

#### 3.2. Assembly nuclear design

The average initial fissile content in the bundle as calculated in Section 3.1 determines the effective lifetime of the fuel. The initial radial distribution of the fissile material within the bundle will affect the power distribution over the whole burnup range. The power distribution will in turn determine the margin to the thermal limits which are set to reduce the risk of fuel failure during in-core operation. In this study, one such thermal limit has been taken into account in bundle design optimization, namely the Linear Heat Generation Rate (LHGR). This limit is used to prevent internal rod over-pressure, pellet centerline melting and harmful pellet-cladding interaction.

The actual LHGR that a fuel pin can be expected to have in the core is roughly proportional to the product of its power relative to the bundle average, i.e. the power peaking factor, denoted  $F_{\text{int}}$ , and the infinite multiplication factor,  $k_{\infty}$ , which indicates the reactivity of the fuel bundle as a whole. Therefore, calculated values of this product for a standard LEU design was used as a guideline when determining the radial distribution of the fissile material within the bundle.

The number of pellet types used in each assembly design was limited to 10. More pellet types would imply very complex fuel manufacturing, whereas fewer types would constrain the possibility of achieving the desired flat power distribution.

In this study, we have used gadolinia as a Burnable Absorber (BA) in the LEU and Th+U-233 cases, where the initial multiplication factor is high at the beginning of life (BOL) and then decreases rapidly with burnup. The other fuel types display a much flatter behavior of the  $k_{\infty}$  vs. burnup curve, which led to the assumption that burnable absorbers would not be necessary. Avoiding burnable absorber would be desirable, as it would make fuel fabrication less complex.

#### 3.3. Neutronic simulation software

The fuel assemblies were designed and analyzed using CASMO-5 (Rhodes et al., 2007), which is a multi-group two-dimensional transport theory code, mostly used to perform fuel assembly depletion calculations and to compute homogenized cross-sections for subsequent input to 3D core simulators. The cross section library used in this study was ENDF-B VII.

#### 3.4. Estimation of reactivity coefficients

Reactivity coefficients were calculated from the CASMO-5 output data. These indicate the change in reactivity of the fuel as a response to a change in operating parameters. It is desirable to have negative reactivity coefficients, in a positive reactivity coefficient would mean that an increase in one operating parameter would lead to an increase in reactivity, which in turn would cause the operating parameter to increase even more, i.e. a positive feedback loop. The coefficients investigated at HFP conditions were the Fuel Temperature (Doppler) Coefficient (FTC), the Coolant Void Coefficient (CVC) and the Moderator Temperature Coefficient (MTC). The Isothermal Temperature Coefficient (ITC) was investigated at CZP conditions.

The reactivity coefficients were estimated by perturbation calculations. The power history of the fuel assembly was simulated up to a certain burnup point under hot full-power conditions, see Table 1, after which the parameter of interest  $x$  (e.g. the fuel temperature) was perturbed by a certain difference, denoted  $\Delta x$ . The infinite multiplication factor at this burnup point was computed for the different states and denoted  $k_P$  and  $k_U$  for the perturbed and the unperturbed states respectively. These were then inserted into Equation (5) for calculating the reactivity coefficient, denoted  $C_x$ .

$$C_x = \frac{k_P - k_U}{\Delta x \cdot k_U} \quad (5)$$

This method does not take into account any leakage effects or interactions between assemblies with different burnup. Thus, the calculated values are rough estimates, but should nevertheless be valid for comparisons of the different fuel types.

#### 3.5. Calculation of control rod worths

An estimate of control rod worths was calculated in a similar way. The fuel irradiation history was simulated up to a certain burnup point, at which  $k_{\infty}$  was calculated with ( $k_P$ ) and without

**Table 2**

Mass compositions of the different fuel assemblies.

Fuel composition	LEU	Th + LEU	MOX	Th + RGPu	Th+U-233	Th + RU + RGPu
Total weight [kg]	175	163	181	163	161	163
Th-232 mass [kg]	–	123.4	–	147.4	155.2	151.5
U-235 mass [kg]	7.2	8.0	0.5	–	–	–
U-238 mass [kg]	167.7	31.6	167.4	–	–	–
RGPu mass [kg]	–	–	13.2	15.6	–	8.3
U-233 mass [kg]	–	–	–	–	5.8	2.9
Gadolinia rods	10	–	–	–	10	–
wt % gadolinia	4.0	–	–	–	4.0	–
NU requirements <sup>a</sup> [kgHM/assembly]	$1.6 \times 10^3$	$1.9 \times 10^3$	–	–	–	–

<sup>a</sup> The tail enrichment was assumed to be 0.3 weight % U-235.

( $k_U$ ) the control rods inserted. The control rod worth, CW, was then determined according to Equation (6).

$$CW = \frac{k_p - k_U}{k_U} \quad (6)$$

The simulation of control rod insertion in the infinite 2D lattice model in CASMO-5 is equivalent to simultaneously inserting all control rods in an infinite lattice of identical fuel assemblies. Hence, also this calculation is only an indicative method for comparing control rod worths between different cases. A higher estimated control rod worth for a certain fuel type indicates that inserting a control rod into a core loaded with this fuel type would have a larger reducing effect on the reactivity of the core.

The CW was calculated at both CZP and HFP conditions, see Table 1. For the CW calculation at HFP, the void fraction was assumed to be zero after control rod insertion.

### 3.6. Calculation of decay heat

The decay heat was calculated using the built-in “SNF lite” module in CASMO-5 (Bahadir, 2008), which uses the end of life (EOL) isotopic number densities given by the CASMO-5 depletion calculation and decay data mainly from the ENDF/B-VI decay data file. Both the short-term and long-term aspects were investigated.

Short-term decay heat after reactor shutdown was calculated in order to assure that the capacity of a heat removal system for the reactor is sufficient for every core loading. Calculations were performed on each fuel type half-way through its life, as intended to give an estimate of a typical equilibrium core decay heat that needs to be removed during the first 30 min after shutdown. The CASMO-5 output, which is in heat rate per unit fuel mass have been integrated over time and multiplied with the total HM mass of the bundle in question. The total accumulated core decay heat relative to the LEU case is then calculated.

The long-term decay heat from a discharged spent fuel assembly was calculated for the first 100 years after discharge. This quantity is significant for considerations related to spent fuel intermediate and final storage, e.g. for the design of canisters and loading capacity.

## 4. Results

2D lattice calculations with CASMO-5 were performed using one model of the lower two thirds of the fuel assembly with the operating parameters given in Table 1 and one similar model for the upper third in which a number of part-length rods are replaced by coolant and the void fraction is changed to 70%. The results for the two different cases are similar and only 2D results from the lower part are presented in this section.

### 4.1. Initial fissile content

Following the methodology of Section 3.1, the initial fissile content for each fuel type was chosen so that the same amount of energy would be produced as in a reference LEU bundle. The resulting fuel compositions and the Natural Uranium (NU) requirements are given in Table 2.

It can be seen that NU requirements are higher in the Th + LEU case than with pure LEU. This means that no uranium savings can be achieved by enriching the uranium to 20% and mixing it homogeneously with thorium in a standard BWR bundle, under the assumed discharge burnup limits.

The amount of RGPu required to produce the same amount of energy is higher when mixed with thorium (the Th + RGPu case) than when mixed with DU (the MOX case). This is mainly due to the contribution of fissions in U-235 and fast fissions in U-238 which are present in the DU. By recovering the uranium, RGPu requirements can be reduced by almost 50%, as can be seen in the last column in Table 2.

### 4.2. Infinite multiplication factor

The infinite multiplication factor calculated at hot, full-power conditions and its variation with burnup is shown in Fig. 1.

In the Th + LEU, MOX, Th + RGPu and Th + RU + RGPu cases,  $k_\infty$  decreases rather slowly with burnup, making it possible to reach the discharge burnup demanded in each case without having a high  $k_\infty$  at BOL. This motivated the choice not to use burnable absorbers in these cases.

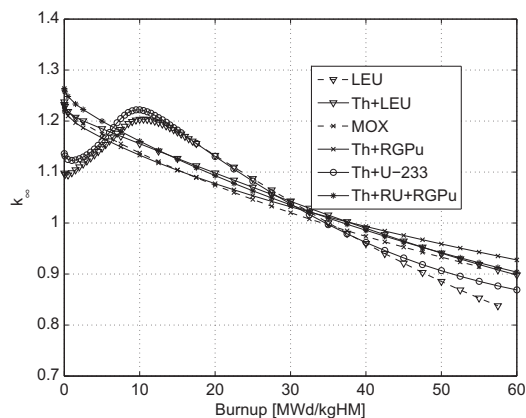


Fig. 1. Infinite multiplication factor dependence on burnup.

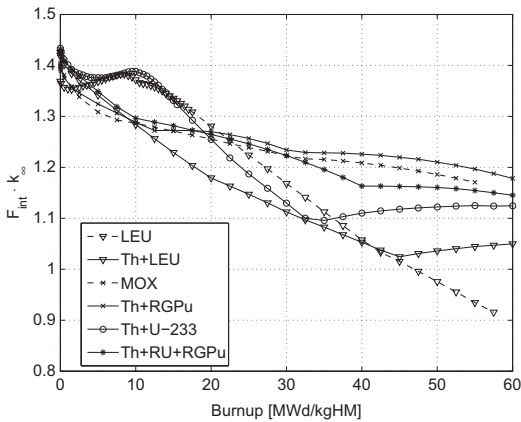


Fig. 2. The intra-assembly radial power peaking factor times the infinite multiplication factor for the different fuel types.

The burning of Th+U-233 fuel, on the other hand, results in a steeper decrease in  $k_{\infty}$ , just as for LEU fuel. The suppressing effect of burnable absorber material on  $k_{\infty}$  early in life can be clearly seen in the LEU and Th+U-233 cases.

#### 4.3. Radial power peaking

Fig. 2 illustrates the power peaking factor of each bundle by drawing the  $F_{\text{int}} \cdot k_{\infty}$  product as a function of burnup. The power distribution is controlled by assigning a suitable fissile content to each group of fuel pins, and hence the power peaking factor depends on the degree of optimization of the fuel bundle design. The optimization process is complicated by the fact that the power profile changes drastically during the life of the fuel assembly due to the efficient breeding in the well-moderated peripheral pins. This is especially true for the Th + RGPu fuel, which is reflected by the fact that the  $F_{\text{int}} \cdot k_{\infty}$  product is comparatively high in this case, especially towards EOL when a considerable amount of U-233 has

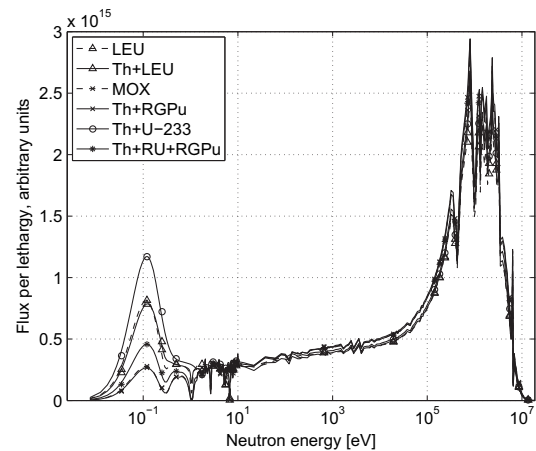


Fig. 3. Neutron energy spectrum at the beginning of life for the different fuel types.

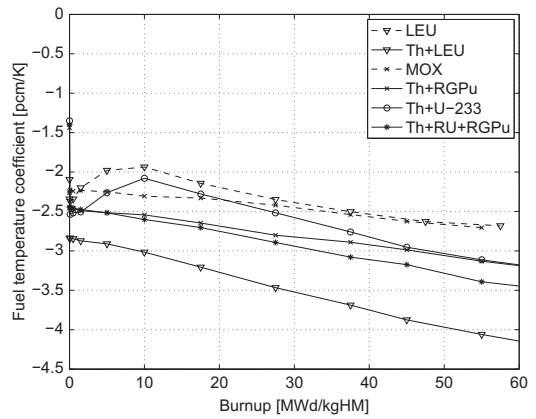


Fig. 4. Fuel temperature to efficient.

been bred in the peripheral fuel pins, thus increasing their reactivity. However, it was possible to design all fuel types so that they had  $F_{\text{int}} \cdot k_{\infty}$  quite similar to that of the LEU reference, at least in the burnup interval 0 – 20 MWd/kgHM in which margins to LHGR limits are usually the lowest in the Forsmark-3 type reactor.

#### 4.4. Neutron energy spectrum

The neutron energy spectrum within an average fuel pin is shown for each fuel type in Fig. 3. It proves to be somewhat harder, i.e. shifted towards higher energy, for all fuel types containing plutonium, which has a large capture cross section for thermal neutrons. In the Th + U-233 fuel, the spectrum is softer than the LEU reference.

#### 4.5. Reactivity coefficients

The reactivity coefficients investigated were the fuel temperature coefficient (FTC), the coolant void coefficient (CVC), the moderator temperature coefficient (MTC) and the isothermal temperature coefficient (ITC). The results are plotted in Fig. 4–7.

The FTC is always negative and larger in amplitude in all the thorium cases, and it remains more or less constant throughout the bundle lifetime. The largest negative amplitude is found for the Th + LEU case, in which the Doppler effect (broadening of capture cross section resonances) is amplified by the simultaneous presence of Th-232 and U-238.

The CVC calculated for the Th + RGPu and Th + LEU fuel types are fairly similar to the reference LEU and MOX cases, and the CVC in the Th + RU + RGPu case is only slightly closer to zero. The CVC in the Th+U-233 case, on the other hand, is positive during the whole lifetime. This would be very severe for reactor safety as it would require other instant negative feedback effects (e.g. the FTC) to be strong enough to grant an overall inherent stability. An accurate estimate of the actual CVC would only be possible with full-core calculation models. Results from a similar study (Insulander Björk, 2008) indicate that the CVC may indeed be negative for a core loaded with 100% Th+U-233 fuel.

The behavior of the MTC is fairly similar to that of the CVC in all cases. Hence, the MTC of the Th+U-233 fuel is positive over its whole lifetime. Again, an accurate assessment would require more sophisticated models to include 3D effects.

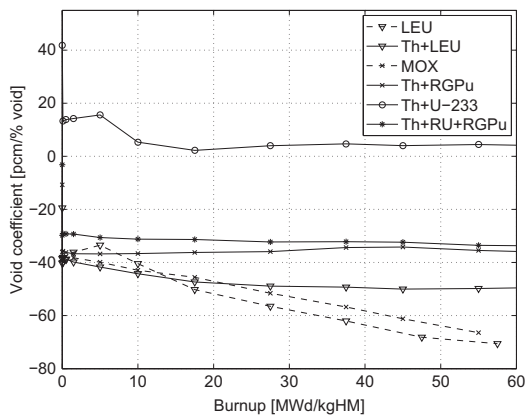


Fig. 5. Coolant void coefficient.

The ITC, calculated at cold conditions, was found to be quite similar for all fuel types. Positive values were calculated over the whole life span, also for the LEU reference. ITC values calculated with this infinite lattice model are conservative as they do not account for the increased neutron leakage and presence of control rods. The use of gadolinium as burnable neutron absorber has a significant reducing effect on ITC.

#### 4.6. Control rod worths

Calculated control rod worths are shown in Fig. 8.

The lower control rod worth observed with fuel that contains plutonium is caused by the harder neutron spectrum, which leaves less thermal neutrons to be captured by boron in control rod blades. This is a well-known phenomenon from MOX-fuelled cores and does not lead to any operational restrictions in modern LWRs, where measures such as increased moderation or boron enrichment have been taken to increase control rod worths (Sonedá et al., 2009; Arslan et al., 2009). With U-233 as the fissile component, the control rod worth is somewhat higher than for LEU. The same trends are observed in both hot and cold conditions, but the difference between fuel types is less pronounced in the latter case.

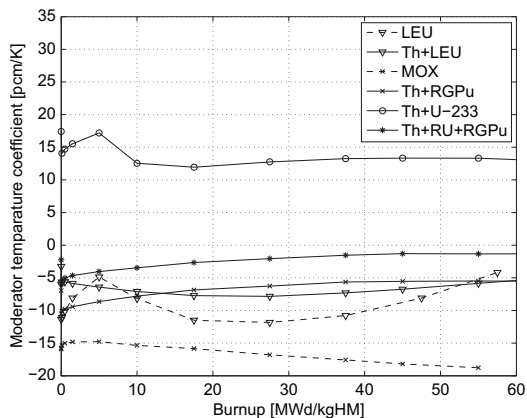


Fig. 6. Moderator temperature coefficient.

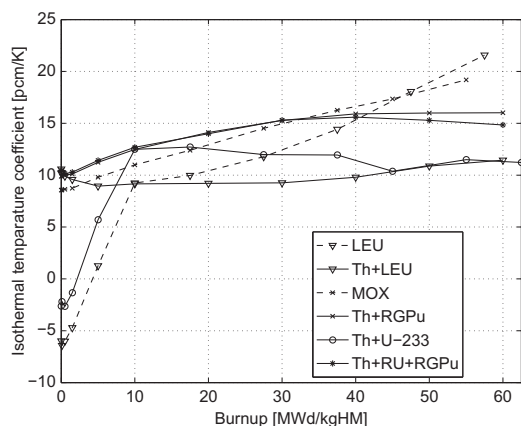


Fig. 7. Isothermal temperature coefficient.

#### 4.7. Delayed neutron fraction

The fraction of fission neutrons emitted with a certain time delay, through decay of unstable fission products, is of major importance to the dynamic properties of the reactor. It is crucial for the ability to control the reactor power during transients that this fraction is not too low. Calculated values of delayed neutron fractions are plotted in Fig. 9.

The delayed neutron fractions in the different fuels clearly reflect the delayed neutron yields of their respective fissile components. Thus, the Th + LEU and reference LEU cases display similar delayed neutron fractions, reflecting the relatively high delayed neutron yield of U-235. The delayed neutron fractions in the Th+U-233, Th + RGPu, Th + RU + RGPu and MOX cases are substantially lower, mirroring the fact that the delayed neutron yield of U-233 and Pu-239 are about half as high as that of U-235. The delayed neutron fractions in the Th + LEU and reference LEU cases also decrease gradually during the cycle as U-233 and Pu-239 build up in the respective fuel types. Since the calculated delayed

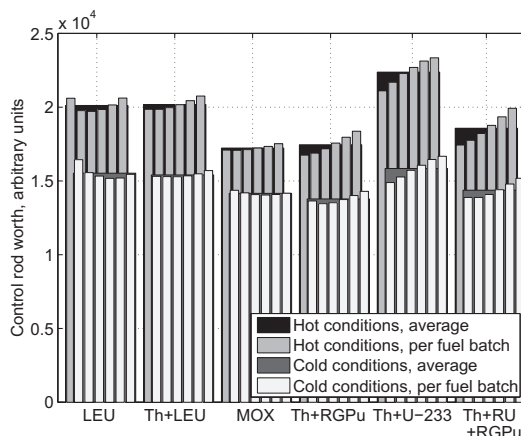


Fig. 8. Control rod worths at HFP and CZP calculated at six burnup points, roughly corresponding to the end of each cycle, along with the burnup averaged value shown as a broad bar in the background.

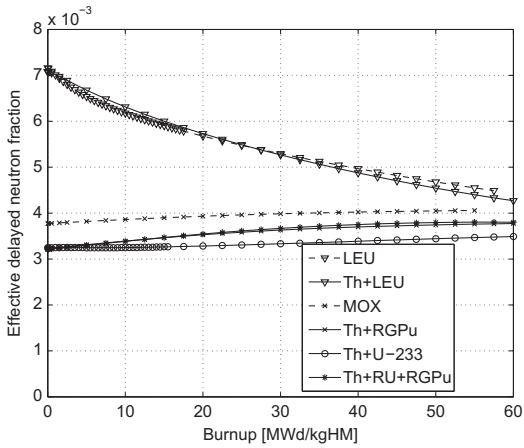


Fig. 9. The effective fraction of delayed neutrons in the different fuel types throughout their lifetime.

neutron fractions for thorium fuels are not significantly lower than for MOX fuel, this in itself is not likely to be an insurmountable issue for reactor safety.

#### 4.8. Power fraction from U-233

As can be seen in Fig. 10, all once-through scenarios involve only a smaller part of power generated by the bred-in U-233. The rate at which fertile Th-232 is converted to U-233 via neutron capture is only sufficient to yield a lifetime average of 25–35% of the total power. For comparison, about 40% of the energy generated in a core fuelled with LEU stems from in-situ fission of plutonium which has been converted from U-238. Closing the cycle, recovering and re-using the bred-in U-233 obviously improves the thorium utilization. Also, the increase with burnup of the power fraction from U-233 indicates that going to higher discharge burnup would also give a higher lifetime average U-233 power share.

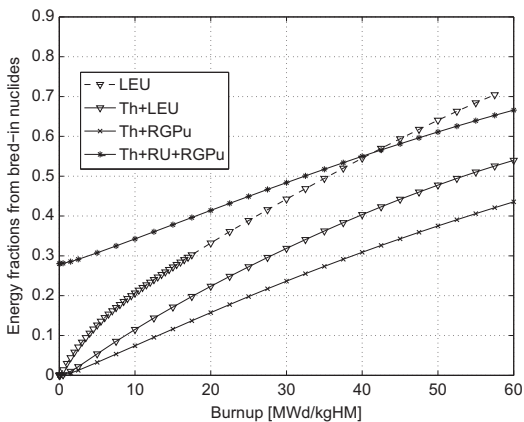


Fig. 10. The fraction of power generated by fission of U-233 in the thorium based cases and the fraction of power generated by fission of Pu-239 and Pu-241 in the LEU case.

Table 3  
Plutonium contents and consumption.

Fuel composition	LEU	Th + LEU	MOX	Th + RGPu	Th+U-233	Th + RU + RGPu
Pu loaded, [kg/assembly]	–	–	13.2	15.7	–	8.2
Pu discharged, [kg/assembly]	1.8	0.56	8.6	7.3	=0	2.7
Pu mass reduction [%]	–	–	35	54	–	67
Fissile fraction of discharged Pu [%]	56	61	48	39	–	28

#### 4.9. Plutonium build-up and destruction

One of the major motivations for the use of thorium fuel is the low production of plutonium and minor actinides. Table 3 shows the plutonium content of the different fuel types at BOL and at EOL. We conclude that about three times more Pu is produced in the discharged LEU fuel compared to the Th + LEU case.

If plutonium is used as the fissile component, a significant net reduction of this material is achieved. Compared to MOX fuel, the plutonium destruction is much more efficient when thorium is used as the fertile matrix since the formation of Pu-239 through conversion of U-238 is avoided.

When RGPu is used as top-up fuel in the "semi-closed" Th + RU + RGPu cycle, less Pu is consumed per bundle, but the fraction of Pu consumed is increased, and the fissile Pu fraction in the spent fuel is as low as 28%.

#### 4.10. Decay heat

As shown in Fig. 11, the accumulated decay heat generated in the core during the first 30 min after shutdown is in all cases less than 5% higher than in the LEU reference case. This indicates that decay heat after shutdown is not likely to pose a great challenge to reactor heat removal systems. For those thorium fuels in which U-233 is the main fissile component, the specific heat rate after shutdown is relatively high, but the lower fuel weight reduces the total decay heat in core.

In the longer term (year scale), Pu bearing fuel yields the highest decay heat among the fuel types studied, see Fig. 12. It will take about 100 years for a Th + Pu fuel bundle to cool down to the heat rate which an LEU fuel bundle cools down to in 15 years.

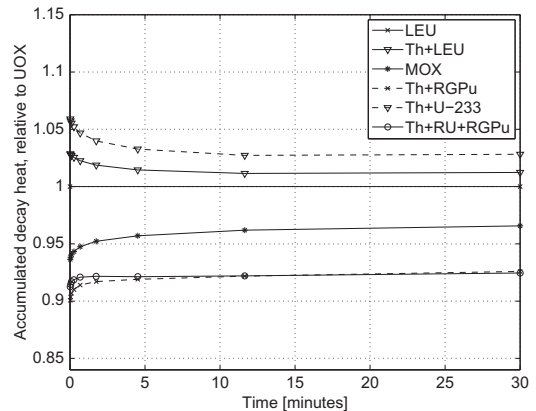


Fig. 11. Accumulated decay heat generated in the core after shutdown, relative to LEU.

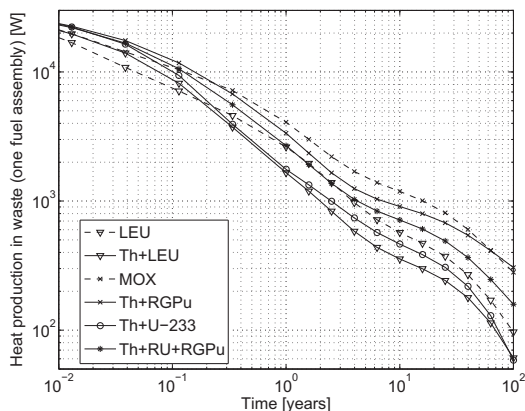


Fig. 12. Total decay heat rate generated in a discharged fuel assembly.

Th + U-233 fuel displays decay heat characteristics very similar to those of LEU.

## 5. Conclusions

The basic reactor physical properties of thorium-fuelled BWR cores have been investigated. Thorium was combined with a number of fissile components into viable nuclear bundle designs and the neutronic properties of these fuels were analyzed using a 2D infinite lattice model.

With each of the fissile driver materials, it was possible to assign a radial distribution of fissile material in a standard BWR assembly design, using a limited number of fuel rod types, such that the bundle internal power peaking could be kept at levels typical to LEU fuel designs.

Introducing the fertile nuclide Th-232 and the fissile U-233 alters the reactivity coefficients of relevance to safe operation of BWRs to a minor degree, with values that are within or near the domain of LEU and MOX fuel. Two exceptions have been highlighted – the CVC and the MTC tend to be positive when U-233 is the dominant fissile component. Calculated values of delayed neutron fraction and control rod worths do not in themselves raise any major concerns for the technical feasibility of introducing any of the fuel types into a modern BWR. However, a more thorough analysis of dynamic core behaviour is needed to fully comprehend the consequences of the observed differences between the investigated thorium-based fuel types and the reference fuel types.

Mixing reactor-grade plutonium with thorium yields a neutronic performance very similar to a corresponding mix of reactor-grade plutonium and depleted uranium (MOX). Hence, it can be expected that the introduction of Th + RGPu fuel will not imply any additional challenges to those faced by MOX fuel. If efficient destruction of stockpile plutonium is targeted, Th + RGPu fuel is superior to MOX. More RGPu is required in the Th + RGPu case than in the MOX case to reach the same total energy release.

It is not possible to make natural uranium savings by mixing LEU with thorium at the discharge burnups studied here.

In the once-through scenarios in which fertile thorium is used together with LEU or RGPu as driver fuel, and discharge burnup is limited to about 50–60 MWd/kgHM, the fraction of power from nuclides in the thorium chain will be about 25–35%. Only when uranium is recovered from spent thorium fuel and re-used in fresh fuel, as in the Th+U-233 and Th + RU + RGPu cases, will more than 50% of the energy be produced by fissions in U-233.

The decay heat generated immediately after shutdown is not expected to be significantly higher in thorium-fuelled cores than in MOX- and LEU-fuelled cores and should be manageable by reactor heat removal systems. The decay heat from discharged thorium fuel in the time frame of 1–100 years depends mostly on the plutonium content, which contributes to a comparatively high decay heat generation.

## Nomenclature

BOL	Beginning of life
BWR	Boiling-water reactor
CVC	Coolant void coefficient
CZP	Cold zero power
DU	Depleted uranium
EOL	End of life
FTC	Fuel temperature coefficient
HFP	Hot full power
HM	Heavy metal
ITC	Isothermal Temperature Coefficient
LEU	Low-enriched uranium
LHGR	Linear heat generation rate
MOX	Mixed oxide fuel (PuO <sub>2</sub> and UO <sub>2</sub> )
MTC	Moderator temperature coefficient
RGPu	Reactor-grade plutonium
RU	Recovered Uranium

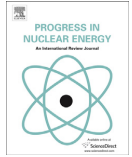
## References

- Arslan, M., Marincic, A., Niquille, A., Dodelier, J., 2009 September 6–11. MOX in Reactors: Present and Future. GLOBAL, Paris.
- Bahadir, T., 2008 September 9 SNF Lite methodology in CASMO-5, Studsvik Scandpower Memorandum.
- Galperin, A., Radkowsky, A., 1999. A Competitive Thorium Fuel Cycle for Pressurized Water Reactors of Current Technology, vol. 1319. International Atomic Energy Agency IAEA-TECDOC, pp. 83–96.
- Graves Jr., H.W., 1979. Nuclear Fuel Management. John Wiley & Sons, Inc., New York.
- Insulander Björk, K., 2008. Nuclear Design of a Thorium Fuelled Boiling Water Reactor. Chalmers University of Technology, Report CTH-NT-215.
- Insulander Björk, K., Fhager, V., 2009 September 6–11. Comparison of Thorium-Plutonium Fuel and MOX Fuel for PWRs. GLOBAL, Paris.
- Merle-Lucotte, E., Heuer, D., Allibert, M., Doglitz, X., Ghetta, V., Le Brun, C., 2008 September 14–19. Optimization and Simplification of the concept of Non-moderated thorium molten salt reactor. In: International Conference on the Physics of Reactors, Interlaken.
- Núñez-Carrera, A., François, J.L., Martín del Campo, C., Espinosa-Paredes, G., 2005. Design of a Boiling water reactor core based on an integrated blanket-seed thorium-uranium Concept. Annals of Nuclear Energy 32, 558.
- Puill, A., 1999. Thorium utilization in PWRs. In: Neutronics Studies, 1319. International Atomic Energy Agency IAEA-TECDOC, 185–197.
- Rhodes, J., Smith, K., Lee, D., 2007. CASMO-5/CASMO-5M, a Fuel Assembly Burnup Program. User's Manual. Studsvik Scandpower Manual. SSP-07/431.
- Salvatores, M., Slessarev, I., Tchistakov, A., Ritter, G., 1997. The potential of accelerator driven systems for transmutation or power production using thorium or uranium fuel cycles. Nuclear Science and Engineering 126 (3), 333.
- Soneda, H., Iwata, Y., Ebisuya, M., 2009. BWR core and fuel development for highly-economical power generation. Hitachi Review 58 (2), 61.

# Paper II

**Irradiation of a Thorium-Plutonium rodlet: Experiment  
and benchmark calculations**





## Irradiation of a thorium–plutonium rodlet: Experiment and benchmark calculations

K. Insulander Björk<sup>a,b,\*</sup>, S. Mittag<sup>c</sup>, R. Nabbi<sup>d</sup>, A. Rineiski<sup>e</sup>, O. Schitthelm<sup>d</sup>, B. Vezzoni<sup>e</sup>

<sup>a</sup>Thor Energy, Sommerrogaten 13–15, Oslo 0255, Norway

<sup>b</sup>Chalmers University of Technology, Göteborg, Sweden

<sup>c</sup>Helmholtz-Zentrum Dresden-Rossendorf, Dresden, Germany

<sup>d</sup>Forschungszentrum Jülich GmbH, Jülich, Germany

<sup>e</sup>Karlsruhe Institute of Technology, Karlsruhe, Germany

### ARTICLE INFO

#### Article history:

Received 1 February 2012

Received in revised form

6 March 2013

Accepted 18 March 2013

#### Keywords:

Thorium  
Plutonium  
Benchmark  
Experiment  
Simulation  
LWR

### ABSTRACT

A benchmark exercise for thorium–plutonium fuel, based on experimental data, has been carried out. A thorium–plutonium oxide fuel rodlet was irradiated in a PWR for four consecutive cycles, to a burnup of about 37 MWd/kgHM. During the irradiation, the rodlet was inserted into a guide tube of a standard MOX fuel assembly. After the irradiation, the rod was subjected to several PIE measurements, including radiochemical analysis. Element concentrations and radial distributions in the rodlet, multiplication factors and distributions within the carrier assembly of burnup and power were calculated. Four participants in the study simulated the irradiation of the MOX fuel assemblies including the thorium–plutonium rodlet using their respective code systems; MCBurn, HELIOS, CASMO-5 and ECCO/ERANOS combined with TRAIN. The results of the simulations and the measured results of the radiochemical analysis were compared and found to be in fairly good agreement when the calculated results were calibrated to give the same burnup of the thorium–plutonium rodlet as that experimentally measured. Average concentrations of several minor actinides and fission products were well reproduced by all codes, to the extent that can be expected based on known uncertainties in the experimental setup and the cross section libraries. Calculated results which could not be confirmed by experimental measurement were compared and only two significant anomalies were found, which can probably be addressed by limited modifications of the codes.

© 2013 Elsevier Ltd. All rights reserved.

### 1. Introduction

This article concerns the benchmarking of numeric tools for prediction of the neutronic behaviour of thorium–plutonium (Th/Pu) mixed oxide fuel in Light Water Reactors (LWRs), with reference to experimental data. The reported work was carried out as part of the LWR-DEPUTY project (Verwerft et al., 2011), which ran from 2006 to 2011 and involved several European research institutes.<sup>1</sup>

The LWR-DEPUTY project aims to study to what extent the existing nuclear power plants in Europe can create markedly less nuclear waste by moving to non plutonium breeding fuels, including

thorium based fuel types. The fact that novel fuels are developed for existing reactors allows for assessing the full scenario of industrial implementation including design, fabrication, licensing, in-reactor performance and safety. The LWR-DEPUTY project builds on the extensive experience gained in previous European projects on advanced nuclear fuel, including the THORIUM-CYCLE (Versteegh et al., 2004) and OMICO (Verwerft et al., 2007) projects.

The deployment route for Th/Pu fuel can be expected to be short compared to other innovative fuel types, since it is neutronically similar to the well established MOX fuel (Insulander Björk and Fhager, 2009). However, one of the key remaining issues is the availability of validated numerical codes and nuclear data for core physics analysis. The objective of the study reported in this article is to assess how well four different nuclear fuel simulation codes can model depletion of Th/Pu fuel under LWR conditions. This is done by comparing calculated concentrations of a number of heavy metals and fission products with those measured by radiochemical analysis of a Th/Pu test fuel rodlet which has been irradiated under

\* Corresponding author. Thor Energy, Sommerrogaten 13–15, Oslo 0255, Norway. Tel.: +47 91117835.

E-mail addresses: [klara.insulander@scatec.no](mailto:klara.insulander@scatec.no), [klaraib@gmail.com](mailto:klaraib@gmail.com) (K. Insulander Björk).

<sup>1</sup> SCK-CEN, FZJ, KIT, HZDR, EC-JRC-ITU, NNL, NRG, PSI and VUJE Inc.

normal PWR conditions. The benchmarked codes include one Monte-Carlo based code system (MCBurn developed at FZJ) and three deterministic codes (HELIOS and CASMO-5, both supplied by Studsvik Scandpower, and a combination of ECCO/ERANOS and TRAIN, using a specific coupling procedure developed by KIT).

The study confirms that the prediction capability of the four benchmarked code systems is generally good with respect to generation and depletion of heavy metals and production of certain fission products. However, two issues are also pointed out, which should be resolved before the concerned codes are used commercially for modelling Th/Pu fuels.

The irradiation experiment and how the benchmark suite was formulated is described in Sections 2 and 3 respectively. The code systems utilized by the benchmark participants are briefly described in Section 4 and the results in Section 5. Finally, the conclusions are presented in Section 6.

## 2. Experiment

In the period 2001–2005 a Th/Pu test rodlet of 14.4 cm height was irradiated for four consecutive cycles at the Obrigheim nuclear power station (KW0) in Germany. The reactor is a PWR with 357 MWe gross electrical output and 1050 MWth thermal power.

The rodlet was placed in one of the inner guide tubes of a MOX fuel assembly, which in turn was placed at the center of the reactor core. During the experiment two carrier assemblies were used, referred to as MOX2310 and MOX2312. These were irradiated simultaneously for one cycle (referred to as cycle 0) to a burnup of approximately 15 MWd/kgHM. After this the rodlet was inserted into MOX2310 and irradiated together with this fuel assembly for two cycles while MOX2312 was cooling. After these two cycles, the partly irradiated rodlet was taken out of MOX2310 and transferred to MOX2312. The rodlet was then irradiated for another two cycles together with MOX2312.

### 2.1. Test rodlet

The rodlet consisted of 17 pellets of mixed Th and Pu dioxides, fabricated at the Institute for Transuranium Elements (ITU). The fuel contained 2.28% of weapons grade Pu. The detailed isotopic composition is given in Table 1. The rodlet was inserted into a device which allowed placing it in the center of the guide tubes. The dimensions of the rodlet and the guide tubes are given in Table 2 and the placement of the rodlet within the assembly is shown in Fig. 1.

The axial position of the center of the rodlet was 85.8 cm below the top of the carrier assembly. In this zone the flux gradient over the active length of the rodlet was small. Due to the short length, the impact on the neutronics of the core is assumed to be limited to the carrier assembly only.

### 2.2. Carrier assemblies

The carrier assemblies were of identical design, employing a standard 14-by-14 PWR fuel design. Three different levels of Pu

**Table 1**  
Isotopic composition of the Th/Pu test rodlet.

Isotope	Concentration 1/(b·cm)	HM vector wt%
Th-232	$2.103 \cdot 10^{-2}$	96.705
Pu-238	$2.175 \cdot 10^{-7}$	0.001
Pu-239	$6.513 \cdot 10^{-4}$	2.995
Pu-240	$5.893 \cdot 10^{-5}$	0.271
Pu-241	$1.087 \cdot 10^{-6}$	0.005
Am-241	$4.784 \cdot 10^{-6}$	0.022
0–16	$4.394 \cdot 10^{-2}$	–

**Table 2**

Geometric dimensions of the fuel rods and the assembly. Fuel rod dimensions apply both to the Th/Pu test rodlet and to the ordinary MOX fuel rods.

Fuel rod diameter	8.05 mm
Fuel-cladding gap width	0.17 mm
Cladding thickness	1.28 mm
Guide tube inner diameter	11.50 mm
Guide tube thickness	1.00 mm
Fuel rod pitch	12.60 mm
MOX rod active length	3650 mm

content were used, distributed as illustrated in Fig. 1. The isotopic composition of the Pu used in the carrier assembly MOX fuel pellets is unknown, and for the benchmark study it was assumed to be reactor grade Pu from LWR fuel with a burnup of 33 MWd/kgHM.

## 3. Benchmark definition

Due to the complexity of the experiment and some unknown experimental conditions, certain simplifications have been made when defining the benchmark.

### 3.1. Geometry

Preliminary studies showed that there is no need to model the whole core for reproducing the neutronic environment of the rodlet. Therefore it was deemed sufficient only to model the carrier assembly, employing a two-dimensional plane model with reflective boundary conditions.

In simulations with software capable of three-dimensional simulations, the full length of the fuel assembly was modelled, adopting a subdivision of the fuel assembly into four parts of length 125 cm, 125 cm, 56.4 cm and 58.6 cm, counting from the bottom and up. The foot and head sections of the fuel assembly were not included in the model due to their negligible impact on the rodlet. Reflective boundary conditions in the radial direction were also used here.

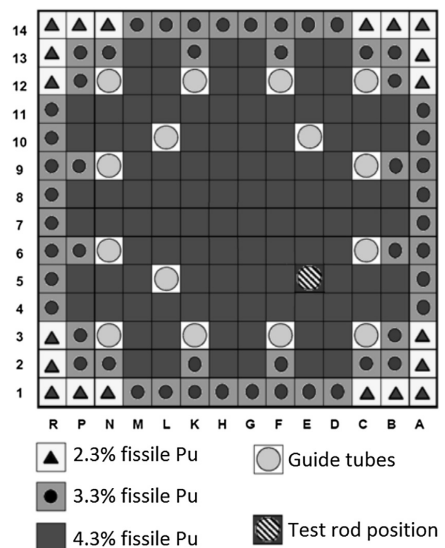


**Fig. 1.** The carrier assembly.

For assessing the radial distribution of fission products and minor actinides within the rodlet, it was subdivided in the employed computer models into ten annular sub-regions of equal volume.

### 3.2. Operating conditions

Some simplifying assumptions had to be made for the operating conditions of the reactor. For example, simulating the decreasing concentration of soluble boron was considered to be of minor importance, so the simulations were carried out at a constant boron concentration for each cycle. The assumed operating parameters during the test irradiation are tabulated in Table 3.

### 3.3. Power history

The power level in the carrier assembly was measured using an aeroball system located at the corner of a next-to-neighbouring fuel assembly, i.e. at a distance of one fuel assembly width from the carrier assembly. The measured values were averaged and one constant power level was assumed for each cycle. However, when using this power history, all participants significantly over-estimated the burnup of the Th/Pu rodlet, compared to the burnup as determined by radiochemical analysis. This discrepancy could be due either to inaccurate predictions based on the aeroball measurements, or to the uncertainties in the isotopic composition of the MOX fuel assembly. It was thus decided that each benchmark participant should recalibrate the power history to yield the same final concentration of Cs-137 as was established by the radiochemical analysis. This would result in approximately the same burnup for all participants. The uncalibrated power levels for each cycle are given in Table 4, along with the duration of each cycle. The calibration factors adopted by each participant are listed in Table 5. The necessity of this power recalibration means that the power measurements are approximate. Thus, the abilities of the employed codes to accurately perform the burn-up calculations are not fully confirmed in this case, so an additional effort on simulation of relevant experimental cases would be of interest.

Furthermore, a shut-down period of 30 days between each cycle was modelled.

## 4. Neutronic codes

Four different code systems were benchmarked. Information on these code systems, the employed nuclear data libraries and the benchmark participants carrying out the simulations is given in Table 5. Each code system is briefly described in the following sections.

### 4.1. MCBurn

The code system MCBurn is an interface routine developed at FZJ which combines the two codes MCNP 5.15 and ORIGEN 2.2 (Schitthelm et al., 2010). MCNP is a well verified and tested Monte-Carlo neutronics code (X-M.C. Team, 2005) while ORIGEN performs the depletion calculations dependent on the local neutron spectra and produced power (Bell, 1973). MCBurn is optimised for

**Table 3**  
Operating parameters assumed for the benchmark exercise.

Fuel temperature	930 K
Clad temperature	586 K
Moderator temperature	586 K
Average boron concentration, cycle 1–3	600 ppm
Average boron concentration, cycle 4	150 ppm

**Table 4**

Power levels as inferred from the aeroball measurements. Except for cycle 0, the power level at the height of the rodlet was measured specifically. All power levels are given as Linear Heat Generation Rates (LHGR) in W/cm. Cycle lengths are given in days.

Cycle number	Axially averaged power	Power at height of rodlet	Cycle duration
0	185	–	363
1	267	280	367
2	196	200	368
3	269	279	361
4	219	209	129

simulation of burnup of LWR fuel elements in very high spatial and temporal resolution.

### 4.2. HELIOS

HELIOS-1.10 is a neutron and gamma transport code for lattice burnup in general two-dimensional geometry developed by Studsvik Scandpower. The particle transport is performed using the current coupling collision probability (CCCP) method (Villarino et al., 1992). The space elements are globally coupled using interface currents. Transport within the space elements is performed by applying collision probabilities.

### 4.3. CASMO-5

CASMO-5, also developed by Studsvik Scandpower, is a two-dimensional characteristics based transport theory lattice physics code (Rhodes et al., 2007). The code has depletion capability and generates effective cross sections and other data for downstream use by 3D-codes. For the benchmark exercise, an extra module for rearrangement of fuel pins, called MOVEROD, was supplied by Studsvik Scandpower. The use of this module does not affect the modeling capability of CASMO-5, so the results of this benchmark exercise are fully representative of the capability of CASMO-5 to model thorium–plutonium oxide fuel.

### 4.4. ECCO/ERANOS and TRAIN

To carry out the benchmark, KIT has developed a specific procedure that enables the coupling between the ECCO/ERANOS neutronic code (Rimpault et al., 2002), for flux and cross section evaluation, and the TRAIN code (Rineiski, 2008), for nuclear density evolution (irradiation and decay). ECCO is a multi-group cell code employing cross-section data originated from the JEFF 3.1, and processed through NJOY/THEMIS and CALENDF, in order to produce the effective cross sections required for reactor calculations. TRAIN is a burn-up code developed at KIT which employs nuclear data from JEFF 3.1 and effective cross-sections from reactor codes. For brevity, this code package will in the following be referred to as EET.

**Table 5**

The benchmarked neutronic simulation codes, the employed nuclear data libraries, the calibration factors referred to in Section 3.3 and the benchmark participant carrying out the calculations in each case (FZJ: Forschungszentrum Jülich, HZDR: Helmholtz-Zentrum Dresden-Rossendorf, KIT: Karlsruhe Institute of Technology, TE: Thor Energy).

Code name	Data library	Calibration factor	Participant
MCBurn	ENDF/B-VII	0.663	FZJ
HELIOS	ENDF/B-VI	0.778	HZDR
CASMO-5	ENDF/B-VII	0.759	TE
ECCO/ERANOS & TRAIN	JEFF 3.1	0.791	KIT

5. Results

5.1. Power history

As described in Section 3.3, the power history had to be recalibrated. The recalibration was done to the Cs-137 content of the Th/Pu test rodlet, since this was judged to be the most reliable burnup indicator under the circumstances, and was done individually by all participants. This, however, implies that every benchmark participant adopted a slightly different burnup history, dependent on the power of the thorium rod relative to the average assembly power level. Fig. 2 illustrates the relative power distribution at the end of cycle 4 in the quarter of the fuel assembly in which the test rodlet was situated. (Since the power distribution is practically symmetrical about the diagonal, only an eighth of the fuel assembly is shown.) This figure shows a significantly higher relative power of the test rodlet for MCBurn compared to the other results (note that numbers in white correspond to negative deviations from average power in Fig. 2). The higher relative power implies that a lower average power is needed in the MCBurn case for the test rodlet to reach the calibration burnup (Cs-137 content). This agrees with the lower calibration factor adopted for the MCBurn calculations, see Table 5. With the ECCO code, the MOX pins were not modelled individually but in three groups according to their Pu content. Thus, the displayed relative power values are the pin group average power values relative to the bundle total power.

As can be seen in Fig. 3, the calibration resulted in essentially similar calculated burnup for all code systems.

It should be noted that power and burnup distributions were calculated and compared at the end of each cycle and at the beginning of cycle 1, but no major findings were made in addition to those already discussed above.

5.2. Multiplication factor

The multiplication factor of the carrier assemblies was calculated by all participants and is plotted in Fig. 4. It is related to the power history in that a higher power results in a more rapid depletion of the fuel and hence a steeper slope of the  $k_{\infty}$  curve. As

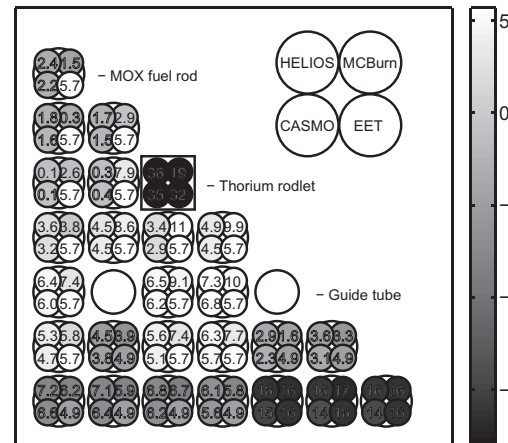


Fig. 2. Relative power distribution in one eighth of the carrier assembly by the end of cycle 4. All numbers are expressed in percent deviation from mean linear heat generation rate. Numbers in white represent deviations in the negative direction, i.e. power below average.

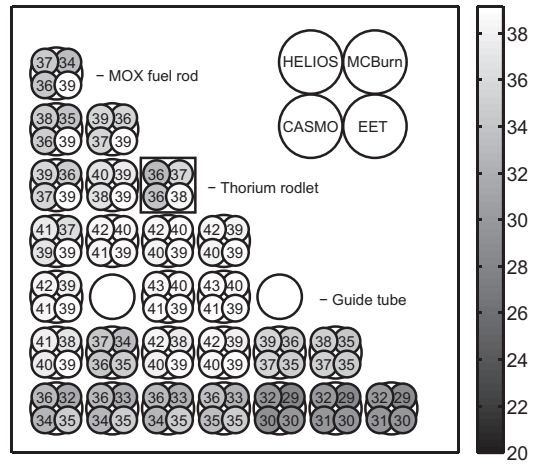


Fig. 3. Burnup distribution in one eighth of the carrier assembly by the end of cycle 4. All numbers are expressed in MWd/kgHM.

previously indicated, a lower power level was adopted for the MCBurn calculations compared to the other codes, which agrees well with the more gentle slope of  $k_{\infty}$  during the first two cycles for these simulations.

The rapid reactivity drop at the beginning of each cycle which can be seen in Fig. 4 corresponds to the buildup of Xe-135. The big discontinuity between cycles two and three corresponds to the change of carrier assembly. The small discontinuity seen between cycles three and four corresponds to a change in soluble boron concentration which was significantly lower in cycle 4 compared to cycles 1–3 (see Table 3). The absence of this discontinuity in the MCBurn case could be due to a different treatment of the soluble boron.

It should be noted that the influence by the Th/Pu rodlet on  $k_{\infty}$  of the carrier assembly is small, so these results mainly indicate differences in modelling of MOX fuel by the different codes.

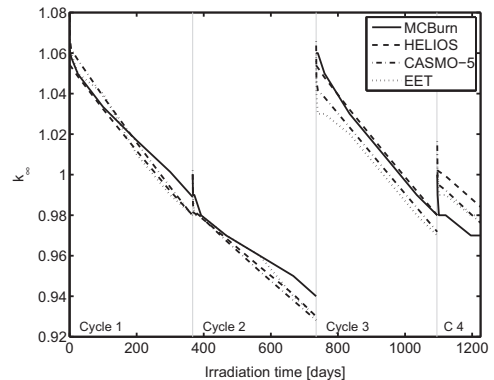


Fig. 4. Infinite multiplication factor of the carrier assembly.

### 5.3. Isotopic analysis

Since the power history was recalibrated to the Cs-137 concentration, the results of the isotopic analysis mainly indicates the yield of different isotopes relative to the Cs-137 yield in the different simulations. The calculated and the experimentally determined (Winkel et al., 2010) isotopic concentrations are tabulated in Table 6. In general, the calculated numbers do not deviate more than 25% from the experimentally measured number for each isotope. A discussion of the more significant deviations follows. In general, a deviation is considered as significant if it exceeds 10%. It should be noted that the statistical error of the measuring devices is estimated to about 5%.

The calibration demand on the burnup indicator Cs-137 was met by all participants within an error margin of 2%. Ce-144 was chosen as a first control nuclide for the burnup estimation. In contrast to Cs-137, this nuclide is relatively short-living with  $T_{1/2} \approx 285$  d and has a stronger dependency on the fissioned parent isotope. All codes overestimate the Ce-144 concentration, which could be due to the shutdown periods between cycles actually being shorter than the modelled 30 days. HELIOS apparently overestimates the Ce-144 content by 50%, however this is due to the shutdown periods not being modelled at all in this case. For Ce-134, all predictions fall within 30% of the experimental data, which is good considering that the fission yield data for this isotope have large error margins (e.g. 64% for ENDF/B-VII).

The production of all Nd isotopes is generally slightly underestimated. The Nd-142 and Nd-150 concentrations are strongly underestimated by all participants. This might be due to the fission yields being underestimated in the cross section libraries, or to experimental measurement errors.

For Eu-155, the difference in fission yields for U-233 and Pu-239 is one order of magnitude and for Eu-154 it is almost three orders of magnitude. In addition the yield data for fission of U-233 and Pu-

239 show uncertainties of more than 10% for Eu-155 and 60% for Eu-154 (ENDF/B-VII), which explains the spread of the calculated concentrations of these isotopes.

The Pa-231 concentration is overestimated by all codes. Pa-231 is mainly produced by  $(n, 2n)$  reactions in Th-232 and subsequent  $\beta$  decay, so one likely cause for this error is an overestimation of the  $(n, 2n)$  reaction cross section in the data libraries or of the computed neutron spectra at high energies. It could also be due to experimental measurement errors.

The production of U-233 and U-234 is overestimated by MCBurn. Since the overestimation is not reproduced by CASMO-5, which uses the same cross section library, this must rather be due to a model difference. A possible cause could be the adopted fission Q-values, i.e. the energy released per fission. A comparison shows that the Q-values adopted by MCBurn are in general about 5% higher than those adopted by the other participants. This would lead to a lower number of fissions being required to reach the same burnup, and consequently a lower consumption of fissile isotopes. This hypothesis is strengthened by the fact that also the consumption of Pu-239 is underestimated by MCBurn, but raises the question of why then the relation between the calculated burnup and the Cs-137 concentration is similar to the other codes. CASMO-5 underestimates the production of U-234 and U-235, and the predicted U-233 concentration is also on the low side. A possible cause for this is discussed in Section 5.4.

There is an underestimation of the U-238 concentration by MCBurn and CASMO-5 (for the HELIOS and EET simulations, there are no predictions of the U-238 concentration). The assumed cause for this is an initial U-238 contamination of the Th/Pu test rodlet, before irradiation. The fact that all codes also underestimate the production of Np-237, which occurs mainly by  $(n, 2n)$  reactions in U-238 and subsequent  $\beta$  decay, confirms this assumption.

The numbers given for Pu-238 through Pu-241 and Am-241 relate to the change in concentration of these nuclides. Considering that the initial Pu-239 concentration was 27.1 mg/g, it is clear that the loaded Pu-239 is almost completely consumed. This consumption is similarly calculated by all codes. The small concentrations of all heavier nuclides indicate that most of the consumed Pu-239 was fissioned. The concentrations of Pu-240, Pu-241 and Am-241 are generally not very well reproduced. This is probably due to the uncertainty concerning the composition of the MOX fuel, since the large absorption cross sections of all Pu isotopes at thermal energies have a strong influence on the spectrum. If for example the Pu-240 concentration in the MOX fuel was overestimated in the benchmark definition, this would cause a stronger suppression of the simulated flux close to the 1 eV absorption resonance, which in turn would cause lower simulated absorption in Pu-240 in the thorium pin. This would explain the underestimated reduction of Pu-240 in the simulations. The contamination of U-238 in the Th/Pu rodlet could also be part of the explanation.

The generation of Am-243, Cm-244 and Cm-245 is generally underestimated, for unknown reasons. Once again, this could be due either to errors in the experimental concentration measurements or in the modelling methods. Since the results of the MCBurn and CASMO-5 calculations (employing the same nuclear data library) are not more coherent than the others, it is less likely that the error lies in the cross section libraries. One probable cause could be different treatment of the metastable state of Am-242 and the Am-241 branching ratio in the different codes.

Summarizing the isotopic results, it can be concluded that most of the larger discrepancies can be explained either by uncertainties in the experimental setup or by known uncertainties in the cross section libraries. The most important isotope concentration for

**Table 6**

Calculated and experimentally determined isotopic concentrations in the Th/Pu test rodlet. Italic numbers indicate difference from initial content. All numbers given in mg/g.

Isotope	Experiment	MCBurn	HELIOS	CASMO-5	EET
Cs-134	0.12	0.14	0.14	0.15	0.15
Cs-137	1.18	1.19	1.19	1.20	1.19
Ce-144	0.22	0.25	0.33	0.24	0.25
Nd-142	0.025	0.021	0.017	0.019	0.018
Nd-143	0.78	0.77	0.77	0.78	0.81
Nd-144	0.87	0.80	0.67	0.80	0.81
Nd-145	0.57	0.57	0.55	0.56	0.58
Nd-146	0.62	0.60	0.59	0.62	0.62
Nd-148	0.33	0.33	0.32	0.32	0.33
Nd-150	0.20	0.17	0.17	0.17	0.17
Eu-154	0.027	0.037	0.040	0.039	0.039
Eu-155	0.0085	0.0065	0.0065	0.0095	0.010
Pa-231	0.07	0.11	0.11	0.12	0.13
U-233	14.3	16.4	14.2	13.3	15.6
U-234	1.90	2.25	1.86	1.74	1.94
U-235	0.43	0.43	0.41	0.35	0.42
U-236	0.05	0.03	0.03	0.03	0.03
U-238	0.30	1.6e-5	–	1.6e-5	–
Np-237	0.010	0.003	0.002	0.002	0.003
Pu-238	0.16	0.17	0.16	0.16	0.19
Pu-239	–26.2	–25.0	–25.2	–25.6	–25.3
Pu-240	–0.93	0.25	–0.04	–0.06	–0.04
Pu-241	2.10	2.71	2.84	2.58	2.68
Pu-242	1.17	1.11	1.12	1.17	1.20
Am-241	–0.082	–0.018	–0.056	–0.017	–0.017
Am-243	0.32	0.22	0.27	0.33	0.32
Cm-244	0.18	0.18	0.13	0.15	0.15
Cm-245	0.018	0.017	0.013	0.016	0.015

evaluation of depletion behaviour and reactivity is probably U-233. This concentration is well reproduced by most codes, MCBurn being slightly off.

#### 5.4. Radial element distributions

The radial distributions of a number of elements are plotted in Fig. 5. Due to limitations in the EET software package, only seven radial zones are simulated, while the other simulations have been carried out with ten radial zones. Due to problems with the analysis

equipment, the radial elemental distributions have not yet been experimentally determined so no comparison with experiment can be made.

The general trend is similar in all plots and also follows reason; elements which have been produced have a concentration peak at the pellet surface, whereas elements which have been reduced in concentration have been more so in the peripheral region. This mirrors the expected shielding effect, leading to higher reaction rates close to the pellet surface. However, the CASMO-5 results indicate a significantly weaker radial dependence of the concentration of some

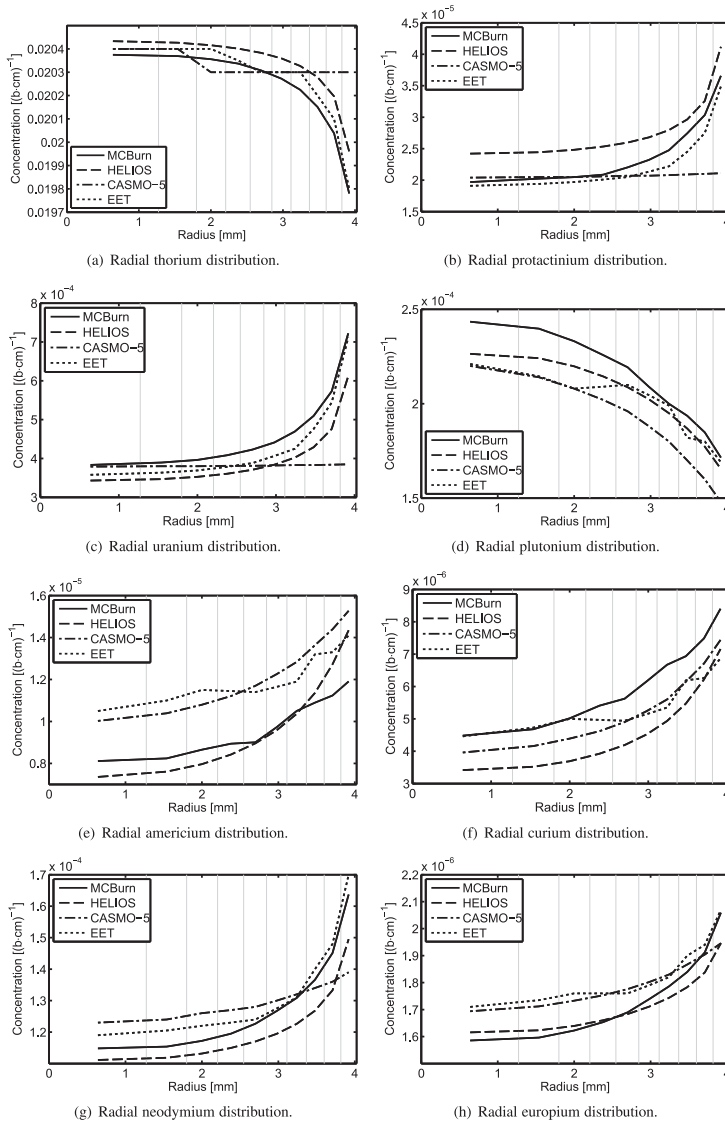


Fig. 5. Radial distribution of several different elements (sum of investigated isotopes) in the Th/Pu test rodlet at the end of burnup. Note that the EET code system could only simulate seven radial zones, so three of the radial points had to be estimated by interpolation.

elements. These elements are thorium and elements derived from thorium, i.e. protactinium (mostly Pa-231), uranium (mostly U-233) and europium, the fission yield of which is much larger for U-233 than for Pu-239, as stated earlier. The CASMO-5 prediction of the radial distribution of plutonium and elements mainly derived from plutonium, i.e. americium and curium, however, agrees well with the other predictions. An exception is the radial distribution of neodymium. The fission yield of most neodymium isotopes is similar for U-233 and Pu-239, and considering that Pu-239 stands for a majority of the fissions, the neodymium profile should follow the Pu-239 profile approximately.

A possible explanation for the deviating CASMO-5 results could be that CASMO-5 normally treats the fuel pellet as one single homogeneous region and uses an empirical radial distribution function for the U-238 resonance integral when a radial subdivision is requested by user input, as it is in this case. This radial distribution function does not necessarily apply to the Th-232 resonance integral. This could also be the reason for the underprediction of the averaged content of the uranium isotopes referred to in Section 5.3.

## 6. Conclusions

The four benchmarked code systems show a general ability to simulate depletion of thorium–plutonium oxide fuel in a light water reactor environment. Considering the uncertainties in the experimental setup and the cross section libraries, the results are in reasonable agreement, with only two exceptions, listed below;

- Compared to the other codes, MCBurn predicts a higher relative power of the Th/Pu pin relative to the surrounding MOX pins.
- CASMO-5 predicts a comparatively flat radial concentration profile of Th-232 and related isotopes, compared to the other codes.

Before existing code packages are used for critical simulations of commercial reactors operating with Th/Pu fuel, these issues should be studied further. However, the general impression is that the issues are limited to a single aspect of the modelling capability, i.e. there is nothing fundamentally wrong with the Th/Pu fuel modelling methodology in any of the benchmarked codes.

To address the issue related to CASMO-5, the radial profiles of Th-232 and related isotopes should be measured, which can be done on the material studied in this benchmark exercise. It is likely that this will be done at the ITU within the coming months. Although it is likely that the CASMO-5 results are the ones which are incorrect in this respect, an experimental confirmation would be valuable.

Further benchmarking exercises may be necessary before Th/Pu is employed on large scale, in particular with respect to burnup prediction. For such future studies, we would like to stress the

importance of documentation of all parameters of any possible impact. In particular, more accurate measurements of the power history would be strongly recommended, for example by a neutron detector located in the guide tube above or below the thorium rodlet. Additional simulations could for example be done for a larger area, which would cover the location where the power measurements were made. To complement this study in the most efficient way, future benchmarks should be made with an experimental setup where thorium fuel dominates the power production, in order to assess the power level and multiplication factor experimentally. This would facilitate addressing the issue related to the power distribution as calculated with MCBurn.

## Acknowledgements

This work was carried out as part of the LWR-DEPUTY project, which was co-funded by the European Commission under the Euratom Research and Training Programme on Nuclear Energy within the Sixth Framework Programme, contract number 036421.

The ECCO model used by KIT was prepared thanks to the help of Dr. F. Gabrielli.

## References

- Bell, M., 1973. ORIGN – the ORNL Isotope Generation and Depletion Code. Technical Report ORNL-4628. ORNL.
- Insulander Björk, K., Fhager, V., 2009. Comparison of thorium–plutonium fuel and MOX fuel for PWRs. In: Proceedings of GLOBAL. Paper 9449.
- Rhodes, J., Smith, K., Lee, D., 2007. CASMO-5/CASMO-5M, a Fuel Assembly Burnup Program. User's manual. Studsvik Scandpower.
- Rimpault, G., et al. (Eds.), 2002. The ERANOS Code and Data System for Fast Reactor Neutronic Analyses, International Conference on the Physics of Reactors, Seoul, Korea.
- Rineiski, A., 2008. Decay heat production in a TRU burner. Progress in Nuclear Energy 50, 377–381.
- Schithelm, O., Nabbli, R., Simons, F. (Eds.), 2010. A MCNP High Resolution Approach for the Simulation of the LWR Fuel Element Configurations. Jahrestagung Kerntechnik, Berlin, Deutschland.
- Versteegh, A., et al., 2004. THORIUM-CYCLE Final Report. Technical report. NRG Petten. FP5-EAECTP C.
- Verwerft, M., Lemehov, S.E., Wéber, M., Vermeeren, L., Gouat, P., Kuzminov, V., Sobolev, V., Parthoens, Y., Vos, B., Van den Bergh, H., ans Segura, S., Blanpain, P., Somers, J., Toury, G., McGinley, J., Staicu, D., Schubert, A., Van Uffelen, P., Haas, D., 2007. OMICO Final Report. Technical Report EUR 23104. European Commission. FIKS-CT-2001–00141.
- Verwerft, M., Gysemans, M., De Breaemacker, A., Schithelm, O., Nabbli, R., Rineiski, A., Vezzoni, B., Romanello, V., Mittag, S., Kliem, S., McGinley, J., Van Winkel, S., Papaioannou, D., Worrall, A., Grove, C., daCruz, D.F., Hania, R., Klaassen, F., Kivel, N., Restani, R., Martin, M., Darilek, P., Breza, J., 2011. LWR-DEPUTY Final Report. External Report SCK-CEN-ER-200, SCK-CEN, SCK-CEN, Boeretang 200, BE-2400 Mol, Belgium. FIGW-036421.
- Villarino, E., Stamm'ler, R., Ferri, A., Casal, J., 1992. HELIOS: angularly dependent collision probabilities. Nuclear Science and Engineering 112, 16–31.
- Winckel, S.V., et al., 2010. Radiochemical Analysis of a High Burn-up (Th, Pu)<sub>2</sub>O<sub>7</sub> Sample, Irradiated in KW0 Obrighheim. Technical Report. JRC–ITU. LWR-DEPUTY Project Deliverable D07c.
- X-M.C. Team, 2005. MCNP – a General Monte Carlo N-particle Transport Code, Version 5. Los Alamos National Laboratory.



# Paper III

**Comparison of Thorium-Plutonium fuel and MOX fuel  
for PWRs**



## Comparison of Thorium-Plutonium fuel and MOX fuel for PWRs

Klara Insulander Björk<sup>a</sup> and Valentin Fhager<sup>a</sup>

<sup>a</sup>Thor Energy A/S

Sommerrogaten 13-15, NO-0255 Oslo, Norway

Tel: +4691117835, Fax: +4722557520, Email: klara.insulander@scatec.no

**Abstract** – Thorium-plutonium (Th,Pu) oxide fuels will provide an evolutionary way to simultaneously reduce plutonium volumes and capture energy from this material. In this work we compare the neutronic properties of Th,Pu-fuel and MOX fuel with different Pu isotope vectors. For these studies, burn-up simulations are performed for a regular MOX PWR fuel assembly and for a thorium-plutonium PWR fuel assembly of the same geometry. The neutronic properties and performance of the assemblies are investigated by lattice calculations using CASMO-5. The plutonium content of the two fuel types is chosen so that the same total energy release per fuel assembly is achieved, which demanded a somewhat higher plutonium content in the thorium-plutonium case. The assemblies are then analyzed with regards to temperature coefficients, delayed neutron fractions, control rod and boron worths, coolant void reactivity (CVR) and decay heat. Overall, the results show that MOX and Th,Pu-fuel have fairly similar neutronic properties in existing PWRs. Th,Pu-fuel offers an advantage over MOX fuel with regards to CVR values and plutonium consumption. The conclusion is therefore that introducing Th,Pu-fuel would improve these factors without imposing any major hurdles from a reactor physics point of view.

### I. INTRODUCTION

Reprocessing spent uranium fuel for re-use of plutonium in MOX fuel is well-established technology. Today, over 30 reactors operate with MOX fuel and international trends indicate that the interest for fuelling reactors with plutonium will increase. In Japan, a new reprocessing plant has been completed, and a MOX fuel fabrication plant will be built. Countries such as the UK are currently considering re-use in MOX as one viable option for disposition of stockpile reactor-grade plutonium. At the same time, a US-Russian program is underway to dispose several tonnes of surplus weapons-grade plutonium, capturing its energy content through burning in power producing reactors.

Traditional MOX utilization in PWRs has been associated with some limitations, such as lower control rod and boron worth, positive CVR at high Pu contents, higher levels of radiotoxicity and decay heat in spent fuel, poorer fission gas retention capability and low plutonium consumption. It is proposed that replacing the DU with thorium in ordinary MOX fuel would mitigate some of these issues. For example, thorium oxides are known to have excellent thermal properties and high fission gas retention capacity, which could be used to the benefit of increasing discharge burnup.

In this paper, we investigate the neutronic aspects of mixing plutonium of various qualities with thorium and we assess the viability of thorium-plutonium oxide fuel as an alternative to MOX fuel in PWRs. We show that thorium-plutonium fuel (Th,Pu-fuel) is similar to MOX fuel in every respect, except for two positive features:

- Burning of Th,Pu-fuel gives a superior net plutonium destruction and reduction of the fraction of fissile plutonium.
- The plutonium fraction, and thus the maximum discharge burnup, can be extended further with Th,Pu-fuels than with MOX fuels, without the CVR becoming positive.

Previous investigations of thorium based fuel for currently operating light water reactors have mainly focused on using uranium as the fissile component, e.g. <sup>1,2</sup>. Although this concept has many merits in terms of actinide waste reduction etc., we consider the possibility of combining thorium with plutonium more interesting from the perspective of effective resource utilization, management of plutonium stockpiles and for facilitating transition to a closed Th+U-233 cycle. A few studies have been made of Th,Pu-fuel for currently operating light water reactors, e.g. <sup>3,4</sup> and we here seek to extend the

understanding of the merits of Th,Pu fuel by a direct comparison to MOX fuel.

The rest of the paper is outlined as follows: The methodology and the assumptions made are described in Section II. The results are presented and discussed in Section III and in Section IV, conclusions are drawn from the calculated results.

## II. METHODOLOGY

In this study a standard 17-by-17 pin PWR fuel assembly is modeled and assumed to be loaded in a regular PWR, operating under the conditions stated in Table I. The boron concentration at hot full power (HFP) conditions is chosen as the cycle average for currently operating UOX fuelled PWRs, whereas the boron concentration at cold zero power (CZP) conditions is chosen as the highest currently used value, which is used at beginning of cycle (BOC). All parameters are calculated at the HFP conditions except for the ITC. Standard oxide pellets and a homogeneous bundle design are assumed. In addition, a uranium oxide PWR fuel assembly is modeled as a reference. With the same demands on total energy production as for the plutonium-containing bundles, the enrichment level is chosen to be 4.55 wt % U-235.

TABLE I  
General operating conditions.

Parameter	Notation	Value
Number of fuel assemblies	$N$	193
Number of fuel batches	$n$	3
Cycle length (days)	$T_C$	450
Reactor thermal power (MW)	$P_{th}$	3400
<i>At hot full power (HFP):</i>		
Boron concentration (ppm)		500
Power density (kW/dm <sup>3</sup> )		104
Moderator temperature (K)		583
Fuel temperature (K)		900
System pressure (bar)		155
<i>At cold zero power (CZP):</i>		
Boron concentration (ppm)		1600
Power density (kW/dm <sup>3</sup> )		0
Moderator temperature (K)		293
Fuel temperature (K)		293
System pressure (bar)		1

### II.A. Neutronic Simulation Software

All calculations are carried out on a 2D infinite lattice level. For these calculations, the fuel assembly burnup simulation program CASMO-5 is used<sup>5</sup>, together with the cross section library ENDFB-VII.

### II.B. Fuel composition

This study focuses on comparing the properties of regular MOX and Th,Pu-fuel in which plutonium of different qualities is used as the initial fissile component. The four plutonium isotope vectors used are (i) reactor grade plutonium (RGPu), (ii) RGPu plutonium with an in-growth of Am-241 (AmPu), (iii) weapons grade plutonium (WGPu) and (iv) plutonium recovered from reprocessed MOX fuel, "second time recycled plutonium" (2RPu). The isotope vectors of the plutonium compositions used in this study are listed in Table II. For the rest of this paper, any mixture of depleted uranium (DU) and Pu will be referred to as MOX, with the Pu composition specified by a prefix, e.g. RG-MOX for a mixture of DU and RGPu.

TABLE II  
Plutonium isotope vectors.

Name	Pu238	Pu239	Pu240	Pu241	Pu242	Am241
RGPu	2%	53%	25%	15%	5%	-
AmPu	2%	53%	25%	10%	5%	5%
WGPu	-	94%	6%	-	-	-
2RPu	3%	37%	30%	19%	11%	-

The fraction of plutonium in each fuel type is adapted to give the same total energy release during the lifetime of the fuel assembly, following a previously described methodology<sup>6</sup>. This implies a demand for higher burnup, i.e. higher energy production per unit mass, in the thorium cases, as thorium oxide fuel has a slightly lower density and hence a lower fuel weight per assembly. The desired total energy release per fuel bundle, equal to the product of the assembly heavy metal weight  $M$  and the assembly average discharge burnup  $B_D$ , is calculated by Eq. (1), using parameters given in Table I.

$$E_{tot} = M \cdot B_D = \frac{P_{th} \cdot T_C \cdot n}{N} \quad (1)$$

### II.C. Temperature Coefficients

The response of the infinite multiplication factor  $k_{\infty}$  to temperature perturbations can be described in terms of temperature coefficients. The temperature coefficients considered in this study are the Fuel Temperature Coefficient (FTC) and the Moderator Temperature Coefficient (MTC) at hot full power and the Isothermal Temperature Coefficient (ITC) at cold zero power. These should preferably be negative, to ensure inherent negative reactivity feedback in the reactor system. The amplitude, though, should not be too large.

The temperature coefficients are estimated by perturbation calculations.  $k_x$  is calculated at several points in life both for the normal, unperturbed operating conditions stated in Table I ( $k_U$ ) and for a perturbed state ( $k_P$ ), where the parameter of interest is increased by a temperature difference  $\Delta T$ . The temperature coefficient  $C$  is then calculated by Eq. (2).

$$C = \frac{k_P - k_U}{\Delta T \cdot k_U} \quad (2)$$

The ITC at CZP is calculated with control rods inserted. It should also be noted that the boron concentration at CZP is chosen to obtain conservative results for the ITC calculation, as a higher boron concentration gives a higher ITC.

#### I.I.D. Coolant Void Reactivity

The Coolant Void Reactivity is calculated by Eq. (3), with  $k_P$  and  $k_U$  being the infinite multiplication factor in the voided and unvoided cases, respectively.

$$CVR = \frac{k_P - k_U}{k_U} \quad (3)$$

The maximum plutonium content, and thus the maximum possible burnup of MOX fuel, is limited by the fact that the CVR is positive for a plutonium content above a certain threshold<sup>7,8</sup>. In order to investigate whether the use of Th,Pu-fuel can offer an advantage in this respect, the CVR dependence on plutonium content is investigated for both MOX and thorium based fuel. Here, the cases where AmPu and 2RPu is used for providing the fissile component are of particular interest, since the demand for a negative CVR might put a limit on the achievable burnup in these scenarios..

#### I.I.E. Control Rod and Boron Worth

One of the factors limiting the core loading fractions of MOX fuel assemblies in most of the currently operating reactors is the reduced worth of control rods and soluble boron in the presence of MOX fuel assemblies<sup>8,9</sup>. This is a result of the high thermal absorption cross section of plutonium compared to uranium, which results in a reduced thermal neutron flux.

The reactivity dependence on soluble boron concentration and control rod presence is investigated. The boron worth ( $BW$ ) is calculated by perturbation calculations;  $k_x$  is calculated for the boron concentration given in Table I ( $k_U$ ), and for a perturbed boron concentration ( $k_P$ ) and the boron worth is calculated by Eq.

(4), where  $\Delta C_B$  is the difference in boron concentration between the perturbed and the unperturbed states.

$$BW = \frac{k_P - k_U}{\Delta C_B \cdot k_U} \quad (4)$$

The control rod worth is calculated just like the CVR (see Eq. (3)), with  $k_P$  and  $k_U$  denoting the infinite multiplication factor with and without control rod presence, respectively. The control rod worth is calculated at end of cycle for each fuel batch, i.e. at the end of six burnup intervals, dividing the life of the fuel assembly into six equal parts. The worth of an average control rod roughly equals the average of the control rod worth at these six burnup points. It should be noted that what is simulated in 2D-lattice calculations is the equivalent of inserting all control rods in an infinite lattice of identical fuel assemblies, which obviously deviates significantly from real conditions. Thus, the calculated values are only valid for comparison between different fuel types in this study.

### III. RESULTS

#### III.A. Fuel composition

Adapting the plutonium fraction of the different fuel types gives the behavior of the  $k_x$  vs. burnup curve shown in Fig. 1. The reactivity swing is similar in the thorium and regular MOX cases, but is significantly larger in the cases where WGPu is used. This is due to less conversion of Pu-240 to Pu-241 in these fuel types. The infinite multiplication factor is somewhat higher in the thorium fuel cases than in the corresponding regular MOX cases for the same burnup, in order to reach a higher discharge burnup, which is needed to compensate for the lower fuel weight when targeting the same total energy production.

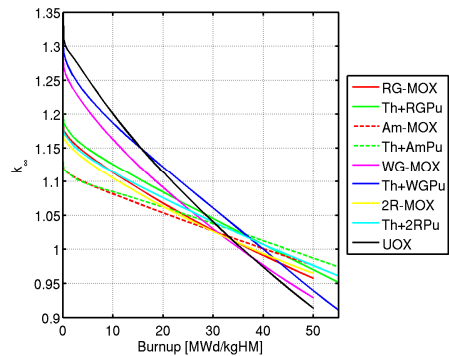


Fig. 1.  $k_x$  vs. burnup for all different fuel types.

The corresponding initial composition of each fuel type is listed in Table III, along with the total assembly heavy metal mass  $M$  and the assembly average discharge burnup  $B_D$ , as calculated from Eq. (1). The DU is assumed to contain 0.25 % U-235.

TABLE III

Fuel compositions and total assembly heavy metal mass  $M$ , expressed in kg, and discharge burnup  $B_D$ , in MWd/kgHM.

Fuel type	DU	Th-232	Pu	$M$	$B_D$
<b>RG-MOX</b>	<b>443.2</b>	-	<b>38.2</b>	<b>481.4</b>	<b>49</b>
Th+RGPu	-	390.2	41.0	431.2	55
<b>Am-MOX</b>	<b>429.9</b>	-	<b>49.0</b>	<b>481.4</b>	<b>49</b>
Th+AmPu	-	397.0	49.6	431.2	55
<b>WG-MOX</b>	<b>458.8</b>	-	<b>22.6</b>	<b>481.4</b>	<b>49</b>
Th+WGPu	-	404.5	26.7	431.2	55
<b>2R-MOX</b>	<b>427.2</b>	-	<b>54.2</b>	<b>481.4</b>	<b>49</b>
Th+2RPu	-	376.0	55.2	431.2	55

It can be seen in Table III that about 7% less RGPu is needed in the RG-MOX case compared to the Th+RGPu case. The reason for this difference is partly the 0.25 wt % U-235 content of the DU, and partly the higher fast fission cross section of U-238 compared to Th-232. For Pu compositions with a higher fissile content, this difference is larger (15% for WGPu) and for lower fissile content it is smaller (5% for 2RPu).

The difference in Pu demand for reaching a certain total lifetime energy release also depends on the energy release target. Fig. 2 shows the RGPu demand as a function of the total energy release in one fuel assembly. The dashed line marks the energy release targeted in this study, as calculated by Eq. (1), which is 24 GWd per fuel assembly. For energy release targets above 42 GWd per fuel bundle (corresponding to 87 MWd/kgHM in the RG-MOX case and 97 MWd/kgHM in the Th+RGPu case), the Pu demand

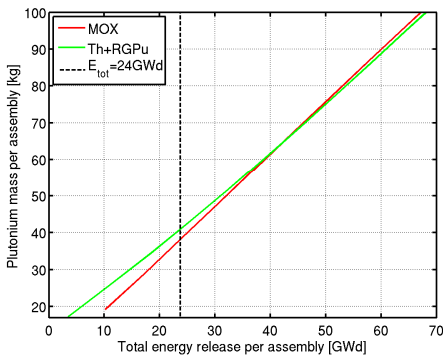


Fig. 2. The plutonium demand as a function of the total energy release in one fuel assembly.

is lower in the thorium case than in the MOX case. At higher burnup the significance of in-situ burning of in-bred U-233 in Th+RGPu fuel increases, and U-233 provides improved neutron economy over Pu-239 and Pu-241 in a PWR.

Another conclusion that can be drawn from the data in Table III is that the in-growth of 5% of Am-241 affects the reactivity slightly more in the regular MOX case than in the thorium case. The initial Pu content must be increased by 28% in the MOX case and by 21% in the thorium case in order to reach the same discharge burnup with AmPu as with RGPu. The Pu demand is only 1.2% lower in the Am-MOX case compared to the Th+AmPu case. This difference in sensitivity between the thorium case and the MOX case can be explained by the increase in Pu fraction which reduces the importance of the difference between DU and Th-232.

### III.B. Plutonium consumption

One reason for burning Pu in a reactor could be to reduce the existing stockpiles of plutonium. In this context, both the reduction of total plutonium and the fissile fraction of the plutonium at discharge are of interest. Another important aspect when Pu is burnt in a thermal spectrum is the production of minor actinides. The initial and final plutonium content of each fuel type is listed in Table IV, along with the final MA content, the fractional plutonium reduction and the final fissile fraction. The MA content here is taken as the content of Am and Cm isotopes.

TABLE IV  
 Plutonium and MA mass data.

Fuel type	Initial Pu mass	Final Pu mass	Pu reduction	Final fissile fraction	Final MA mass
<b>RG-MOX</b>	<b>38.2</b>	<b>27.5</b>	<b>28%</b>	<b>57%</b>	<b>1.90</b>
Th+RGPu	41.0	18.9	54%	43%	1.97
<b>Am-MOX</b>	<b>49.0</b>	<b>37.8</b>	<b>23%</b>	<b>56%</b>	<b>3.12</b>
Th+AmPu	49.6	26.7	46%	44%	3.05
<b>WG-MOX</b>	<b>22.6</b>	<b>14.8</b>	<b>35%</b>	<b>64%</b>	<b>0.494</b>
Th+WGPu	26.7	7.4	72%	47%	0.499
<b>2R-MOX</b>	<b>54.2</b>	<b>41.3</b>	<b>24%</b>	<b>50%</b>	<b>3.10</b>
Th+2RPu	55.2	31.3	43%	38%	3.12

The conclusion to be drawn from the numbers in Table IV is that thorium based fuel is superior to MOX in a context where destruction of plutonium is the main objective. In the thorium cases, a significantly larger mass of plutonium is destroyed. Also, the fissile fraction is decreased to below 50% in all thorium cases, whereas this is not the case for any of the MOX cases. The production of minor actinides is similar in all cases.

### III.C. Temperature Coefficients

The temperature coefficients are generally similar for the thorium and MOX cases, and only the ITC is significantly different in the plutonium containing fuels compared to the UOX reference.

The FTC is very similar in all plutonium containing cases, see Fig. 3. Although the FTC of the UOX fuel is initially higher than all Pu cases, the assembly lifetime average FTC magnitude is only 8% smaller in the UOX case compared to the regular MOX case. The difference in average FTC between MOX and thorium based fuels is even smaller; 6% for the RGPu-containing cases. Because of this, we believe that possible challenges or benefits that could be encountered as a result of the larger FTC magnitude would be similar in MOX and thorium cases.

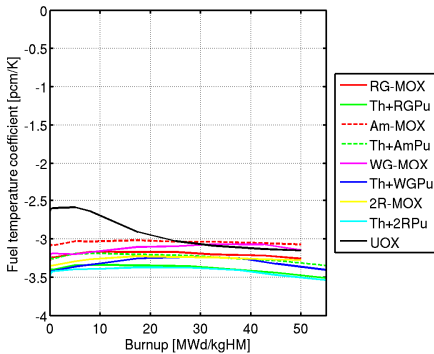


Fig. 3. The FTC dependence on burnup.

The MTC is negative in all cases. For the RG-MOX and the WG-MOX fuel types, the MTC is significantly lower than for the UOX reference, whereas it in the thorium cases is fairly similar to that of UOX, see Fig. 4. The MTC, thus, is not foreseen to cause any problem for the introduction of thorium based fuel.

It is worth noting that the burnup dependence of the MTC in the Th+WGPu case differs from that of the others. This is due to the rapidly increasing fraction of fissions that take place in U-233 nuclei in this case. Whereas the optimum reactivity of plutonium containing fuel lies at a lower fuel-to-moderator ratio than that of a normal PWR bundle, the optimum reactivity for U-233 fuels lies at a higher fuel-to-moderator ratio. An increase in moderator temperature, giving a lower moderator density, thus brings the conditions closer to the optimum for a U-233 bearing fuel.

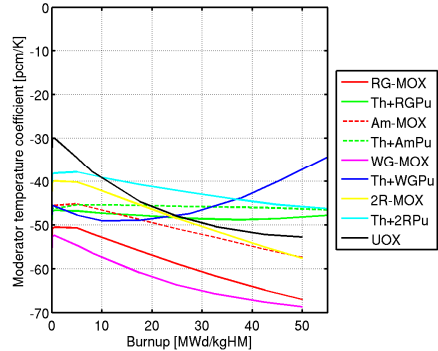


Fig. 4. The MTC dependence on burnup.

The ITC at CZP is significantly closer to zero in all plutonium containing cases compared to the UOX reference, but very similar in all plutonium containing cases, see Fig. 5. As with the FTC, we see that if any challenges are met in this respect, they will be similar in the MOX and thorium cases.

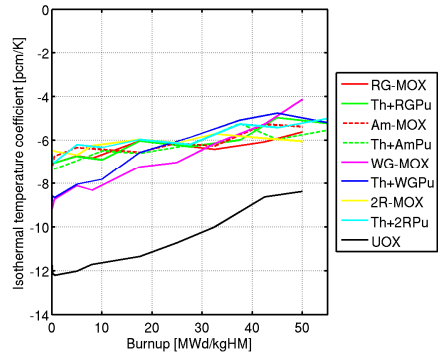


Fig. 5. The ITC dependence on burnup at CZP.

### III.D. Coolant Void Reactivity

The CVR proves to depend more strongly on the total initial plutonium content than on the fertile matrix used (DU or Th). For a given Pu vector, the CVR is generally lower in the thorium case than in the MOX case. The exception is the Th+WGPu case where the CVR increases with burnup to become larger than in the WG-MOX case. The explanation for the increasing MTC in the Th+WGPu case also applies to this situation.

Another important conclusion that should be drawn from Fig. 5 is that the CVR is closer to zero in all plutonium containing cases, compared to that of the UOX reference, and significantly so in the RGPu and 2RPu cases. Although the CVR does not become positive in any of the cases, this should call for close attention. It should be noted that these simulations are only carried out for one particular set of operating conditions and one operating history, and another combination of parameters could potentially lead to a positive CVR, which constitutes a grave safety hazard.

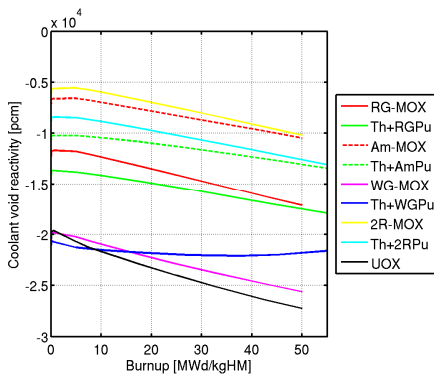


Fig. 6. The CVR dependence on burnup.

As previously noted, this risk of the CVR becoming positive limits the fraction of plutonium that could be contained in PWR fuel, and thus also limits the achievable discharge burnup. For the purpose of investigating how the use of thorium can enable the use of higher initial Pu contents, the CVR at beginning of life of the fuel assembly

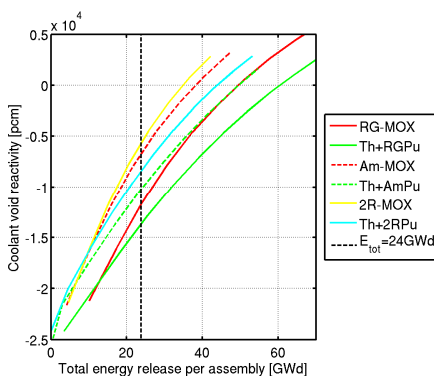


Fig. 7. The CVR dependence on total energy release for RG-MOX, Th+RGPu, WG-MOX and Th+2RPu fuel.

(which is the limiting case, as seen in Fig. 6) has been calculated for different Pu contents, and plotted against the resulting discharge burnup in Fig. 7. For reference, a vertical line is plotted, marking a total energy release of 24 GWd/fuel assembly which is the case investigated in this paper.

The conclusion is clearly that a higher initial plutonium content, and thus a higher discharge burnup, can be allowed with thorium based fuel than with regular MOX without the CVR becoming positive, although exactly how much higher remains unclear. Fig. 7 suggests that fuel assembly energy release can be extended to 35 GWd in the 2R-MOX case, to 44 GWd in the Th+2RPu case, to 38 GWd in the Am-MOX case, to 50 GWd in the Th+AmPu case, to 50 GWd in the RG-MOX case and to 61 GWd in the Th+RGPu case. The corresponding discharge burnup and Pu contents are listed in Table V.

TABLE V

Total energy release  $E_{tot}$ , discharge burnup (bur.), Pu fraction and Pu mass per fuel assembly for the value of these parameters at which the CVR of the corresponding fuel becomes positive.

Fuel type	$E_{tot}$ (GWd)	Discharge burnup (MWd/kgHM)	Pu fraction (%)	Pu mass (kg)
<b>RG-MOX</b>	<b>50</b>	<b>103</b>	<b>15.6</b>	<b>75</b>
Th+RGPu	61	140	20.7	89
<b>2R-MOX</b>	<b>35</b>	<b>73</b>	<b>15.4</b>	<b>74</b>
Th+2RPu	44	102	20.4	88
<b>Am-MOX</b>	<b>38</b>	<b>80</b>	<b>15.3</b>	<b>74</b>
Th+AmPu	50	115	20.4	88

Judging from these numbers, the CVR should not be the limiting factor for extending discharge burnup, as the values listed in Table V lie far above the currently prevailing discharge burnup limits, which are not set by neutronic properties but rather by irradiation behavior of the fuel material, such as fission gas release. Previous work<sup>7</sup>, though, suggests that the Pu fraction at which the CVR becomes positive is 13% for MOX fuel, rather than the 15-16% concluded in this study. As a 13% Pu content corresponds to a discharge burnup of only 59 MWd/kgHM in the 2R-MOX case, the CVR issue seems to be more limiting than indicated by the numbers above. This would make the Th alternative more interesting.

### III.E. Control Rod and Boron Worth

The reactivity worth of control rods and soluble boron are slightly higher in the thorium cases than in the corresponding MOX cases, see Figs. 8 and 9. The differences between fuel types with different Pu isotope vectors, though, are larger than the differences between the corresponding thorium and MOX cases. In all plutonium containing cases, the control rod and boron worths are significantly lower than in the UOX reference case. The

remedies to these issues used in modern reactors, in order to allow a 100% MOX loading, is the use of enriched boron and/or a larger number of control rods. This will thus also be needed for Th,Pu-fuel.

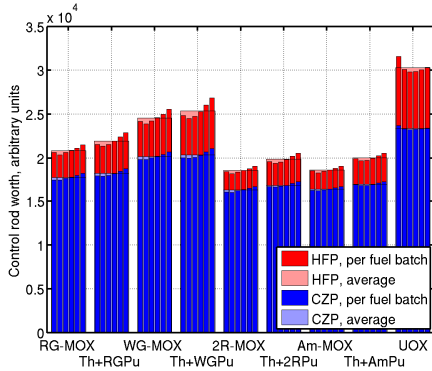


Fig. 8. The control rod worth at HFP and CZP.

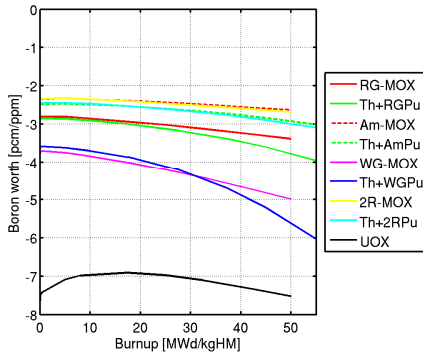


Fig. 9. The boron worth dependence on burnup.

### III.F. Delayed Neutron Fraction

The delayed neutron fraction indicates the rapidness with which the reactor responds to perturbations. This is known to be significantly smaller for Pu-239 (0.0022), Pu-241 (0.0054) and U-233 (0.0026) than it is for U-235 (0.0067)<sup>10</sup>. Consequently, the delayed neutron fractions of the fuels containing these isotopes are all lower than that of UOX fuel. It is very similar between all plutonium containing fuels. Consequently, potential challenges are once again similar in the MOX and Th,Pu-fuel cases.

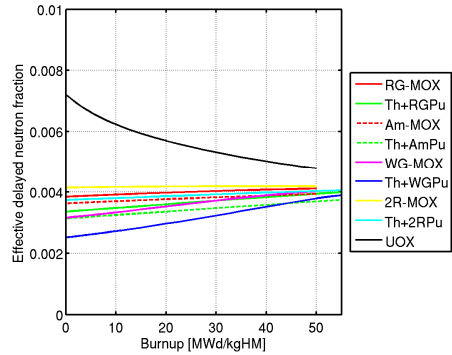


Fig. 10. The delayed neutron fraction dependence on burnup.

### III.G. Heat production

The heat production during the first 30 minutes after shut down is important for dimensioning of the emergency cooling system. It is seen in Fig. 11 that this will most certainly not limit the use of either MOX or Th,Pu-fuel. In all cases, the decay heat accumulated in the core during this time range is lower than the UOX reference, except for the Am-MOX case, where it is only slightly higher. The thorium based fuels show a lower decay heat than the MOX fuels in this time range.

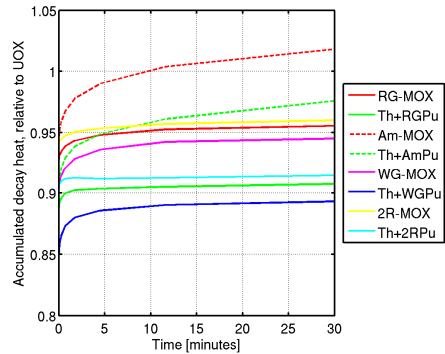


Fig. 11. The heat production in spent fuel in the emergency cooling time range.

For intermediate storage of spent fuel, i.e. during the first 1-100 years, the decay heat of the plutonium containing fuels is comparatively high. This turns out to depend strongly upon the initial plutonium content and hardly to any extent on whether DU or Th has been used as the fertile matrix. Thus, basically the same conditions which apply to storage of spent MOX fuel also apply to the case of Th,Pu-fuels.

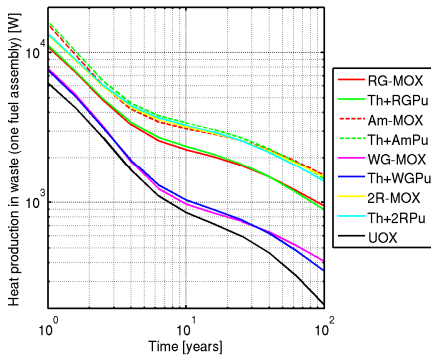


Fig. 12. The heat production in spent fuel in the intermediate storage time range.

#### IV. CONCLUSIONS

The results show that Th,Pu-fuel is similar to MOX fuel in several respects when compared, as here, using a homogeneous fuel design. Therefore, introduction of Th,Pu-fuel should be very similar to that of MOX fuel. Many properties, such as the CVR, the control rod and boron worths and the long term decay heat depend rather on the plutonium quality than on whether DU or Th-232 is used as the fertile matrix. In the cases where MOX has proven to have properties significantly different to those of UOX, the properties of Th,Pu-fuel are generally similar to those of MOX fuel.

MOX and Th,Pu-fuel only display significant differences in two respects, discussed below.

##### IV.A. Plutonium destruction

Burning of Th,Pu-fuel gives a superior capability of plutonium destruction and reduction of the fraction of fissile plutonium in the spent fuel.

Plutonium is also consumed at a higher rate for the same energy production targets, as thorium fuel demands a higher initial plutonium content than MOX fuel. This can be regarded as either beneficial or detrimental to the

Th,Pu-fuel case, depending on viewpoint. The relationship is reversed for high discharge burnups.

It should also be mentioned that previous work<sup>11</sup> indicates that a higher hydrogen to heavy metal ratio could improve the Pu destruction efficiency even further.

##### IV.B. Coolant Void Reactivity

The plutonium fraction, and thus the maximum discharge burnup, can be extended further with Th,Pu-fuels than with MOX fuels, without the CVR becoming positive. This could eliminate the current limits on recycling of spent MOX fuel.

#### NOMENCLATURE

2RPu	Twice Recycled Plutonium
AmPu	RGPu with 1% Am-241
CVR	Coolant Void Reactivity
CZP	Cold Zero Power
DU	Depleted Uranium
FTC	Fuel Temperature Coefficient
HFP	Hot Full Power
ITC	Isothermal Temperature Coefficient
MA	Minor Actinides
MOX	Mixed oxide fuel (DU and Pu)
MTC	Moderator Temperature Coefficient
RGPu	Reactor Grade Plutonium
UOX	Uranium oxide
WGPu	Weapons Grade Plutonium

#### REFERENCES

1. J. L. FRANÇOIS, A. NÚÑEZ-CARRERA "Core Design of a Boiling Water Reactor Based on an Integrated Blanket-Seed Thorium-Uranium Concept", *Proc. of Advances in Nuclear Fuel Management III*, American Nuclear Society, LaGrange Park, IL (2003)
2. A. GALPERIN, A. RADKOWSKY, "A competitive thorium fuel cycle for pressurized water reactors of current technology", *Proceedings of three IAEA meetings held in Vienna in 1997, 1998 and 1999*, IAEA-TECDOC 1319, pp. 83-96, International Atomic Energy Agency, Vienna, Austria, (1999)
3. A. PULL, "Thorium utilization in PWRs. Neutronics studies", *Proceedings of three IAEA meetings held in Vienna in 1997, 1998 and 1999*, IAEA-TECDOC 1319, pp. 185-197, International Atomic Energy Agency, Vienna, Austria, (1999)
4. A. GALPERIN, M. SEGEV, M. TODOSOW, "A Pressurized Water Reactor Plutonium Incinerator Based on Thorium Fuel and Seed-Blanket Assembly

Geometry”, *Nuclear Technology*, **132**, pp. 214-225, (2000).

5. J. RHODES, K. SMITH and D. LEE, *CASMO-5M A fuel assembly burnup program Users manual*, Studsvik Scandpower (2007).
6. K. INSULANDER BJÖRK, V. FHAGER, C. DEMAZIÈRE, “Methodology for Investigating the Applicability of Thorium-Based Fuels in Existing BWRs”, *Proc. of ICAPP'09*, Tokyo, Japan (2009).
7. IAEA, *Technical Reports Series no. 415; Status and advances in MOX fuel technology*, p. 55, IAEA, Vienna (2003).
8. OECD NUCLEAR ENERGY AGENCY, *Physics of Plutonium Recycling — Issues and Perspectives*, Vol. 1, OECD NEA, Paris (1995).
9. OECD NUCLEAR ENERGY AGENCY, *Plutonium Management in the Medium Term*, p. 17, OECD NEA, Paris (2003).
10. WESTON M. STACEY, *Nuclear Reactor Physics*, p. 144, WILEY-VCH, Weinheim (2007).
11. E. SHWAGERAUS, P. HEJZLAR, M. KAZIMI, “Use of thorium for transmutation of plutonium and minor actinides in PWRs”, *Nuclear technology*, **147**, pp. 53-68 (2004).



# Paper IV

**Study of Thorium-Plutonium Fuel for Possible Operating Cycle Extension in PWRs**



## Research Article

# Study of Thorium-Plutonium Fuel for Possible Operating Cycle Extension in PWRs

Klara Insulander Björk,<sup>1,2</sup> Cheuk Wah Lau,<sup>2</sup> Henrik Nylén,<sup>3</sup> and Urban Sandberg<sup>3</sup>

<sup>1</sup> Thor Energy AS, Sommerrogaten 13-15, 0255 Oslo, Norway

<sup>2</sup> Division of Nuclear Engineering, Department of Applied Physics, Chalmers University of Technology, 412 96 Gothenburg, Sweden

<sup>3</sup> Ringhals AB, 432 85 Väröbacka, Sweden

Correspondence should be addressed to Klara Insulander Björk; [klara.insulander@scatec.no](mailto:klara.insulander@scatec.no)

Received 14 October 2012; Accepted 11 January 2013

Academic Editor: Hangbok Choi

Copyright © 2013 Klara Insulander Björk et al. This is an open access article distributed under the Creative Commons Attribution License, which permits unrestricted use, distribution, and reproduction in any medium, provided the original work is properly cited.

Computer simulations have been carried out to investigate the possibility of extending operating cycle length in the Pressurised Water Reactor Ringhals 3 by the use of thorium-plutonium oxide fuel. The calculations have been carried out using tools and methods that are normally employed for reload design and safety evaluation in Ringhals 3. The 3-batch reload scheme and the power level have been kept unchanged, and a normal uranium oxide fuel assembly designed for a 12-month operating cycle in this reactor is used as a reference. The use of plutonium as the fissile component reduces the worth of control rods and soluble boron, which makes it necessary to modify the control systems. The delayed neutron fraction is low compared with the reference, but simulations and qualitative assessments of relevant transients indicate that the reactor could still be operated safely. Differences in reactivity coefficients are mainly beneficial for the outcome of transient simulations for the thorium based fuel. A 50% extension of the current 12-month operating cycle length should be possible with thorium-plutonium mixed oxide fuel, given an upgrade of the control systems. More detailed simulations have to be carried out for some transients in order to confirm the qualitative reasoning presented.

## 1. Introduction

The objective of the work described herein is to investigate the possibility of extending operating cycle length in a Pressurised Water Reactor (PWR) by the use of Thorium-Plutonium Mixed Oxide (Th-MOX) fuel.

The general viability of Th-MOX fuel in light water reactors (mainly PWRs) has been confirmed by several recent studies [1–5]. In addition, the neutronic and physical properties of Th-MOX indicate that the fuel is not only viable, but may also improve the economy of a nuclear power plant by allowing for longer operating cycles and hence a higher availability of the reactor. Most importantly, the good material properties [6, 7] of the Thorium-Plutonium Mixed Oxide ceramic indicate that Th-MOX fuel may be capable of sustaining higher burnups than Uranium-Oxide- (UOX-) based fuel types. Secondly, the currently practiced uranium enrichment limit of 5% U-235 does not affect Th-MOX, which

can be loaded with high amounts of plutonium. Finally, the slow change of the multiplication factor with depletion of Th-MOX makes it possible to achieve high burnups without having an excessively high initial multiplication factor [4].

In this paper, we present and discuss the simulation of a standard PWR fuel assembly loaded with Th-MOX fuel and a full Reload Safety Evaluation (RSE) of the Ringhals 3 PWR core when loaded with this fuel assembly. The content of Pu and Burnable Absorbers (BA) in the fuel is adapted for achieving an 18-month cycle, which is an operating cycle extension of 50% compared with the normal cycle length in Ringhals 3. The fuel assembly design is developed using the fuel assembly burnup simulation program CASMO-4E [8], and the RSE is carried out with SIMULATE-3 [9].

The simulated fuel and reactor systems are described in Section 2 and the calculation tools and methods used in this study in Section 3. The results in terms of depletion behaviour

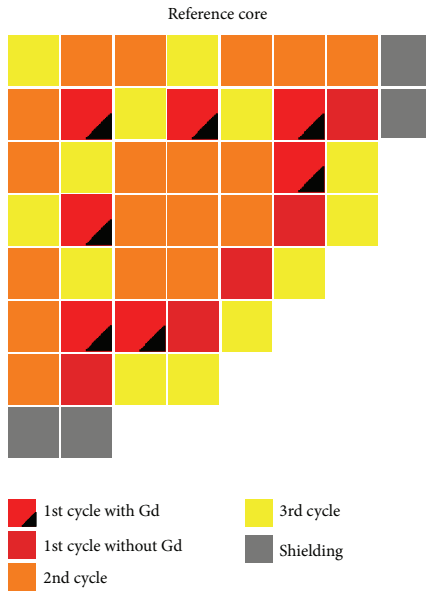


FIGURE 1: The UOX reference core.

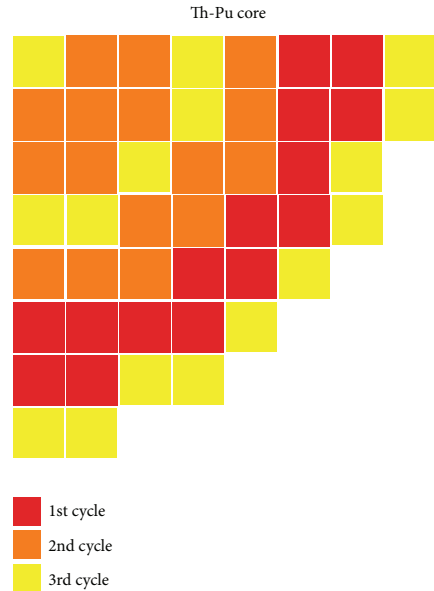


FIGURE 2: The Th-MOX core.

and neutronic safety parameters are presented in Section 4 and conclusions are drawn in Section 5.

## 2. Description of the Modelled System

**2.1. Reactor.** The reactor simulated in this study is the Swedish Ringhals 3 reactor, which is a 3135 MW<sub>th</sub> reactor of Westinghouse design. This reactor operates with a 12-month cycle and a 3-batch reload scheme. In the reference case, which is a typical operation cycle, the Ringhals 3 core is loaded with 28 fuel assemblies containing the BA Gd<sub>2</sub>O<sub>3</sub> and 20 fuel assemblies without BA. Such a reload is used as a reference in this work. The core design is shown in Figure 1 and the fuel assemblies will be discussed in more detail in Section 2.2.

The Th-MOX core is designed for an 18-month cycle using a different core layout, designed to reduce the power of the oldest fuel assemblies. Without this change of the layout, the oldest fuel assemblies (having the highest burnup) would run at a power level which would be too high considering the deterioration of the fuel material at high burnup. This core design is shown in Figure 2.

**2.2. Fuel Assemblies.** The reference fuel is a UOX fuel assembly designed for a standard 12-month cycle in Ringhals 3, which requires an enrichment of 4.4% in most fuel rods. The assembly comprises 264 fuel rods, arranged in a standard 17-by-17 lattice with a central instrumentation thimble and 24 control rod guide tubes. In the assemblies containing Gd<sub>2</sub>O<sub>3</sub>, this is located in 12 rods. Since the addition of Gd<sub>2</sub>O<sub>3</sub> lowers

the thermal conductivity of the fuel, a lower enrichment (2.8%) is used in order to avoid high power in these fuel rods. The reference fuel design with Gd<sub>2</sub>O<sub>3</sub> is shown in Figure 3. The reference fuel without BA is identical except that all rods have 4.4% enrichment and no BA. The fuel assembly heavy metal weight is 461 kg.

The Th-MOX fuel design uses the same mechanical structure as the reference fuel, but differs in two important aspects.

Firstly, the uranium oxide fuel is exchanged for a mixture of thorium and plutonium oxides. The Pu isotope vector used in the Th-MOX fuel is 2%<sup>238</sup>Pu, 53%<sup>239</sup>Pu, 25%<sup>240</sup>Pu, 15%<sup>241</sup>Pu, and 5%<sup>242</sup>Pu. This corresponds to the Pu vector in spent light water reactor fuel burnt to approximately 42 MWd/kgHM, if reprocessed immediately [10].

Secondly, the Integral Fuel Burnable Absorber (IFBA) concept is preferred over the use of Gd<sub>2</sub>O<sub>3</sub> as a BA. The reason not to use Gd<sub>2</sub>O<sub>3</sub> is that it is normally mixed into the fuel matrix. Since Th-MOX is already a mixed oxide, using Gd<sub>2</sub>O<sub>3</sub> would require a ternary mixture of ThO<sub>2</sub>, PuO<sub>2</sub>, and Gd<sub>2</sub>O<sub>3</sub> which is very difficult to fabricate with good homogeneity. The IFBA concept entails a thin layer of zirconium boride applied to the surface of the fuel pellets [11].

In order to achieve an even power profile within the fuel assembly, three different levels of Pu content are used. The rods with the highest Pu content contain 13.7% Pu, the lowest 9% Pu, and the rest 11.7% Pu. The fuel assembly design is shown in Figure 4.

The mixture of ThO<sub>2</sub> and PuO<sub>2</sub> has a slightly lower density than UO<sub>2</sub> due to the lower mass number of Th. Given

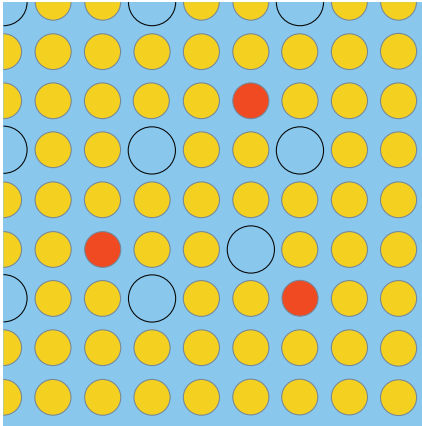


FIGURE 3: The BA-containing UOX reference fuel assembly design (a quarter of the fuel assembly). Yellow rods consist of 4.4% enriched uranium; red rods consist of 2.8% enriched uranium and 6%  $Gd_2O_3$ . The non-BA-containing reference fuel design is identical except that all rods are of the former (yellow) type.

that the same mechanical structure is used, this results in a slightly lower assembly heavy metal weight; 431 kg, assuming the same porosity.

### 3. Method

**3.1. Simulation Tools.** The fuel assembly simulations are carried out in two dimensions, using the fuel assembly burnup simulation program CASMO-4E [8] together with the microscopic cross-section library JEF2.2. CASMO-4E generates cross-section data for the subsequent use in core simulations.

The core simulations are carried out in three dimensions, using SIMULATE-3 [9] and the macroscopic cross-section libraries generated by CASMO-4E and converted by the linking program CMS-link (Studsvik Scandpower's Core Management System (CMS) linking program [12]). SIMULATE-3 is a two-group steady-state nodal code. All the used softwares are supplied by Studsvik Scandpower, Inc.

**3.2. Reload Safety Evaluation.** The Swedish Radiation Safety Authority requires that an RSE is performed for every core reload, in order to ensure that the reactor can be operated safely with the new core design during the whole cycle. The reload safety evaluation employed at Ringhals 3 is based on the Westinghouse reload methodology which is licensed by the United States Nuclear Regulatory Commission (USNRC) as described in the topical report WCAP-9272 [13]. This is a bounding analysis approach, and it is employed in this work in the same way as is usually done when a new reload is designed for Ringhals 3.

In the RSE, a number of key parameters are calculated. These are effective delayed neutron fraction  $\beta_{\text{eff}}$ , boron worth,

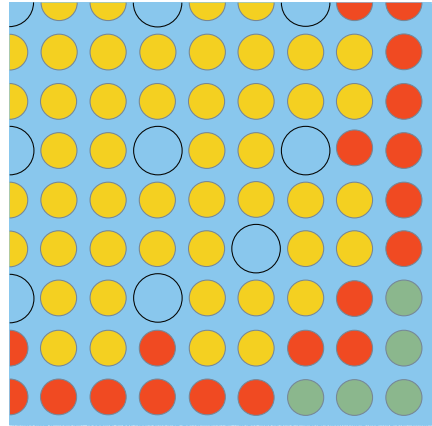


FIGURE 4: The Th-MOX fuel assembly design (a quarter of the fuel assembly). Yellow rods contain 13.7%, red rods 11.7%, and grey rods 9.0% Pu (weight percent of heavy metal content). The zirconium boride layer is too thin to be visible in the figure.

Shut Down Margins (SDM), Moderator Density Coefficient (MDC), Moderator Temperature Coefficient (MTC), Isothermal Temperature Coefficient (ITC), Doppler Temperature Coefficient (DTC), and Doppler Power Coefficient (DPC). For each of these (except for the MTC, in the case of Ringhals 3), there are a lower and/or upper safety limits, specific to the reactor for which the calculations are done. These safety limits take into account the uncertainty in the calculations.

The calculated values of key parameters are then used for checking whether safety conditions are fulfilled for a large number of transients; that is, whether there is departure from nucleate boiling and whether the burnup-dependent limit on the linear heat generation rate (LHGR) is contained.

### 4. Results

**4.1. Depletion Behaviour.** The infinite multiplication factor  $k_{\infty}$  for the different fuel assemblies is shown in Figure 5. One clear difference between the Th-MOX and the reference fuel is that the reactivity decreases more slowly in the Th-MOX case. Another difference is seen during the first cycle (approximately the first 1/3 of the curves), and that is the difference in the rate with which the BA burns out. Whereas the  $Gd_2O_3$  burns out fairly rapidly and almost linearly, the effect of the IFBA in the Th-MOX assembly lingers for a longer time and decays rather exponentially. In both cases, the objective of avoiding an exceedingly high  $k_{\infty}$  at the Beginning Of Life (BOL) is fulfilled. If BA would not be used, the much higher reactivity of the fresh fuel assemblies compared with the once or twice burnt would cause locally high-power levels where the fresh fuel is located, which would limit the power at which the reactor can be safely operated.

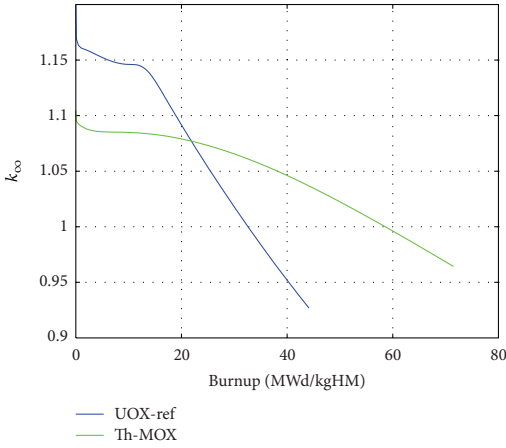


FIGURE 5: Infinite multiplication factor dependence on burnup.

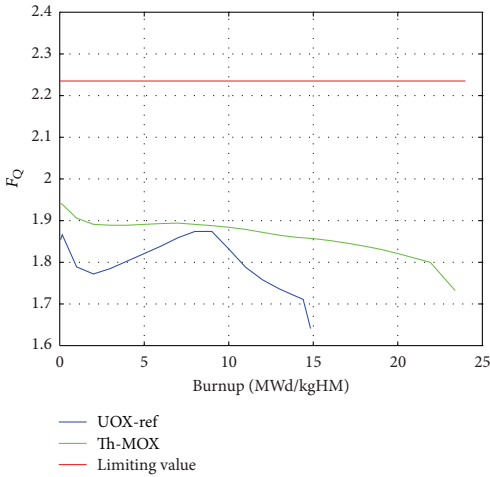


FIGURE 6:  $F_Q$ , that is, local power relative to core average power as a function of burnup.

Also, a higher concentration of soluble boron would be needed to keep the reactor critical.

In order to reach the desired operating time of three 18-month cycles, the assembly average discharge burnup is increased to 78 MWd/kgHM in the Th-MOX case. It should be noted that this discharge burnup is considerably higher than the currently employed limits on UOX fuel. There are several reasons to believe that this burnup will in fact be achievable. Firstly, although the burnup is high, the residence time within the reactor is only 4.5 years. Whereas this residence time is quite long for PWR fuel, it is a normal residence time for boiling water reactor fuel, so fuel aging factors related to the residence time should be within acceptable range.

Secondly, it is expected that thorium-based fuel will have a capacity to keep its thermal and mechanical robustness to high burnup, for several reasons. One is that the thermal conductivity of the Thorium-Plutonium Mixed Oxide ceramic is higher than that of a corresponding uranium oxide ceramic, up to about 14% Pu [6]. This means that the fuel temperature will remain lower in the pellet, causing less swelling, less pellet-cladding mechanical interaction, and a larger margin to fuel melting. Another reason is that fission gases have a lower mobility in the thorium oxide matrix, which results in a lower fission gas release. The higher thermal conductivity also has a beneficial effect on the fission gas release, since the lower fuel temperature makes the fission gases diffuse more slowly.

Deterioration of the cladding integrity may constitute an obstacle to safe operation at high burnups. This is partially mitigated by the fact that the residence time is not extremely long, and there are documented cases of cladding operating well up to such burnups [14]. There are also interesting initiatives towards combining thorium fuel with silicon carbide cladding for realizing much higher burnups than the current standard [15].

**4.2. Power Distribution.** As mentioned, the development of the infinite multiplication factor with burnup is important for maintaining an even power distribution within the core. The parameter  $F_Q$  denotes the maximum local fuel rod linear power density divided by the average fuel rod linear power density.

$F_Q$  is calculated for equilibrium xenon at Beginning Of Cycle (BOC), Middle Of Cycle (MOC), End Of Gadolinium (EOG), and at End Of Full Power (EOFP). The highest  $F_Q$  in the core, for normal operating conditions, is plotted in Figure 6 as a function of burnup. As can be seen,  $F_Q$  is higher for the Th-MOX fuel than for the reference fuel but stays comfortably below the limiting value.

Another measure of the evenness of the power distribution is  $F_{\Delta H}$ , which for each fuel rod denotes the integral rod power of that fuel rod relative to the average integral rod power. This parameter is calculated similarly to  $F_Q$  and the highest value, corresponding to the hottest rod, is plotted in Figure 7. In this case, the value for Th-MOX is similar and even a bit lower than that for the reference fuel, and also below the limiting value.

The limits are set by the material properties of the fuel, and the same limits are employed for the Th-MOX core and the reference core. The limits displayed in these plots are the least restrictive ones, which are applicable for fresh fuel. For older fuel, lower limits are applied. A more detailed analysis shows that some of the older fuel assemblies break the applicable age-dependent limits in the Th-MOX case. However, as discussed in Section 4.1, there are reasons to believe that Th-MOX fuel will have better material properties than UOX fuel also at high burnup.

Keeping the power distribution even has two main purposes, one being economical utilization of the fuel and the other one being to allow operation at high power without reaching departure from nucleate boiling anywhere

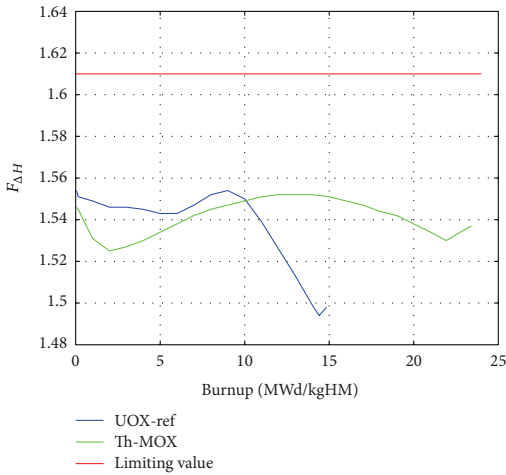


FIGURE 7:  $F_{\Delta H}$ , that is, maximum rod power relative to core average rod power as a function of burnup.

in the core. A measure of how large the margin is to departure from nucleate boiling is the Departure from Nucleate Boiling Ratio (DNBR). This is the ratio between the heat flux which would cause departure from nucleate boiling and the actual local heat flux at a fuel rod surface and should thus be kept above unity, and preferably above a certain threshold to provide margin to departure from nucleate boiling in the case of transient events. The threshold employed in Ringhals 3 is 1.36. The reference fuel is very slightly above the limit, whereas the Th-MOX fuel has a larger margin with a cycle minimum DNBR of 1.43. This is a very positive feature of the core, which provides extra margin in a large number of transients.

**4.3. Control Systems.** The boron worth is calculated for boron concentrations between 0 and 2500 ppm and for the whole power range, from Hot Zero Power (HWP) with no xenon to Hot Full Power (HFP) with xenon equilibrium. Usually natural boron is used for reactivity control, that is, with 19.8%  $^{10}\text{B}$ , which is the isotope having the largest thermal neutron capture cross section. Using this isotopic composition, the boron worth is significantly reduced (closer to zero) in the Th-MOX case. This is expected, since the presence of large absorption resonances in several of the Pu isotopes causes the flux to decrease at the thermal energies where  $^{10}\text{B}$  has its highest absorption cross section. In order to cope with this problem, the Th-MOX cycle is simulated with boron enriched to 60% in  $^{10}\text{B}$ . As can be seen in Table 1, this gives a boron worth for the Th-MOX core similar to that in the reference UOX core, and within the safety limits.

The flatter slope of  $k_{\infty}$ , which allows for a lower initial  $k_{\infty}$  of the Th-MOX assembly, lowers the boron concentration needed for keeping  $k_{\text{eff}}$  equal to unity. The use of enriched

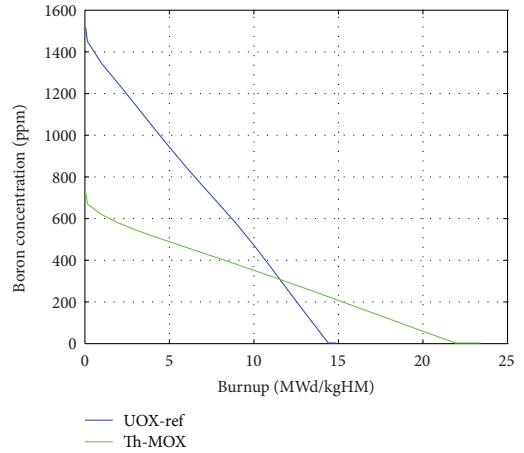


FIGURE 8: Boron concentration as a function of burnup.

TABLE 1: Control rod and boron worth, their limits, and the calculated values for the Th-MOX and the reference UOX core. For the Th-MOX core, the boron used for reactivity control is enriched to 60% in  $^{10}\text{B}$  instead of the usual 19.8% (natural isotopic composition), and stronger control rods are used.

Parameter	Limit	UOX-ref	Th-MOX
Min boron worth [pcm/ppm]	-15	-8.3	-8.7
Max boron worth [pcm/ppm]	-5	-6.2	-5.2
Min SDM [pcm]	2000	2559	3895
Max rod worth [pcm]	—	6505	7808

boron enhances this effect significantly, and the result is shown in Figure 8.

The same mechanisms that cause the lower boron worth for Th-MOX fuel also cause a significant lowering of the control rod worth. In order to adhere to the limits on SDM, the normal control rods, containing a silver-indium-cadmium alloy as the neutron absorber, had to be exchanged for stronger ones containing  $\text{B}_4\text{C}$ . This shortens the lifetime of the control rods but improves the shutdown margin significantly. Furthermore, the four extra openings available in the Ringhals 3 pressure vessel have been utilized for inserting four extra control rods in addition to the 48 which are normally used. The values shown in Table 1 show that the minimum SDM with the  $\text{B}_4\text{C}$  control rods is well above the lower limit.

Also the maximum control rod worth is shown in Table 1 and proves to be higher than the reference. This gives a higher value of the Ejected Rod Worth (ERW) in case of a Rod Ejection Accident (REA) when this transient is evaluated at HWP. However, when evaluated at HFP, the ERW is smaller than the reference, as discussed in Section 4.5. This is most likely due to the strong DTC, discussed in Section 4.4. The same tendency can be seen for the Differential Rod Worth

TABLE 2: Key safety parameters, their limits, and the calculated values for the Th-MOX and the reference UOX core. No limit is specified for moderator temperature coefficient in Ringhals 3.

Parameter	Limit	UOX-ref	Th-MOX
Max MDC [( $\Delta k/k$ )/(g/cm <sup>3</sup> )]	0.50	0.41	0.34
Max MTC [pcm/K]	—	-1.3	-4.0
Max ITC [pcm/K]	0.0	-4.4	-7.9
Min DTC [pcm/K]	-4.00	-3.72	-4.53
Max DTC [pcm/K]	-1.70	-2.10	-2.36
Min DPC [pcm/% power]	-21.0	-15.5	-21.5
Max DPC [pcm/% power]	-6.5	-9.8	-14.6
Min $\beta_{\text{eff}}$ EOC [pcm]	430	502	350
Max $\beta_{\text{eff}}$ BOC [pcm]	720	647	370

(DRW) in case of Rod Withdrawal At Power (RWAP), also discussed in Section 4.5.

**4.4. Key Safety Parameters.** The MDC quantifies the reactivity change caused by a change in moderator density when all other parameters, such as core power, moderator flow, and fuel temperature, are kept constant. The highest and hence most limiting MDC occurs at End Of Cycle (EOC), HFP, All control Rods Inserted (ARI), a boron concentration of 0 ppm, and the highest average moderator temperature, 305.3°C. This is clearly not a set of authentic operating parameters; for example, the core is never operated at HFP with ARI, but it guarantees that the calculated value of MDC is conservative. As can be seen in Table 2 the MDC of the Th-MOX core is smaller than that of the reference core and is well within the safety limits. As will be discussed below, this small value of the MDC is beneficial in many transient scenarios. Many transients involve a cooling of the core, which leads to an increase of the moderator density. The small positive MDC in the Th-MOX core means that the associated reactivity increase is comparatively small.

A high MDC corresponds to a low MTC and vice versa, so the highest MTC occurs at the operating conditions corresponding to the lowest MDC, which are BOC, HZP, All control Rods Out (ARO), no xenon, and critical boron concentration. The MTC is the ratio between the reactivity change caused by a change in moderator temperature, divided by the magnitude of that temperature change. For Ringhals 3, a limit is defined for the ITC instead of the MTC although the MTC is used in many transient simulations and is thus of great interest. The MTC at BOC for Th-MOX fuel is significantly lower than that of the reference, providing a larger margin to becoming positive. Later in the cycle, however, the MTC of the Th-MOX fuelled core is higher than that of the reference core (-75 pcm/K at EOC to be compared with -89 pcm/K for the reference). This means, once again, that many transients are handled in a better way, since the reactivity increase related to a temperature decrease is smaller for Th-MOX fuel than for the reference UOX fuel.

The ITC corresponds to the change in reactivity caused by a simultaneous increase of the temperature of all present

materials while all other parameters are kept constant. The limiting ITC occurs at BOC, HZP, no xenon, and maximum samarium. The ITC for both the Th-MOX and the reference core is well within the safety limits, the ITC for the Th-MOX core being significantly larger in amplitude than that of the reference core.

The MDC, MTC, and ITC all show the same tendency of larger amplitudes for the Th-MOX fuel than for the reference. This is primarily due to the two competing effects of a moderator density increase (associated with a temperature decrease in the MTC and ITC cases). An increase in the moderator density causes an increase in the parasitic neutron absorption by the moderator. This effect is independent on fuel type. However, the density increase also improves the moderation which causes a thermalization of the neutron spectrum. This in turn increases the macroscopic fission cross section to an extent which depends on the specific energy dependence of the microscopic fission cross sections of the fissile nuclei present in the fuel. In the Th-MOX fuel, the dominating fissile isotopes are <sup>239</sup>Pu and <sup>241</sup>Pu, which have large peaks in their microscopic fission cross sections at about 0.3 eV. The main fissile isotope in the reference UOX fuel is <sup>235</sup>U, which has a smaller peak at 0.3 eV. Pu bearing fuels thus benefit more than UOX fuel from the thermalization of the neutron spectrum caused by a density increase.

The DTC indicates the reactivity response caused by a change in fuel temperature only, due to the Doppler broadening of the absorption resonances of the fuel material. This parameter varies quite irregularly with power and burnup, so it is calculated for several different sets of operating conditions and a minimum and maximum value is sought. Due to the presence of several nuclides in the Th-MOX fuel, the DTC is lower (larger in amplitude, negative) in the Th-MOX core than in the reference UOX core, below the lower safety limit. When the result is outside the safety limits, a closer investigation must be made of the transient simulations where the minimum value of the DTC is used. These are Feed Water Malfunction (FWM), Steam Line Break (SLB), at HFP and HZP, Feed Line Break (FLB), Inadvertent Safety Injection (ISI) and the previously mentioned REA and RWAP transients. These are the same transient simulations that use the minimum value of  $\beta_{\text{eff}}$  and will be discussed in the following section.

A closely related parameter is the DPC. It is defined as the reactivity change due to a change in core power, which is related to a corresponding change in fuel and cladding temperatures while the moderator temperature is fixed. The physical principle behind the DPC is thus the same as for the DTC. The DPC is also calculated at a large number of burnup and power levels. For illustration, the DPC at 100% power is listed in Table 2, since most transients start at this power level. As can be seen, the DPC is slightly below the lower safety limit in the Th-MOX fuelled core. The transients where the minimum DPC is used are the following: Loss Of Normal Feedwater/Offsite Power (LONF/LOOP), Partial/Complete Loss of Flow (PLOF/CLOF), Locked Rotor (LR), and Steam Generator Tube Rupture (SGTR) and also some of the same transients that use the minimum DTC: FLB, RWAP, and ISI. Also these transients will be discussed in Section 4.5.

TABLE 3: Calculated safety parameters for the representative transients SLB, REA, and RWAP. For REA, the parameters and limits are for EOC conditions. For SLB and RWAP, the same limits are employed throughout the cycle and the parameters which are listed for the moment in the cycle where they are closest to these limits.

Parameter	Limit	UOX-ref	Th-MOX
SLB at HZP, limiting moment			
Min DNBR [-]	2.93	4.56	5.37
SLB at HFP, limiting moment			
Min DNBR [-]	1.36	1.86	1.93
Max LHGR [W/cm]	545	426	440
REA at HZP, EOC			
Max ERW [\$]	2.55	0.99	1.12
Max $F_Q$ [-]	59.2	15.3	9.48
REA at HFP, EOC			
Max ERW [\$]	0.30	0.056	0.047
Max $F_Q$ [-]	5.75	2.183	2.079
RWAP at HFP, limiting moment			
Max DRW [pcm/cm]	50	11.95	10.88

The effective delayed neutron fraction  $\beta_{\text{eff}}$  is calculated at BOC and EOC for HZP, ARO, no xenon, and maximum samarium.  $\beta_{\text{eff}}$  is strongly affected by the fissioning isotope. The numbers in Table 2 mainly reflect the fact that the delayed neutron fraction is considerably lower (less than half) in  $^{239}\text{Pu}$  and  $^{233}\text{U}$  compared with  $^{235}\text{U}$ , which leads to a  $\beta_{\text{eff}}$  below the lower safety limit. This indicates that the Th-MOX-core will have a smaller margin to prompt criticality compared with the reference. As mentioned, the minimum value of  $\beta_{\text{eff}}$  is used in the same transients as the minimum DTC: FWM, SLB at HZP and HFP, FLB, RWAP, ISI, and REA. These transients are discussed below.

**4.5. Transient Simulations.** A large number of transients have previously been simulated in large detail for the accepted values of the safety parameters, that is, for the values between the upper and lower limits shown in Table 2. As long as the key parameters fall within the safety limits, these general simulations are applicable and the outcome of the transient is known to be acceptable. When any of the key parameters discussed above falls outside the safety limits, the affected transients must be checked in order to determine whether the outcome is acceptable. As noted above,  $\beta_{\text{eff}}$ , DPC, and DTC fall outside these safety limits for Th-MOX fuel, which means that the transient simulations which have been carried out for Ringhals 3 have not been carried out for the calculated values for these parameters. A discussion of the affected transients follows, indicating why they are likely to be acceptable even though the simulation results are not exactly applicable. Some representative simulation results are listed in Table 3, showing that the margins are large in all cases, and in many cases larger for Th-MOX than for the reference fuel.

All of the transients where the minimum value of  $\beta_{\text{eff}}$  is used, except for REA, are rather slow transients; that is,

they happen over a time scale of a few seconds. Within this time frame, there is time for the comparatively slow feedback process provided by the MTC and the MDC to contribute.

In the cases of FWM, SLB, and FLB, the moderator temperature sinks and the density increases. The generally weaker reactivity feedback provided by the higher MTC and lower MDC in the Th-MOX case makes the consequent reactivity increase smaller compared with the reference case, which causes the Th-MOX core to behave well in these transients despite the lower  $\beta_{\text{eff}}$ . DNBR and in the HFP case also LHGR are checked and the calculated values for SLB are listed in Table 3. As previously mentioned, the margins to the limiting values are seen to be large. There are small differences between Th-MOX and the reference, which depend partly on the fuel type and partly on the core design in each case.

An ISI involves an increased flow of borated water to the core. This transient has large margins and the power never increases above 100%, neither for the Th-MOX core nor the reference core, so this transient does not imply any safety concerns.

For the REA transient, the minimum value of  $\beta_{\text{eff}}$  is of larger importance, since the transient is fast. However, the results of the analysis show that all investigated parameters (the maximum ejected rod worth and  $F_Q$ ) were within the employed limits with good margins throughout the transient. The reason for this is that the large negative DPC and DTC of the Th-MOX core provide strong and rapid negative reactivity feedback. In the HFP case, where the fuel temperature is high, the ERW is even lower for the Th-MOX fuel than for the reference. Given the large margins there is good reason to believe that a Th-MOX-fuelled core would cope well with this transient even though the actual value of  $\beta_{\text{eff}}$  is smaller than the one used in the simulations.

RWAP is similar to REA but happens more slowly, so the large negative DPC should make also this transient acceptable. The listed value of the maximum differential rod worth for the Th-MOX case, showing an even larger margin to the limit than the reference, strengthens this assumption.

As mentioned above, the transients in which the minimum DPC plays a role also involve the value of  $\beta_{\text{eff}}$ , but the maximum value of  $\beta_{\text{eff}}$  rather than the minimum value discussed above. The main concern in these cases is the reactivity increase after a SCRAM caused by the low DPC. However, the strong (and added) control rods provide an extra reactivity margin during and after a SCRAM, which makes it very likely that also these transients will turn out well. Also, the small value of the maximum  $\beta_{\text{eff}}$  makes the power decrease at SCRAM come faster than in the reference case, which leaves a smaller decay power that needs to be cooled off.

## 5. Conclusions

The simulations, which have been carried out according to the same routines which are normally employed when designing a new reload, do not show any fundamental obstacles to loading the Ringhals 3 core with Th-MOX fuel with maintained safety margins in normal operation and transient scenarios. However, the condition is that the control

systems are upgraded: Boron enriched to 60% in  $^{10}\text{B}$  must be used for reactivity control, and stronger control rods than the current ones must be used for shutdown. In our simulations, control rods with  $\text{B}_4\text{C}$  are used, which fulfil the safety conditions. In addition, it might be necessary to utilize the four currently unused control rod openings for inserting four additional control rods.

Three kinetic parameters, namely, the minimum Doppler power, temperature coefficients, and the minimum effective delayed neutron fraction  $\beta_{\text{eff}}$ , have values outside the current safety limits. However, differences in the values of the reactivity coefficients along with the extra margins at SCRAM provided by the use of stronger control rods make it possible to argue that the Th-MOX-fuelled core will behave acceptably also in transients where these parameters are of importance.

What remains to be done is to carry out the transient simulations in detail, using the exact calculated values of the key parameters for Th-MOX fuel. This is a major undertaking, which does not only require a large amount of computing capacity and modelling work, but also that temperature and power limits specific to Th-MOX fuel are determined experimentally. These parameters are assessed in an upcoming experiment which will be carried out in the Halden research reactor [16]. This experiment also aims to experimentally confirm the claims made about Th-MOX fuel being able to withstand higher burnup than UOX fuel while maintaining acceptable thermal and mechanical robustness.

Ringhals 3 is a typical PWR, which started commercial power production as early as 1981. Hence, it has no features which would make it particularly suited for using Th-MOX fuel. Thus, our conclusion, based on this limited set of simulations, is that PWRs in general can be loaded with Th-MOX fuel, given that the control systems are strong enough and that the properties of the Th-MOX fuel material become experimentally determined.

## Acknowledgments

The authors would like to thank Ringhals AB for the scientific and technical support and the Norwegian Research Council, Vattenfall AB, Oskarshamns Kraftgrupp AB, and the Swedish Centre for Nuclear Technology for the financial support. The support from the Norwegian Research Council was provided through the industrial Ph.D. program.

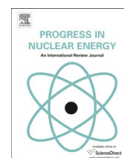
## References

- [1] H. R. Trellue, C. G. Bathke, and P. Sadasivan, "Neutronics and material attractiveness for PWR thorium systems using monte carlo techniques," *Progress in Nuclear Energy*, vol. 53, no. 6, pp. 698–707, 2011.
- [2] E. Fridman and S. Kliem, "Pu recycling in a full Th-MOX PWR core—part I: steady state analysis," *Nuclear Engineering and Design*, vol. 241, no. 1, pp. 193–202, 2011.
- [3] H. Tsige-Tamirat, "Neutronics assessment of the use of thorium fuels in current pressurized water reactors," *Progress in Nuclear Energy*, vol. 53, no. 6, pp. 717–721, 2011.
- [4] K. Insulander Björk, V. Fhager, and C. Demazière, "Comparison of thorium-based fuels with different fissile components in existing boiling water reactors," *Progress in Nuclear Energy*, vol. 53, no. 6, pp. 618–625, 2011.
- [5] M. Todosow and G. Raites, "Thorium based fuel cycle options for PWRs," in *Proceedings of the International Congress on Advances in Nuclear Power Plants (ICAPP '10)*, pp. 1888–1897, San Diego, Calif, USA, June 2010.
- [6] C. Cozzo, D. Staicu, J. Somers, A. Fernandez, and R. Konings, "Thermal diffusivity and conductivity of thorium-plutonium mixed oxides," *Journal of Nuclear Materials*, vol. 416, no. 1-2, pp. 135–141, 2011.
- [7] M. Karam, F. Dimayuga, and J. Montin, "Fission gas release of (Th,Pu) $\text{O}_2$  CANDU fuel," Tech. Rep. CW-124950-CONF-002, Atomic Energy of Canada Limited, 2008.
- [8] J. Rhodes, D. Lee, and K. Smith, *CASMO-4E: Extended Capability CASMO-4—User's Manual*, Studsvik Scandpower, 2009.
- [9] D. W. Dean, *SIMULATE-3 Advanced Three-Dimensional Two-Group Reactor Analysis Code*, Studsvik Scandpower, 2007.
- [10] "Plutonium," World Nuclear Association, 2009, <http://www.world-nuclear.org/info/inf15.html>.
- [11] A. Biancheria and R. J. Allio, "Nuclear fuel elements," US patent 3.427.111, 1969.
- [12] T. Bahadir, *CMS-LINK User's Manual*, Studsvik Scandpower, 1999.
- [13] "Westinghouse reload evaluation methodology," Tech. Rep. WCAP-9272, US Nuclear Regulatory Commission, 1978.
- [14] G. Ledergerber, S. Valizadeh, J. Wright et al., "Fuel performance beyond design—exploring the limits," in *Proceedings of the LWR Fuel Performance Meeting/Top Fuel/WRFPM*, pp. 513–524, Orlando, Fla, USA, September 2010.
- [15] E. Shwageraus and H. Feinroth, "Potential of silicon carbide cladding to extend burnup of Pu-Thmixed oxide fuel," *Transactions of the American Nuclear Society*, vol. 104, pp. 658–660, 2011.
- [16] J. F. Kelly and V. Fhager, "Designing a thorium fuel irradiation experiment," in *Advanced Fuel Pellet Materials and Fuel Rod Design for Water Cooled Reactors*, no. TECDOC 1654, International Atomic Energy Agency, 2010.

# Paper V

**A BWR fuel assembly design for efficient use of plutonium in thorium-plutonium fuel**





## A BWR fuel assembly design for efficient use of plutonium in thorium–plutonium fuel

Klara Insulander Björk<sup>a,b,\*</sup>

<sup>a</sup> Thor Energy, Sommerrogaten 13-15, NO-0255 Oslo, Norway

<sup>b</sup> Chalmers University of Technology, Department of Applied Physics, Division of Nuclear Engineering, SE-412 96 Göteborg, Sweden

### ARTICLE INFO

#### Article history:

Received 1 June 2012

Received in revised form

15 January 2013

Accepted 26 January 2013

#### Keywords:

Thorium

Plutonium

Boiling water reactor

Fuel assembly design

High moderation

High burnup

Plutonium incineration

### ABSTRACT

The objective of this study is to develop an optimized BWR fuel assembly design for thorium–plutonium fuel. In this work, the optimization goal is to maximize the amount of energy that can be extracted from a certain amount of plutonium, while maintaining acceptable values of the neutronic safety parameters such as reactivity coefficients, shutdown margins and power distribution. The factors having the most significant influence on the neutronic properties are the hydrogen-to-heavy-metal ratio, the distribution of the moderator within the fuel assembly, the initial plutonium fraction in the fuel and the radial distribution of the plutonium in the fuel assembly. The study begins with an investigation of how these factors affect the plutonium requirements and the safety parameters. The gathered knowledge is then used to develop and evaluate a fuel assembly design. The main characteristics of this fuel design are improved Pu efficiency, very high fractional Pu burning and neutronic safety parameters compliant with current demands on UOX fuel.

© 2013 Elsevier Ltd. All rights reserved.

### 1. Introduction

The objective of the work described herein is to develop a Boiling Water Reactor (BWR) fuel assembly design adapted to thorium–plutonium (Th/Pu) fuel, as a part of the fuel development program at the Norwegian company Thor Energy. The broad goal of our company's research is to develop a safe, reliable and cost effective Light Water Reactor (LWR) fuel which effectively consumes the world's growing stockpiles of plutonium, either it is present in nuclear waste or as surplus weapons material. The fuel is intended for use in currently operating and future LWRs and will be similar to currently used uranium oxide (UOX) and mixed oxide (MOX) fuel, except that the fuel pellets will consist of a homogeneous mixture of thorium and plutonium oxides. The specific goal of this work is to develop a fuel assembly design which maximizes the amount of energy that can be extracted from a certain amount of plutonium, a property hereafter referred to as Pu efficiency. This goal is based on the perception that an entity in possession of a certain amount of plutonium would like to maximize its value,

which effectively means extracting as much energy from it as possible.

The general viability of Th/Pu fuel in LWRs (mainly PWRs) has been confirmed by several recent studies (Trellue et al., 2011; Fridman and Kliem, 2011; Tsige-Tamirat, 2011; Insulander Björk et al., 2011; Todosow and Raitses, 2010). In these studies, conventional fuel assembly designs are used, since the main goal is to investigate the inherent differences between Th/Pu fuel and other fuel types. However, it is known that when Pu is the main fissile element, the optimal (for reactivity) hydrogen-to-heavy-metal ratio (H/HM ratio) is much larger than it is for UOX fuel (Puill, 2002; Kloosterman and Bende, 2000). This fact applies to Th/Pu fuel as well as to MOX fuel, and has been used to some extent for creating more optimized MOX fuel assembly designs (Ramirez-Sanchez et al., 2008; Bairiot et al., 2003; Hamamoto et al., 2001). New fuel designs for Th/Pu fuel have also been presented, aiming to improve conversion of  $^{232}\text{Th}$  to  $^{233}\text{U}$  (Galperin et al., 2000). There are however, to our knowledge, no previous studies of fuel assembly designs for Th/Pu fuel aiming to improve Pu efficiency.

The current study concerns BWR fuel assembly design. This choice was made since the location of the cruciform control rods outside the BWR fuel assembly and the channel allows for comparatively large freedom in designing the layout of the fuel within the channel. It is our intention to also create an optimized PWR fuel assembly design later.

\* Corresponding author. Thor Energy, Sommerrogaten 13-15, NO-0255 Oslo, Norway. Tel.: +47 460735939862.

E-mail addresses: [klaraib@gmail.com](mailto:klaraib@gmail.com), [klara.insulander@scatec.no](mailto:klara.insulander@scatec.no).

Varying the H/HM ratio affects the reactivity of the fuel assembly, but also several important safety parameters such as the control rod worth, shutdown margins and reactivity coefficients. These effects are investigated and, where necessary and possible, mitigated. An effort is made to keep the power distribution in the assembly even, in order to avoid excessive individual rod Linear Heat Generation Rate (LHGR). Ultimately, the LHGR which will be achievable with Th/Pu fuel will depend on the thermal, mechanical and chemical properties of the fuel material. Investigations of these properties are underway, but are not part of this study.

The implications of the changed design for the thermal hydraulic parameters, such as pressure drop and margin to dryout, will need to be evaluated too. This is also left for later study.

The constraints for the fuel design and the reactor system that is simulated are described in Section 2. The calculation tools and methods used in this study are described in Section 3. Within this framework, a number of different studies were carried out, investigating how different parameters affect the properties of the fuel assembly. Using the results of these, a fuel assembly was designed. This process is described in Section 4. The properties of the new fuel assembly design were calculated and compared to those of reference fuel assemblies. This phase of the work is reported in Section 5. In Section 6, finally, the conclusions are presented along with an outlook where future investigations and directions for the assembly design work are suggested.

## 2. Premises

### 2.1. Design constraints

In order to design a fuel assembly that would be commercially feasible in the sense that it is fabricable with current manufacturing facilities and licensable in current BWRs, certain constraints were put on the fuel assembly design. These constraints are summarized in the list below.

- The neutronic safety parameters should be within currently practiced limits.
- The size and shape of the fuel assembly should allow it to be loaded into a normal BWR.
- Normal cylindrical oxide fuel pellets should be used.
- Well-known materials should be used for the cladding, external channel and internal water channel(s).
- Geometrical parameters such as the fuel rod thickness, rod pitch, rod-channel distance etc. should not be outside current experience.

### 2.2. Reactor operation parameters

As a framework for the calculations, the Swedish BWR Forsmark 3<sup>1</sup> was considered. The standard operation parameters of this reactor are listed in Table 1. Fuel assembly mass and burnup depend on the fuel design and are listed separately in Table 3 in the Results section.

The modern and commonly used fuel assembly design GE-14N was used as a reference. For comparing the properties of the improved design with those of normally used fuel, reference designs were created with both UOX and MOX fuel, as well as with Th/Pu fuel. The fissile content of the reference fuel designs, as well as the new fuel assembly design, was adapted to release the same amount of energy during the lifetime of the fuel assemblies. This

**Table 1**

Reactor parameters. The numerical value of the neutron leakage is based on experience of normal reload design for Forsmark 3.

Parameter	Notation	Value
Number of fuel assemblies	$N$	700
Number of fuel batches	$n$	6
Cycle length [days]	$t_c$	350
Reactor thermal power [MW]	$P_{th}$	3300
Neutron leakage [pcm]	$\Delta\rho$	2000
At hot full power (HFP)		
Power density [kW/dm <sup>3</sup> ]		53.5
Coolant temperature [K]		559
System pressure [MPa]		7.02
Average void fraction [%]	$V$	40
At cold zero power (CZP)		
Power density [kW/dm <sup>3</sup> ]		0
Coolant temperature [K]		293
System pressure [MPa]		0.1
Void fraction [%]	$V$	0

gives a fair comparison between the fuel types since the released energy is directly related to the revenue of the reactor operation. Due to different fuel masses in the different designs, equal energy release implies different burnup, which will be discussed in Section 3.4. The higher discharge burnup implied by the lower fuel mass in the Th/Pu cases is discussed and justified in Section 5.4.

The UOX design had an average enrichment of 4.1 wt% <sup>235</sup>U, yielding the required amount of energy as described in Section 3.4. The Pu content of the reference MOX and Th/Pu reference designs was adjusted to reach the same energy release, demanding 7.0% Pu in the MOX case and 9.2% Pu in the Th/Pu case. The Pu isotope vector used both in the reference fuel and in the created new designs was: 2% <sup>238</sup>Pu, 53% <sup>239</sup>Pu, 25% <sup>240</sup>Pu, 15% <sup>241</sup>Pu and 5% <sup>242</sup>Pu. This corresponds to the Pu vector in spent LWR fuel burnt to approximately 42 MWd/kgHM, if reprocessed and used immediately after discharge (World Nuclear Association, 2009). In all three reference cases, a number of different enrichment levels (8–9) was used in order to create an even power distribution. Gadolinium was used as a Burnable Absorber (BA) in all cases, in order to suppress the reactivity of the fuel at the Beginning Of Life (BOL). Due to the small slope of the reactivity curve in the Th/Pu and MOX reference cases, only very small amounts of BA were required.

## 3. Calculation tools and methods

### 3.1. Neutronic simulation software

All calculations were carried out on a 2D infinite lattice level. For these calculations, the fuel assembly burnup simulation program CASMO-5 (Rhodes et al., 2007) was used, together with the cross section library ENDF/B-VII.0 (Chadwick et al., 2006). It should be noted that some changes were made to the <sup>232</sup>Th and <sup>233</sup>U cross sections in ENDF/B-VII short before its release (Mosteller, 2004; Mosteller, 2008). These data sets have not been subject to the same level of testing as the other data sets in the library. Benchmarks for <sup>233</sup>U cross sections in the thermal spectrum show some improvement over the last ENDF/B-VI version. For <sup>232</sup>Th cross sections, there are not many well-validated benchmarks, so we must settle with regarding the results with some scepticism and await further testing and possibly improvements of the data sets.

These lattice calculations do not take leakage or spectral interactions between assemblies of differing type or age into account, except for that the neutron energy spectrum is corrected for the energy dependence of the leakage probability. The numerical values of the calculated parameters are thus only correct for the

<sup>1</sup> The ongoing power uprate at Forsmark 3 is not accounted for.

two-dimensional infinite lattice and not for a real, three-dimensional system. Nevertheless, they are useful for comparing the merits of different candidate fuel designs, and for giving an indication of the behavior of the fuel assemblies in a reactor.

### 3.2. Estimation of reactivity coefficients

The reactivity coefficients were estimated by perturbation calculations. The life of the fuel assembly was simulated up to a certain burnup point with constant operation parameters as given in Table 1, and  $k_\infty$  was calculated and denoted  $k_U$ , where  $U$  stands for unperturbed. One of the operating parameters was then changed by a certain amount  $\Delta x$ , and  $k_\infty$  was calculated for the perturbed state and denoted  $k_P$ . The reactivity coefficient  $\alpha_x$  was then calculated from Eq. (1).

$$\alpha_x = \frac{k_P - k_U}{\Delta x \cdot k_U} \quad (1)$$

This estimation obviously neither accounts for the leakage effects between assemblies of different age or out of the core, nor for absorption by control rods. These effects generally give significant negative contributions to some reactivity coefficients, notably the void coefficient and the isothermal temperature coefficient, which have to be calculated by full-core simulations. Given the assumption of similar core loading patterns (see Section 3.4), the mentioned effects are likely to be similar for Th/Pu fuel and UOX fuel.

### 3.3. Estimation of control rod worth

The control rod worth depends on the type and burnup of the fuel assemblies surrounding it and also on its position in the reactor. In the simulations performed in the current study, control rod insertion corresponds to inserting all control rods simultaneously in an infinite lattice of identical fuel assemblies, so the worth of one single specific control rod in a reactor cannot be calculated by this method. Nevertheless, it is possible to use the infinite lattice simulations to estimate the difference in actual control rod worth between two fuel types. The control rod worth in the infinite lattice was calculated as the difference in  $k_\infty$  between a lattice with all rods inserted and a lattice with all rods withdrawn.

### 3.4. Total energy release

In order to compare fuel assemblies of, in some sense, equal value, it was decided to adjust the fissile content of all designs so that the assemblies release an equal amount of energy during their lives. This strategy also implies that the same number of batches and hence the same core loading pattern can be used for all different designs. This improves the reliability of the comparison of fuel design properties as calculated in 2D, since the errors introduced by the omission of all 3D (core level) effects can be assumed to be similar. In addition, the chosen strategy implies that all materials in the core and in each fuel assembly, except for the fuel material itself, will receive the same amount of radiation and have the same core residence time with the new designs as with the reference cases.

Since the total energy release is the product of the fuel mass  $M$  and the discharge burnup  $D_B$ , a light fuel assembly will need to reach a higher specific discharge burnup in order to release the same amount of energy as a heavier one. This increased exposure will have consequences for the fuel material, which is discussed in Section 5.4. The demanded total energy release  $E_{\text{tot}}$  can be calculated from the operation parameters given in Table 1, using Eq. (2).

$$E_{\text{tot}} = M \cdot D_B = \frac{P_{\text{th}} t_{\text{c}} n}{N} = \frac{3300 \text{ MW} \cdot 350 \text{ d} \cdot 6}{700} = 9900 \text{ MWd} \quad (2)$$

To determine the achievable discharge burnup from the CASMO-5 output, the reactivity of the whole core can be calculated as the average of the reactivities of each of the six fuel batches present in the core at end of cycle (Driscoll et al., 1990). This calculated value of the core reactivity must then be adjusted to take into account the neutron leakage out of the reactor, which is not accounted for in the infinite lattice simulations. Thus, in order for the core to be critical, the reactivity must comply with the condition set by Eq. (3).

$$\sum_{i=1}^n \rho(i \cdot B_C) = \Delta \rho \quad (3)$$

Here,  $\rho = (k_\infty - 1)/k_\infty$  is the reactivity, which is a function of burnup, and  $\Delta \rho$  and  $n$  are the neutron leakage and the number of batches, respectively, as listed in Table 1.  $B_C$  is the cycle burnup. For determining the achievable discharge burnup, the largest  $B_C$  is sought for which  $\rho$  fulfills the condition, and the discharge burnup  $B_D$  is calculated as  $n B_C$ .

## 4. Design procedure

### 4.1. Hydrogen-to-heavy-metal ratio

A first step in the development was to find the H/HM ratio that is optimal from a reactivity point of view, while maintaining a negative void coefficient. The H/HM ratio is defined in this paper as the ratio of the number of hydrogen atoms to the number of heavy metal atoms in a fresh fuel assembly. To study the effect of varying the H/HM ratio, a basic fuel assembly was simulated. The assembly consisted of a simple 10-by-10 lattice of fuel rods enclosed in a quadratic tubular channel box of Zr-alloy sheet material. The H/HM ratio was varied by varying the fuel pellet radius from 2.1 mm to 5.7, at which point the fuel rods almost made contact, rendering the fuel design infeasible. At the operating conditions for HFP listed in Table 1, this gives a variation of the H/HM ratio from about 24 to 1.8, depending on the number density of heavy metal atoms in the investigated fuel type. The ratio between the pellet radius, the pellet-clad gap and the cladding thickness was kept constant.

For illustration, this investigation was made for four different fuel types; normal UOX fuel, conventional MOX fuel, Th/Pu fuel and Th/U-233 fuel. The latter fuel type consists of thorium with pure U-233 used as a fissile component. The fissile content of all fuel types was adjusted so that each fuel assembly delivered 9900 MWd during its lifetime for a pellet radius of 4.4 mm. The initial  $k_\infty$  was calculated for each pellet radius and plotted against the corresponding H/HM ratio. This corresponds to the dashed lines in Fig. 1. For clarity, all curves are normalized to their respective maxima. It can be seen from this figure that the optimal H/HM ratio depends mainly on the fissile component and not much on the fertile ( $^{232}\text{Th}$  or  $^{238}\text{U}$ ). This is expected, since it is mainly the fission cross sections which determine the reactivity and depend strongly on the H/HM ratio. Increasing the H/HM ratio increases the parasitic absorption of neutrons by hydrogen nuclei equally for all fuel types. It also improves the moderation, i.e. thermalizes the neutron spectrum, which in turn increases the macroscopic fission cross section to an extent which is determined by the specific energy dependence of the microscopic fission cross sections of the fissile nuclei.  $^{239}\text{Pu}$  and  $^{241}\text{Pu}$  have large peaks in their microscopic fission cross sections at about 0.3 eV.  $^{235}\text{U}$  has a slightly smaller peak at 0.3 eV and  $^{233}\text{U}$  a very small peak at 0.2 eV. Pu bearing fuels thus benefit strongly from a thermalization of the neutron spectrum, compared to one which is optimal for  $^{235}\text{U}$ . For a  $^{233}\text{U}$  bearing fuel, on the other hand,

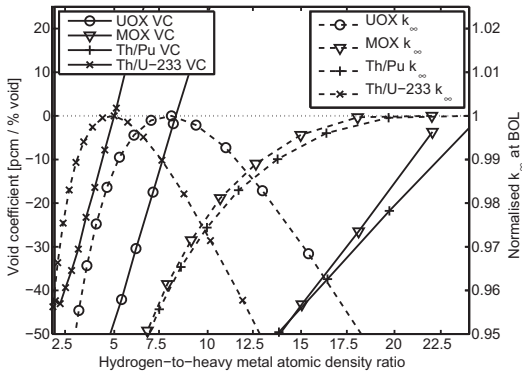


Fig. 1. Void coefficient at BOL (solid lines) and normalized  $k_{\infty}$  at BOL (dashed lines) dependence on H/HM ratio.

the weak energy dependence of the microscopic fission cross section gives a comparatively small penalty for impaired moderation with decreasing H/HM ratio, so the effect of the decreased parasitic absorption dominates, resulting in a smaller optimum H/HM ratio. A mixture of two fissile components gives an optimum H/HM ratio between those of the two pure cases.

Fig. 1 is illustrative but gives only an approximate indication of what H/HM ratio is optimal for a certain fuel type. There are several reasons for this. One is that the fuel constitution changes with burnup, especially for fuel types where the bred fissile isotopes are different from the original ones, as is the case for Th/Pu fuel. As  $^{233}\text{U}$  is bred into the fuel and Pu is burnt out, the optimal H/HM ratio will move closer to that of  $\text{Th}/^{233}\text{U}$ . Thus, the H/HM ratio giving the highest  $E_{\text{tot}}$  is lower than the one giving the highest initial  $k_{\infty}$ .

Further investigations of the effect of varying the H/HM ratio for Th/Pu fuel showed that the optimum H/HM ratio depends of the initial Pu content; a higher Pu content gives a higher optimal H/HM ratio. The optimal H/HM ratio also depends on whether the H/HM ratio is increased by decreasing the fuel rod radius or by removing rods or replacing them with moderator channels. This indicates, not surprisingly, that the H/HM ratio is not the only geometric parameter affecting the reactivity.

However, the decidedly most important limitation on the H/HM ratio is illustrated by the solid lines in Fig. 1. These show the void coefficient dependence on the H/HM ratio. As can clearly be seen, the void coefficient becomes positive exactly at the optimum H/HM ratio. This is explained by the fact that an increase in the coolant void fraction is also a decrease in the H/HM ratio. As long as a decrease in H/HM ratio leads to a lowered  $k_{\infty}$ , as it does below the optimum, the void coefficient is negative. However, above the optimum, the void coefficient is positive.

As explained above, many different factors affect the optimal H/HM ratio. Given the clear relationship between the H/HM ratio and the void coefficient, these factors also affect the void coefficient. No exact value of the limiting H/HM ratio can thus be given, but the burnup averaged void coefficient for a specific fuel assembly design must be calculated at the limiting operating conditions, in order to give an indication of the feasibility of that design.

#### 4.2. Ways to increase the H/HM ratio

The conclusion of the study described above was that the H/HM ratio should be increased significantly. This could be done in several ways. The options to decrease the void fraction or the moderator temperature were discarded immediately, since we intend to

develop a fuel assembly which could be used without any changes to the normal operation of the reactor. Further options are to make the fuel rods smaller and to leave some empty spaces in the lattice.

The most straightforward alternative is using an existing fuel assembly design and only decreasing the diameter of the fuel rods to increase the H/HM ratio. This was done with the reference GE-14 assembly design, and a moderate improvement of the Pu efficiency was found. It was decided to investigate the potential of the remaining alternative; leaving some empty spaces in the lattice, which proved to be a more effective way of improving the Pu efficiency. For the final design, a combination of leaving empty spaces and decreasing the fuel rod diameter was used.

#### 4.3. Improving shut-down margin

The strategy of leaving some empty spaces in the lattice offers the advantage to replace them with moderator channels containing water which is not in contact with the fuel rods and thus does not boil. This makes it possible to keep a high H/HM ratio also at the upper part of the fuel assembly, where the void fraction in the coolant is high. Furthermore, the moderator channels fill a second, even more important function, namely to improve the Shut Down Margin (SDM). The SDM is the margin to criticality in the situation that the reactor is in cold shut down and the control rod (or group of control rods) having the highest reactivity value stays out of the core. Since this parameter depends on the specific core loading, it cannot directly be calculated by the infinite lattice simulations done here. However, the SDM can be estimated by calculating the Hot-to-Cold-Swing (HCS), which is the reactivity difference between HFP conditions with all control rods withdrawn, and CZP conditions with all control rods inserted. The HCS can be estimated by lattice calculations. In addition to the HCS, the absolute value of the reactivity of the core affects the SDM. This is most commonly controlled by burnable absorbers.

The main contribution to the HCS is the Control Rod Worth (CRW). The currently used control rods contain boron which has its largest absorption cross section in the thermal part of the spectrum. Due to the large absorption resonances of the Pu isotopes at thermal energies, the spectrum becomes harder when Pu is present, decreasing the CRW. However, a second contribution to the HCS comes from the reactivity difference caused by the change in operating parameters when the reactor goes from HFP to CZP. The H/HM ratio increases when the reactor is shut down, since the void fraction goes to 0% and the water density increases. For an under-moderated fuel assembly with negative void- and moderator temperature coefficients, this generally gives a positive reactivity contribution. Also the negative Doppler coefficient gives a positive contribution to the HCS.

However, the increased water density also decreases the neutron migration area, which can be used to create a negative reactivity contribution at shut down. If the moderator channels have a cross section area larger than the migration area at CZP but smaller than the migration area at HFP, this results in a negative reactivity contribution. At HFP, neutrons which enter the moderator channels have a high probability of escaping them again, moderated, but at CZP most neutrons which enter the moderator channels will be absorbed and never escape. A study was made to determine the channel size giving the largest reactivity difference between HFP and CZP and the result was used in the design.

#### 4.4. Power distribution

Finally, the fuel assembly should be designed to have an even power distribution. This is desirable since an uneven power distribution would mean that some rods operate at a much higher

power level, and thus a higher LHGR, than the average. Since the LHGR of all rods must stay below the Thermal-Mechanical Operating Limit (TMOL), this effectively limits the power which the fuel assembly can be allowed to produce.

The power distribution also affects the flow and boiling patterns in the fuel assembly, which puts another constraint on the reactor operation. The Minimum Critical Power Ratio (MCPR) is defined as the ratio of the critical power to the actual operating power of the fuel assembly, where the critical power is the power which causes transition boiling to occur. The MCPR must be kept above unity, and this can be achieved partly by an even power distribution and partly by other means, such as enhancing the turbulence in the coolant flow or introducing part length rods which vanish in the upper part of the core where the MCPR is generally lower due to the high void fractions. Direct assessment of the MCPR requires knowledge of the thermo-dynamic properties of the fuel assembly, which is outside the scope of this work. So is also the consideration of part length rods.

An even power distribution can be achieved partly by placing the water channels so that the moderation is evenly distributed within the fuel assembly, and partly by using a varying Pu fraction, giving well moderated rods, such as the corner rods, a lower Pu content to prevent them from becoming much hotter than the average. While most of the moderation was concentrated to one large moderator channel, in order to improve the SDM, some rods were removed in positions evenly distributed in the assembly, just to create an even power distribution. In addition, four different levels of Pu content were used.

Simulations also showed that a very uneven distribution of the moderation not only limits the power of the fuel assembly due to the consequent uneven power distribution, but also decreases the total energy release. This is due to a lot of fissile material remaining unused in the less-moderated rods when the more well-moderated rods are already burnt out.

## 5. Results

### 5.1. Reactivity swing and power distribution

Several different fuel designs were evaluated and adapted to perform well in terms of safety parameters, power distribution and Pu efficiency, under the constraint that they should release the same amount of energy as calculated by Equation (2). Since most factors are interdependent, the process had to be iterative. Basically, the H/HM ratio was changed by removing or adding fuel rods and fine tuned by adjusting the fuel rod diameter. Then, the fissile content was adjusted to yield an even power profile and the required total energy release and finally the safety parameters and the Pu efficiency were calculated to evaluate the result of the initial change. The final fuel design was denoted TT-01. Compared to the reference design, the new design features more and thinner pins. This will have consequences for the reactor stability, since it makes the heat transfer from fuel to coolant faster, an issue which is outside the scope of the current work.

A BWR fuel assembly normally contains fuel rods with about five to ten different enrichments. The evenly distributed moderation in TT-01 made it possible to achieve power peaking factors comparable to that of the reference with only four different enrichment levels. A low power peaking factor is most important where  $k_{\infty}$  and thus the relative power of the fuel assembly is high. Weighting the maximum LHGR in the assembly with  $k_{\infty}^3$  gives an indication of the core maximum LHGR (Helmersson, 2011). A comparison of this product between the reference fuel types and a preliminary version of TT-01 indicated that use of Burnable Absorbers (BA) would be necessary not only to improve the SDM, but also to suppress the reactivity at the beginning of life, just as is done with the UOX fuel.

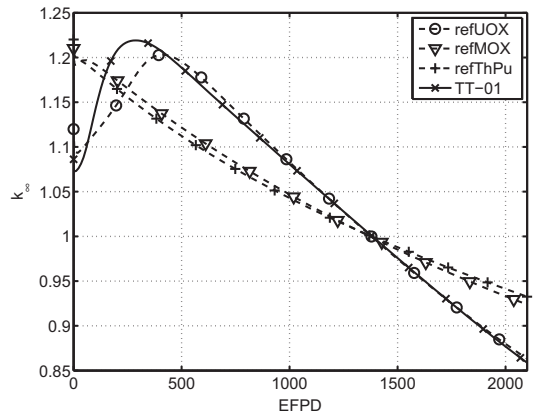


Fig. 2. Development of  $k_{\infty}$  with time.

In a conventional fuel assembly design, the reactivity swing of Th/Pu fuel is smaller than it is for UOX fuel, i.e.  $k_{\infty}$  decreases more slowly, as can clearly be seen in Fig. 2. This is due to a comparatively high conversion. With a significantly higher H/HM ratio, however, the conversion is lower and  $k_{\infty}$  decreases just as fast as for UOX fuel. To reach the desired total energy release, an increased fissile fraction becomes necessary in order to keep  $k_{\infty}$  from dropping too low towards the end of life. This results in a very high  $k_{\infty}$  at the beginning of life, which must be suppressed by the use of BA. Thus, BA was included in the TT-01 design, which made it possible to reach a core maximum LHGR slightly lower than the reference UOX case.

The  $k_{\infty}$  of TT-01 is plotted in Fig. 2 together with the  $k_{\infty}$  of the reference fuel designs. The effect of a significant amount of BA is clear at the beginning of life for the reference UOX fuel and TT-01, where  $k_{\infty}$  is increasing while the BA is burnt out. The effect of the very small amount of BA used in the reference MOX and Th/Pu fuels is barely noticeable in the plot, but prevents the initial  $k_{\infty}$  to reach up to about 1.25. Despite the rapid rise in  $k_{\infty}$  for TT-01 seen in the figure, the global reactivity increase of the core never exceeds 0.1 pcm/(MWd/kgHM), and thus adheres to a common design criterion (Helmersson, 2011).

### 5.2. Shutdown margins and control rod worth

The Hot-to-Cold Swing (HCS), i.e. reactivity difference between HFP with ARO and CZP with ARI, is a qualitative measure of how large shutdown margin can be expected, which can be assessed by lattice calculations. As previously described, this difference mainly depends on the reactivity contributions from the Control Rod Worth (CRW) and from the change in operating parameters. As can be seen in Fig. 3, the total reactivity difference is improved for TT-01 compared to the Th/Pu reference case, and is essentially similar to the UOX reference case. As expected, the CRW is smaller in amplitude for all Pu-bearing fuel types compared to the UOX reference, so the improvement can be accounted to the reactivity contribution from the change in operating conditions. For the reference assemblies, this difference is positive due to the improved moderation and Doppler-enhanced resonance absorption at CZP – effects that are expressed as negative reactivity coefficients, listed in Table 2 below. For TT-01, the mentioned effects, and thus also the reactivity coefficients, are smaller, as can be seen in Table 2. Combined with the design of the moderator channel as

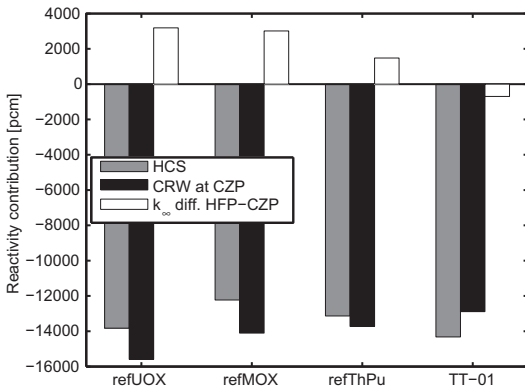


**Fig. 3.** The reactivity swing (HCS) between Hot Full Power (HFP) conditions with All Rods Out (ARO) and Cold Zero Power (CZP) conditions with All control Rods In (ARI), the Control Rod Worth (CRW) at CZP and the  $k_{\infty}$  difference between HFP conditions and CZP conditions.

described in Section 4.3, this results in a negative reactivity difference.

### 5.3. Reactivity coefficients and delayed neutron fraction

The reactivity coefficients and the delayed neutron fraction ( $\beta$ ) generally change with burnup. However, since fuel assemblies having different burnup are simultaneously present in the core, the general core behavior is reasonably well captured by the burnup averaged value, which is shown in Table 2.

The Isothermal Temperature Coefficient (ITC) corresponds to the change in reactivity caused by simultaneous heating of all present materials. This parameter is thus important for the safety at startup, since nuclear heating is regularly used at startup in BWRs. The demand on the ITC practiced at Forsmark 3 is that it should be negative for temperatures above 493 K (Gotthardsson, 2007). The ITC was calculated at isothermal zero power conditions at several different temperatures with all control rods inserted, and was found to decrease with increasing temperatures. As can be seen in Table 2, the ITC is higher than the reference for TT-01, but fulfills the requirement since it is negative at 493 K.

The average void coefficient is negative but is somewhat smaller in amplitude for TT-01 compared to the reference MOX and UOX cases. This may be an advantage in transients involving a pressure increase causing void collapse, such as a turbine trip, and also improves the stability of the reactor. It might however be a disadvantage in cases where a flow decrease is used to regulate the reactor, since this will have a smaller reactivity effect.

The Doppler coefficient is also negative in all cases, and larger in the Th/Pu reference case than in the two other reference cases, due

**Table 2**

Burnup averaged reactivity coefficients and  $\beta$  for the reference assemblies and TT-01. All parameters are calculated for HFP conditions, except for the isothermal temperature coefficient which is calculated for isothermal conditions at 493 K and 0% void fraction.

Fuel name	refUOX	refMOX	refThPu	TT-01
Void coefficient [pcm/% void]	-55	-52	-37	-41
Doppler coefficient [pcm/K]	-2.4	-2.5	-2.9	-2.1
Isothermal temperature coefficient [pcm/K]	-28	-26	-21	-12
Delayed neutron fraction [pcm]	551	399	365	369

to the specific resonance structure of  $^{232}\text{Th}$ . It is smaller in amplitude for TT-01 than for the reference assemblies. The cause for this is once again the increased H/HM ratio, since the Doppler coefficient is proportional to the fuel mass and volume and inversely proportional to the moderator mass and volume (Demaziere, 2000). However, the differences are small.

The delayed neutron fraction is not strongly affected by the changed design. The numbers in Table 2 mainly reflect the fact that the delayed neutron fraction is considerably lower (less than half) in  $^{239}\text{Pu}$  and  $^{235}\text{U}$  compared to  $^{235}\text{U}$ .

### 5.4. Depletion performance

The mass balance of relevant elements is listed in Table 3 along with related data of importance.

As can be seen, the H/HM ratio is almost doubled compared to the reference case. In order to achieve this, the fuel mass had to be significantly reduced, and the burnup is correspondingly increased in order to reach the same total energy release. The average initial Pu fraction can be seen to be higher in TT-01 than in the reference Th/Pu case. With the smaller total fuel mass, this nevertheless results in a smaller initial Pu mass and hence in a better Pu efficiency, since the total released energy is equal by design. The improvement in Pu efficiency for TT-01 is 20%, relative to the reference Th/Pu fuel. Using the straightforward approach of decreasing the diameter of the fuel pins in the reference assembly resulted in a 13% improvement of the Pu efficiency for the same H/HM ratio.

The Pu efficiency of the reference Th/Pu fuel is lower than that of the reference MOX fuel, partly due to the  $^{235}\text{U}$  present in the depleted uranium matrix, and partly due to the higher fast fission cross section of  $^{238}\text{U}$  compared to  $^{232}\text{Th}$ . This difference is eliminated by the new fuel design, which has the same Pu efficiency as the reference MOX design.

In a context where destruction of Pu is the ultimate goal, the fractional Pu consumption is of great interest. Whereas the net consumption is about a third in ordinary MOX fuel, the reference Th/Pu fuel consumes about half of the initial Pu and TT-01 as much as two thirds of the Pu that was initially added. The quality of the remaining Pu, i.e. the fraction of fissile Pu isotopes of the total Pu, is also very much deteriorated, rendering it very unattractive as weapons material.

The production of  $^{233}\text{U}$  has also been assessed. As expected, the improved moderation decreases the breeding of  $^{233}\text{U}$  in TT-01. Although  $^{233}\text{U}$  has been judged as comparatively unattractive as weapons material (Dekoussar et al., 2005), the resulting lower  $^{233}\text{U}$  content may be regarded as another advantage from a proliferation safety point of view.

Finally, the production of minor actinides (Np, Am, Cm, Bk, Cf, Es and Fm) is listed. The produced masses of Bk, Cf, Es and Fm were insignificant. Thus, the masses listed are the added masses of  $^{237}\text{Np}$ – $^{239}\text{Np}$ ,  $^{241}\text{Am}$ – $^{243}\text{Am}$  and  $^{242}\text{Cm}$ – $^{246}\text{Cm}$ . As can clearly be

**Table 3**

Mass balance and related data for reference GE14 assemblies and for TT-01.

Fuel name	refUOX	refMOX	refThPu	TT-01
H/HM ratio	4.6	4.4	4.8	9.0
Fuel mass [kg]	186	192	172	108
$B_D$ [MWd/kgHM]	53	52	58	91
Initial Pu fraction [%]	–	7.0	9.2	12.3
Initial Pu mass [kg]	–	13.4	15.8	13.4
Pu efficiency [MWd/kgPu]	–	741	625	741
Pu consumption [%]	–	34	54	67
Final Pu quality [%]	59	49	40	24
Final $^{233}\text{U}$ mass [kg]	–	–	2.3	1.4
Final minor actinide mass [kg]	0.20	0.74	0.75	0.62

seen, the production of minor actinides is lower in TT-01 compared to the MOX and ThPu references (19% and 21% lower, respectively). It should be noted that the fraction of minor actinides in the spent fuel is nevertheless higher in spent TT-01, but that the lower fuel mass gives a lower absolute amount.

It is noted that the average discharge burnup of 91 MWd/kgHM in the TT-01 case is far beyond current standard in commercial reactors. One of the factors most likely to limit the burnup in this case is cladding degradation. Studies of cladding with a burnup of up to 92 MWd/kgHM have been carried out, suggesting that such high burnups could indeed be feasible also with current cladding materials (Ledergerber et al., 2010). In addition, all degradation factors proportional to core residence time, such as water side hydriding, corrosion and crud deposit, will be the same as for the reference fuel, since the same loading pattern, and hence the same core residence time, is assumed for all fuel types.

The thermal and mechanical integrity of the fuel material itself at such high burnups must also be addressed, in particular for transient and accident scenarios such as reactivity insertion accidents and loss of coolant accidents. This has to be investigated experimentally by irradiation of Th/Pu fuel material to high burnup and ultimately ramp testing and post irradiation examination of such material. Such an irradiation program is underway in the HBWR research reactor in Halden, Norway, under the direction of Thor Energy (Kelly and Fhager, 2010; Kelly, 2012). The scope of this program is to obtain irradiation data supporting the licensing case for Th/Pu fuel in LWRs and in particular to validate fuel performance codes which are necessary for licensing of Th/Pu fuel.

There are several reasons to believe that thorium based fuel will have a capacity to keep its thermal and mechanical robustness to a higher burnup compared to UOX. One reason is that the thermal conductivity of the thorium plutonium mixed oxide ceramic is higher than that of a corresponding uranium oxide ceramic, up to about 14% Pu (Cozzo et al., 2011). This implies that the fuel temperature will remain lower in the pellet, causing less swelling and less pellet-cladding mechanical interaction. The margin to fuel melting is also larger, providing an advantage in transient and accident scenarios. Another reason to expect a better burnup performance from thorium based fuel than from corresponding uranium fuel is that fission gases have a lower mobility in the thorium oxide matrix, which results in a lower fission gas release (Belle and Berman, 1984). The higher thermal conductivity also has a beneficial effect on the fission gas release, since the lower fuel temperature makes the fission gases diffuse more slowly.

### 5.5. Design flexibility

As mentioned, several different designs were evaluated, and the one designated TT-01 was chosen as the best one based on a somewhat arbitrary evaluation of its advantages. It should be stressed that there is a large design flexibility, and that the design may well be adapted to another set of demands than the one applied here. For example, the specific properties of Th/Pu fuel can be used to design a fuel for operating cycle extension (Insulander Björk, 2012).

## 6. Conclusions

The created fuel assembly design shows significant improvements in Pu efficiency and reduction, compared with the reference fuel which is a normal fuel assembly loaded with Th/Pu oxide pellets. 20% more energy can be extracted from the same amount of Pu, which makes it just as Pu-efficient as the MOX reference. A large

fraction of the initially added Pu is consumed and the fissile fraction of the final Pu vector is very low, which makes this fuel type very useful for Pu incineration purposes.

This efficient Pu burning is achieved by increasing the hydrogen-to-heavy-metal ratio through reduction of the fuel mass, which makes it necessary to increase the specific burnup in order to fulfill the same demands on total energy release. This results in a smaller mass of waste for the same energy production, and in addition, the produced mass of minor actinides is reduced. Together with the low solubility of the Th matrix (Hubert et al., 2001), this makes the fuel less cumbersome from the perspective of long term waste storage.

The reactivity coefficients fulfill currently practiced safety requirements and the shut-down margin is expected to be improved through the improvement of the hot-to-cold swing, which makes the fuel usable in currently operating BWRs.

### 6.1. Outlook

First of all, the properties of the fuel assembly design should be evaluated on core level and in three dimensions. Most importantly, modern fuel assembly designs, including the one used as reference assembly here, have a number of part-length fuel rods, so that the upper part of the fuel assembly has a reduced number of fuel rods. This has been ignored in this work, and the calculations have been based on the properties of the lower, dominant part of the fuel assembly. Continued work would include finding out if the introduction of part-length rods is a suitable strategy also for Th/Pu fuel, and in such case finding out how many and which fuel rods should be part-length, how long they should be and what the consequences would be for parameters such as BWR stability and the MCPR.

The development work will need to continue along two lines: experimental assessment of the TMOL and evaluation of thermal-hydraulic and kinetic behavior of the assembly design, which are intimately connected.

The TMOL depends on several material properties such as thermal conductivity of the fuel material, fission gas release and burnup behavior. All of these will be assessed in the upcoming test irradiation planned by Thor Energy (Kelly and Fhager, 2010).

The consequences of the altered reactivity coefficients must be assessed by reactor kinetic simulation of adequate transients. Since these simulations are dependent on the thermal-hydraulic properties of the fuel assembly, these properties will need to be assessed simultaneously. The thermal-hydraulic calculations will most probably show a need for further modification of the assembly design in order to deal with thermal-hydraulic issues, which in turn will affect the neutronics. Hence, the design work will be an iterative process where the neutronic and the thermal-hydraulic development go hand in hand.

Finally, it should be noted that many of the limitations described in Section 2.1 are not definite, but rather a means to limit the scope of the study to designs which could be fabricated with existing licensed materials and facilities. On the material side, there are interesting indications that the use of silicon carbide cladding in conjunction with Th/Pu fuel could be advantageous (Shwageraus and Feinroth, 2011).

### Acknowledgments

In addition to the scientists whose work is cited, Sture Helmersson should be thanked for sharing his deep understanding of BWR fuel assembly design, Valentin Fhager for his input in the early phases of this work and the Norwegian Research Council for financial support through the industrial PhD program.

## Nomenclature

ARI	All Rods In
ARO	All Rods Out
BA	Burnable Absorber
BOL	Beginning Of Life
CRW	Control Rod Worth
CZP	Cold Zero Power
EOL	End Of Life
H/HM ratio	Hydrogen to Heavy Metal ratio
HCS	Hot-to-Cold Reactivity Swing
HFP	Hot Full Power
ITC	Isothermal Temperature Coefficient
LHGR	Linear Heat Generation Rate
LOCA	Loss Of Coolant Accident
MTC	Moderator Temperature Coefficient
RIA	Reactivity Insertion Accident
TMOL	Thermal-Mechanical Operating Limit

## References

- Bairiot, H., Blanpain, P., Farrant, D., Ohtani, T., Onoufriev, V., Porsch, D., Stratton, R., 2003. Status and Advances in MOX Fuel Technology. Technical Report TECDOC 415. International Atomic Energy Agency, Vienna.
- Belle, J., Berman, R.M., 1984. Thorium Dioxide: Properties and Nuclear Applications. Technical Report DOE/NE-0060. Naval Reactors Office, United States Department of Energy.
- Chadwick, M., Obložinský, P., Herman, M., Greene, N., McKnight, R., Smith, D., Young, P., MacFarlane, R., Hale, G., Frankle, S., Kahler, A., Kawano, T., Little, R., Madland, D., Moller, P., Mosteller, R., Page, P., Talou, P., Trellue, H., White, M., Wilson, W., Arcilla, R., Dunford, C., Mughabghab, S., Pritychenko, B., Rochman, D., Sonzogni, A., Lubitz, C., Trumbull, T., Weinman, J., Brown, D., Cullen, D., Heinrichs, D., McNabb, D., Derrien, H., Dunn, M., Larson, N., Leal, L., Carlson, A., Block, R., Briggs, J., Cheng, E., Huriá, H., Zerkle, M., Kozier, K., Courcelle, A., Pronyayev, V., van der Marck, S., 2006. ENDF/B-VII.0: next generation evaluated nuclear data library for nuclear science and technology. Nuclear Data Sheets 107, 2931–3060.
- Cozzo, C., Staicu, D., Somers, J., Fernandez, A., Konings, R.J.M., 2011. Thermal diffusivity and conductivity of thorium-plutonium mixed oxides. Journal of Nuclear Materials 416, 135–141.
- Dekoussar, V., Dyck, G., Galperin, A., Ganguly, C., Todosow, M., Yamawaki, M., 2005. Thorium Fuel Cycle – Potential Benefits and Challenges. Technical Report TECDOC 1450. International Atomic Energy Agency, Vienna.
- Demaziere, C., 2000. Analysis of the reactivity coefficients and the stability of a BWR loaded with MOX fuel. In: Proceedings of PHYSOR 2000, Pittsburgh, Pennsylvania, USA.
- Driscoll, M.J., Downar, T.J., Pilat, E.E., 1990. The Linear Reactivity Model for Nuclear Fuel Management. American Nuclear Society.
- Fridman, E., Kliem, S., 2011. Pu recycling in a full Th-MOX PWR core. Part I: steady state analysis. Nuclear Engineering and Design 241, 193–202.
- Galperin, A., Segev, M., Todosow, M., 2000. Pressurized water reactor plutonium incinerator based on thorium fuel and seed-blanket assembly geometry. Nuclear Technology 132, 214–226.
- Gotthardsson, R., 2007. Technical Requirements Reload Fuel for Forsmark 1/2/3. Technical Report FF-2007-1265 Rev 0. Forsmarks Kraftgrupp AB.
- Hamamoto, K., Kanagawa, T., Hiraiwa, K., Sakurada, K., Moriwaki, M., Aoyama, M., Yamamoto, T., Ueji, M., 2001. High moderation MOX cores for effective use of plutonium in LWRs. Nippon Genshiryoku Gakkaiishi/Journal of the Atomic Energy Society of Japan 43, 503–517.
- Helmerson, S. Personal Communication, 2011.
- Hubert, S., Barthelet, K., Fourest, B., Lagarde, G., Dacheux, N., Baglan, N., 2001. Influence of the precursor and the calcination temperature on the dissolution of thorium dioxide. Journal of Nuclear Materials 297, 206–213.
- Insulander Björk, K., 2012. Thorium-plutonium fuel for long operating cycles in PWRs – preliminary calculations. In: Thorium and Rare Earths Conference 2012, Cape Town, South Africa.
- Insulander Björk, K., Fhager, V., Demaziere, C., 2011. Comparison of thorium-based fuels with different fissile components in existing boiling water reactors. Progress in Nuclear Energy 53, 618–625.
- Kelly, J.F., 2012. Imminent: physical testing of a thorium-based LWR fuel. In: Thorium Energy Conference 2012, Shanghai, China.
- Kelly, J.F., Fhager, V., 2010. Designing a thorium fuel irradiation experiment. In: Advanced Fuel Pellet Materials and Fuel Rod Design for Water Cooled Reactors, Technical report TECDOC1654. International Atomic Energy Agency, Vienna, pp. 165–171.
- Kloosterman, J., Bende, E., 2000. Plutonium recycling in pressurized water reactors: influence of the moderator-to-fuel ratio. Nuclear Technology 130, 227–241.
- Ledergerber, G., Valizadeh, S., Wright, J., Limbäck, M., Hallstadius, L., Gavillet, D., Abolhassani, S., Nagase, F., Sugiyama, T., Wiesenack, W., Tverberg, T. Fuel performance beyond design – exploring the limits, in: Proceedings of 2010 LWR fuel performance/Top Fuel/WRFPF.
- Mosteller, R., 2008. ENDF/B-VII.0, ENDF/B-VI, JEFF-3.1, and JENDL-3.3 results for the MCNP criticality validation suite and other criticality benchmarks. In: Proceedings of PHYSOR 2008, Interlaken, Switzerland.
- Mosteller, R., 2004. Comparison of results from the MCNP criticality validation suite using ENDF/B-VI and preliminary ENDF/B-VII nuclear data. In: Proceedings of AIP Conference Santa Fe, New Mexico, USA.
- Puill, A., 2002. Thorium utilization in PWRs. Neutronics studies. In: Thorium Fuel Utilization: Options and Trends, TECDOC 1319. International Atomic Energy Agency, Vienna, pp. 185–197.
- Ramirez-Sanchez, R., Perry, R., Gustavo Alonso, V., Javier Palacios, H., 2008. MOX fuel assembly design equivalent to enriched uranium fuel for BWR. In: Proceedings of PHYSOR 2008, Interlaken, Switzerland.
- Rhodes, J., Deokjung, L., Smith, K., 2007. CASMO-5/CASMO-5M, A Fuel Assembly Burnup Program, User's Manual. Studsvik Scandpower, Inc.
- Shwageraus, E., Feinroth, H., 2011. Potential of silicon carbide cladding to extend burnup of Pu–Th mixed oxide fuel. Transactions of the American Nuclear Society 104, 658–660.
- Todosow, M., Raites, G., 2010. Thorium based fuel cycle options for PWRs. In: Proceedings of ICAPP 2010, San Diego, California, USA.
- Trellue, H., Bathke, C., Sadasivan, P., 2011. Neutronics and material attractiveness for PWR thorium systems using Monte Carlo techniques. Progress in Nuclear Energy 53, 698–707.
- Tsige-Tamirat, H., 2011. Neutronics assessment of the use of thorium fuels in current pressurized water reactors. Progress in Nuclear Energy 53, 717–721.
- World Nuclear Association, 2009. Plutonium. <http://world-nuclear.org/info/inf15.html>, (Date accessed: 03.11.11).

# Paper VI

**Commercial thorium fuel manufacture and irradiation:  
Testing (Th,Pu)O<sub>2</sub> and (Th,U)O<sub>2</sub> in the “Seven-Thirty”  
program**





## Commercial thorium fuel manufacture and irradiation: Testing (Th,Pu)O<sub>2</sub> and (Th,U)O<sub>2</sub> in the “Seven-Thirty” program



Klara Insulander Björk<sup>a,f,\*</sup>, Saleem S. Drera<sup>a</sup>, Julian F. Kelly<sup>a</sup>, Carlo Vitanza<sup>b</sup>, Christian Helsingreen<sup>b</sup>, Terje Tverberg<sup>b</sup>, Matylda Sobieska<sup>b</sup>, Barbara C. Oberländer<sup>b</sup>, Harri Tuomisto<sup>c</sup>, Laura Kekkonen<sup>c</sup>, Jonathan Wright<sup>d</sup>, Uffe Bergmann<sup>d</sup>, Daniel P. Mathers<sup>e</sup>

<sup>a</sup>Thor Energy, Sommerrogaten 13–15, NO-0255 Oslo, Norway

<sup>b</sup>Institute for Energy Technology, Os allé 5, NO-1777 Halden, Norway

<sup>c</sup>Fortum Corporation, P.O. Box 1, FI-00048 Fortum, Finland

<sup>d</sup>Westinghouse Electric Sweden AB, SE-721 63 Västerås, Sweden

<sup>e</sup>National Nuclear Laboratory, Chadwick House, Risley, Warrington WA3 6AE, United Kingdom

<sup>f</sup>Chalmers University of Technology, Department of Applied Physics, Division of Nuclear Engineering, SE-412 96 Göteborg, Sweden

### ARTICLE INFO

#### Article history:

Received 19 March 2014

Received in revised form 18 June 2014

Accepted 19 June 2014

Available online 24 August 2014

#### Keywords:

Thorium

Plutonium

Halden test reactor

Irradiation

Thorium fuel manufacture

### ABSTRACT

Thorium based fuels are being tested in the Halden Research Reactor in Norway with the aim of producing the data necessary for licensing of these fuels in today's light water reactors. The fuel types currently under irradiation are thorium oxide fuel with plutonium as the fissile component, and uranium fuel with thorium as an additive for enhancement of thermo-mechanical and neutronic fuel properties. Fuel temperatures, rod pressures and dimensional changes are monitored on-line for quantification of thermo-mechanical behavior and fission gas release. Preliminary irradiation results show benefits in terms of lower fuel temperatures, mainly caused by improved thermal conductivity of the thorium fuels. In parallel with the irradiation, a manufacturing procedure for thorium–plutonium mixed oxide fuel is developed with the aim to manufacture industrially relevant high-quality fuel pellets for the next phase of the irradiation campaign.

© 2014 Elsevier Ltd. All rights reserved.

### 1. Introduction

From an engineering standpoint, most types of nuclear reactor can operate with fuels that contain thorium. Proposals have been made to produce energy from thorium using various reactor platforms, including numerous interesting engineering concepts for utilizing thorium in novel reactor designs (Delpech et al., 2009; Herrera-Martinez et al., 2007), but in reality it will take a long time before these facilities can be financed, built, tested and approved for commercial operation. Meanwhile, the light water reactor (LWR) will remain the work horse of the nuclear generating industry. For these reasons, the first modern-era commercial electricity production using thorium on large scale will most likely be achieved in a LWR.

This paper describes a research program in which several candidate LWR thorium-based fuels are being physically tested with the intent that they are qualified for commercial deployment. Their

operational performance is being measured in simulated LWR conditions in irradiation rig IFA-730 (hence the program name) in the boiling heavy water research reactor (HBWR) in Halden, Norway. The aim of this undertaking is to produce a suite of detailed performance and post-irradiation examination (PIE) data that will support fuel performance code development and subsequent irradiation trials in a commercial reactor for typical thorium oxide fuels that can be used in current and new build Generation III + LWRs. The program is premised on modern fuel cycle realities, focusing on two applications for thorium use in LWRs: Thorium–plutonium mixed oxide fuel and thorium as an additive to uranium fuel.

Thorium based fuels have been tested before in numerous experiments since the very beginning of civil nuclear development. Many of the early trials used mixed oxide fuels of thorium and highly enriched uranium, a configuration which would not be considered today due to proliferation concerns. The reactors using these fuels were the Thorium High Temperature Reactor (HTR) (Baumer and Kalinowski, 1991) and the Atomversuchsreaktor (AVR) (Gottaut and Krüger, 1990) in Germany, the Peach Bottom (Steward, 1978) and Fort St Vrain (Walker, 1978) HTRs in the

\* Corresponding author at: Thor Energy, Sommerrogaten 13–15, NO-0255 Oslo, Norway. Tel.: +47 91117835.

E-mail address: [klara.insulander@scatec.no](mailto:klara.insulander@scatec.no) (K. Insulander Björk).

USA and the Dragon HTR in the UK (Price, 2012). The Shippingport Light Water Breeder Reactor (Clayton, 1993) and the Oak Ridge molten salt demonstration reactor (Haubenreich and Engel, 1970) in the US both used U-233 as the fissile component of the thorium based fuel and demonstrated the feasibility of closed thorium cycles, however they used highly specialized reactor designs. The irradiation of thorium–plutonium and thorium–LEU (low enriched uranium) mixed oxide fuels has been carried out on a small scale (a small number of rods rather than full cores) in PHWR/CANDU reactors (Karam et al., 2008) and in a number of trials in both commercial and test reactors (Hellwig et al., 2006; Verwerft et al., 2007). However, these tests were not on fuels that are prototypical for those that would be manufactured on an industrial scale for commercially operating reactors.

The objectives and scheduling of the Seven-Thirty program are laid out in Section 2. Thereafter, the program is presented by describing the test materials in Section 3, the fuel manufacture campaign in Section 4 and the irradiation test matrix in Section 5. Some of the first results of the Seven-Thirty program are presented in Section 6 and in Section 7 the continuation of the program is outlined.

## 2. The Seven-Thirty program

### 2.1. Objectives

The primary objective of the thorium fuel manufacture and irradiation program is to generate information that enables the licensing of thorium-based fuels that can be used in commercially operating light water reactors. To achieve this, data needs to be collected on how candidate thorium-based fuels change as they operate for long periods under typical operation conditions. Fuel irradiation behavior information is drawn from direct on-line measurements, including fuel temperature, rod pressure and cladding elongation, and post irradiation examination which yields data on chemical and mechanical interactions within the fuel rod. Since the pellets are isolated within the fuel rod the only effect of the heavy water moderator in the HBWR is its effects on the fast flux which can be taken into account by physics codes. For these reasons, the Halden Research Reactor is ideal for studying online pellet behavior and has provided a rich source of data which has been long used to support fuel licensing efforts.

The data gathered during this program will serve the safety licensing case for subsequent lead test thorium-based fuel rods (LTR) and/or lead test assemblies (LTA) in a commercial reactor. Furthermore, the understanding of thorium oxide fuel performance gained from this test campaign will enable the development of a fuel performance code for predicting thorium fuel behavior during commercial operation – a vital part of the fuel developer's intellectual property. Since an important benefit of thorium based fuel is the potential for high burnup, an important objective of the irradiation campaign is to measure high burnup data.

Only data representative of the final commercial product can be used for fuel licensing. To be able to guarantee the representativeness of the collected data, the research program includes work on fuel manufacture procedures to ensure that relevant thorium fuel ceramics are tested, prototypic of future commercial fuels.

### 2.2. Schedule

The Seven-Thirty program started in late 2011 with experiment design and material procurement efforts. Burnup

accumulation started with the loading of a first irradiation rig in April 2013, with the view of collecting high burnup data within five years. In parallel, the alpha laboratory at IFE Kjeller has been extended to enable manufacture of (Th,Pu)<sub>2</sub>O<sub>7</sub> material.

Three batches of experimental and reference fuel have been manufactured at the IFE Kjeller laboratory and loaded into the reactor together with (Th,Pu)<sub>2</sub>O<sub>7</sub> pellets procured from an earlier thorium fuel research program. The development of (Th,Pu)<sub>2</sub>O<sub>7</sub> fuel manufacture using powder metallurgical routes is underway at IFE, Kjeller, so that a second batch of (Th,Pu)<sub>2</sub>O<sub>7</sub> pellets can be loaded in the Halden Research Reactor in 2014.

The irradiation campaign includes online measurements of operating characteristics and discharge of fuel for PIE at the end of the campaign and at intermediate points. The (Th,Pu)<sub>2</sub>O<sub>7</sub> fuel pellets manufactured at IFE Kjeller will be loaded into the rig which is already under irradiation, at which point some of the currently irradiated rods will be extracted from the rig for PIE or storage for later use.

## 3. Materials

The flexibility of the Halden Research Reactor allows for the irradiation of a large number of different thorium fuel materials within the scope of a single irradiation campaign. In addition to the thorium fuels, a number of reference rods of more well-known materials are irradiated. Table 1 lists the basic characteristics of each material. Sample manufacturing is dealt with briefly in Section 4 along with a motivation for each composition. The placement and instrumentation of the different materials in the irradiation rig is discussed in Section 5.

## 4. Fuel manufacture

### 4.1. Th<sub>0.92</sub>Pu<sub>0.08</sub>O<sub>2</sub>

Pellets of mixed thorium and plutonium oxides were manufactured at ITU in 2003 as part of the European “OMICO” project (Verwerft et al., 2007) and were made available by JRC-ITU (Joint Research Centre – Institute for Transuranium Elements). The Sol–Gel (co-precipitation) technique was used, resulting in the relatively homogenous Pu distribution shown in Fig. 1.

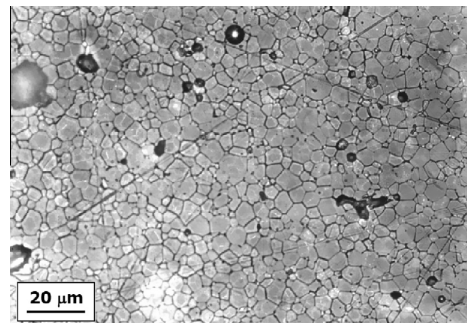


Fig. 1. Micrograph of the Th<sub>0.92</sub>Pu<sub>0.08</sub>O<sub>2</sub> material manufactured at ITU by the Sol–Gel technique, from Verwerft et al. (2007).

**Table 1**

Basic characteristics of the fuel materials being tested in the Seven-Thirty program. Compositions are given as oxide weight percentages.

Fuel type	Th <sub>0.92</sub> Pu <sub>0.08</sub> O <sub>2</sub>	Th <sub>0.42</sub> U <sub>0.58</sub> O <sub>2</sub>	Th <sub>0.07</sub> U <sub>0.93</sub> O <sub>2</sub>	UO <sub>2</sub>	Th <sub>0.86</sub> Pu <sub>0.14</sub> O <sub>2</sub>
Th content [%]	92.1	42	7	–	86
Pu content [%]	7.9	–	–	–	14
U content [%]	–	58	93	100	–
U enrichment [% U-235]	–	19.8	9.0	8.4	–
Pressing force [t/cm <sup>2</sup> ]	4.1	2.5	4.0	4.0	–
Sintering temperature [°C]	1650	1680	1680	1680	–
Sintering time [h]	6	4	4	4	–
Sintering atmosphere	Wet Ar/H <sub>2</sub>	Dry H <sub>2</sub>	Dry H <sub>2</sub>	Dry H <sub>2</sub>	–
Diameter [mm]	5.9	5.9	8.48	8.48	8.48
Theoretical density (TD) [g/cm <sup>3</sup> ]	10.11	10.58	10.90	10.96	10.19
Density [% of TD]	97	80	95	97	–
Cladding inner diameter [mm]	6.03	6.03	8.63	8.63	8.63
Cladding outer diameter [mm]	7.0	7.0	9.84	9.84	9.84

#### 4.2. UO<sub>2</sub>

Enriched UO<sub>2</sub> pellets were manufactured using a standard powder blending procedure at IFE, Kjeller, to provide a reference material for the Th<sub>0.07</sub>U<sub>0.93</sub>O<sub>2</sub> test rods. These were manufactured from a blend of 10% enriched uranium powder manufactured by the ADU method and dry milled, and 4.9% enriched uranium powder manufactured by the AUC method. 0.5 weight% zinc stearate was added as a lubricant before pressing. The currently loaded pellets have an enrichment chosen so that the power level of the reference rods is similar to that of the Th<sub>0.07</sub>U<sub>0.93</sub>O<sub>2</sub> pellets throughout the irradiation. In the next phase of the experiment, a new UO<sub>2</sub> reference rod will be manufactured with a different enrichment, matching that of the Th<sub>0.86</sub>Pu<sub>0.14</sub>O<sub>2</sub> rods.

#### 4.3. Th<sub>0.42</sub>U<sub>0.58</sub>O<sub>2</sub>

Th<sub>0.42</sub>U<sub>0.58</sub>O<sub>2</sub> pellets were designed to have a reactivity closely matching that of the Th<sub>0.92</sub>Pu<sub>0.08</sub>O<sub>2</sub> pellets so that they would run at similar power levels throughout the irradiation, in order to avoid power discontinuities at the interfaces between the different fuel sections. The thorium content was chosen to be as high as possible given that the highest enriched uranium available for the manufacture of these pellets had an enrichment of 19.8 weight% U-235. The purpose is to mitigate end effects in the short Th<sub>0.92</sub>Pu<sub>0.08</sub>O<sub>2</sub> rod sections and to provide a reference to their performance. Another beneficial aspect was realized with these pellets as they represent a valuable reference to past Th–U fuel irradiations. These pellets were also manufactured at IFE, Kjeller, using the standard uranium fuel manufacturing procedure following a dry ball-mill blending of the constituent oxide powders. A polished cross section of the resulting fuel pellets is shown in Fig. 2.

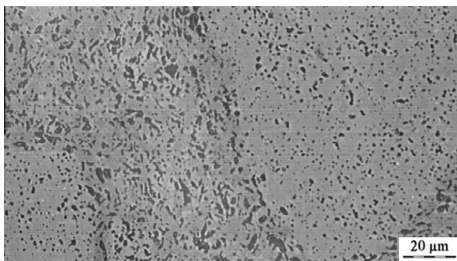


Fig. 2. Polished section from center of a Th<sub>0.42</sub>U<sub>0.58</sub>O<sub>2</sub> pellet with 6 vol% porosity.

#### 4.4. Th<sub>0.07</sub>U<sub>0.93</sub>O<sub>2</sub>

Th-additive fuel is recognized as potentially a means for the first introduction of thorium into the nuclear fuel cycle, with a Th fraction of about 7% being typical for this application (Lau et al., 2012). Th-additive fuel was manufactured at IFE, Kjeller, also with a standard uranium fuel manufacturing procedure. The pore size distribution at the rim had a mean size of 1.61 μm with a standard deviation of 1.52 μm as shown in Fig. 3. The pore size distribution at the center of pellet has an average size of 1.48 μm with a standard deviation of 1.36 μm as shown in Fig. 4.

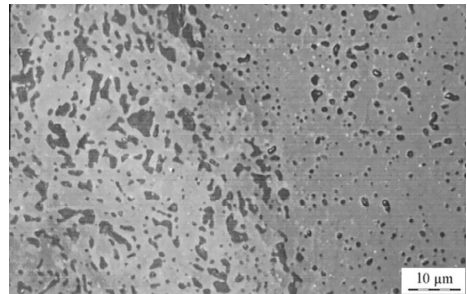


Fig. 3. Porosity depiction in a polished section from the rim of a Th<sub>0.07</sub>U<sub>0.93</sub>O<sub>2</sub> additive pellet.

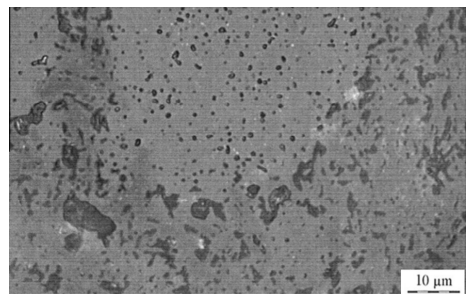


Fig. 4. Porosity depiction in a polished section from the center of a Th<sub>0.07</sub>U<sub>0.93</sub>O<sub>2</sub> additive pellet.

#### 4.5. $\text{Th}_{0.86}\text{Pu}_{0.14}\text{O}_2$ – manufacture trials

The Seven-Thirty program will test the irradiation performance of  $(\text{Th},\text{Pu})\text{O}_2$  fuel pellets having an elemental plutonium fraction of 14 weight%, chosen to give a fissile plutonium fraction in the fuel of 10 weight%, which is the upper limit for fissile plutonium content in fuel tested at IFE. A high plutonium content is desirable for this experiment. The addition of plutonium oxide to the thorium oxide matrix is assumed to degrade fuel performance, and a high plutonium content pellet will provide some conservatism with respect to fuel behavior. These fuel pellets will be manufactured in 2014 for loading into the Halden Research Reactor.

Surrogate  $(\text{Th},\text{Ce})\text{O}_2$  ceramic pellets have been manufactured to develop procedures for manufacturing good quality  $(\text{Th},\text{Pu})\text{O}_2$  fuel. From this work it is clear that commercially procured thorium dioxide powder is not necessarily ideal for nuclear fuel manufacturing. The raw powder used in the Seven-Thirty program has a coarse microstructure, a specific surface area that is only  $2\text{ m}^2/\text{g}$ , and high carbon impurity due to the calcining step. Nevertheless, it is representative of current world supplies of thorium dioxide derived from the oxalate method and hence it represents a logical starting point for this work.

A desirable thorium dioxide powder for fuel pellet production has a specific surface area in the order of  $8\text{ m}^2/\text{g}$  and a moderate distribution of particle sizes. To achieve such a powder state the thorium dioxide powder is milled for an extended period in a planetary ball mill. The powder can then be pressed with  $3.5$  to  $4\text{ t}/\text{cm}^2$  force to produce a green pellet that is roughly 67–68% of TD.

The sintering process should be performed in an oxidizing atmosphere such as air, to ensure that the oxygen-to-metal ratio in the ceramic is exactly 2.0.  $(\text{Th},\text{Ce})\text{O}_2$  pellets sintered in argon-hydrogen lose some oxygen mass but can be re-oxidized in air in regular furnaces running several hundred degrees lower than sintering furnaces. Final fuel pellet densities are typically 95% of TD.

### 5. Irradiation campaign

#### 5.1. Instrumentation and measured quantities

The instrumentation used for on-line measurements in the IFA-730 rig is listed below.

- **Fuel thermocouples:** The centerline temperature of the fuel pellets is measured by means of a thermocouple inserted into a narrow hole carefully drilled through a few pellets at the top or bottom of the fuel stack as shown in Fig. 5.

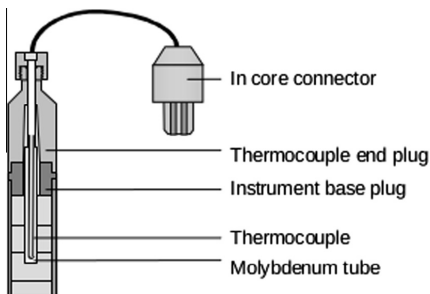


Fig. 5. Schematic drawing of a fuel rod instrumented with a thermocouple, from Bennett et al. (2008).

- **Pressure transducers:** The internal gas pressure of a fuel rod is measured by means of a pressure bellows within the fuel rod that communicates with a sensitive transformer mounted on the rod exterior as shown in Fig. 6.
- **Cladding extensometers:** Elongation of the cladding is measured by means of a magnetic rod mounted on the cladding, extending through a magnetic coil picking up its longitudinal movements as shown in Fig. 7.

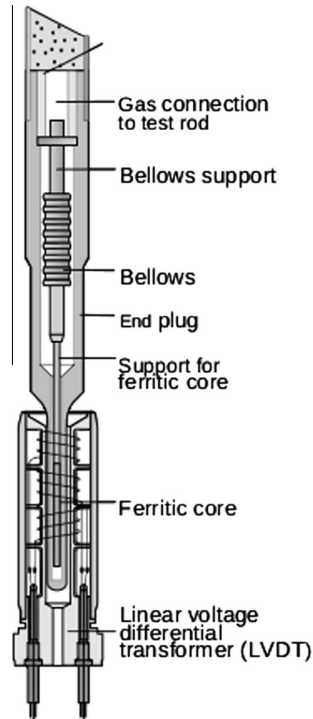


Fig. 6. Schematic drawing of a fuel rod instrumented with a pressure bellows, from Bennett et al. (2008).

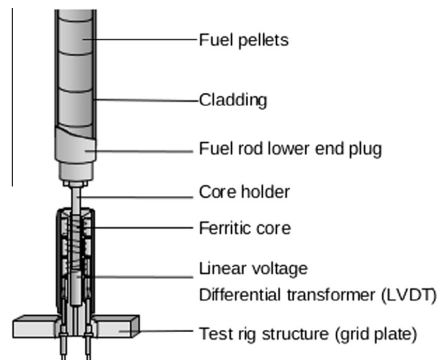


Fig. 7. Schematic drawing of a fuel rod instrumented with a cladding extensometer, from Bennett et al. (2008).

In addition, the neutron flux is monitored by means of neutron detectors at several locations in the rig, the moderator temperature is monitored by thermocouples at the coolant inlet and outlet and the flow is measured by an inlet coolant flowmeter.

### 5.2. The irradiation rig

The rig which is currently loaded in the Halden Research Reactor comprises six rods of 30 cm active length, arranged and instrumented as shown in Fig. 8.

Rods 1 and 3 contain the  $\text{Th}_{0.92}\text{Pu}_{0.08}\text{O}_2$  pellets manufactured at ITU. There were however only eight pellets available of sufficient quality. Hence, each rod contains only four pellets of this type. In order to avoid adverse end effects which would yield unrepresentative data, the rest of these two rods are filled with pellets of  $\text{Th}_{0.42}\text{U}_{0.58}\text{O}_2$  material which have been designed and manufactured to match the reactivity and spectrum of the  $\text{Th}_{0.92}\text{Pu}_{0.08}\text{O}_2$  pellets as closely as possible. The  $\text{Th}_{0.92}\text{Pu}_{0.08}\text{O}_2$  pellets had a small diameter of only 5.9 mm and the  $\text{Th}_{0.42}\text{U}_{0.58}\text{O}_2$  pellets were manufactured with the same diameter. This choice of diameter was

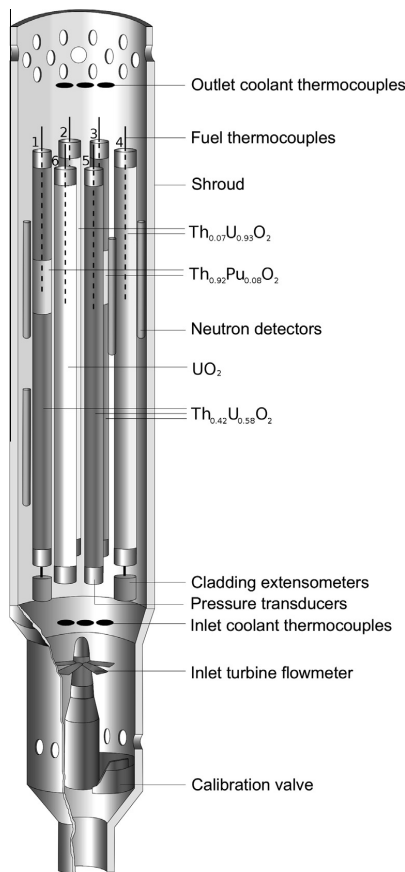


Fig. 8. The IFA-730 irradiation rig.

made during the OMICO project for which the pellets were originally designed. Reducing the diameter and increasing the fissile plutonium loading allows for an acceleration of the irradiation, which was prioritized in that context.

The  $\text{Th}_{0.92}\text{Pu}_{0.08}\text{O}_2$  pellets are located close to the upper end of the rods so that the thermocouple extends into these and measures the operating temperature of these pellets. Five  $\text{Th}_{0.42}\text{U}_{0.58}\text{O}_2$  pellets of approximately 9 mm height are located above the  $\text{Th}_{0.92}\text{Pu}_{0.08}\text{O}_2$  section in each rod, in order to catch most of the end effects. In addition to the thermocouples, rod 1 is instrumented with a cladding extensometer and rod 3 with a pressure transducer.

Rod 5 is a reference rod for rods 1 and 3, containing only  $\text{Th}_{0.42}\text{U}_{0.58}\text{O}_2$  pellets of the same diameter. This rod is also instrumented with a fuel thermocouple and a pressure transducer. This experiment setup does not allow for an accurate assessment of the fission gas release behavior of the  $\text{Th}_{0.92}\text{Pu}_{0.08}\text{O}_2$  material, but a difference in rod pressure between rod 3 and its reference rod 5 would indicate that there may be a difference between the  $\text{Th}_{0.42}\text{U}_{0.58}\text{O}_2$  and  $\text{Th}_{0.92}\text{Pu}_{0.08}\text{O}_2$  material in this respect.

Rods 2 and 4 contain  $\text{Th}_{0.07}\text{U}_{0.93}\text{O}_2$  pellets with a diameter of 8.48 mm. This is a standard BWR diameter and was chosen to yield data representative for commercial reactors. Choosing the same diameter as the other rods would have facilitated intercomparison of the fuel types, but the representativity aspect was prioritized since the applications of the differential fuel types are quite different, so that a choice between them will not primarily be based on differences in fuel performance. Both rods 2 and 4 are instrumented with fuel thermocouples, rod 2 with a pressure transducer and rod 4 with a cladding extensometer. Rod 6 is a reference rod for rods 2 and 4 with 8.4% enriched uranium ( $\text{UO}_2$ ) pellets of the same diameter, and is instrumented with a fuel thermocouple and a pressure transducer.

All pellets are enclosed in standard Zircalloy-2 cladding tubes with the dimensions listed in Table 1.

In the following phase of the experiment, three rods will be discharged from the current rig and replaced by two rods containing the freshly manufactured  $\text{Th}_{0.86}\text{Pu}_{0.14}\text{O}_2$  pellets from the IFE Kjeller laboratory, and a uranium oxide reference rod for this material. These three rods will have the same diameter of 8.48 mm and be instrumented similarly to the current rods, i.e. with fuel thermocouples on all rods, as well as a cladding extensometer on one of the  $\text{Th}_{0.86}\text{Pu}_{0.14}\text{O}_2$  rods and pressure transducers on the remaining two.

## 6. First irradiation results

### 6.1. Fuel temperatures

Figs. 9 and 10 show the fuel centerline temperatures during the first 100 days of irradiation for all fuel types normalized to a power level of 30 kW/m for the large diameter rods and 20 kW/m for the small diameter rods, which is close to actual operating levels and representative for normal reactor operation. Note that the temperatures displayed by the  $\text{Th}_{0.92}\text{Pu}_{0.08}\text{O}_2$  pellets are not typical for normal LWR fuel due to their small diameter. The plutonium used in these pellets has a fissile content higher than typical recycled plutonium, which together with the small diameter yields a burnup rate approximately 40% higher than that of the large diameter pins. This explains why the accumulated burnup is larger for these rods although the plotted time span is the same for all rods.

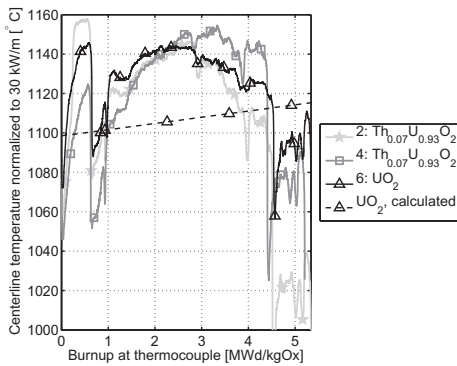


**Fig. 9.** Fuel centerline temperatures for the large diameter rods (rods 2, 4 and 6), normalized to 30 kW/m. The calculated temperature for the  $\text{UO}_2$  rod is also plotted.

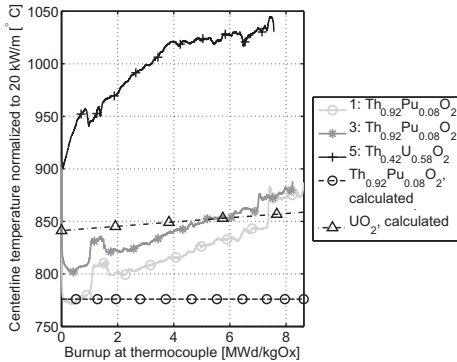


**Fig. 10.** Fuel centerline temperatures for the small diameter rods (rods 1, 3 and 5), normalized to 20 kW/m. The calculated temperature for the  $\text{Th}_{0.92}\text{Pu}_{0.08}\text{O}_2$  rod is shown, and also the calculated temperature of a comparable  $\text{UO}_2$  rod with the same diameter and power level as the other rods in this plot.

These first measurements show that the normalized fuel temperature is slightly lower (30–40 K) in the  $\text{Th}_{0.07}\text{Pu}_{0.93}\text{O}_2$  rods compared to their reference  $\text{UO}_2$  rod, indicating a higher thermal conductivity of the Th-doped pellets. This is an intriguing result, but one to treat with caution. During the course of the irradiation, the normalized fuel temperatures have drifted relative to each other due to different densification behavior and different free volumes in the respective fuel rods causing differing pellet-cladding gaps. The current data base is too small to draw any conclusions regarding the long term behavior of this fuel ceramic. Continued irradiation should shed light on the magnitude of this apparent conductivity enhancement effect.

The temperature of the  $\text{Th}_{0.92}\text{Pu}_{0.08}\text{O}_2$  pellets compared to their reference  $\text{Th}_{0.42}\text{U}_{0.58}\text{O}_2$  pellets indicates a better thermal conductivity of the  $\text{Th}_{0.92}\text{Pu}_{0.08}\text{O}_2$  material, a trend which prevails throughout the current irradiation period.

Theoretical predictions of the fuel temperatures are also shown in Figs. 9 and 10. The temperatures have been calculated with IFE's

in-house code FTMP3 (Pihlatie, 2000) which, for the prediction of the temperature of the  $\text{Th}_{0.92}\text{Pu}_{0.08}\text{O}_2$  material, has been modified using a published correlation for  $(\text{Th},\text{Pu})\text{O}_2$  conductivity (Cozzo et al., 2011). The fuel temperature has been calculated for the  $\text{UO}_2$  pellets, for the  $\text{Th}_{0.92}\text{Pu}_{0.08}\text{O}_2$  pellets and for a hypothetical small diameter  $\text{UO}_2$  pellet for comparison with the data for the other small diameter pellets.

Initially spurious readings from the pressure transducer on the  $\text{UO}_2$  rod makes it difficult to assess the swelling and densification of this material, so the assumptions for these parameters are based on previous experience with similar material. A swelling rate of about 0.07% per MWd/kgOx and a densification of 1.5% were assumed. The assumption for the densification is smaller than the 2% usually assumed for  $\text{UO}_2$  fuel, because of the high initial density of the  $\text{UO}_2$  pellets used in this experiment, and is chosen to give good agreement with the measured data. The same assumptions were made for the small  $\text{UO}_2$  pellet.

The prediction agrees well with the measured data for the  $\text{UO}_2$  pellets, so it is assumed that the prediction is reasonably accurate also for the hypothetical small diameter  $\text{UO}_2$  pellet. Comparison with measured data for the other small diameter pellets then shows that the  $\text{Th}_{0.92}\text{Pu}_{0.08}\text{O}_2$  pellets perform better than corresponding  $\text{UO}_2$  pellets, in terms of lower operating temperature. This could be expected from comparison between the thermal conductivity correlation for  $(\text{Th},\text{Pu})\text{O}_2$  by Cozzo et al. (2011) and the corresponding correlation for  $\text{UO}_2$  used in FTMP3 or the similar correlation published by the IAEA (Kim et al., 2006). It is noted that the model does not capture the gradual temperature increase with burnup displayed by the  $\text{Th}_{0.92}\text{Pu}_{0.08}\text{O}_2$  pellets. Fuel performance code development work is ongoing, and more irradiation data is awaited before any firm conclusions are drawn regarding the development of the fuel temperature with burnup.

The measured temperatures of  $\text{Th}_{0.42}\text{U}_{0.58}\text{O}_2$  pellets, however, are significantly higher than those predicted for a  $\text{UO}_2$  pellet of the same diameter, which could be expected given their low density and also from comparison of literature data for  $\text{UO}_2$  and  $(\text{Th},\text{U})\text{O}_2$  (Yang et al., 2004). This correlation for  $(\text{Th},\text{U})\text{O}_2$  was chosen because it includes measurements on compositions close to that of the  $\text{Th}_{0.42}\text{U}_{0.58}\text{O}_2$  composition used in this experiment.

In fact, the correlation published by Yang et al. (2004) also indicates that the conductivity of the  $\text{Th}_{0.07}\text{Pu}_{0.93}\text{O}_2$  is lower than that of pure  $\text{UO}_2$ , which does not agree with our measurements on that material. However, in the absence of any measurement data on  $(\text{Th},\text{U})\text{O}_2$  material with low Th content (<20%), the temperature data measured in this experiment is considered reliable for the time being.

## 6.2. Fuel rod pressures

At this early stage of the irradiation campaign, fission gas release is not expected. Instead, the recorded changes in fuel rod pressure shown in Fig. 11 correspond to the dimensional changes of the fuel, i.e. irradiation growth, which during the first part of operation is over-compensated by densification (shrinkage) caused by resintering of the fuel ceramic. Discontinuities are seen at burnups corresponding to shutdown periods.

The pressure transducer on the  $\text{UO}_2$  reference rod initially gave spurious readings, probably due to internal friction in the instrument. After a rapid drop at approximately four irradiation days, the instrument responds as expected to power changes but the absolute value of the given pressure should be regarded with some skepticism. At the end of the irradiation, the absolute pressure can

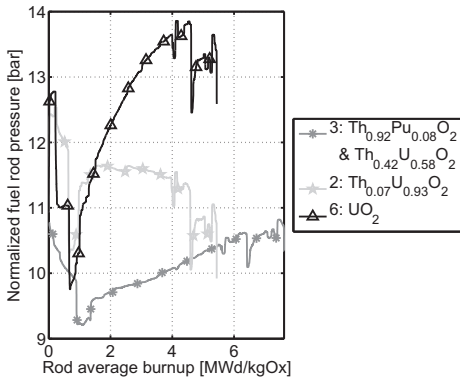


Fig. 11. Internal fuel rod pressures in rods 2, 3 and 6, normalized to zero power and 20 °C.

nevertheless be confirmed by rod puncture and the measurements recalibrated accordingly.

The readings from the pressure transducer on the  $\text{Th}_{0.42}\text{U}_{0.58}\text{O}_2$  rod ended after about 12 irradiation days, due to water penetration into the cable. The initial readings also showed unexpected behavior, so it is assumed that the cable was in bad condition already when loaded.

### 6.3. Cladding elongation

The primary reason for measuring the cladding elongation is to detect when the pellet-cladding gap closes. This is expected to appear after around two years of irradiation, so the readings recorded so far and shown in Fig. 12 only show cladding length changes due to friction between the cladding and the pellets before the pellets become perfectly aligned and centered, and a weak irradiation growth of the cladding material of 0.01 mm per MWd/kgOx, corresponding well with previous experience. As with the fuel rod pressures, discontinuities are seen after shutdown periods, in particular in connection with a shutdown period during which the rig was moved.

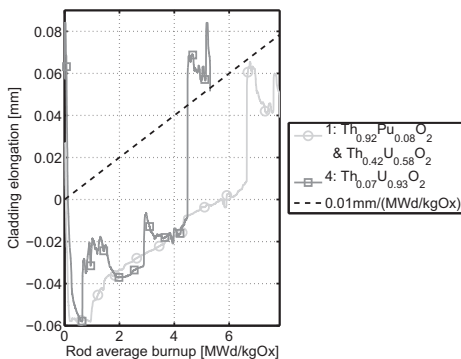


Fig. 12. Cladding elongation of rods 1 and 4 and a line representing the expected cladding irradiation growth of 0.01 mm per MWd/kgOx.

## 7. Outlook

### 7.1. Continued irradiation

In the third phase of the Seven-Thirty program a new test-rig will be introduced for testing  $(\text{Th,Pu})\text{O}_2$  pellets manufactured at a new alpha laboratory, operated by the UK National Nuclear Laboratory (NNL). This rig will comprise a 12-rod double cluster consisting of two stacked 6-rod clusters. The upper cluster will be located at the axial flux peak in the Halden Research Reactor, a location chosen to accumulate burnup as fast as possible. The lower cluster will experience a tapered flux profile, which is useful for acquiring samples of varying burnup for PIE. Irradiation of these two rigs will continue until late 2017 at which point the oldest material will have accumulated a burnup of approximately 50 MWd/kgHM.

### 7.2. Proposed PIE program

While the online measurements are invaluable for understanding in-pile fuel behavior, post irradiation examination is crucial for understanding the physical mechanisms behind the manifested macroscopic behavior. The characterization of microscopic phenomena such as grain growth, formation of high burnup structure and diffusion of oxygen and fission products within the fuel ceramic is important for building reliable fuel behavior models. In order to assess these processes, a PIE program is proposed comprising rod puncture and gas spectrometry, non-destructive neutron radiography and gamma scanning of the fuel rod, optical microscopy and SEM, punch tests for micro-hardness measurements, and measurement of elemental composition by mass spectrometry.

### 7.3. Testing in a commercial reactor

As mentioned in Section 2.1, the objective of the Seven-Thirty program is to provide requisite data that can enable the licensing of thorium based fuels for use in commercially operating light water reactors. After completion of this program, the target is inserting Lead Test Rods (LTRs) and thereafter Lead Test Assemblies (LTAs) into a commercial reactor. The fuel pellets for these rods will be manufactured in accordance with the process developed within the Seven-Thirty program. For licensing purposes, a well benchmarked fuel performance code must also be in place. The development of such a code is in progress, and the collected data will be used for benchmarking. Full-core simulations such as the ones described and partly completed by Insulander Björk et al. (2013) must also confirm the feasibility with respect to neutronic behavior. With all these pieces in place, thorium based fuels will be ready for large scale deployment in currently operating light water reactors.

## Acknowledgments

The Seven Thirty consortium is grateful for support from the Norwegian Research Council through its program for user-driven research-based innovation (BIA). The authors would like to thank the many IFE employees who have been crucial in enabling this experiment, in particular Margaret McGrath. We also thank Joseph Somers at JRC-ITU for making the  $\text{Th}_{0.92}\text{Pu}_{0.08}\text{O}_2$  pellets available and for his advice.

## References

- Baumer, R., Kalinowski, I., 1991. THTR commissioning and operating experience. *Energy* 16 (1–2), 59–70.

- Bennett, P.J., Helsingreen, C., McGrath, M.A., Tverberg, T., 2008. In-core fuel performance characterization in the Halden reactor. Technical Report F1.9 HWR-884, OECD Halden Reactor Project, Halden, Norway.
- Clayton, J., 1993. The shippingport pressurized water reactor and light water breeder reactor. Technical Report WAPD-T-3007, Westinghouse Bettis Atomic Power Laboratory.
- Cozzo, C., Staicu, D., Somers, J., Fernandez, A., Konings, R., 2011. Thermal diffusivity and conductivity of thorium–plutonium mixed oxides. *J. Nucl. Mater.* 416 (1–2), 135–141.
- Delpech, S., Merle-Lucotte, E., Heuer, D., Allibert, M., Ghetta, V., Le-Brun, C., Doligez, X., Picard, G., 2009. Reactor physic and reprocessing scheme for innovative molten salt reactor system. *J. Fluorine Chem.* 130 (1).
- Gottaut, H., Krüger, K., 1990. Results of experiments at the AVR reactor. *Nucl. Eng. Des.* 121 (2), 143–153.
- Haubenreich, P., Engel, J., 1970. Experience with the molten-salt reactor experiment. *Nucl. Appl. Technol.* 8, 118–136.
- Hellwig, C., Streit, M., Blair, P., Tverberg, T., Klaassen, F., Schram, R., Vettrano, F., Yamashita, T., 2006. Inert matrix fuel behaviour in test irradiations. *J. Nucl. Mater.* 352 (1–3), 291–299.
- Herrera-Martinez, A., Kadi, Y., Parks, G., Dahlfors, M., 2007. Transmutation of nuclear waste in accelerator-driven systems: fast spectrum. *Ann. Nucl. Energy* 34 (7), 564–578.
- Insulander Björk, K., Lau, C.W., Nylén, H., Sandberg, U., 2013. Study of thorium–plutonium fuel for possible operating cycle extension in PWRs. *Sci. Technol. Nucl. Installations* 2013 (Article ID: 867561).
- Karam, M., Dimayuga, F., Montin, J., 2008. Fission gas release of (Th,Pu)O<sub>2</sub> CANDU fuel. Technical Report CW-124950-CONF-002, Atomic Energy of Canada Limited.
- Kim, Y.-E., Park, J.-W., Cleveland, J., 2006. Thermophysical properties database of materials for light water reactors and heavy water reactors. Technical Report IAEA-TECDOC-1496, International Atomic Energy Agency.
- Lau, C.W., Demazière, C., Nylén, H., Sandberg, U., 2012. Improvement of LWR thermal margins by introducing thorium. *Prog. Nucl. Energy* 61, 48–56.
- Pihlatie, M., 2000. Modifications of FTEMP to produce fuel temperature calculation code FTEMP3. F-Note 1697, OECD Halden Reactor Project, Halden, Norway.
- Price, M., 2012. The dragon project origins, achievements and legacies. *Nucl. Eng. Des.* 251, 60–68.
- Steward, K., 1978. Final summary report on the peach bottom end-of-life program. Technical Report GA-A14404, General Atomics.
- Verwerf, M., Lemehov, S.E., Wéber, M., Vermeeren, L., Gouat, P., Kuzminov, V., Sobolev, V., Parthoens, Y., Vos, B., Van den Bergh, S., ans Segura, H., Blanpain, P., Somers, J., Toury, G., McGinley, J., Staicu, D., Schubert, A., Van Uffelen, P., Haas, D., 2007. OMICO final report. Technical Report EUR 23104, European Commission, FKS-CT-2001-00141.
- Walker, R., 1978. Experience with the Fort St. Vrain reactor. *Ann. Nucl. Energy* 5 (8–10), 337–356.
- Yang, J., Kang, K., Song, K., Lee, C., Jung, Y., 2004. Fabrication and thermal conductivity of (Th,U)O<sub>2</sub> pellets. *Nucl. Technol.* 147 (1), 113–119.

# Paper VII

Development of a fuel performance code for thorium-plutonium fuel



# DEVELOPMENT OF A FUEL PERFORMANCE CODE FOR THORIUM-PLUTONIUM FUEL

**Klara Insulander Björk and Patrik Fredriksson**

Thor Energy, NO-0255 Oslo, Norway

Department of Applied Physics, Division of Nuclear Engineering  
Chalmers University of Technology, SE-412 96 Göteborg, Sweden

[klara.insulander@scatec.no](mailto:klara.insulander@scatec.no)

[patrik@nephy.chalmers.se](mailto:patrik@nephy.chalmers.se)

## ABSTRACT

Thorium-plutonium Mixed OXide fuel (Th-MOX) is considered for use as light water reactor fuel. Both neutronic and material properties show some clear benefits over those of uranium oxide and uranium-plutonium mixed oxide fuel, but for a new fuel type to be licensed for use in commercial reactors, its behaviour must be possible to predict. For the thermomechanical behaviour, this is normally done using a well validated fuel performance code, but given the scarce operation experience with Th-MOX fuel, no such code is available today.

In this paper we present the ongoing work with developing a fuel performance code for prediction of the thermomechanical behaviour of Th-MOX for light water reactors. The well-established fuel performance code FRAPCON is modified by incorporation of new correlations for the material properties of the thorium-plutonium mixed oxide, and by development of a new subroutine for prediction of the radial power profiles within the fuel pellets. This paper lists the correlations chosen for the fuel material properties, describes the methodology for modifying the power profile calculations and shows the results of fuel temperature calculations with the code in its current state of development. The code will ultimately be validated using data from a Th-MOX test irradiation campaign which is currently ongoing in the Halden research reactor.

*Key Words:* **Fuel performance code, FRAPCON, Thorium, Plutonium**

## 1. INTRODUCTION

Thorium-plutonium Mixed OXide fuel (Th-MOX) is considered a promising technology for plutonium incineration [1, 2], and also offers several benefits in terms of neutronic [3, 4] and material properties compared with the traditional fuel types, Uranium OXide (UOX) and Uranium-plutonium Mixed OXide (U-MOX). The Norwegian company Thor Energy is currently developing Th-MOX fuel for use in current and future Light Water Reactors (LWRs), assessing both the particularities of Th-MOX fuel manufacture and its irradiation behaviour through an irradiation campaign in the Halden Research Reactor within the research program "Seven-Thirty" [5].

In order for a new nuclear fuel type, such as Th-MOX, to be licensed for use in a commercially operating nuclear reactor, its material properties and thermal-mechanical behaviour must be well known and predictable for all operation modes of the reactor. These predictions are normally done

using a fuel performance code, in which established correlations for the properties of the fuel in question are integrated, along with models of various processes in the fuel such as fission gas release and variations of power profiles. Thor Energy has chosen to develop a modified version of the well-established code FRAPCON [6] for this purpose, and the first phase of this work is described here.

Similar work was conducted previously in connection with the OMICO project [7], for prediction of the behaviour of the experimental fuel which was irradiated within the scope of this project, but no validation of the code with experimental data was performed. A version of FRAPCON for modelling of thorium-uranium mixed oxide fuel has also been created by Loewen et al. [8]. Our work has to a large extent been guided by their methodology. For the purpose of modifying FRAPCON for use with Th-MOX fuel, the available literature on the material properties of  $\text{Th}_{1-y}\text{Pu}_y\text{O}_{2-x}$  has been reviewed and the found correlations have been incorporated into the FRAPCON code. Since Th-MOX fuel differs from UOX and U-MOX fuel also with respect to neutronic properties, the power distribution within the fuel pellet is expected to be different, which affects the temperature and burnup profiles directly and thus, indirectly, all the material properties. To account for this, we also develop a new subroutine for prediction of power profiles.

All physical properties of the fuel material will change with the burnup of the fuel. Quantitative assessments of these dependencies are however very scarce. As the "Seven-Thirty" program proceeds, information will become available to make such assessments, but for the time being, the burnup dependence of the thermomechanical properties is left as they are in the current version of the FRAPCON code.

A brief account on the working mode of the FRAPCON code is given in Section 2. In Section 3 we list the correlations chosen for the material properties which have been incorporated in the code. The development of a new subroutine for power profile prediction is described in Section 4, preliminary results are presented in Section 5 and in Section 6 we conclude and summarize our plans for future development and validation of the code.

## 2. THE FRAPCON CODE

Our starting point is the current version of the FRAPCON code, FRAPCON-3. This code iteratively calculates temperature, pressure, and deformation of a light-water reactor fuel rod during long-term burnup, modeling phenomena such as heat conduction through the fuel and cladding to the coolant, fuel-cladding mechanical interaction, stored energy, and fission gas release. For this purpose, properties for fuel and cladding materials are incorporated in the code. The cladding material properties are left unchanged, whereas the fuel material and neutronic properties are being updated in this work. The state of the fuel rod is determined for each time step by iterative calculations, until the fuel-cladding gap temperature difference and internal gas pressure converge. The radial power profiles within the fuel pellets are calculated in each time step, but there is no feedback from the thermomechanical simulations to the neutronic calculations.

Looking specifically at the modeling of the fuel pellet, it is divided into several radial nodes within each of which all properties are averaged. The fuel material is specified by user input in terms of

porosity, oxygen to metal (O/M) ratio, plutonium weight fraction and the plutonium vector. For the purpose of calculating material properties, these entities are regarded as constant throughout the life of the fuel pin. Possible changes of these parameters with burnup are implicitly taken into account through the burnup dependence of the thermomechanical material properties. The temperature and burnup is calculated separately for every radial node, and the material properties are determined using the locally calculated temperature and burnup of the fuel material. The subroutine for prediction of radial pellet power profiles, in contrast, uses local concentrations of all important actinide isotopes, and also updates these with every time step. This is also the only instance in the code where the isotopic composition of the plutonium is taken into account.

### 3. THERMOMECHANICAL PROPERTIES

The fuel thermomechanical properties, listed in Table I, predominantly depend on the fuel temperature and burnup. The fuel temperature is denoted  $T$  and is always assumed to be given in units of Kelvin. As previously stated, burnup dependence is excluded at the current stage of the code development due to lack of experimental data. In many instances the properties also depend on the porosity of the fuel, which is denoted  $P$ , and the oxygen to metal (O/M) ratio. We let  $x$  denote the negative deviation from stoichiometry, i.e. from the  $O/M = 2.00$ . Since neither  $\text{ThO}_2$  nor  $\text{PuO}_2$  become hyperstoichiometric,  $x$  will always be a positive number [9]. Due to the limited experience with Th-MOX, and also due to the fact that  $\text{ThO}_2$  in itself does not readily deviate from stoichiometry, the stoichiometry dependence of most thermomechanical properties is unknown for  $\text{ThO}_2$ . Since the thermal conductivity is such an important property, with the by far largest impact on simulation results, an attempt has nevertheless been made of introducing a stoichiometry dependence of this property.

Most thermomechanical properties also depend on the plutonium weight fraction  $y$ . In case of the lattice parameter (also after thermal expansion), this can be found by simple linear interpolation (Vegard's law) between the lattice parameters for the pure constituents  $\text{ThO}_2$  and  $\text{PuO}_2$  [10, 11]. The correlation for thermal expansion of  $\text{PuO}_2$  is kept unchanged, whereas the implemented correlation for  $\text{ThO}_2$  is listed in Table I. Similarly, heat capacity and enthalpy increments can be calculated using linear interpolation, following Neumann-Kopp's law [12] and the correlation used for  $\text{PuO}_2$  is left unchanged whereas the implemented correlation for  $\text{ThO}_2$  is listed in Table I. The factor used for correction of the thermal conductivity for the influence of the fuel porosity is also left unchanged.

For the simulation of mechanical interactions between fuel and pellet, FRAPCON assumes the pellet to be rigid. The subroutine for calculation of the Young's modulus is thus only used for the stoichiometry correction factor for the thermal conductivity. Finally, the code's sensitivity to the emissivity of the fuel material is negligible for all normal applications, for which reason this correlation is left unchanged.

Table I: Thermomechanical properties of  $\text{Th}_{1-y}\text{Pu}_y\text{O}_{2-x}$  implemented in the FRAPCON code.

Lattice parameter at STP of $\text{ThO}_2$ [13].	5.597 Å
Thermal expansion of $\text{ThO}_2$ [10].	$\frac{\Delta L}{L_0} = -0.2426 \cdot 10^{-2} + 7.837 \cdot 10^{-6}T + 9.995 \cdot 10^{-10}T^2$
Heat capacity of $\text{ThO}_2$ ( $\theta = 408.14$ K) [10].	$C_P = \frac{260.1\theta^2 e^{\frac{\theta}{T}}}{T^2 (e^{\frac{\theta}{T}} - 1)^2} + 3.65 \cdot 10^{-2}T$
Enthalpy of $\text{ThO}_2$ relative to $T_{\text{ref}}$ [10].	$\Delta H_T = H_T - H_{T_{\text{ref}}} = \frac{260.1\theta^2 e^{\frac{\theta}{T}}}{T^2 (e^{\frac{\theta}{T}} - 1)^2} + 3.65 \cdot 10^{-2}T$
Solidus temperature of $\text{Th}_{1-y}\text{Pu}_y\text{O}_2$ <sup>1</sup> .	$T_s = -34.86y^3 + 233.1y^2 - 832.3y + 3651$
Liquidus temperature of $\text{Th}_{1-y}\text{Pu}_y\text{O}_2$ .	$T_l = -99.54y^3 - 24.59y^2 - 509.7y + 3651$
Young's modulus of $\text{ThO}_2$ [10].	$E = 2.491 \cdot 10^{11}(1 - 2.21P)(1.0230 - 1.405 \cdot 10^{-4}e^{\frac{181}{T}})$
Thermal conductivity $\text{Th}_{1-y}\text{Pu}_y\text{O}_2$ [14] <sup>2</sup> .	$\kappa = (6.071 \cdot 10^{-3} + Cx + 5.72 \cdot 10^{-1}y - 5.937 \cdot 10^{-1}y^2 + 2.4 \cdot 10^{-4}T)^{-1}$
Stoichiometry correction factor for conductivity <sup>3</sup> .	$C = \frac{\pi^2 \theta_D \bar{m}}{3Eh} \left( \frac{a_{\text{ThPuO}_2}}{a_{\text{ThO}_2}} \right)^2 \left( - \left( \frac{m_{\text{O}^{2-}}}{\bar{m}} \right)^2 + \frac{\epsilon}{\bar{r}^2} \left( 2(r_{\text{Pu}^{3+}}^2 - r_{\text{Pu}^{4+}}^2) + (r_{\text{O}^{2-}}^2 - r_{\text{O}^{2-}}^2) \right) \right)^{\frac{1}{2}}$

<sup>1</sup> The equations for the solidus and liquidus temperatures are polynomial fits to the solutions to the system of equations given in reference [15], using the melting points 3017 K for  $\text{PuO}_2$  [16] and 3651 K for  $\text{ThO}_2$  [17].

<sup>2</sup> The factor  $C$  quantifying the stoichiometry dependence has been introduced by the authors, based on the reasoning by Duriez et al. for U-MOX fuel [8], and is given as a separate function in the table.

<sup>3</sup> This formulation of the stoichiometry correction factor is based on [8], using  $\theta_D = 259$  K [19],  $\epsilon = 7.5$  [14], ionic radii  $r_i$  from [20] ( $\text{O}_v$  denotes an oxygen vacancy) and the lattice parameter  $a_{\text{ThPuO}_2}$  and Young's modulus  $E_{\text{ThPuO}_2}$  as calculated by their corresponding FRAPCON subroutines.  $h$  denotes the Planck constant,  $m_{\text{O}^{2-}}$  the mass of the  $\text{O}^{2-}$  ion,  $\bar{m}$  the mean atomic mass of the lattice and  $\bar{r}$  the mean ionic radius.

## 4. RADIAL PELLETT POWER PROFILES

As previously mentioned, power is not generated homogeneously in the fuel pellet, with the important consequence that the fuel material in the different radial nodes will have different burnup and hence different material properties. In addition, the inhomogeneous heat generation affects the temperature profile in the pellet directly. The difference in neutronic properties between Th-MOX and UOX fuel affects the radial power profiles, for which reason a new subroutine for prediction of radial pellet power profiles was created.

First, power profiles in Th-MOX fuel pellets were calculated using Monte-Carlo simulations, which is time consuming but yields accurate data, to the extent that the used cross section libraries are accurate. A simplified theoretical model was then developed and implemented in the FRAPCON code, which is capable of rapidly calculating the power profiles using a set of effective cross sections for the important isotopes in Th-MOX fuel. Then a genetic algorithm was employed to find the set of effective cross sections which, when used by the simplified theoretical model, best reproduces the power profiles given by the Monte Carlo simulations. Last, these effective cross sections were incorporated in the FRAPCON code. These steps are described in greater detail below.

### 4.1. Monte-Carlo simulations

For the purpose of calculating power profiles, the Monte-Carlo based code *Serpent* [21] was used. *Serpent* is a continuous-energy Monte Carlo reactor physics burnup calculation code. First, a sensitivity study was made, concluding that the parameters having a strong influence on the power profile were the plutonium fraction and composition, the pellet radius and the neutron energy spectrum, which is primarily determined by the moderator-to-fuel ratio. Since the moderator-to-fuel ratio is not adjustable in the FRAPCON input, this was kept roughly constant at a value close to what is a normal average in currently operating light water reactors, yielding a typical LWR spectrum and correspondingly typical power profiles. A separate set of cases was run, simulating the conditions in the Halden Research Reactor. Fuel average temperature and linear heat generation rates had negligible impact on the calculated power profiles. A set of 60 cases was simulated to 70 MWd/kgHM, in which the pellet radius and the plutonium fraction and composition were varied. For every case, the relative power in each radial node was recorded for every burnup step of 1 MWd/kgHM.

### 4.2. Theoretical model

The theoretical model implemented in the power profile subroutine for Th-MOX is similar to that implemented in the current version of the FRAPCON code. First, the local concentration  $N_i(r)$  of each isotope  $i$  is calculated (dependent on the radial position  $r$ ), then the flux  $\phi(r)$  is calculated and finally the power profile, i.e. the normalized local volumetric heat generation  $q'''(r)$  is calculated

by Equation 1, where  $\sigma_{f,i}$  is the fission cross section of isotope  $i$  and  $C$  is a normalization constant.

$$q'''(r) = C \sum_i \sigma_{f,i} N_i(r) \phi(r) \quad (1)$$

The isotopic concentrations in each radial node are calculated by solving a system of coupled ordinary differential equations, known as the Bateman equations, which have the form:

$$\frac{dN_i(r)}{dt} = -\sigma_{a,i} N_i(r) \phi(r) + \sigma_{c,i-1} N_{i-1}(r) \phi(r) \quad (2)$$

where  $i$  is the isotope in question and  $i-1$  is the parent isotope from which the isotope  $i$  is produced by neutron capture (and possible subsequent beta decays, as for example in the case of production of  $^{233}\text{U}$  from  $^{232}\text{Th}$ ).

In the current FRAPCON version, the generation of  $^{239}\text{Pu}$  is treated specially, to account for resonance capture of epithermal neutrons close to the periphery. This is done by using the average  $^{238}\text{U}$  concentration multiplied by a shape function, instead of a radius-dependent concentration. The shape function  $f(r)$  has the form given in Equation 3,

$$f(r) = 1 + p_1 e^{-p_2(R-r)^{p_3}}, \quad (3)$$

where  $R$  is the pellet radius and  $p_i$  are empirically determined parameters. In the new subroutine, similar shape functions are used to account for the epithermal neutron capture in  $^{232}\text{Th}$  and  $^{239}\text{Pu}$ . However, instead of using the function directly in the calculation of the concentration of their respective daughter nuclides  $^{233}\text{U}$  and  $^{240}\text{Pu}$ , the function is multiplied with their microscopic cross sections. This gives effectively the same result in the calculation of the isotopic concentrations, but also allows the neutron flux, and thereby the power profile, to be directly dependent on the capture of epithermal neutrons.

To calculate the neutron flux, the one-group diffusion equation is solved in cylindrical coordinates, assuming that the flux is in steady state, anisotropic and radially symmetrical. In the current FRAPCON version it is assumed that for the purpose of the calculation of the flux, the isotopic concentrations are homogeneous throughout the pellet so that the diffusion equation can be solved analytically, yielding a solution of the form of Bessel functions. This model proved to be too inaccurate for modeling of Th-MOX fuel, since the absorption in Th-MOX fuel is quite strong compared to UOX fuel - the predominant isotopes  $^{232}\text{Th}$  and  $^{239}\text{Pu}$  have larger thermal absorption cross sections (approximately 7.4 barn and 1022 barn respectively [22]) than  $^{238}\text{U}$  and  $^{235}\text{U}$  (2.7 barn and 681 barn [22]).

To maintain the simplicity of the current FRAPCON algorithm, it was decided to continue to use the diffusion approximation. However, by solving the diffusion equation numerically, using a finite difference method, radially varying cross sections of  $^{232}\text{Th}$  and  $^{239}\text{Pu}$  as described above could be

used. The shape functions giving the radial dependence of the microscopic cross sections were empirically adapted by introducing dependence on the pellet outer radius  $R$  and  $N_{Pu-239}$  of the parameters  $p_i$ , introducing some additional parameters. A genetic algorithm was then used as described in Section 4.3, so that the shape functions satisfactorily could compensate for the inaccuracies of the diffusion approximation.

### 4.3. Genetic algorithm

In the above equations, the microscopic cross sections  $\sigma_{a,i}$  and  $\sigma_{c,i}$  and the parameters  $p_i$  are undetermined. Neglecting the energy dependence in the model introduces a need for finding "effective" microscopic cross sections, i.e. constant values of the cross sections that reasonably well reproduce the neutronic behaviour of the modeled system. The complex spectral interactions between the present isotopes, including various shielding effects at different energies, makes it a very difficult task to find these effective cross sections by classical methods. Instead, we employ the pragmatic approach of searching for the set of effective cross sections that best reproduces the observed behaviour of the system, i.e. the reference data generated by the Monte-Carlo simulations described in Section 4.1. The same approach is held for the parameters  $p_i$ , which are inherently empirical.

The number of unknown parameters in this system is large; 10 isotopes are present, giving 20 cross sections ( $\sigma_a$  and  $\sigma_c$ ) to be determined, to which we add 11 parameters  $p_i$  for the shape functions. The total number of unknown parameters is thus 31. Searching for the best solution to a system with a large number of unknowns is a very difficult task using classical optimization methods, for which reason we have chosen to use a genetic algorithm.

A genetic algorithm is a biologically inspired method, in which a *population* of different solutions, referred to as *individuals*, compete to *reproduce*. In this case, each *individual* (set of  $\sigma_{a,i}$ ,  $\sigma_{c,i}$  and  $p_i$ ) is evaluated in terms of how well the simplified theoretical model described in Section 4.2 reproduces the Monte-Carlo generated power profiles. The best *individuals* are then allowed to *reproduce* in the sense that a new generation of *individuals* is generated from them by combining them in a process similar to biological *crossover* of chromosomes. Also a process corresponding to *mutation* has been implemented. The first *population* consisted of 100 *individuals*, i.e. parameter sets, generated as random small variations around measured cross sections from [22] and initial guesses for  $p_i$ .

## 5. PRELIMINARY RESULTS

Using a genetic algorithm as described in Section 4.3, a good set of cross sections and function parameters was found. When the simplified theoretical model described in Section 4.2 was implemented using this set, the Monte-Carlo generated power profiles were reproduced with a mean relative error of 0.67% for all radial nodes and burnup steps. Over 99.8% of the predictions had an error less than 5%. This proves that the theoretical model is a reasonably good description of the system. A separate set of cross sections and function parameters was generated for the operation conditions of the Halden research Reactor.

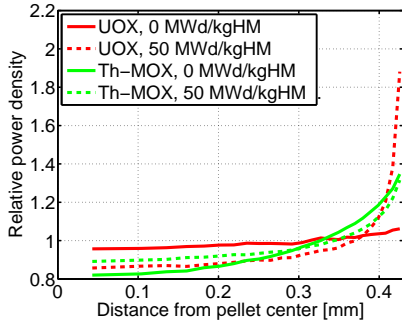


Figure 1: Radial pellet power profiles for UOX and Th-MOX fuel. In the UOX fuel the enrichment is 5% and in the thorium fuel the Pu concentration is 8% with 80%  $^{239}\text{Pu}$ .

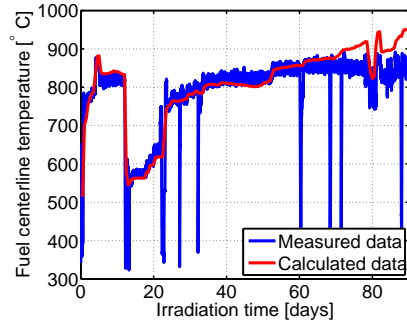


Figure 2: Online measured fuel centerline temperature of Th-MOX rods irradiated in the Halden Research Reactor and the new FRAPCON version's prediction of the same.

In addition to modeling the less homogeneous power generation in fresh fuel, the model captured another interesting feature of Th-MOX fuel, which occurs at higher burnup.  $^{232}\text{Th}$  has a narrower range and a weaker intensity of its resonance capture peaks than  $^{238}\text{U}$ . This will lead to weaker shielding effects and less build up of fissile isotopes in the rim region and thus the power profile will not change as much during irradiation as is the case with UOX fuel, as seen in Figure 1. The reduced generation of a high burnup structure close to the pellet periphery in Th-MOX fuel is likely to have a beneficial impact on fission gas release.

The new FRAPCON version, as it now stands with implementations of Th-MOX thermomechanical property correlations and the new radial pellet profile model, was used to model the behaviour of the Th-MOX pellets which are currently irradiated in the Halden Research Reactor. The result is shown in Figure 2. As can be seen, the code predicts the centerline temperature very well for low burnups but starts to overpredict it after about 60 days. This is probably due to the fact that the burnup dependence of the thermomechanical parameters is not adapted to Th-MOX behaviour yet.

## 6. CONCLUSION AND OUTLOOK

The modified FRAPCON code is currently able to predict the fuel centerline temperature well for fresh Th-MOX fuel under normal operating conditions. The new prediction of the power profiles agrees well with the Monte-Carlo simulations used as reference data to build the model, but validation using experimental data remains to be done. The code does not currently model the changes of the fuel behaviour with burnup, so the burnup dependence of the thermomechanical fuel material properties must be experimentally determined and implemented in the code. The dependence of the thermomechanical properties on deviations from stoichiometry should also be investigated, but may be deemed unimportant given that  $\text{ThO}_2$ -based fuel is likely to be manufactured at and remain very close to stoichiometry.

The work with modifying the FRAPCON code is ongoing. Monte-Carlo simulation output will also be used for modifying the subroutines relating to the generation of fission gases, and when experimental fission gas release data becomes available, a new fission gas release model will also be developed. Burnup dependence of the material parameters will be incorporated in the code, which will be possible when more results, in particular post irradiation data, are available from the "Seven-Thirty" program. The measured online data will also be used for validation of the code.

## ACKNOWLEDGMENTS

The authors would like to thank Klas Jareteg for his assistance with the Serpent simulations. Financial support was given by the Norwegian Research council through the Industrial PhD Programme.

## REFERENCES

- [1] B. A. Lindley and G. T. Parks. "Near-complete transuranic waste incineration in a thorium fuelled pressurised water reactor." *Annals of Nuclear Energy*, **40(1)**: pp. 106 – 115 (2012).
- [2] K. Insulander Björk. "A BWR fuel assembly design for efficient use of plutonium in thorium-plutonium fuel." *Progress in Nuclear Energy*, **65(0)**: pp. 56 – 63 (2013).
- [3] K. Insulander Björk and V. Fhager. "Comparison of thorium-plutonium fuel and MOX fuel for PWRs." In: *Proceedings of Global 2009*. Paper 9449 (2009).
- [4] C. W. Lau *et al.* "Conceptual study on axial offset fluctuations by stepwise power changes in a thorium-plutonium core to improve load-following conditions." *Accepted for publication in Annals of Nuclear Energy* (2014).
- [5] S. S. Drera and K. Insulander Björk. "Thorium fuel production and results from beginning of life irradiation." *Progress in Nuclear Energy*. Article in press (2014).
- [6] K. Geelhood, W. Luscher, and C. Beyer. *FRAPCON-3.4: A Computer Code for the Calculation of Steady-State Thermal-Mechanical Behavior of Oxide Fuel Rods for High Burnup*. Pacific Northwest National Laboratory, P.O. Box 999, Richland, WA 99352. NUREG/CR-7022 (2011).
- [7] M. Verwerft *et al.* *Oxide Fuels: Microstructure and Composition Variations (OMICO)*. Technical Report EUR 23104, European Commission (2007).
- [8] E. Loewen *et al.* "Preliminary frapcon-3th steady-state fuel analysis of ThO<sub>2</sub> and UO<sub>2</sub> fuel mixtures." *Nuclear Technology*, **136(3)**: pp. 261–277. ISSN 0029-5450 (2001).
- [9] T. Kutty *et al.* "Densification behaviour of ThO<sub>2</sub>-PuO<sub>2</sub> pellets with varying PuO<sub>2</sub> content using dilatometry." *Journal of Nuclear Materials*, **312(2-3)**: pp. 224 – 235 (2003).
- [10] J. Belle and R. M. Berman. *Thorium Dioxide: Properties and Nuclear Applications*. Technical Report DOE/NE-0060, Naval Reactors Office, United States Department of Energy (1984).

- [11] I. Cohen and R. Berman. “A metallographic and x-ray study of the limits of oxygen solubility in the  $\text{UO}_2\text{-ThO}_2$  system.” *Journal of Nuclear Materials*, **18(2)**: pp. 77–107 (1966).
- [12] O. Valu *et al.* “The high temperature heat capacity of the  $(\text{Th,Pu})\text{O}_2$  system.” *The Journal of Chemical Thermodynamics*, **68(0)**: pp. 122 – 127 (2014).
- [13] K. Bakker *et al.* “Critical evaluation of the thermal properties of  $\text{ThO}_2$  and  $\text{Th}_{1-y}\text{U}_y\text{O}_2$  and a survey of the literature data on  $\text{Th}_{1-y}\text{Pu}_y\text{O}_2$ .” *Journal of Nuclear Materials*, **250(1)**: pp. 1–12 (1997).
- [14] C. Cozzo *et al.* “Thermal diffusivity and conductivity of thorium-plutonium mixed oxides.” *Journal of Nuclear Materials*, **416(1-2)**: pp. 135–141 (2011).
- [15] L. F. Epstein. “Ideal solution behaviour and heats of fusion from the  $\text{uO}_2\text{-puO}_2$  phase diagram.” *Journal of Nuclear Materials*, **22**: pp. 340–349 (1969).
- [16] F. D. Bruycker *et al.* “The melting behaviour of plutonium dioxide: A laser-heating study.” *Journal of Nuclear Materials*, **416**: pp. 166–172 (2011).
- [17] C. Ronchi and J. P. Hiernaut. “Experimental measurement of pre-melting and melting of thorium dioxide.” *Journal of Alloys and Compounds*, **240**: pp. 179–185 (1996).
- [18] C. Duriez *et al.* “Thermal conductivity of hypostoichiometric low Pu content  $(\text{U,Pu})\text{O}_{2x}$  mixed oxide.” *Journal of Nuclear Materials*, **277(2-3)**: pp. 143 – 158 (2000).
- [19] M. Ali and P. Nagels. “Evaluation of the debye temperature of thorium dioxide.” *Physica Status Solidi B*, **21(1)**: pp. 113–116 (1967).
- [20] R. D. Shannon. “Revised effective ionic radii and systematic studies of interatomic distances in halides and chalcogenides.” *Acta Crystallographica*, **A32**: p. 751 (1976).
- [21] J. Leppänen. *Serpent - a Continuous-energy Monte Carlo Reactor Physics Burnup Calculation Code*. VTT Technical Research Centre of Finland (2012).
- [22] J. Magill and J. Pfennig, Galy. *Karlsruher Nuklidkarte*. European Commission - Joint Research Centre - Institute for Transuranium Elements, 7 edition (2006).

# Paper VIII

**Thermal-mechanical performance modelling of thorium-plutonium oxide fuel and comparison with experimental data**



# Thermal-mechanical performance modelling of thorium-plutonium oxide fuel and comparison with experimental data

Klara Insulander Björk<sup>a,b</sup>, Laura Kekkonen<sup>c,d</sup>

<sup>a</sup>Thor Energy, Sommerrogaten 13-15, NO-0255 Oslo, Norway

<sup>b</sup>Chalmers University of Technology, Department of Applied Physics, Division of Nuclear Engineering, SE-412 96 Göteborg, Sweden

<sup>c</sup>Fortum Power and Heat Ltd, P.O. Box 100, FI-00048 Fortum, Finland

<sup>d</sup>Institute for Energy Technology, Os allé 5, NO-1777 Halden, Norway

---

## Abstract

Thorium-plutonium Mixed OXide (Th-MOX) fuel is considered for use in light water reactors fuel due to some inherent benefits over conventional fuel types in terms of neutronic properties. The good material properties of ThO<sub>2</sub> also suggest benefits in terms of thermal-mechanical fuel performance, but the use of Th-MOX fuel for commercial power production demands that its thermal-mechanical behaviour can be accurately predicted using a well validated fuel performance code. Given the scant operational experience with Th-MOX fuel, no such code is available today.

This article describes the first phase of the development of such a code, based on the well-established code FRAPCON 3.4, and in particular the correlations reviewed and chosen for the fuel material properties. The results of fuel temperature calculations with the code in its current state of development are shown and compared with data from a Th-MOX test irradiation campaign which is underway in the Halden research reactor. The results are good for fresh fuel, and an adjustment of the burnup dependence of the thermal conductivity gives fair agreement also for higher burnup.

*Key words:* Nuclear fuel, thermal-mechanical performance, FRAPCON, thorium, plutonium

---

## 1. Introduction

Thorium-plutonium Mixed OXide fuel (Th-MOX) is considered a promising technology for plutonium incineration in light water reactors [1, 2, 3], and also offers benefits in terms of neutronic [4, 5] properties compared with the traditional fuel types, Uranium OXide (UOX) and Uranium-plutonium Mixed OXide (U-MOX). A research program is currently addressing both the particularities of Th-MOX fuel manufacture and its irradiation behaviour, through a test irradiation in the Halden research reactor [6].

In order for a new nuclear fuel type such as Th-MOX to be licensed for use in a commercially operating nuclear reactor, its material properties and thermal-mechanical behaviour must be well known and predictable for all operation modes of the reactor. These predictions are normally done using a fuel performance

code, in which established correlations for the various property changes are integrated. A modified version of the well-established code FRAPCON 3.4 [7] is being developed for this purpose, and the first phase of this development is described here. The modified version is referred to as FRAPCON-ThMOX, and has been used to model the Th-MOX pellets within the mentioned irradiation program, enabling a comparison between calculated and measured fuel temperatures.

Similar work was conducted previously in connection with the OMICO project [8], for prediction of the behaviour of the experimental fuel which was irradiated within the scope of this project. We bring this work onward by using some data unavailable at the time of this study, and by comparison of calculated temperatures with experimental data. A version of FRAPCON for modelling of thorium-uranium mixed oxide fuel has also been created by Long et al. [9]. Our work has to a large extent been guided by their methodology. Other relevant studies include: Work on a more generalized FRAPCON-based code ongoing at MIT [10], adaptations of the fuel performance code TRANSURANUS

---

\*Corresponding author

Email address: klara.insulander@scatec.no (Klara Insulander Björk)

Preprint submitted to Journal of Nuclear Materials

April 8, 2015

to simulations of thorium-containing fuels is ongoing at Technische Universität München, and the National Nuclear Laboratory in the UK are developing a thorium-capable version of the fuel performance code ENIGMA.

For the purpose of modifying FRAPCON 3.4 for use with Th-MOX fuel, the literature on the material properties of thorium dioxide and mixtures with plutonium dioxide was reviewed and appropriate data was incorporated into FRAPCON-ThMOX. A previous review of the literature data was done in 1997 by Bakker et al. [11], concluding that very little was known at that time. Several new findings have been published since this review was made [12, 13], in particular regarding the important thermal conductivity [14]. However, for some properties, data is still lacking and in such cases a best estimate is suggested.

Since Th-MOX fuel also differs from UOX and U-MOX fuel with regard to neutronic properties, the power distribution within the fuel pellet is expected to be different, and this affects the temperature profile. To account for this, a new subroutine for prediction of power profiles has also been developed [15].

Some properties of the fuel material will change with the burnup of the fuel. Quantitative assessments of these dependencies are however very scarce. As the above-mentioned Th-MOX irradiation experiment proceeds, information is becoming available to make such assessments, but for the time being, the burnup dependence of most of the physical properties is left as they are in FRAPCON 3.4.

A brief account on the working mode of the FRAPCON code is given in Section 2. In Sections 3 - 9, we describe the correlations chosen for the material properties and behaviours which have been incorporated in the code. The subroutine for power profile prediction is described in Section 10 and a comparison between the preliminary calculated results and the experimental data is shown and discussed in Section 11. Comments on the future development and validation of the code are provided in Section 12. Finally, conclusions are drawn in Section 13.

## 2. The FRAPCON code

FRAPCON 3.4 iteratively calculates temperature, pressure and deformation of a light-water reactor fuel rod during long-term burnup, thereby describing phenomena such as heat conduction through the fuel and cladding to the coolant, fuel-cladding mechanical interaction and fission gas release. For this purpose, the thermal-mechanical properties of fuel and cladding materials are incorporated in the code through calls to spe-

cific subroutines, each calculating a single property. In this work, the subroutines relating to the cladding material properties are left unchanged.

The fuel rod is subdivided into nodes in the axial direction, and the total heat generation in the fuel at any axial node is normalized to the local LHGR specified by user input. Each axial node is further subdivided into concentric cylindrical radial nodes with a finer spacing towards the pellet periphery. The radial distribution of the heat generation is assumed to be proportional to the local fission rates, which are calculated as described in Section 10.

At each axial node, the temperature is calculated for every radial node using the heat conduction equation with the normalized local heat generation as the source term. The temperature dependent material properties are determined using the locally calculated temperature of the fuel material. The temperature, denoted  $T$  in the following, is always assumed to be given in units of Kelvin.

The state of the fuel rod is determined for each time step by iterative calculations which can be summarized as follows:

1. The fuel temperature and dimensional changes are calculated, then the resulting cladding mechanical response and ultimately the temperature drop over the pellet-cladding gap, which in turn affects the fuel temperature. This sequence is iterated until the pellet-cladding gap temperature drop converges. This is the only step essentially affected by the currently performed code modifications.
2. Local power, burnup and cladding properties are calculated and step 1 is carried out for each axial node.
3. The resulting gas release into the rod's free gas volume (total from all nodes) is calculated. An updated FGR subroutine would affect also this step. Since the FGR affects the pellet-cladding gap temperature drop in all nodes, steps 1 and 2 are repeated until the rod internal pressure converges.
4. The state of the fuel rod resulting from step 3 is used as input to the next time step.

The fuel material is specified by user input in terms of, most importantly, (a) porosity, which in the following will be denoted  $P$ , (b) the plutonium dioxide weight fraction and (c) the oxygen to metal (O/M) ratio. The plutonium dioxide weight fraction is recalculated to give the molar plutonium dioxide fraction, which we denote  $y$ . We will let  $x$  denote the negative deviation from stoichiometry, i.e. from O/M = 2.00. Since neither  $\text{ThO}_2$  nor  $\text{PuO}_2$  become hyperstoichiometric,  $x$

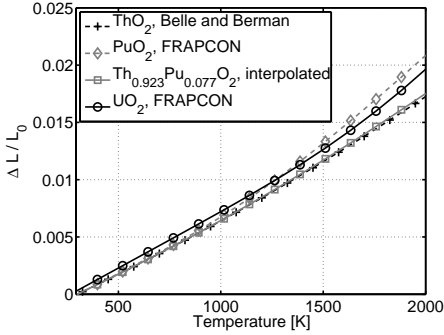


Figure 1: Linear thermal expansion of relevant actinide oxides and the irradiated Th-MOX fuel composition,  $\text{Th}_{0.923}\text{Pu}_{0.077}\text{O}_2$ .

will always be a positive number [16]. It should be noted that FRAPCON 3.4 does not track stoichiometry changes, but only uses the stoichiometry value that is input from initial conditions, which need not be exactly 2.00. We will nevertheless discuss the stoichiometry dependence of the material properties, since it is foreseen that this study will be complemented with further studies in which stoichiometry is treated with more detail.

In order to improve readability in formulae,  $\text{Th}_{1-y}\text{Pu}_y\text{O}_2$  will sometimes be simplified to  $(\text{Th}, \text{Pu})\text{O}_2$ .

### 3. Thermal expansion

#### 3.1. Thermal Expansion of $\text{ThO}_2$

The linear thermal expansion of  $\text{ThO}_2$  is treated by several sources [11, 17, 18, 19, 20] which all agree well. In FRAPCON, the thermal expansion is calculated in terms of percent linear dimensional change,  $\Delta L/L_0$

The correlation recommended by Belle and Berman [20] and shown in Equation 1 is adopted in preference to the others, since it is based on several different data sets and claims the largest temperature interval of validity,  $150 \text{ K} < T \lesssim 2500 \text{ K}$ . This correlation is plotted in Figure 1.

$$\left(\frac{\Delta L}{L_0}\right)_{\text{ThO}_2} = -0.243 \cdot 10^{-2} + 7.84 \cdot 10^{-6} T + 10.0 \cdot 10^{-10} T^2. \quad (1)$$

The correlation used for the thermal expansion of  $\text{PuO}_2$  is unchanged from FRAPCON 3.4.

#### 3.2. Thermal expansion of $\text{Th}_{1-y}\text{Pu}_y\text{O}_2$

Due to the fact that  $\text{ThO}_2$  and  $\text{PuO}_2$  form a nearly ideal solid solution [11, 20], the lattice parameter of  $\text{Th}_{1-y}\text{Pu}_y\text{O}_2$  can to good approximation be derived from the lattice parameters of  $\text{ThO}_2$  and  $\text{PuO}_2$  by simple linear interpolation. Such interpolation across a compositional range is often referred to as Vegard's law [21]. This has also been experimentally confirmed [22]. The lattice parameter of  $\text{ThO}_2$  at Standard Temperature and Pressure (STP),  $a_{0,\text{ThO}_2}$ , is quoted by several sources which all agree well [11, 20, 23]. We use the value  $a_{0,\text{ThO}_2} = 5.597 \text{ \AA}$ , which is recommended by Bakker et al. [11]. The same applies to the lattice constant at STP for  $\text{PuO}_2$ ,  $a_{0,\text{PuO}_2}$ , which is given as  $5.396 \text{ \AA}$  [23, 24, 25].

Using Vegard's law, we can calculate the lattice parameter for  $\text{Th}_{1-y}\text{Pu}_y\text{O}_2$  at any temperature, and derive the linear thermal expansion as shown in Equation 2. This equation is implemented in the FRAPCON subroutine `fthexp`.

$$\begin{aligned} \left(\frac{\Delta L}{L_0}\right)_{(\text{Th}, \text{Pu})\text{O}_2} &= \frac{a_{(\text{Th}, \text{Pu})\text{O}_2}(T)}{a_{0,(\text{Th}, \text{Pu})\text{O}_2}} - 1 = \\ &= \frac{y a_{0,\text{PuO}_2} \left(\left(\frac{\Delta L}{L_0}\right)_{\text{PuO}_2} + 1\right) + (1-y) a_{0,\text{ThO}_2} \left(\left(\frac{\Delta L}{L_0}\right)_{\text{ThO}_2} + 1\right)}{y a_{0,\text{PuO}_2} + (1-y) a_{0,\text{ThO}_2}} - 1 \quad (2) \end{aligned}$$

The lattice parameter of  $\text{PuO}_{2-x}$  depends on the stoichiometry [24], and also that of  $\text{Th}_{1-y}\text{U}_y\text{O}_{2-x}$  [21] and  $\text{U}_{1-y}\text{Pu}_y\text{O}_{2-x}$  [26]. To the small extent that  $\text{ThO}_2$  becomes non-stoichiometric, this also affects the lattice parameter, according to the single measurement that could be found in the open literature; reduction of  $\text{ThO}_2$  to  $\text{ThO}_{1.997}$  caused a decrease in the unit cell size by 0.5% [20]. No measurements could however be found of the stoichiometry dependence of the  $\text{Th}_{1-y}\text{Pu}_y\text{O}_{2-x}$  lattice parameter. Since the stoichiometry is not expected to have a significant impact on the thermal expansion behaviour and the lattice parameter in itself is only used very indirectly (see Section 4), the stoichiometry dependence is currently left unaddressed.

The thermal expansion is assumed to have no dependence on burnup in FRAPCON 3.4, an assumption which is kept in the modified version. The actual density of the fuel, however, depends of course on burnup, due to the effect of irradiation swelling, see Section 9.

### 4. Thermal conductivity

The thermal conductivity of  $\text{Th}_{1-y}\text{Pu}_y\text{O}_2$ ,  $\kappa_{(\text{Th}, \text{Pu})\text{O}_2}$ , was most recently measured by Cozzo et al. [14], who fitted their data with an expression of the form  $\kappa =$

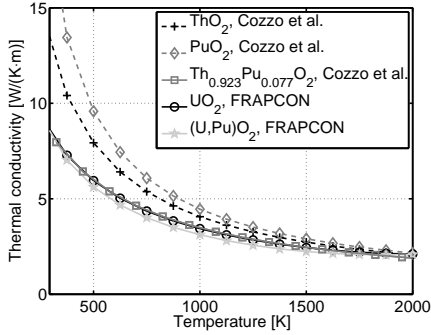


Figure 2: Thermal conductivity of relevant actinide oxides and mixtures thereof, for 95% density.

$1/(A + BT)$ , where the  $A$  coefficient was confirmed to depend on the plutonium fraction, and the  $B$  coefficient showed no such dependence. The fitted relation is shown in Equation 3. It applies to material with a porosity  $P = 5\%$ , i.e. with a density 95% of the theoretical density (TD), and is valid in the temperature interval 500 K - 1500 K. The correction factor used to account for the porosity dependence of the thermal conductivity is left unchanged.

$$\kappa_{(Th,Pu)O_2} = \frac{1}{6.07 \cdot 10^{-3} + 0.57y - 0.59y^2 + 2.4 \cdot 10^{-4}T} \quad (3)$$

The thermal conductivity as calculated by this expression is plotted in Figure 2, with  $y = 7.7\%$ , which corresponds to the composition currently being tested in the Halden research reactor (7.9 wt% PuO<sub>2</sub>), and for  $y = 0$  and  $y = 1$  (pure ThO<sub>2</sub> and PuO<sub>2</sub> respectively). The expressions for the thermal conductivity of 95% dense UO<sub>2</sub> and U-MOX used in FRAPCON 3.4 are also plotted for comparison. The thermal conductivity of pure PuO<sub>2</sub> as calculated by this expression is higher than previously published data on the thermal conductivity of PuO<sub>2</sub> [14], however, since it is expected that the Pu fraction in Th-MOX used as nuclear fuel for LWRs will not be larger than 30%, this discrepancy is deemed to have low relevance to the correlation for candidate Th-MOX compositions.

A different correlation was developed within an IAEA coordinated research project [27], based on measurements with up to 10 wt% PuO<sub>2</sub>. Since the Pu fraction in Th-MOX for LWRs will often exceed 10 wt%, the correlation by Cozzo et al. is preferred since the

measurement series and data fit also includes a plutonium fraction of 30%, making the correlation more suitable for calculation of the conductivity in the composition range 10-30% Pu.

The thermal conductivity of pure ThO<sub>2</sub> is approximately 10% higher than that of pure UO<sub>2</sub> at typical operating temperatures around 1000 K. However, when another oxide is added, such as PuO<sub>2</sub>, this component acts as an impurity, increasing phonon scattering and thus decreasing the conductivity. The conductivity decreases rapidly with increasing Pu fraction up to about 50% PuO<sub>2</sub> and then increases again for higher Pu fractions. For U-MOX fuel, however, the correlation implemented in FRAPCON ignores any dependence on the Pu fraction, with the limitation that it can only claim to be valid for fuels with a Pu fraction between 3% and 15%. One justification for this apparently drastic approximation is that the majority UOX component of U-MOX fuel easily becomes hyperstoichiometric, which affects the conductivity so strongly that the effect of varying Pu fraction becomes negligible in comparison [28]. Neither ThO<sub>2</sub> nor PuO<sub>2</sub> readily become hyperstoichiometric [29], so stoichiometry changes in the (Th,Pu)O<sub>2</sub> mixture plays a minor role in determining the bulk thermal conductivity for these fuel ceramics. However, the effect of Pu fraction variation is much stronger for (Th,Pu)O<sub>2</sub> than for (Th,U)O<sub>2</sub>. This is primarily due to the fact that the reduction of the thermal conductivity depends on the relative mass difference and the relative lattice parameter difference between the two components [14]. These differences are larger for the (Th,Pu)O<sub>2</sub> case than for the (U,Pu)O<sub>2</sub> case.

It is also noted that the thermal conductivity of UO<sub>2</sub> is expected to be higher than that of ThO<sub>2</sub> at high temperatures (above approximately 2000 K). At these temperatures, the heat conduction by electrons starts to play a significant role, and the higher electron mobility in the UO<sub>2</sub> lattice gives a higher electronic contribution to the thermal conductivity compared with the thorium analog [30]. Since these temperatures are far above the recorded temperatures in the current irradiation experiment, above normal LWR fuel operating temperatures, and also above the temperature interval of validity for the Th-MOX thermal conductivity correlation developed by Cozzo et al. [14], this aspect is of minor importance for the current study and is not factored in.

#### 4.1. Correction for deviation from stoichiometry

Duriez et al. [28] studied the thermal conductivity of hypostoichiometric U<sub>1-y</sub>Pu<sub>y</sub>O<sub>2-x</sub> and found a linear stoichiometry dependence of the term  $A$  discussed

above, so a stoichiometry dependent term was introduced, yielding the expression given in Equation 4.

$$\kappa = \frac{1}{A(y) + BT} = \frac{1}{A_{2,00}(y) + xC + BT} \quad (4)$$

Whereas this stoichiometry correction coefficient  $C$  could be experimentally determined for  $U_{1-y}Pu_yO_{2-x}$  in the work by Duriez et al., it has to be calculated for  $Th_{1-y}Pu_yO_{2-x}$  drawing on the scarce physical data that is available, using the expression shown in Equation 6.

$$\begin{aligned} A_{2-x} &= A_{2,00} + xC = \\ &= A_{2,00} + x \frac{\pi^2 \theta_D \bar{m}}{3Eh} \left( \frac{a_{Th,PuO_2}}{a_{ThO_2}} \right)^2 \left( - \left( \frac{m_{O^{2-}}}{\bar{m}} \right)^2 + \right. \\ &\quad \left. + \frac{\epsilon}{\bar{r}} \left( 2(r_{Pu^{3+}}^2 - r_{Pu^{4+}}^2) + (r_{O_v}^2 - r_{O^{2-}}^2) \right) \right) \frac{1}{3} \end{aligned} \quad (5)$$

This formulation of the stoichiometry correction factor  $C$  is based on the reasoning by Duriez et al. [28]. The parameter  $\epsilon$  was estimated to 7.5 by Cozzo et al. [14], the ionic radii  $r_i$  are taken from [31] ( $O_v$  denotes an oxygen vacancy, the radius of which was estimated by Ohmichi et al. [32]) and the lattice parameter  $a_{ThPuO_2}$  and Young's modulus  $E$  as calculated by the FRAPCON subroutines `fthexp` and `felmod` respectively.  $h$  denotes the Planck constant,  $m_{O^{2-}}$  the mass of the  $O^{2-}$  ion,  $\bar{m}$  the mean atomic mass of the lattice and  $\bar{r}$  the mean ionic radius. The Debye temperature is calculated by Neumann-Kopp's rule using  $\theta_{D_{ThO_2}} = 259$  K [33] and  $\theta_{D_{PuO_2}} = 239$  K [34].

There are large uncertainties in this calculation, the most significant one being that of the parameter  $\epsilon$ , which was estimated as a data fitting parameter by Cozzo et al. Also, the value of the ionic radius of the oxygen vacancy is based on measurements made on  $UO_2$ , which is likely not accurate for  $ThO_2$ , but is used as a best estimate. Above all, it must be remembered that this term was introduced to explain a behaviour which was observed for  $U_{1-y}Pu_yO_{2-x}$ , and may not describe  $Th_{1-y}Pu_yO_{2-x}$  behaviour well. Experimental assessment is necessary for understanding stoichiometry effects on the thermal conductivity of  $Th_{1-y}Pu_yO_{2-x}$ .

#### 4.2. Burnup dependence

The burnup dependence of the thermal conductivity is introduced in FRAPCON 3.4 as an additive term  $f(Bu)$  in the denominator of the expression for the thermal conductivity shown in Equation 6, where  $Bu$  is the burnup. The numerical value of this term is empirically derived. As explained in Section 11, an increase of this factor provided good agreement with the measured fuel temperatures.

$$\kappa = \frac{1}{A + BT + f(Bu)} \quad (6)$$

### 5. Heat capacity and enthalpy

Enthalpy increments of several  $Th_{1-y}Pu_yO_2$  compositions were recently measured by Válu et al. [13]. The experimental results were compared to values obtained by linear interpolation between the corresponding values for  $ThO_2$  and  $PuO_2$ , which in this context is referred to as Neumann-Kopp's rule. The agreement was found to be good, so we adopt this way of calculating both the enthalpy increments  $\Delta H$  and its derivative with respect to temperature, which is the heat capacity  $C_P$ . The calculation of  $\Delta H$  and  $C_P$  is implemented in the subroutines `fenth1` and `fcP` respectively.

No assessment has, to our knowledge, been made of the stoichiometry dependence of the enthalpy and heat capacity of  $Th_{1-y}Pu_yO_{2-x}$ . FRAPCON 3.4, however, introduces a stoichiometry dependence in the enthalpy and heat capacity of  $PuO_{2-x}$ . The currently used correlation for the heat capacity of  $PuO_{2-x}$ , including its stoichiometry dependence, is left unchanged. Both  $\Delta H$  and  $C_P$  are assumed to be independent on burnup in FRAPCON 3.4 as well as FRAPCON-ThMOX.

#### 5.1. Heat capacity of $ThO_2$

Several measurements of enthalpy increments of  $ThO_2$  have been made in the past [11] and these have been used as a basis for developing correlations which all agree acceptably well at temperatures typical for LWR fuel under normal operation. We adopt an expression given by Belle and Berman [20] which has the same form as the expression for the  $PuO_{2-x}$  heat capacity used in FRAPCON, but excluding the term which expresses an electronic contribution to the heat capacity which is not present in  $ThO_2$  [35]. For  $ThO_2$ ,  $\theta = 408.14$  K.

$$C_P = \frac{260.1\theta^2 e^{\frac{\theta}{T}}}{T^2 \left( e^{\frac{\theta}{T}} - 1 \right)^2} + 3.65 \cdot 10^{-2} T \quad (7)$$

#### 5.2. Enthalpy increments of $ThO_2$ and $PuO_2$

The enthalpy increments of  $ThO_2$  are calculated using Eq. 8, which is the integral with respect to temperature of Eq. 7. The correlation for  $PuO_2$  is left unchanged.

$$\Delta H_T = H_T - H_{T_{ref}} = \frac{260.1\theta^2 e^{\frac{\theta}{T}}}{T^2 \left( e^{\frac{\theta}{T}} - 1 \right)^2} + 3.65 \cdot 10^{-2} T - H_{T_{ref}} \quad (8)$$

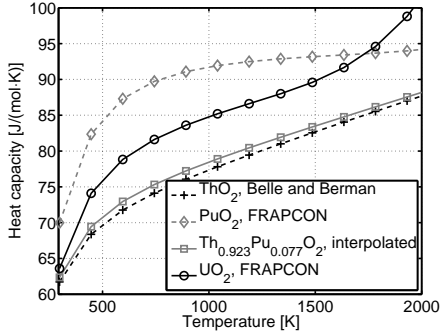


Figure 3: Heat capacity of relevant actinide oxides and  $\text{Th}_{0.923}\text{Pu}_{0.077}\text{O}_2$ .

## 6. Elastic properties

FRAPCON 3.4 assumes the fuel pellet to be rigid, i.e. fuel dimensional changes are only modelled using initial densification, thermal expansion, irradiation swelling and relocation. Thus, the subroutines calculating the Young's modulus and the Poisson ratio are not called in FRAPCON 3.4. As mentioned in the discussion on the stoichiometry correction of the thermal conductivity, the Young's modulus is used in FRAPCON-ThMOX if the fuel is non-stoichiometric, so a modified subroutine for calculation of a best estimate of the Young's modulus for  $\text{Th}_{1-y}\text{Pu}_y\text{O}_{2-x}$  is needed. Also a remark on the Poisson ratio is made, although the corresponding subroutine, `fpoir`, is not called in FRAPCON-ThMOX.

### 6.1. Young's Modulus of $\text{ThO}_2$

The Young's modulus of  $\text{ThO}_2$ ,  $E_{\text{ThO}_2}$ , for temperatures  $298 \text{ K} < T < 1300 \text{ K}$  is given by Equation 9, according to Belle and Berman [20].

$$E_{\text{ThO}_2} = 2.491 \cdot 10^{11} (1 - 2.21P) (1.0230 - 1.405 \cdot 10^{-4} e^{\frac{181}{T}}) \quad (9)$$

### 6.2. Young's Modulus of $\text{Th}_{1-y}\text{Pu}_y\text{O}_{2-x}$

No measurements of the Young's modulus of  $\text{Th}_{1-y}\text{Pu}_y\text{O}_2$  could be found in the literature, and no temperature dependent measurements seem to have been performed on pure  $\text{PuO}_2$ . In FRAPCON 3.4, however, the Young's modulus is corrected for the addition of  $\text{PuO}_2$  by multiplying the value for  $\text{UO}_2$  with a factor

$(1 + 0.15y)$ , where the constant 0.15 is empirically deduced. This rule is applied over the entire temperature range. At standard temperature and pressure, the values calculated by this rule agree well with the values calculated by linear interpolation of the Young's moduli of  $\text{UO}_2$  and  $\text{PuO}_2$  as given by Sobolev [23] (233.4 GPa and 268.4 GPa respectively). Hence, we suggest using the same approach for  $\text{Th}_{1-y}\text{Pu}_y\text{O}_2$ . The Young's modulus of  $\text{PuO}_2$  is 2.84% larger than that of  $\text{ThO}_2$  at standard temperature and pressure (261 GPa [23]), so the Young's modulus of  $\text{ThO}_2$  is modified for addition of  $\text{PuO}_2$  by multiplication with a factor  $(1 + 0.0284y)$ .

To the small extent that  $\text{ThO}_2$  becomes hypostoichiometric, this affects the Young's modulus quite strongly: According to one measurement [20], the reduction of  $\text{ThO}_2$  to  $\text{ThO}_{1.997}$  decreased the Young's modulus by 9%. The addition of (possibly non-stoichiometric)  $\text{PuO}_2$  however introduces the possibility for the presence of a second phase in the material, for which the elastic properties may be different. The elastic properties of the bulk material are then somewhere between those of the two phases [36]. Lacking any data on this, we leave the stoichiometry dependence of the Young's modulus as it is currently expressed in FRAPCON 3.4, i.e. by multiplication with a factor  $e^{-1.75x}$ .

The complete expression for the Young's modulus of  $\text{Th}_{1-y}\text{Pu}_y\text{O}_2$  is shown in Equation 10 and implemented in the FRAPCON subroutine `fe1mod`.

$$E_{(\text{Th,Pu})\text{O}_2} = E_{\text{ThO}_2} (1 + 0.0284y) e^{-1.75x} \quad (10)$$

The burnup dependence of the Young's modulus is negligible [37], and no burnup dependence is implemented neither in FRAPCON 3.4 nor in FRAPCON-ThMOX.

### 6.3. Poisson Ratio of $\text{Th}_{1-y}\text{Pu}_y\text{O}_2$

The unitless Poisson ratio  $\nu$ , for randomly oriented cubic polycrystalline materials that behave isotropically on a macroscopic scale, equals  $E/2G - 1$  where  $G$  is the shear modulus. Since the Young's modulus and the shear modulus behave comparably with regard to temperature for  $\text{ThO}_2$  [20] the Poisson ratio is taken to be independent on temperature for  $\text{ThO}_2$ . This is also the case for  $\text{U}_{1-y}\text{Pu}_y\text{O}_2$  [37], so we assume the approximation to hold well for  $\text{Th}_{1-y}\text{Pu}_y\text{O}_2$  too.

Sobolev [23] gives the Poisson ratios of both  $\text{ThO}_2$  and  $\text{PuO}_2$ , which have the same numerical value; 0.28. This value can thus be used for all temperatures and compositions. It is slightly lower than the corresponding value for  $\text{UO}_2$ , 0.316, indicating a slightly higher

dimensional stability of  $(\text{Th,Pu})\text{O}_2$ . The effect of stoichiometry or burnup on the Poisson's ratio has, to our knowledge, not been assessed, but we expect that it is similar for the Young's modulus and the shear modulus, thus leaving the Poisson ratio unaffected.

## 7. Melting points

The melting point of pure  $\text{ThO}_2$  was determined by Ronchi and Hiernaut [38] to be 3651 K. This value is also recommended by both Bakker et al. [11] and Sengupta [27]. The melting point of pure  $\text{PuO}_2$  was measured by Bruycker et al. [39] to be 3017 K, which is significantly higher than previously published results [40, 41, 42]. This difference is attributed to undesired chemical reactions in the  $\text{PuO}_2$  samples during the previous measurements.

According to Epstein [43], systems such as  $\text{Th}_{1-y}\text{Pu}_y\text{O}_2$ , which form a continuous series of ideal solid solutions, have a lenticular phase diagram, i.e. the solidus and liquidus temperatures are not identical for any given composition except for the end members. The system is then determined by Equations 11 and 12.

$$y_l = \frac{1 - t_1}{t_2 - t_1} \quad (11)$$

$$y_s = y_l t_2, \quad (12)$$

where  $t_i = e^{3(1-T_i/T)}$ ,  $y_l$  and  $y_s$  are the atomic Pu fractions in the case of the liquidus and solidus temperatures respectively and  $T_i$  is the melting point of  $\text{ThO}_2$  ( $i = 1$ ) or  $\text{PuO}_2$  ( $i = 2$ ). In order to compute the solidus and liquidus temperatures for a certain composition, the solution to this system was approximated by a polynomial expression, given in Equation 14.

$$T_s = -34.86y^3 + 233.1y^2 - 832.3y + 3651 \quad (13)$$

$$T_l = -99.54y^3 - 24.59y^2 - 509.7y + 3651$$

Here,  $T_s$  is the solidus temperature,  $T_l$  is the liquidus temperature and  $y$  is the atomic Pu fraction. This expression is plotted in Figure 4, together with the FRAPCON 3.4 model for  $\text{U}_{1-y}\text{Pu}_y\text{O}_2$ . The value used for the melting point of pure  $\text{PuO}_2$  in FRAPCON 3.4, 2373 K, is considerably lower than the one measured by Bruycker et al. and used for modeling  $\text{Th}_{1-y}\text{Pu}_y\text{O}_2$ .

Recent measurements by Böhler et al. [12] on  $\text{Th}_{1-y}\text{Pu}_y\text{O}_2$  show that the phase diagram does not agree with the expressions assumed by Epstein [43], but has a minimum solidus temperature at a Pu fraction around

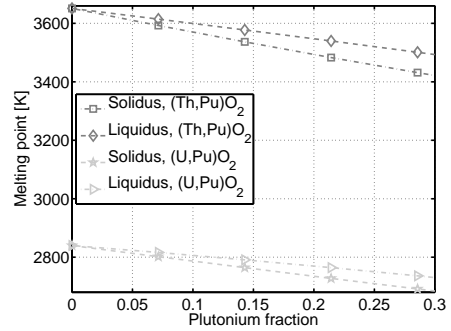


Figure 4: Solidus and liquidus temperatures of  $\text{Th}_{1-y}\text{Pu}_y\text{O}_2$  and  $\text{U}_{1-y}\text{Pu}_y\text{O}_2$ .

95%. A series of melting point measurements on  $\text{PuO}_2$ -rich mixtures of  $\text{PuO}_2$  and  $\text{ThO}_2$  was made by Freshley and Mattys [44], which suggests that such a minimum might indeed be present. Also, recent measurements [45] on  $\text{U}_{1-y}\text{Pu}_y\text{O}_2$  indicate that the phase diagram of that mixture has a minimum solidus temperature at Pu fraction somewhere between 50% and 80%. However, Equation 14 agrees well with the data points obtained by Böhler et al. [12] for Pu fractions at and below 8% Pu, and also with their data fit up to about 30% Pu, which is well above the expected Pu fraction in Th-MOX fuel for LWR applications.

The work of Bruycker et al. clearly indicates that the melting point depends on stoichiometry such that any deviation from  $\text{O}/\text{M} = 2.00$  leads to a lower melting point. Their analysis is difficult to transfer to the case of  $\text{Th}_{1-y}\text{Pu}_y\text{O}_{2-x}$ , so for the moment, the stoichiometry dependence is left out of the correlation. The melting point is assumed to be independent on stoichiometry in FRAPCON-ThMOX as well as in FRAPCON 3.4.

The melting point is calculated in FRAPCON 3.4 as the solidus temperature, minus a term proportional to the fuel burnup, to factor in a number of ceramic crystal damage mechanisms. Lacking any data to support a change in this term, it is maintained in FRAPCON-ThMOX.

### 7.1. Heat of fusion

The heat of fusion  $\Delta H$  for  $\text{ThO}_2$  and  $\text{PuO}_2$  can be estimated from their respective melting points by using Richard's rule, stated in Equation 14 [43, 39].

$$\Delta H = NRT_M \quad (14)$$

Here,  $R$  is the gas constant,  $T_M$  is the melting point and  $N$  is the number of atoms in the molecular unit, i.e. 3 for the actinide dioxides. This expression for the heat of fusion assumes ideal behaviour of the material and is thus only indicative, but the results agree well with previously published values of the heat of fusion for  $\text{PuO}_2$  [39]. The agreement is good also for  $\text{UO}_2$  [42]. Lacking any measured data for  $\text{ThO}_2$ , we assume that the approximation holds well for this material too. Linear interpolation is used for determining the heat of fusion for  $\text{Th}_{1-y}\text{Pu}_y\text{O}_{2-x}$  fuel ceramic mixtures.

The correlations for the melting point and the heat of fusion are implemented in the subroutine `phyprp`.

## 8. Emissivity

The emissivity of the fuel material is used for the calculation of radiative heat transport over the pellet-cladding gap. This parameter has negligible impact on calculated results for all normal applications of the code. Only for very large gap sizes and poor gas conductivity does the emissivity play an important role. Furthermore, the few measurements of the emissivity of  $\text{ThO}_2$  and mixed oxides which could be found in the literature [20] indicate a strong dependence on the composition of the mixture. This would be interesting to explore in more detail in separate studies, however, for code development purposes the emissivity correlation is left as it is currently implemented in the subroutine `femiss` in FRAPCON 3.4. The correlation for the emissivity  $\epsilon$  does not include any dependence on stoichiometry or burnup.

## 9. Irradiation Swelling

Measurements of irradiation swelling of  $\text{Th}_{1-y}\text{Pu}_y\text{O}_2$  are scarce. One assessment was made within the Thorium-Cycle project [46], in which a  $\text{Th}_{0.89}\text{Pu}_{0.11}\text{O}_2$  sample was irradiated. At a burnup of 45 MWd/kgHM, the radial and axial swelling was 3.6% and 5.6% respectively, which is larger than the swelling of the corresponding UOX fuel in the same experiment. Measurements of axial swelling have also been published in a fast reactor fuel context [47], where it is stated that 16  $\text{Th}_{0.65}\text{Pu}_{0.35}\text{O}_{1.95}$ -pins had an average length increase of 2.5 mm. Without knowledge of the total pin length or the burnup, this number is however difficult to interpret. The irradiation swelling of  $\text{Th}_{1-y}\text{Pu}_y\text{O}_2$  cannot be deduced from online measurements from the ongoing test irradiation, but will be possible from post irradiation examination.

Given the very scarce measurements, we leave the irradiation swelling subroutine `fswell` unchanged until more supporting data has been collected.

## 10. Radial pellet power profiles

Power is not generated homogeneously in the fuel pellet, with the important consequence that the fuel material in the different radial nodes will have different burnup and hence different material properties. In addition, the inhomogeneous heat generation directly affects the temperature profile in the pellet. The continuous-energy Monte Carlo reactor physics burnup calculation code *Serpent* [48] was used to simulate the life of the respective fuel types in order to quantify these differences.

The differences in neutronic properties between Th-MOX and UOX fuel depend partly on the high thermal absorption cross section of Th-232, combined with the large absorption resonances in some of the Pu isotopes. The higher thermal absorption results in a more pronounced self shielding effect for thermal neutrons, causing a power profile in the Th-MOX pellet which is more peaked towards the periphery at the beginning of life, see Figure 5.

The production of new fissile isotopes (U-233 in the Th-MOX case and Pu-239 in the UOX case) also differs between the fuel types. The narrow resonance region of Th-232, with comparatively small capture resonances, causes a weaker self shielding of epithermal neutrons compared to UOX fuel, so that conversion takes place relatively homogeneously throughout the pellet, resulting in an increase of the relative power centrally in the pin, as can be seen in Figure 5.

In UOX fuel, the conversion of U-238 to Pu-239 takes place close to the periphery of the pellet, resulting in a very high relative power generation in that region towards the end of life. This has the adverse effect that the local burnup becomes very high, severely degrading the local material structure. This effect is sometimes referred to as the rim effect. Based on the observed differences in the power profiles, it can be expected that this effect will be much less pronounced for Th-MOX fuels. This finding could be significant on the larger scheme of assessing relative merits of plutonium fuel strategies, but firm conclusions will have to await experimental confirmation of this hypothesis.

The differences in power profiles between Th-MOX and UOX have been taken into account by modification of appropriate subroutines in FRAPCON, see Insulander Björk and Fredriksson [15]. The main difference with respect to FRAPCON 3.4 is that appropriate cross

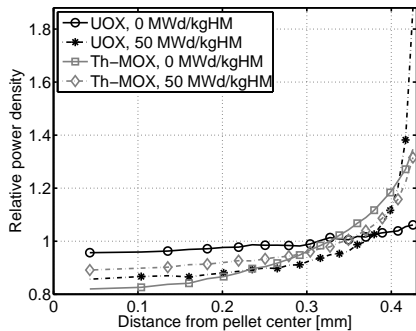


Figure 5: Radial pellet power profiles for UOX and Th-MOX fuel. In the UOX fuel the enrichment is 5% and in the Th-MOX fuel the Pu fraction is 8% with 80%  $^{239}\text{Pu}$ .

sections have been integrated into the relevant subroutine and that the diffusion equation is solved numerically in order to account for radial variations in the concentrations of heavy metal isotopes.

## 11. Early results

### 11.1. Irradiation experiment

The irradiation experiment in the Halden research reactor comprises two fuel rods with Th-MOX fuel pellets (*ThMOX-1* and *ThMOX-3*) and a UOX reference rod (*UOX-6*). The specifications of these pellets are summarized in Table 1. There were eight Th-MOX fuel pellets available at the start of the experiment, these having been manufactured at the Institute for Transuranium Elements (ITU) in Germany as part of the joint European "OMICO" project [8]. Four Th-MOX pellets are in each of the Th-MOX rods. The remaining pellets are composed of 42%  $\text{ThO}_2$  and 58%  $\text{UO}_2$  (enriched to 20%), a composition which was chosen to minimize the axial heterogeneity of the macroscopic cross sections (and given material availabilities when the experimental fuel rods were constructed). The density of the  $\text{Th}_{0.42}\text{U}_{0.58}\text{O}_2$  material was initially measured to 94% of TD, however, it underwent very high densification early in the irradiation and so the density was re-measured on remaining un-irradiated pellets, and found to be about 80% of TD. One rod, *ThUOX-5*, is composed of only this material.

The centerline temperature of each rod during irradiation is measured by means of a thermocouple inserted

into a hole extending along the central axis of the uppermost six pellets in each fuel stack. The rods are also instrumented with pressure transducers or cladding elongation detectors, primarily to detect fission gas release (FGR) and pellet-cladding gap closure.

Table 1: Basic characteristics of the simulated fuel pellets. Compositions are given as weight percentages.

Fuel type	Th-MOX	UOX
Pu fraction [%]	7.9	-
U enrichment [% U-235]	-	8.4
Density [% of TD]	97	95.5
Central hole $\varnothing$ [mm]	1.2	1.2
Pellet $\varnothing$ [mm]	5.9	8.48

### 11.2. Simulation of the test rods

FRAPCON input files have been prepared based on the rod and pellet specifications and the detailed power history of each rod. The individual pin power levels are calculated using a rig-internal pin power distribution obtained from simulations with HELIOS [49]. The input power level of the rig is calibrated using measured values of the coolant flow and temperature at the rig inlet and outlet during the first startup. The calculated radial power distribution between the pins is corrected for a possible flux tilt over the rig quantified by three neutron detectors located in the same horizontal plane as the thermocouples. Finally, the axial power distribution can be calculated using the signal from a fourth neutron detector located below the other three.

For the *UOX-6* rod, the entire rod of 30 cm active length has been simulated as is, using FRAPCON 3.4. For the Th-MOX rods, the simulation needed to be simplified due to the fact that only a small fraction of the pellets are Th-MOX pellets. Since FRAPCON does not support the modelling of different fuel types within the same fuel stack, all axial dependencies have been neglected and only the Th-MOX rod segment (into which the thermocouple is inserted) has been simulated, using FRAPCON-ThMOX in its current state of development.

The calculated centerline temperatures at the location of the thermocouple tip in each rod are plotted in Figure 6 along with the measured temperatures.

In the FRAPCON input files, the absolute power level of the rig (and thus all the simulated fuel rods) has been increased by 12% relative to the calculated power levels. This adjustment of the power level is chosen to make the calculated fuel temperature agree with the measured data for the UOX reference rod at beginning of life. The reasons for this are twofold:

Firstly, there is an uncertainty of about 5% in the prediction of the total rig power (not affecting the power distribution between the individual pins in the rig). The systematic underprediction of the temperatures for all fuel rods when using the nominal power as input indicates that the total rig power is indeed higher than assumed, which motivates the use of a higher power for the corrected temperature calculations.

Secondly, FRAPCON 3.4 is known to underpredict many fuel temperatures for Halden research reactor conditions by up to about 7% [50]. The exact reason for this is unknown, but it is likely that a systematic underprediction at Halden irradiation conditions would affect UOX rods and Th-MOX rods in the same irradiation rig similarly.

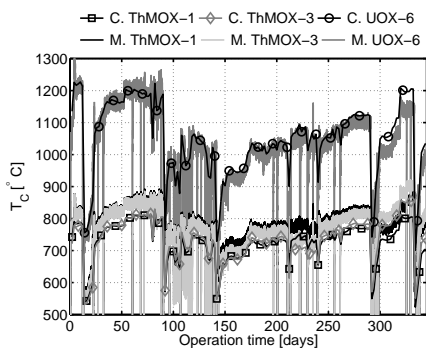


Figure 6: Measured (M.) and calculated (C.) fuel centerline temperatures for the two irradiated Th-MOX rods (*ThMOX-1* and *ThMOX-3*) and the UOX reference rod (*UOX-6*). The discussed 12% power correction factor has been applied for the calculations. Note that the large difference in temperature between the rod types mainly depends on the differences in diameter and linear heat generation rates.

With this adjustment of the input power level, the calculations still underestimate the fuel centerline temperature for the Th-MOX fuel. This underprediction is assumed to be caused - at least in part - by heat conduction in the axial direction (not modelled by FRAPCON) from the  $\text{Th}_{0.42}\text{U}_{0.58}\text{O}_2$  material, which is hotter than the Th-MOX material. The interface between the  $\text{Th}_{0.42}\text{U}_{0.58}\text{O}_2$  material and the Th-MOX material is located only 2 cm from the thermocouple tip. The high temperature of the  $\text{Th}_{0.42}\text{U}_{0.58}\text{O}_2$  material is due to its low density causing a correspondingly low thermal conductivity and a large pellet cladding gap for these pellets (due in turn to the excessive densification and shrinkage of this fuel).

The temperature contribution from the adjacent

$\text{Th}_{0.42}\text{U}_{0.58}\text{O}_2$  material to the temperature at the thermocouple tip is difficult to estimate without very fine-meshed neutronic and heat conduction simulations which is outside the scope of this work. The size of this contribution may be estimated using the temperatures recorded for the *ThUOX-5* rod. The difference in normalized temperature between the Th-MOX rods and the *ThUOX-5* rod is approximately constant after the initial period of approximately a week during which the main part of the densification of the  $\text{Th}_{0.42}\text{U}_{0.58}\text{O}_2$  material takes place. However, the difference in absolute temperature is increasing, due to a decrease in reactivity of the Th-MOX material relative to the  $\text{Th}_{0.42}\text{U}_{0.58}\text{O}_2$  material. It is difficult to estimate the local power in the  $\text{Th}_{0.42}\text{U}_{0.58}\text{O}_2$  material directly adjacent to the Th-MOX material, so it cannot be excluded that there may be a gradual increase in the temperature contribution from axial heat conduction.

### 11.3. Burnup dependent factors

Initially, a trend of close to linearly increasing underprediction was observed, growing to almost 100K within the current irradiation period, that is, to a burnup of 22 MWd/kgOx. Possible causes for this were investigated.

By far the most important parameter for the temperature prediction is the local power. Additional neutronic simulations were performed using *Serpent*, in order to investigate whether the power balance between the short Th-MOX segments and the *UOX-6* reference rod was mispredicted by the HELIOS simulations. No obvious errors in the previous simulations were found.

As mentioned, there may be a gradual increase in the temperature contribution from axial heat conduction from the hotter  $\text{Th}_{0.42}\text{U}_{0.58}\text{O}_2$  material. It is difficult to say whether this accounts for all of the observed increase of the underprediction, so reasons for the increasing underprediction were also sought among the key burnup dependent fuel behaviours.

The swelling behaviour is likely to be different for the different fuel types, but lacking data, the swelling calculation is left unchanged in FRAPCON-ThMOX. The scarce data available, however, indicates that there is a higher swelling rate for Th-MOX fuel, consistent with a higher fission gas retention ability [51]. A higher swelling rate would cause a lowering of the temperature through reduction of the pellet-cladding gap. The sensitivity of the calculated temperature to the swelling rate was checked, and even setting the swelling rate to zero (i.e. decreasing it, despite the expectation that it should be higher than for UOX) only partly decreased the underprediction, by about 40 K at 22 MWd/kgOx.

The calculation in FRAPCON 3.4 of the effective gap reduction due to fuel fragment relocation is based entirely on empirical data from measurements on UOX fuel. The relocation behaviour may well be different for Th-MOX fuel. The temperature calculations are quite sensitive to the gap size, and changes in the calculated temperature caused by changes in the magnitude of gap reduction are largest at the beginning of the fuel's life. Thus, although an incorrect relocation model may cause mispredictions, it would not cause an increasing underprediction.

Finally, the new model for radial power profile predictions also affects the calculated temperatures. However, the change from the UOX-specific model to the new model only introduced a lowering of the calculated temperature of about 10 K, a difference which remained almost constant for the entire irradiation period. This is expected for such a small pin radius and low burnup.

The burnup dependence of the thermal conductivity is modeled by a burnup dependent term,  $f(Bu)$  as shown in Equation 6. This term comprises the small host of physical factors that cause the thermal conductivity of ceramic fuels to degrade with burnup. An increase of this term eliminated the gradual increase of the underprediction, indicating that a more rapid decrease of the thermal conductivity of Th-MOX fuel compared with that of UOX fuel may indeed be the cause for the initially observed increase of the underprediction. The hypothesis is strengthened by a second set of measurements. When the reactor is scrammed, the fuel temperature exponentially approaches the coolant temperature. The time constant for this exponential decay is partly determined by the thermal conductivity, a lower conductivity causing a slower temperature drop and hence a larger time constant. As seen in Figure 7, the scram time constant for the UOX rods remains almost constant throughout the irradiation period, whereas an increasing trend is observed for the Th-MOX rods, although the large uncertainty in the determination of the time constants makes the trend somewhat unclear.

It can be noted in Figure 6 that the simulations for rod UOX-6 suddenly overestimate the measured temperature after 300 operation days. This could be due to closing of the pellet-cladding gap. Recordings from similar rods in the same irradiation rig indicates impending gap closure, although the FRAPCON 3.4 simulations show some remaining gap. Also the low values of the time constants for rod UOX-6 from the last two scrams indicates that the heat conductance between the thermocouple and the coolant has suddenly improved, e.g. through gap closure.

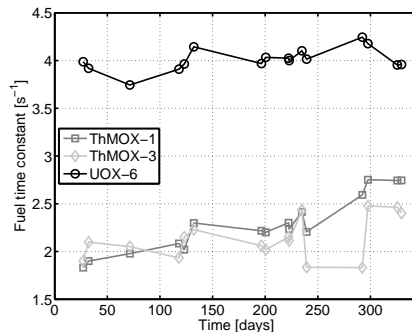


Figure 7: Scram time constants for the simulated fuel rods.

## 12. Discussion

The thermal-mechanical properties of  $\text{Th}_{1-y}\text{Pu}_y\text{O}_{2-x}$  fuel materials clearly need to be better understood, including via further experimental measurements. Thermal conductivity, thermal expansion, heat capacity, enthalpy and melting point are reasonably well investigated, but only for stoichiometric, fresh material. On the other hand, estimates of the elastic properties are based on theoretical reasoning which is not experimentally confirmed, and the irradiation swelling and emissivity subroutines are left unchanged for the lack of useful experimental data. Furthermore, the existing data is only known for solid fuel. For fuel performance analysis under severe accident conditions, properties of molten material may need to be known.

Also, most reasoning regarding the stoichiometry dependence of the thermal-mechanical property changes is based on theory rather than experiment. Although thorium based fuels are expected to maintain O/M = 2.00 stoichiometry to a larger extent than uranium based ones, this needs to be confirmed, and the sensitivity of the properties to deviations from stoichiometry needs to be assessed in order to confirm or discard the hypothesis that neglecting this dependence does indeed not introduce significant errors. Mihaila et al. [52] have shown that the inclusion of oxygen diffusion models in  $\text{UO}_2$  fuel performance modelling does indeed have a significant impact on the predicted fuel temperature, and similar simulations should be carried out for the  $\text{Th}_{1-y}\text{Pu}_y\text{O}_{2-x}$  system.

Irradiation effects on Th-MOX fuel performance are still unknown. The burnup dependence of the thermal conductivity must be much more thoroughly in-

vestigated. The burnup dependence of the melting point needs to be experimentally assessed, and perhaps more importantly, purely irradiation-induced phenomena such as irradiation swelling, cracking, relocation and fission gas production and release will require revised models.

Some measurements of irradiation swelling have been made [46, 47], and more data will become available after post-irradiation examination (PIE) of the Th-MOX pellets being irradiated in the Halden research reactor. Cracking and relocation behaviour will also be possible to assess at least qualitatively after PIE, but given the very empirical relocation model employed in FRAPCON 3.4, data for several different pellet and cladding dimensions will need to be gathered to support a revised model. A new fission gas release model has been developed for thorium-uranium fuel [9] and a similar approach can be used for Th-MOX. Fission gas production rates can be calculated by neutronic codes. The fission gas release can not be assessed from the current irradiation experiment due to the dominance of the (Th,U)O<sub>2</sub> material in the test fuel rods, but an extension of the program to include full Th-MOX rods will allow for such assessments.

It should also be noted that of the modified subroutines, only those related to thermal conductivity, thermal expansion and the radial power profiles have a significant impact on the calculated results. Further experiments and corresponding simulations need to be performed to assess the impact of the changes made to the subroutines related to enthalpy and heat capacity.

Finally, it is noted that FRAPCON 3.5 was released during the course of this development work. The difference between the results as calculated by FRAPCON 3.4 and FRAPCON 3.5 for the cases discussed here were negligible (about 2K for the centerline temperature) after the same thermal-mechanical property correlations were changed for both releases. Unfortunately, the new model for radial power profile prediction could not be directly implemented in FRAPCON 3.5, however this is not affecting the ongoing refinement of correlations tailored for Th<sub>1-y</sub>Pu<sub>y</sub>O<sub>2-x</sub> fuel ceramics.

### 13. Conclusion

The performed calculations indicate that FRAPCON-ThMOX predicts the centerline temperature of fresh Th-MOX fuel with the same precision as FRAPCON 3.4 when applied to UOX fuel. Given that the thermal-mechanical properties of un-irradiated Th<sub>1-y</sub>Pu<sub>y</sub>O<sub>2</sub> are reasonably well known, this could be expected. An increase of the burnup dependent term in the expression

for the thermal conductivity also gave good predictions for higher burnups. The hypothesis that the thermal conductivity of Th-MOX fuel decreases more rapidly with burnup compared with that of UOX fuel is strengthened by the time constants shown in Figure 7, but further experimental confirmation is needed.

### Acknowledgments

The authors would like to thank Julian F. Kelly, Ian D. Palmer and Alexander J. Mieloszyk for their advice and Bogdan Mihaila for his support during the early phases of the literature study. Financial support was given to the first author by the Norwegian Research council through the Industrial PhD program, and to the test irradiation project through the BIA program.

### References

- [1] H. Gruppelaar, J. P. Schapira, Thorium as a waste management option, final report, Technical Report EUR 19142 EN, European Commission, 2000.
- [2] B. A. Lindley, G. T. Parks, Near-complete transuranic waste incineration in a thorium fuelled pressurised water reactor, *Annals of Nuclear Energy* 40 (2012) 106 – 115.
- [3] K. Insulander Björk, A BWR fuel assembly design for efficient use of plutonium in thorium-plutonium fuel, *Progress in Nuclear Energy* 65 (2013) 56 – 63.
- [4] K. Insulander Björk, V. Fhager, Comparison of thorium-plutonium fuel and MOX fuel for PWRs, in: *Proceedings of Global 2009*, Paper 9449.
- [5] C. W. Lau, H. Nylén, K. Insulander Björk, U. Sandberg, Feasibility study of 1/3 thorium-plutonium mixed oxide core, *Science and Technology of Nuclear Installations 2014* (2014). Paper 709415.
- [6] K. Insulander Björk, S. S. Drera, J. F. Kelly, C. Vitanza, C. Helsingreen, T. Tverberg, M. Sobieska, B. C. Oberländer, H. Tuomisto, L. Kekkonen, J. Wright, U. Bergmann, D. P. Mathers, Commercial thorium fuel manufacture and irradiation: Testing (Th,Pu)O<sub>2</sub> and (Th,U)O<sub>2</sub> in the "Seven-Thirty" program, *Annals of Nuclear Energy* 75 (2015) 79–86.
- [7] K. Geelhood, W. Luscher, C. Beyer, FRAPCON-3.4: A Computer Code for the Calculation of Steady-State Thermal-Mechanical Behavior of Oxide Fuel Rods for High Burnup, Pacific Northwest National Laboratory, P.O. Box 999, Richland, WA 99352, 2011. NUREG/CR-7022.
- [8] M. Verwerf, S. E. Lemehov, M. Wéber, L. Vermeeren, P. Gouat, V. Kuzminov, V. Sobolev, Y. Parthoens, B. Vos, H. Van den Berghe, S. ans Segura, P. Blanpain, J. Somers, G. Toury, J. McGinley, D. Staicu, A. Schubert, P. Van Uffelen, D. Haas, OMICO Final Report, Technical Report EUR 23104, European Commission, European Commission, 2007. FIKS-CT-2001-00141.
- [9] Y. Long, L. J. Siefken, P. Hejzlar, E. P. Loewen, J. K. Hohorst, P. E. MacDonald, M. S. Kazimi, The behavior of ThO<sub>2</sub>-based fuel rods during normal operation and transient events in LWRs, *Nuclear Technology* 147 (2004) 120–139.
- [10] A. Mieloszyk, Y. Sukjai, S. Xu, M. S. Kazimi, FRAPCON-MIT: A fuel performance tool for innovative fuel designs, in: *Proceedings of TopFuel*.

- [11] K. Bakker, E. H. P. Cordfunke, R. J. M. Konings, R. P. C. Schram, Critical evaluation of the thermal properties of  $\text{ThO}_2$  and  $\text{Th}_{1-x}\text{U}_x\text{O}_2$  and a survey of the literature data on  $\text{Th}_{1-x}\text{Pu}_x\text{O}_2$ , *Journal of Nuclear Materials* 250 (1997) 1–12.
- [12] R. Böhler, P. Çakır, O. Beneš, H. Hein, R. Konings, D. Manara, High temperature phase transition of mixed ( $\text{puo}_2+\text{tho}_2$ ) investigated by laser melting, *The Journal of Chemical Thermodynamics* 81 (2015) 245–252.
- [13] O. Válu, O. Beneš, R. Konings, H. Hein, The high temperature heat capacity of the (Th,Pu) $\text{O}_2$  system, *The Journal of Chemical Thermodynamics* 68 (2014) 122–127.
- [14] C. Cozzo, D. Staicu, J. Somers, A. Fernandez, R. Konings, Thermal diffusivity and conductivity of thorium-plutonium mixed oxides, *Journal of Nuclear Materials* 416 (2011) 135–141.
- [15] K. Insulander Björk, P. Fredriksson, Development of a fuel performance code for thorium-plutonium fuel, in: *Proceedings of PHYSOR 2014*, Kyoto, Japan, September 28 - October 3.
- [16] T. Kutty, P. Hegde, J. Banerjee, K. Khan, A. Sengupta, G. Jain, S. Majumdar, H. Kamath, Densification behaviour of  $\text{ThO}_2$ - $\text{PuO}_2$  pellets with varying  $\text{PuO}_2$  content using dilatometry, *Journal of Nuclear Materials* 312 (2003) 224–235.
- [17] T. Yamashita, N. Nitani, T. Tsuji, H. Inagaki, Thermal expansions of  $\text{NpO}_2$  and some other actinide dioxides, *Journal of Nuclear Materials* 245 (1997) 72–78.
- [18] A. K. Tyagi, M. D. Mathews, Thermal expansion of  $\text{ThO}_2$ -2 wt%  $\text{UO}_2$  by HT-XRD, *Journal of Nuclear Materials* 278 (2000) 123–125.
- [19] A. Momin, E. Mirza, M. Mathews, High-temperature x-ray diffractometric studies on the lattice thermal-expansion behaviour of  $\text{UO}_2$ ,  $\text{ThO}_2$  and  $(\text{U}_{0.2}\text{Th}_{0.8})\text{O}_2$  doped with fission-product oxides, *Journal of Nuclear Materials* 185 (1991) 308–310.
- [20] J. Belle, R. M. Berman, Thorium Dioxide: Properties and Nuclear Applications, Technical Report DOE/NE-0060, Naval Reactors Office, United States Department of Energy, 1984.
- [21] I. Cohen, R. Berman, A metallographic and x-ray study of the limits of oxygen solubility in the  $\text{UO}_2$ - $\text{ThO}_2$  system, *Journal of Nuclear Materials* 18 (1966) 77–107.
- [22] S. Hubert, J. Purans, G. Heisbourg, P. Moisy, N. Dacheux, Local structure of actinide dioxide solid solutions  $\text{Th}_{1-x}\text{U}_x\text{O}_2$  and  $\text{Th}_{1-x}\text{Pu}_x\text{O}_2$ , *Inorganic Chemistry* 45 (2006) 3887–3894.
- [23] V. Sobolev, Modelling thermal properties of actinide dioxide fuels, *Journal of Nuclear Materials* 344 (2005) 198–205.
- [24] T. D. Chikalla, C. E. McNeilly, R. E. Skavdahl, The plutonium-oxygen system, *Journal of Nuclear Materials* 12 (1964) 131–141.
- [25] T. A. Sandenaw, Heat capacity of plutonium dioxide below 325 K, *Journal of Nuclear Materials* 10 (1963) 165–172.
- [26] S. G. Popov, J. J. Carbajo, V. K. Ivanov, G. L. Yoder, Thermophysical Properties of MOX and  $\text{UO}_2$  Fuels Including the Effects of Irradiation, Technical Report ORNL/TM-2000/351, Oak Ridge National Laboratory, 2000.
- [27] Y.-E. Kim, J.-W. Park, J. Cleveland, Thermophysical properties database of materials for light water reactors and heavy water reactors, Technical Report IAEA-TECDOC-1496, International Atomic Energy Agency, 2006.
- [28] C. Duriez, J.-P. Alessandri, T. Gervais, Y. Philipponneau, Thermal conductivity of hypostoichiometric low Pu content  $(\text{U,Pu})\text{O}_{2-x}$  mixed oxide, *Journal of Nuclear Materials* 277 (2000) 143–158.
- [29] D. Das, S. R. Bharadwaj (Eds.), *Thoria based Nuclear Fuels*, Springer, London, UK, 2013.
- [30] E. P. Loewen, P. E. MacDonald, J. K. Hohorst, J. P. Sharp, L. Siefken, Development of Material Property Correlations for Analysis of Mixed Thoria-Urania Fuel Performance in Light Water Reactors and Augmentation of the FRAPCON-3 Computer Code, Technical Report INEEL/EXT-2000-00275, Idaho National Engineering and Environmental Laboratory, 2000.
- [31] R. D. Shannon, Revised effective ionic radii and systematic studies of interatomic distances in halides and chalcogenides, *Acta Crystallographica A32* (1976) 751.
- [32] T. Ohmichi, S. Fukushima, A. Maeda, H. Watanabe, On the relation between lattice parameter and O/M ratio for uranium dioxide-trivalent rare earth oxide solid solution, *Journal of Nuclear Materials* 102 (1981) 40–46.
- [33] M. Ali, P. Nagels, Evaluation of the Debye temperature of thorium dioxide, *Physica Status Solidi B* 21 (1967) 113–116.
- [34] S. FUKUSHIMA, T. OHMACHI, A. MAEDA, M. HANDA, Thermal conductivity of stoichiometric  $(\text{Pu,Nd})\text{O}_2$  and  $(\text{Pu,Y})\text{O}_2$  solid solutions, *Journal of Nuclear Materials* 114 (1983) 260–266.
- [35] J. Fink, Enthalpy and heat capacity of the actinide oxides, *International Journal of Thermophysics* 3 (1982) 165–200.
- [36] N. Igata, K. Domoto, Fracture stress and elastic modulus of uranium dioxide including excess oxygen, *Journal of Nuclear Materials* 45 (1972/73) 317–322.
- [37] L. J. Siefken, E. W. Coryell, E. A. Harvego, J. K. Hohorst, SC-DAP/RELAP5/MOD3.3 Code Manual: MATPRO - A Library of Materials Properties for Light-Water-Reactor Accident Analysis, Technical Report NUREG/CR-6150, Vol. 4, Rev. 2 INEL-96/0422, Idaho National Engineering and Environmental Laboratory, 2001.
- [38] C. Ronchi, J. P. Hiernaut, Experimental measurement of pre-melting and melting of thorium dioxide, *Journal of Alloys and Compounds* 240 (1996) 179–185.
- [39] F. D. Bruycker, K. Boboridis, P. Pöml, R. Eloiirdi, R. Konings, D. Manara, The melting behaviour of plutonium dioxide: A laser-heating study, *Journal of Nuclear Materials* 416 (2011) 166–172.
- [40] W. L. Lyon, W. E. Baily, The solid-liquid phase diagram for the  $\text{UO}_2$ - $\text{PuO}_2$  system, *Journal of Nuclear Materials* 22 (1967) 332–339.
- [41] J. J. Carbajo, G. L. Yoder, S. G. Popov, V. K. Ivanov, A review of the thermophysical properties of MOX and  $\text{UO}_2$  fuels, *Journal of Nuclear Materials* 299 (2001) 181–198.
- [42] M. Kato, K. Morimoto, H. Sugata, K. Konashi, M. Kashimura, T. Abe, Solidus and liquidus temperatures in the  $\text{UO}_2$ - $\text{PuO}_2$  system, *Journal of Nuclear Materials* 373 (2008) 237–245.
- [43] L. F. Epstein, Ideal solution behaviour and heats of fusion from the  $\text{uo}_2$ - $\text{puo}_2$  phase diagram, *Journal of Nuclear Materials* 22 (1969) 340–349.
- [44] Y. Katayama, D. Carroll, R. Skavdahl, J. Burnham, J. Christensen, M. Freshley, H. Mattys, D. Brite, K. Sump, J. Bates, J. Daniel, L. Pember, H. Anderson, J. McPartland, W. Ross, L. Merker, R. Smith, J. Hauth, D. Burrough, C. Bloomster, R. Bardsley, R. Sharp, L. C. Lemon, W. Ross, L. P. Murphy, W. Bailey, J. Burnham, G. Horn, M. Millhollen, W. Flaherty, L. Mill, T. Chikalla, W. Roake, S. Woodcock, Ceramics Research and Development Operation Quarterly Report, October - December 1962, Technical Report HW-76300, General Electric Co. Hanford Atomic Products Operation, 1963.
- [45] F. D. Bruycker, K. Boboridis, R. Konings, M. Rini, R. Eloiirdi, C. Guneau, N. Dupin, D. Manara, On the melting behaviour of uranium/plutonium mixed dioxides with high-pu content: A laser heating study, *Journal of Nuclear Materials* 419 (2011) 186–193.
- [46] F. C. Klaassen, J. C. Kuijper, K. Bakker, R. P. C. Schram, THORIUM CYCLE: Development Steps for PWR and ADS Applications, Technical Report Th5-DOC-041, NRG, 2008.
- [47] L. A. Lawrence, Performance of LMFBR fuel pins with  $(\text{Pu,Th})\text{O}_{2-x}$  and  $\text{UO}_2$ , *Transactions of the American Nuclear*

- Society 45 (1983) 301–302.
- [48] J. Leppänen, Serpent - a Continuous-energy Monte Carlo Reactor Physics Burnup Calculation Code., VTT Technical Research Centre of Finland, 2012.
  - [49] J. Casal, R. Stammler, E. Villarino, A. Ferri (Eds.), HELIOS: Geometric Capabilities of a New Fuel Assembly Program, Intl. Topical Meeting on Advances in Mathematics, Computations and Reactor Physics, Pittsburgh, Pennsylvania, USA, 1991.
  - [50] K. Geelhood, W. Luscher, C. Beyer, FRAPCON-3.4: Integral Assessment, Pacific Northwest National Laboratory, P.O. Box 999, Richland, WA 99352, 2011. NUREG/CR-7022.
  - [51] M. Karam, F. Dimayuga, J. Montin, Fission Gas Release of (Th,Pu)O<sub>2</sub> CANDU Fuel, Technical Report CW-124950-CONF-002, Atomic Energy of Canada Limited, 2008.
  - [52] B. Mihaila, M. Stan, J. Ramirez, A. Zubelewicz, P. Cristea, Simulations of coupled heat transport, oxygen diffusion, and thermal expansion in UO<sub>2</sub> nuclear fuel elements, Journal of Nuclear Materials 394 (2009) 182–189.